Cytokine gene and protein expression in BCG vaccinated and non-vaccinated *Mycobacterium bovis* infected cattle

Jaydene Witchell

Submitted to the University of Hertfordshire in partial fulfilment of the requirements of the degree of PhD

July 2008

Abstract

The persistent increase of bovine tuberculosis (bTB) over the past twenty years has put a substantial strain on both the British economy and the welfare of livestock. However, the development of an effective bTB vaccine has been continually hindered by the lack of knowledge on the immune response following *Mycobacterium bovis* (*M. bovis*) infection. In collaboration with the TB Research Group at the Veterinary Laboratories Agency (VLA, Surrey), this thesis is part of a much wider strategy managed by the Department of Environment, Food and Rural Agency (DEFRA) aimed at elucidating the immunopathogenesis of *M. bovis* and to develop more effective infection control measures. The specific focus of this thesis was to enable a stronger understanding of the bovine immune response over different periods of *M. bovis* infection and to apply this new knowledge in evaluating the efficacy of a novel BCG vaccination.

Time Course Study: Knowledge of time dependent cytokine expression following *M. bovis* infection would aid vaccine development by revealing potential correlates of protection. Interferon gamma (IFN-γ), tumour necrosis factor alpha (TNF-α), interleukin (IL) 4 and 10 expression were analysed using quantitative (q) PCR in formalin fixed bovine lymph nodes following five, twelve and nineteen weeks of *M. bovis* infection. A strong pro-inflammatory/ T helper 1 (T_H1) lymphocyte response was evident at five weeks post *M. bovis* infection, represented by IFN-γ and TNF-α expression (log_2 copies of 6.5 and 2.15, respectively) in the absence of IL4. Between five and twelve weeks of infection, a significant increase was observed in IL10 (log_2 copies from 5.97 to 8.27, $p<0.01$, Mann Whitney test), accompanied by an increase in both IFN-γ (log_2 7.53) and TNF-α (log_2 3.94). This data conformed to a recently described aspect of T_H1 lymphocytes, a 'self-limiting' nature in which cells produced both IFN-γ and IL10 with the aim of controlling the heightened pro-inflammatory response. The role of IL10 as an immunosuppressive became evident when comparing cytokine expression between four different types of thoracic lymph node; the left bronchial (LB), cranial mediastinal (CRM), caudal mediastinal (CM) and cranial tracheobronchial (CRT) nodes. The LB and CRM lymph nodes produced significantly higher levels of IFN-γ expression (log_2 copies between 8.2 and 10) as compared to the CM and CRT (log_2 copies between 2.6 and 5.5, $p<0.001$, Mann Whitney test). Further analysis of the data as a profile of cytokine expression for each lymph node type revealed that IFN-γ was dominantly expressed within the LB and CRM nodes,

whereas within the CM and CRT nodes, IL10 was the dominant cytokine. The former nodes also displayed a higher level of pathological damage (represented by mean percentage area coverage of granuloma, 33.6 and 20%, respectively) as compared to the CM (13%) and the CRT lymph node types (10.8 %). This suggests conflicting roles for IFN-γ and IL10 in the development of immune-associated pathology. Following nineteen weeks of infection, the expression levels of IFN-γ, TNF-α and IL10 reduced (log_2 6.22, 3.02 and 7.03, respectively) implying a loss of the cellular response. The later stages of bovine tuberculosis have been shown within the literature to display characteristics of a humoral rather than cell mediated response. However, within this study at nineteen weeks post infection IL4 (an important cytokine in the development of the humoral response) remained undetectable.

The results from this study therefore confirm the importance of the cell mediated immune profile in response to *M. bovis* infection as well as the integral role of IFN-γ in both protection and pathology. It also further demonstrates the involvement of IL10 in controlling the IFN-γ response and highlights this cytokine as being potentially important in future immunology-based vaccination studies.

BCG Vaccination Study: The current vaccine used against human tuberculosis, BCG, has provided variable results on protection against infection in experimental bovine studies. The BCG bacterium has lost a comparatively large quantity of genomic DNA through attenuation since its primary production in 1921, of which the majority represented genes encoding antigenic proteins. MPB70 and MPB83 are differentially expressed between BCG sub-strains due to a single nucleotide polymorphism in the alternative sigma factor K (SigK). BCG Pasteur has been shown to produce low levels of these antigenic proteins; however complementation of BCG Pasteur with a copy of *sigK* from BCG Russia resulted in up-regulating expression. It was therefore hypothesised that the recombinant BCG (*sigK*) Pasteur would prove more efficient in controlling *M. bovis* infection by inducing a stronger protective immune response post vaccination.

IFN-γ, TNF-α, IL 4 and 10 expression were analysed using qPCR within the freshly dissected lymph nodes of five experimental cattle groups; BCG Pasteur vaccinated *M. bovis* challenged, BCG (*sigK*) Pasteur vaccinated challenged, non-vaccinated infected, non-vaccinated non-infected and BCG Pasteur vaccinated non-infected. Five weeks following infection, a strong IFN-γ mRNA response was detected in both the non-vaccinated and vaccinated cattle (mean log_2 copies between 9.6 and 10.5 as compared to between 7.84 and 8.58 in the non-infected

cattle). *M. bovis* infection also induced a significant reduction in IL10 mRNA levels in both vaccinated and non-vaccinated cattle (mean $\log_2$ 14.4 in the infected groups compared to 15.5 in the non-infected cattle, $p<0.005$, Mann Whitney test) although there was little difference in TNF-α expression (mean $\log_2$ copies between 11.06 and 11.8 in all five groups). Interestingly, IL4 mRNA was detectable only within the two non-infected control groups (mean $\log_2$ 12.4), further supporting the concept of a strong cell mediated response after five weeks of infection.

Vaccination prior to challenge had an effect on IFN-γ mRNA levels only, as both the BCG Pasteur and BCG (*sigK*) Pasteur vaccinated groups displayed a smaller increase in IFN-γ mRNA following challenge (mean $\log_2$ 10.3 and 9.6, respectively) as compared to the non-vaccinated group (mean $\log_2$ 10.5). This reflected the role of vaccination in priming the immune response to enable more rapid elimination of the bacteria and subsequently inducing a lesser pro-inflammatory response. Interestingly, the BCG Pasteur vaccinated group appeared to control the immune response to a greater extent, as IFN-γ mRNA was significantly similar to that observed in the non-vaccinated non-infected group (mean $\log_2$ 8.58, $p>0.05$, Mann Whitney test).

In addition to the qPCR data, levels of IFN-γ and TNF-α protein (represented by the number of cells producing these proteins) were also analysed by immunohistochemistry. IFN-γ protein in the five experimental groups displayed the same pattern as that observed for IFN-γ mRNA expression ($p<0.001$, Spearmans correlation coefficient). However, analysis of TNF-α protein revealed significant differences between the five groups ($p<0.005$, Kruskal Wallis test) in contrast to that observed for the mRNA levels ($p>0.05$, Spearmans correlation coefficient) suggesting that posttranscriptional controls may play an important role in TNF-α translation.

The difference in IFN-γ mRNA and protein expression between the two vaccination groups was also reflected within the pathological data. Although both BCGs reduced levels to below that of the non-vaccinated group (represented by mean percentage area coverage of granuloma, 59%), the BCG Pasteur group displayed less pathology (mean 6%) compared to the BCG (*sigK*) Pasteur cattle (mean 35%). It was suggested that the increased antigenic repertoire of the recombinant BCG (*sigK*) Pasteur did result in a stronger stimulation of the immune response post vaccination but that, as a consequence the bacterial threat was eliminated more rapidly. This resulted in shortening the duration of antigenic stimulation thereby effecting the development of the memory T cell response. These results imply that enhancing the antigen repertoire of the current BCG alone is not sufficient in improving upon protection against *M. bovis* infection. They further support the benefits of a prime/boost vaccination protocol, in which primary antigenic stimulation of the bovine immune response is boosted at a later stage.

Supplementary studies: To complement the above studies, supplementary work was also performed to investigate the effect of tissue fixation on the quality of extracted RNA and the impact of *M. bovis* dosage on the bovine immunological response post infection. Archived tissues provide an extensive source of experimental material on which to perform molecular techniques many years after the initial investigations. Formalin is a popular choice of fixative however its ability to conserve the molecular composition of tissue sections has been questioned. This has led to the development of new alternatives such as the Hepes glutamic acid buffer-mediated organic solvent protection effect (HOPE) fixative. In order to analyse the efficacy of formalin and HOPE fixation in preserving RNA integrity, total RNA was extracted from fixed bovine lymph node samples and the mRNA expression of housekeeping gene glyceraldehyde-3-phosphate dehydrogenase (GAPDH) measured using qPCR. Using two different extraction procedures (a commercial kit from Ambion (UK) and an in-house trizol method), the HOPE-fixed lymph node tissue provided total RNA of a high integrity, shown by producing two strong rRNA bands following gel electrophoresis. The total RNA extracted from the formalin-fixed tissues using the Optimum Ambion kit appeared to be of a slightly lesser quality, as only one of the two rRNA bands was visualised on the agarose gel following electrophoresis. The use of the trizol method on formalin fixed tissues failed to provide total RNA, confirmed by both the absence of rRNA bands and a negative spectrophotometry reading. QRT-PCR for GAPDH expression using total RNA extracted from HOPE-fixed tissues displayed higher levels of messenger RNA (4.05×10^{-2} pg/100ng total RNA using the commercial Ambion kit and 6.45×10^{-2} pg/100ng total RNA using the trizol method) as compared to that extracted from formalin-fixed tissues (5.69×10^{-4} pg/100ng total RNA using the Ambion kit). These results suggest that the RNA did experience a certain degree of degradation whilst exposed to formalin-fixation and that HOPE fixative did provide a total RNA template of better quality. This was reflected in the gene expression study, as the RNA of higher integrity extracted from the HOPE-fixed tissues displayed a higher concentration of GAPDH mRNA. The consequences of this study are extensive, particularly when considering the results of the time course study, as it suggests that the expression levels observed were probably lower than what might have been observed if HOPE-fixed tissues were available. It also supports the use of HOPE rather than formalin fixative in future molecular expression studies.

The second supplementary study focused on the possible effects of different *M. bovis* inoculation concentrations on bovine cytokine expression levels. Experimental infection of cattle has traditionally involved the use of extremely high concentrations of *M. bovis* inoculum

(between 10^4 and 10^6 cfu's) so as to ensure that the animal successfully display disease. However, recent field studies have shown that cattle need only inhale one to two bacterial cells to become infected and therefore experimental models using high dosage levels may not be representative of natural disease. A study performed at the VLA confirmed that there was no pathological difference between cattle infected with 1, 10, 100 or 1,000 cfu's of *M. bovis,* suggesting that dosage concentration had little effect on disease progression. This study aimed to further this comparison by measuring the genetic expression of IFN-γ, TNF-α, IL10 and IL4 within the same lymph node samples (this work was performed entirely by an MSc student using the RNA extraction and qRT-PCR methods developed for this thesis). The results showed that expression of these four cytokines increased as the infecting dose of *M. bovis* increased. Between 1 and 1,000 cfu's of *M. bovis*, there was a significant increase in IFN-γ (2.1 $x10^5$ and 9.0 $x10^5$ copies, respectively), IL10 (9.3 $x10^4$ and 5.1 $x10^5$, respectively) and IL4 (2.0 $x10^5$ and 6.3 $x10^5$, respectively, $p<0.05$, Mann Whitney test). Although there was a simultaneous increase in TNF-α, the difference was not significant (2.5 $x10^5$ and 7.1 $x10^5$, respectively, $p>0.05$, Mann Whitney test). The increasing expression of these cytokines may be a direct effect of the increased level of antigenic stimulation from a higher concentration of bacterial cells. Expression of IFN-γ and IL10 experienced the largest increase between 1 and 1,000 cfu's (fold increase of 4.23 and 5.5, respectively) as both are produced by CD4+ T cells, an important part of the immune response against *M. bovis* infection. In contrast, TNF-α expression showed little difference over the four *M. bovis* concentrations and this may be due to the role of posttranscriptional regulation in controlling protein production.

In conclusion, although there were no obvious differences in lymph node pathology, there were significant differences in the expression of these four cytokines. This would suggest that the levels of expression observed at higher concentrations of *M. bovis* would be greatly increased in comparison to those observed at lower concentrations (i.e. natural infection). However, it is important to note that, as all of the cytokines increased in expression relative to each other, the patterns observed at high *M. bovis* concentrations may still be relevant to lower *M. bovis* concentrations.

Contents

Acknowledgements.

I would firstly like to thank my supervisors Dr. Madhu Goyal, Dr. Martin Vordermeier and Dr. Arun Wangoo for all of their advice, support and encouragement during my PhD. I am extremely appreciative for having been given this opportunity and also for being able to work so closely with the Veterinary Laboratories Agency (Weybridge, Surrey).

I would also like to express my sincere gratitude to all of those at the Veterinary Laboratories Agency who I have had the pleasure of working with; I have been overwhelmed by their generosity. In particular to Dr. Paul Golby for his help in RNA extraction and Dr. Shelley Rhodes for her invaluable guidance in quantitative PCR. Dr. Adam Whelan deserves a medal for his endless patience despite my constant e-mailing and I am indebted to Dr. Sarah Marsh for her unwavering enthusiasm in this thesis.

To the students and staff at the University of Hertfordshire I extend my deepest thanks. When times were tough and the work seemed never-ending, they were there with a smile when I needed it the most. Thank you to Di, Jon, Wanwisa, Alex, Anita and countless others – you made life at the university more than bearable.

I would also like to thank my parents Sally and Keith, my friends and my partner Sean. Words can not express how eternally grateful I will be for their support, both emotional and financial. Without them, I would never have got this far.

Finally, I dedicate this thesis to my late grandmother, Joyce Drodge and my late uncle, Steven Drodge. Although they were not able to see me complete my PhD, the love and inspiration they provided me with at the beginning saw me through to its end.

Publications

Witchell, J., Varshney, D., Gajjar, T., Wangoo, A., Goyal, M. (2008) RNA isolation and quantitative PCR from HOPE and formalin fixed bovine lymph node tissues. *Pathology; Research and Practice*. **204** (2): 105-11

Boddu-Jasmine, H. C., Witchell, J., Vordermeier, M., Wangoo, A., Goyal, M. (2008) Cytokine mRNA expression in cattle infected with different dosages of *Mycobacterium bovis*. *Tuberculosis.* **88** (6): 610-5

.

Conference posters

Witchell, J., Vordermeier, M., Wangoo, A., Goyal, M. (2007) Cytokine mRNA expression levels within BCG vaccinated and non-vaccinated, *Mycobacterium bovis* challenged cattle. *British Society of Immunology International Congress*: Glasgow, Scotland

Witchell, J., Vordermeier, M., Wangoo, A., Goyal, M. (2008) Immunological responses to BCG vaccination in *Mycobacterium bovis* challenged cattle. *European Congress of Clinical Microbiology and Infectious Diseases*: Barcelona, Spain.

Witchell, J., Vordermeier, M., Wangoo, A., Goyal, M. (2008) Time dependent cytokine mRNA expression in *Mycobacterium bovis* infected cattle. *3rd International Conference on Cytokine Medicine*: London, UK

List of figures

List of tables

Abbreviations

Acid fast bacilli	AFB
Alpha beta lymphocytes	αβ lymphocytes
Alternative sigma factor K	SigK
Analysis of variance	ANOVA
Antigen presenting cells	APCs
Bacillus Calmette-Guérin	BCG
Black Hole Quencher-1	BHQ-1
(Bovine) Tuberculosis	(B) TB
Cluster of differentiation	CD
Cell-mediated delayed-type hypersensitivity reaction	DTH reaction
Culture filtrate protein-10	CFP-10
Colony forming unit	Cfu
Complementary deoxyribose nucleic acid	cDNA
Crossing point value	CP value
Cytotoxic T lymphocytes	CTLs
Dendritic cells	DCs
Deoxyribose nucleic acid	DNA
Department of Environment, Food and Rural Agency	DEFRA
Diaminobenzidine	DAB
Diethyl pyrocarbonate	DEPC
Escherichia coli	*E. coli*
Enzyme linked immunosorbent assays	ELISA
Early secretory antigenic-target-6	ESAT-6

Formalin fixed, paraffin embedded tissues	FFPE
Gamma delta T cells	γδ T cells
Glyseraldehyde-3-phosphate dehydrogenase	GAPDH
Granulocyte macrophage-colony stimulating factor	GM-CSF
Immunohistochemistry	IHC
Independent Scientific Review group	ISR group
Inducible nitric oxide	iNOS
Interferon gamma	IFN-γ
Interleukin	IL
Lipopolysaccharide	LPS
Major Histocompatability complex	MHC
Messenger RNA	mRNA
Modified Vaccinia Ankara	MVA
Mycobacterium bovis	*M. bovis*
Mycobacterium tuberculosis	*M. tuberculosis*
Natural killer cells	NK cells
Non-tuberculous mycobacteria	NTM
Optical density	OD
Pathogen recognition receptors	PRRs
Pathogen-associated molecular patterns	PAMPs
Peripheral blood mononuclear cells	PBMCs
Primary macrophage-activating factor	MAF
P-selectin glycoprotein ligand-1	PSGL-1
Purified protein derivative (bovine/avium)	PPD (B/A)

Quantitative polymerase chain reaction	QPCR
Quantitative reverse-transcriptase polymerase chain reaction	QRT-PCR
Regulatory T cells type one	Tr1
Restriction fragment length polymorphisms	RFLP
Ribonucleic acid	RNA
Single intradermal comparative tuberculin test	SICTT
Single nucleotide polymorphisms	SNP
Sodium tris EDTA buffer	STE buffer
Statistical Package for the Social Sciences	SPSS
T central memory cells	T_{CM} cells
T cytotoxic cells	T_C cells
T effector memory cells	T_{EM}
T helper cells	T_H cells
T lymphocytes	T cells
TNF-α receptor type 2	TNFR2
Toll-like receptors	TLRs
Transforming growth factor beta	TGF-β
Transmembrane TNF	TmTNF
Tris Acetate EDTA buffer	TAE buffer
Tumour necrosis factor alpha	TNF-α
Veterinary Laboratories Agency	VLA
Workshop cluster molecule	WC molecule

Chapter 1

Introduction

Introduction

Mycobacterium bovis and bovine tuberculosis

Mycobacterium bovis (*M. bovis*) was first described as the causative agent of bovine tuberculosis (bTB) in 1896 by the American bacteriologist Theobald Smith (Sakula, 1982). Predominantly a pathogen of animals and in particular cattle (Francis, 1947 and 1958), *M. bovis* has the ability to cross the species barrier from animal to human.

In 1934, the first government applied statistical survey was performed to quantify the spread of bTB within Britain (Reynolds 2006). This concluded that approximately 40% of cattle within each individual dairy herd were infected with bTB and an estimated 0.5% of these animals were releasing tubercle bacilli within their milk (DEFRA 2005a). *M. bovis* infection was held accountable for over 2,500 human deaths and more than 50,000 new cases of human TB each year (DEFRA 2005a).

Systematic testing, compulsory slaughter of infected animals and the restricted movement of potentially infected herds resulted in the dramatic reduction of British bTB cases, from 40% in 1934 to 0.41% in 1996 (Krebs *et al*, 1997). Similar control programs applied across the world also led to complete eradication of bTB from Australia (Radunz, 2006), Canada and some American states (Essey and Koller, 1994). However the last twenty years have seen a dramatic resurgence in British bTB levels (Jalava *et al* 2007), with a reported annual increase of approximately 18% (Reynolds 2006). BTB has had extensive economical and welfare consequences, as it dramatically reduces farm productivity, impedes export to the EU and results in the premature death of animals. In 2006/2007, bTB cost the British tax payer an average of £79.8 million of which £24.5 million was paid to farmers as compensation for the slaughter of infected cattle and £37.8 million towards cattle bTB testing (DEFRA, 2008). In response to the increase in bTB, research into developing an effective bovine vaccination and more sensitive testing regimes are now regaining their significance as both veterinary and economical priorities.

Mycobacterium complex

The *Mycobacterium* genus (belonging to the phylum Actinobacteria) currently consists of approximately 139 different species (including subspecies) of mycobacteria (Klenk, 2008,

Pitulle *et al*, 1992). The majority of these species are environmental saprophytes (able to absorb dead organic matter) and have been found to exist around the world in a variety of habitats including drinking water (McSwiggan and Collins, 1974, Goslee and Wolinsky, 1976) soil (Jones and Jenkins, 1965) and dust (Dawson, 1971). These non-tuberculous mycobacteria (NTM) have generally been considered harmless, although a large number have been known for their opportunistic pathogenic properties in humans (Grange, 1987), commonly producing *M. tuberculosis*-like pulmonary symptoms. The remainder of the *Mycobacterium* genus consists of the highly pathogenic species *M. leprae, M. lepraemurium, M. avium* subspecies *paratuberculosis* and the *Mycobacterium* complex

The *Mycobacterium* complex includes the major causative agents of TB in humans (*M. tuberculosis*, *M. africanum*, *M. canetti*), in animals (*M. bovis*) and in rodents (*M. microti*). Commonly known as tubercle bacilli, the evolutionary development of these five species has long been a topic of debate (Frothingham *et al*, 1994, Aranaz *et al*, 1999, van Embden *et al*, 2000, Huard *et al*, 2006). Using molecular techniques such as the polymerase chain reaction (PCR), genetic sequencing and restriction fragment length polymorphisms (RFLP), the species of the *Mycobacterium* complex have been found to possess highly conserved genetic sequences with approximately 99.9% similarity (Brosch *et al*, 2002). However, there are clear differences in the pathogenicity and structural properties of each species (Garnier *et al*, 2003). *M. bovis* is known to have an extremely wide host spectrum with the ability to produce disease within a variety of animal species as well as humans, whereas the other members of the complex appear to be more restricted in their host tropisms.

A major advancement in the area of genetic evolution was the complete mapping of the bacterial genome sequences for *M. tuberculosis* strain H37Rv (Cole *et al*, 1998) and *M. bovis* strain AF2122/97 (Garnier *et al*, 2003). It has been hypothesised that *M. bovis* evolved at a much later point than *M. tuberculosis*, from the same common ancestor (Brosch *et al*, 2002). The genomes of *M. africanum*, *M. canetti* and *M. microti* are also currently being sequenced (Wellcome Trust Sanger Institute) and the information gained will add much to our knowledge on the *Mycobacterium* complex.

Mycobacterium bovis phenotype

M. bovis is a rod shaped bacilli approximately 1-10 μm in length and 0.2-0.6 μm in width (Kaneda *et al*, 1988). The bacilli are microaerophilic, as they require oxygen at a preferentially

reduced level to grow and are unable to survive in oxygen-depleted environments (Wayne and Diaz, 1967). However, research has shown that both *M. tuberculosis* (Wayne and Sohaskey, 2001) and *M. smegmatis* (a fast growing NTM species closely related to the *Mycobacterium* complex, Dick *et al*, 1998) are able to survive within anaerobic environments that have been slowly depleted of oxygen, thus allowing the bacilli to adapt accordingly to anaerobiosis. This has also been described for the attenuated form *M. bovis* Bacillus Calmette-Guerin or BCG (Lim *et al*, 1999) and has been suggested as the means by which tubercle bacilli are able to persist within anaerobic phagocytic cells in a non-replicating state, followed by latent reactivation of the disease many years later (Wayne and Sohaskey, 2001).

The durability and pathogenesis of the tubercle bacilli is in part aided by its unique cell wall (Takayama *et al*, 2005). Approximately 60% of the cell wall is composed of wall-associated lipids and mycolic acids (long-chained, branched fatty acids) subsequently providing a strongly hydrophobic structure (Asselineau and Lederer, 1950, Minnikin and Goodfellow, 1980, Ducati *et al*, 2006). The mycolic acids are covalently bonded to arabinogalactan, a polysaccharide that is linked in turn to peptidoglycan to produce an immensely thick cross linked matrix (Petit *et al*, 1975). The mycobacterial cell wall consists of an unusually high number of cross-links (approximately 70-80% in *M. tuberculosis* compared to 20-30% in *E. coli*) providing immense mechanical support to the bacterial cell (Palomino *et al*, 2007). The presence of mycolic acids within the cell wall has also provided a means of identification for the mycobacterial species as they have the ability to retain arylmethane dyes (such as red carbol fuchsin) after decolourisation with acidic-alcohol solutions (Wade, 1952, Sakula, 1982). Acid fast staining of pathological specimens is now a universal diagnostic test for mycobacterial infection, although there are some reports on the failure of acid fast staining due to alterations in the bacterial cell wall (Palomino *et al*, 2007).

As mentioned previously, there is a 99.95% genetic homology between *M. tuberculosis* and *M. bovis*, despite their vast differences in host tropisms (Brosch *et al*, 2002). It has been reported that the majority of the 0.05% genetic variation between the two species is located within the genes encoding for secreted and cell wall proteins (Garnier *et al*, 2003). An example of differential protein expression between *M. bovis* and *M. tuberculosis* is the ESAT-6 family of secreted proteins (including culture filtrate proteins (CFP) 10 and 7). These proteins are known for their antigenic properties in stimulating the host immune response and have been used widely in experimental infection models (Meher *et al*, 2007, Maue *et al*, 2007, Meher *et al*, 2006). They are actively secreted by *M. tuberculosis* but studies on *M. bovis* have shown that six of these proteins are either missing or altered (Garnier *et al*, 2003). Little is known of the

consequences to *M. bovis* in losing these proteins. It has been suggested that certain genes may prove unfavourable in specific host-bacterial interactions and so are selectively deleted (Brosch *et al*, 2001). Interestingly, murine studies have shown *M. bovis* strains to have a considerably higher level of virulence as compared to *M. tuberculosis* strains (in relation to their ability to cause progressive pathology and premature mortality of the host, Dunn and North, 1995). This suggests that the specific deletion of the ΔRD4 region may have had extensive beneficial effects on the pathogenicity of *M. bovis*.

Immunology of bovine tuberculosis

M. bovis is believed to be spread predominantly between cattle via aerosols of bacterial cells exhaled by an infectious host (Palmer, 2002, Goodchild and Clifton-Hadley, 2001, Wells *et al*, 1948, Gannon *et al*, 2007); however transmission is possible via other means such as ingestion of milk during the nursing of calves. An infectious host releases airborne particles containing the bacilli (termed respiratory droplets) of various sizes upon coughing or sneezing (Louden and Roberts, 1968, Louden and Spohn, 1969). The smaller respiratory droplets or droplet nuclei (1-5 μm in diameter) evaporate immediately after exhalation and can be carried on normal air currents for long periods of time (Gannon *et al*, 2007). Droplet nuclei need only to contain a small number of bacilli (two or more cells) to initiate TB within a potential host (Schafer *et al*, 1999). This theory has been supported by recent experimental models of bovine infection, reporting that levels of pathological disease were indistinguishable between animals infected with 1 colony forming unit (cfu) and those infected with 1000 cfu (Dean *et al*, 2005). As previously mentioned, pro-longed periods within the vicinity of an infected host may also increase the probability of becoming infected due to the high numbers of bacilli exhaled into the surrounding environment (Goodchild and Clifton-Hadley, 2001).

Innate immune response to *M. bovis* infection

Upon inhalation of the bacterial cells, the innate immune response is the first line of defence against progressive disease (Metchnikoff, 1905). The innate immune response can be divided into four categories, anatomic, phagocytic, inflammatory and physiologic (Goldsby *et al*, 2003). The anatomic innate response includes the respiratory cilia that prevent bacteria from travelling down the trachea by using mucus to coat the bacilli and propel them away from the hosts' lungs (Ganz, 2002, Fleming, 1922, Metchnikoff, 1905). If bacilli are able to evade these

mechanisms they encounter firstly alveolar macrophages and dendritic cells within the bronchial airways and then neutrophils and monocytes, initiating the phagocytic innate immune response (Chan *et al*, 1994). Within the infiltrating phagocytic cells, neutrophils are the more abundant cell type (Cassidy, *et al*, 1998), ingesting bacterial cells quickly in response to the infection and surviving only a few hours. Monocytes are less abundant and upon ingesting the bacilli within the tissue can differentiate into either macrophages or dendritic cells which are able to survive for longer time periods (Goldsby *et al*, 2003). These phagocytic cells recognise pathogens via pathogen recognition receptors (PRRs) including Toll-like receptors (Medzhitov and Janeway, 2000), mannose receptors and complement receptors (Schlesinger *et al*, 1990). Mannose receptors complimentary to the terminal mannose residue on bacterial glycoproteins facilitate binding of the bacterial cell to the phagocytic cells (Schlesinger *et al*, 1994) subsequently aiding endocytosis of the invading bacilli. Toll-like receptors (TLRs) are transmembrane proteins on the surfaces of phagocytic cells that recognise conserved bacterial structures termed pathogen-associated molecular patterns (PAMPs) (Underhill and Ozinsky, 2002, Kopp and Medzhitov, 2003). The two major TLRs involved in mycobacterial infection are TLR2 and TLR4 (Means *et al*, 1999, Gilleron *et al*, 2006, Nicolle *et al*, 2004). Recognition of PAMPs by TLRs induces the phagocytic cell to produce specific cytokines, for example the *M. tuberculosis* 19-kD lipoprotein has been shown to induce monocyte-produced interleukin 12 (IL12) through recognition by TLR2 (Brightbill *et al*, 1999).

In response to bacterial cell endocytosis and TLR2 activation, macrophages release cytokines tumour necrosis factor alpha (TNF-α) and interleukin 1 (IL1) which act on the neighbouring endothelial cells to increase expression of adhesion molecules E (Sung *et al*, 1994) and P – selectin. Dendritic cells (DCs) circulating within the peripheral blood have been shown to bind to E and P- selectins via a glycosylated form of P-selectin glycoprotein ligand (PSGL) –1 expressed upon their cell surface (Robert *et al*, 1999). Activated macrophages and neighbouring endothelial cells simultaneously produce chemokines (chemoattractant cytokines) to stimulate an increase in the affinity of phagocyte integrins to the associated ligands upon the endothelium surface (Algood *et al*, 2003). The integrin-ligand interaction strengthens the bonds between the phagocytes and the endothelium surface and with associated re-arranging of the phagocyte cytoskeleton, allows the cells to spread out over the alveolar wall (Lasunskaia *et al*, 2006). The phagocytic cells are then able to move via chemotaxis along a concentration gradient supplied by the chemokines to the site of infection (Goldsby *et al*, 2003). This is termed inflammatory recruitment and directs the accumulation of phagocytes, lymphocytes and

effector cells to the site of inflammation by the recognition of various chemokine-specific receptors on the cell surface (Peters and Ernst, 2003). TNF-α has been shown to be essential within this process, as mice lacking TNF-α displayed significantly reduced chemokine expression and reduced T cell infiltration to the lungs (Roach *et al*, 2002).

The inflammatory part of the innate response involves accumulation of leukocytes to the infected area accompanied by vasodilation (an increase in blood vessel diameter producing tissue redness and high temperatures) and increased vascular permeability (producing tissue swelling or edema). Lastly, the physiologic innate response includes soluble and cell associated molecules such as lysozymes (capable of breaking down bacilli cell membranes) and the complement system. The complement system involves a large number of membrane-bound and freely circulating proteins which act as chemoattractants to leukocytes initiating localised inflammation. They also form polymeric proteins that disrupt the permeability of bacterial cell membranes leading to either osmotic lysis or apoptotic death and they are able to coat bacilli (termed opsinisation) to enhance phagocytosis (Goldsby *et al*, 2003).

Phagocytes, primarily macrophages and dendritic cells have the ability to internalise bacterial cells (phagocytosis) by extending pseudopods around the bacilli and containing them within a phagosome (Maxwell and Marcus, 1968). Proton ATP-ase pumps located along the membrane of the phagosome are activated following bacterial ingestion (Lukacs *et al*, 1990) and create an acidic environment of approximately pH 5.3-5.4 that is detrimental to the bacilli. The phagosome then fuses with lysosomes to form a phagolysosome inducing the release of proteolytic enzymes into the compartment to digest the bacterial cell (Armstrong and Hart, 1971). In addition to these mechanisms, a metabolic process known as the respiratory burst, involving the activation of oxidase embedded within the phagolysosome membrane catalyzes the reduction of oxygen into superoxide anions and creates an extremely toxic environment alongside hypochlorite and nitric oxide radicals (Goldsby *et al*, 2003). By effectively breaking down the bacterial cell wall, the phagocytic cell is able to process bacterial antigens and present them upon their cell surface to activate specific T lymphocyte cells for a cell mediated immune response.

Cytokines have been shown to be heavily involved within the development of the innate immune response. As previously mentioned, activation of TLR2 via the *M. tuberculosis* 19-kDa lipoprotein induces TNF-α and IL12 (Brightbill *et al*, 1999) expression within macrophages. TNF is initially produced as a transmembrane (26-kD TmTNF) precursor before it is cleaved by a membrane-bound metalloprotease-disintegrin termed the TNF-α-converting enzyme (Black *et*

al, 1997). This generates a soluble TNF molecule (17-kD sTNF). A study involving knockout mouse models expressing TmTNF in the absence of sTNF and lymphotoxin-α revealed a role for both TmTNF and sTNF in the control of mycobacterial growth (Olleros *et al*, 2005). TmTNF in particular is able to reduce the bacterial population by inducing apoptosis of *M. tuberculosis*-infected alveolar macrophages (Keane *et al*, 1997). However, virulent *M. tuberculosis* strain H37Rv has also shown the ability to block TNF-α-dependent macrophage apoptosis by producing soluble TNF-R2 (Balcewicz-Sablinska *et al*, 1998). This allows proliferation of the bacterial cells within macrophages and is favourable for progressive infection.

IL12 is a covalently linked heterodimer (Podlaski *et al*, 1992) consisting of a 35 kDa light chain (p35 or IL12α) and a 40 kDa heavy chain (p40 or IL12β). Activation of the TLRs of phagocytic cells induces very low concentrations of IL12 p40 (monomer or homodimer) and TNF-α has been shown to be essential in up-regulating IL12 p40 expression within *M. tuberculosis* infected guinea pig macrophages (Cho *et al*, 2005).

The receptor for IL12 consists of two chains, IL-12Rβ1 and IL-12Rβ2 which are expressed predominantly by natural killer (NK) lymphocytes and activated T lymphocyte cells, although they have also been found on dendritic cells (Grohmann *et al*, 1998). The constitutive expression of low levels of the IL12 receptor on NK cells (unlike resting T cells where it is undetectable), enables them to respond quickly to activation by IL12 secreted from phagocytic cells (Trinchieri 2003). NK cells are extremely important constituents of the innate immune response (Denis *et al*, 2007) as they are able to recognise infected host cells independent of direct antigenic stimulation and destroy them to suppress bacterial spread (Hamerman *et al*, 2005). IL12 induces NK cells to secrete IFN-γ in the presence of low levels of TNF and IL1 (Gazzinelli *et al*, 1994), producing a positive feedback effect on the macrophage by increasing phagocytosis efficiency. Un-stimulated bovine NK cells have also been reported to reduce *M. bovis* growth within macrophages even in the absence of IFN-γ, suggesting that IFN-γ may act as a contributing mediator but is not solely responsible for macrophage activation (Denis *et al*, 2007). IL12 is potent in inducing IFN-γ expression within T lymphocytes (this will be discussed later in this chapter) and in turn, IFN-γ acts synergistically with TNF-α to produce reactive nitrogen intermediates during phagocytosis (Chan *et al*, 1992b). The ability to control *M. tuberculosis* infection in mice has been shown to positively correlate with the ability of the mouse to produce the nitrogen intermediate inducible nitric oxide (iNOS, Olleros *et al*, 2005) due to its importance in the phagocytic pathway.

In addition to phagocytic cells, γ/δ T cells accumulate early within the site of infection (Cassidy *et al*, 2001). Bovine γ/δ T cells are characterised based on the presence of the workshop cluster 1 (WC1) molecule (Clevers *et al*, 1990). Both $WC1^+$ and $WC1^-$ γ/δ T cells are differentially distributed throughout bovine tissues, however $WC1^+$ are found mainly within the peripheral blood and skin (MacHugh *et al*, 1997) allowing a faster response to bacterial infection (Hein and Mackay, 1991). $WC1^+$ γ/δ T cells play a supportive role in the delayed-type hypersensitivity (DTH) reaction which is characteristically produced by the detection of tuberculosis infection via the intradermal skin test (Doherty *et al*, 1996). An injection with purified protein derivative (PPD) is typically followed 6-24 hours later by a perivascular aggregation of $WC1^+$ γ/δ T cells and neutrophils. By 72 hours post injection, $WC1^+$ cells play only a minor role in the reaction (Doherty *et al*, 1996) and so it is believed that the kinetics of $WC1^+$ cells are associated primarily with the earlier stages of *M. bovis* infection (Pollock *et al*, 1996). As the γ/δ T cells are not major histocompatibility complex (MHC) molecule restricted and rarely express CD4 or CD8 membrane proteins, they are able to have a broader range of action. They also produce IFN-γ to activate macrophages and lyse infected phagocytic cells (Rhodes *et al*, 2001).

The innate immune response is extremely effective in removing the disease threat and is essential in the development of an effective adaptive immune response which dictates subsequent progression of the disease (Pollock and Neill, 2002). It has been speculated that bacterial transmission within whole cattle herds may only produce disease within one or two cattle, while the other cattle appear to have successfully dealt with the infection at the innate immune stage (Morrison *et al*, 2000). There have been a number of suggestions as to the reasons behind increased cattle susceptibility to *M. bovis* infection, including nutrition deficiencies (Doherty *et al*, 1995) and concurrent infections of immunosuppressive viruses (such as bovine viral diarrhoea virus or BVD) (Menzies and Neill, 2000). However, bacterial cells have also developed a number of mechanisms to evade the innate immune response. Virulent mycobacteria species have the ability to reside within the hosts phagocytes and produce persistent infection, essentially hidden from the hosts' immune response. Early studies showed that *M. tuberculosis* infected macrophage vacuoles did not fuse with the lysosomal compartment (Armstrong and Hart, 1971 and 1975) and therefore led to the arrestment of phagosomal maturation. Modern molecular studies have added to this hypothesis by illustrating that different cell markers are expressed upon the phagosomal membrane surface specific to early and late stages of phagosomal maturation (Hestvik *et al*,

2005). Typically, the phagosomes of cells infected with virulent, live mycobacteria bacilli express cell markers associated with early phagosomal development. The proton ATP-ase pump proteins are a feature of late phagosomal development and appear to be absent form bacilli infected cells (Sturgill-Koszycki *et al*, 1994). This may explain why mycobacterial infected phagosomes generally display a pH of around 6.2-6.3, less acidic than during the normal phagocytic process (Sturgill-Koszycki *et al*, 1994). This therefore suggests that the bacteria are able to arrest phagosomal maturation and survive within immature phagosomes which contain a less harmful environment (Flynn and Chan, 2005).

Adaptive immune response to *M. bovis* infection

Macrophages and dendritic cells are termed antigen presenting cells (APCs) as they both have the ability to process bacterial antigens during the phagocytic process and display these to the naïve T lymphocytes (Bodnar *et al*, 2001, Gonzalez-Juarrero and Orme, 2001, Hickman *et al*, 2002). The presence of the metabolically active bacterial cell within the phagosome allows direct access of mycobacterial antigens to the major histocompatibility complex (MHC) class II molecules (Barnes *et al,* 1994), to which they bind and are transported to the cell surface. MHC class II molecules displaying antigen are specific to activating T lymphocytes expressing the membrane glycoprotein CD4 (Orme *et al*, 1993). Mycobacterial cells that are effectively destroyed within the phagocytic cell give rise to somatic proteins which are broken down into peptide fragments within the cytoplasm. These antigens are displayed via MHC class I molecules and are specific to activating T lymphocytes expressing the dimeric membrane glycoprotein CD8 (Barnes *et al*, 1994).

There is ample evidence to suggest that the priming of naïve T lymphocytes occurs primarily within the lung draining lymph nodes (Flynn and Chan, 2001, Bhatt *et al*, 2004, Thacker *et al*, 2007, Widdison *et al*, 2006). The lymph nodes are bean-like structures located at the junctions of the lymphatic system and can be separated into the cortex, paracortex and medulla regions containing α/β lymphocytes (B and T cells) integrated with large numbers of dendritic cells (Steinman *et al*, 1997). It is believed that the infected phagocytic cells move within the lymphatic fluid to the local lymph nodes via the lymphatic system (Fu *et al*, 1999). They are then able to filter through the lymph nodes thus giving a high level of contact with the T lymphocytes and increasing the chance of activating the specific adaptive immune response. Within the lungs of *M. tuberculosis* infected mice, macrophages have been shown to be the main population of cells containing the invading bacteria (Humphreys *et al*, 2006). However, the same study using Green Fluorescent Protein (GFP)-labelled *M. tuberculosis* to track the

movement of infection from the lungs to the mediastinal lymph nodes of murine models implicated dendritic cells as the main cell type responsible for mycobacterial dissemination (Humphreys *et al*, 2006).

Pre-infection, immature dendritic cells display the ability for efficient phagocytosis (Romani *et al*, 1989) and respond particularly to chemokines MIP-3α, RANTES and MIP-1α (Sozzani *et al*, 1995, Xu *et al*, 1996). Following mycobacterial infection and TLR activation, dendritic cells undergo a maturation process characterised by up-regulation of co-stimulatory molecules CD40 (Rescigno, 2002), B7.1 and B7.2 (Larsen *et al*, 1994), increased expression of adhesion molecules and up-regulation of chemokine receptor CCR7 (Dieu *et al*, 1998). Chemokines are believed to aid in the migration of the dendritic cells to the lymph nodes along a concentration gradient (Bhatt *et al*, 2004). Macrophages however do not express CCR7 before infection and express only minimal levels post infection, thus reducing their ability to detect chemokines and severely hampering their ability to migrate to the draining lymph nodes (Bhatt *et al*, 2004). The immature dendritic cells express low levels of MHC class II and I molecules and therefore are unable to act as antigen presenting cells until after maturation, during which the MHC molecules are significantly up-regulated (Cella *et al*, 1997, Mellman and Steinman, 2001). Conversely, the cells ability to capture and process bacterial antigens is reduced post maturation (Romani *et al*, 1989, Streilein *et al*, 1989, Larsen *et al*, 1992).

Following CD4+ T cell (also known as T helper (T_H) cells) activation via the MHC class II-antigen complex, the cells divide to produce effector cell clones specific also for the same antigen-MHC class II complex. There are two main types of T_H class response, T_H1 which is predominately pro inflammatory and cell mediated and T_H2 which is associated with B cells and the humoral immune response (Mosmann *et al*, 1986). The type of response that is activated is based primarily on the associated cytokine environment that the naïve T_H cells experience early on in the infection (Trinchieri 2003). *M. tuberculosis* infection of bone marrow-derived murine macrophages and dendritic cells illustrate the different abilities of the two cells to induce naïve T cell development towards a T_H1 phenotype (Hickman *et al*, 2002). Upon infection, dendritic cells have been shown to secrete both IL12 and IL10 (Hickman *et al*, 2002). IL-12 is a potent T_H1 type inducer and previous reports of IL10 suggest the ability to suppress cell mediated immunity (Akbari *et al*, 2001). Despite this, the dendritic cells still displayed the ability to induce naïve T cell differentiation into T_H1 effector cells (Hickman *et al*, 2002). The authors suggested that the rapid production of IL12 meant that the later presence of IL10 did not effect the polarisation of the T cells. In contrast, macrophages have been shown to secrete IL10 but

be unable to produce IL12 following infection unless co-stimulated by IFN-γ (the primary macrophage-activating factor, MAF) first (Schultz *et al*, 1983). This is believed to be due to the role of IL10 in inhibiting IL12 expression, supported by the ability of macrophages to secrete IL12 in IL10 knock-out mouse models (Hickman *et al*, 2002). The dendritic cells are therefore extremely important in priming the initial differentiation of the T cells to a T_H1 cell mediated immune response and mark the progression from innate to adaptive immunity.

Upon antigenic stimulation, it has been shown that activated human and murine T lymphocytes experience an up-regulation in the transcription and expression of the receptor for IL12. The increased expression of the IL12 receptor and in particular the IL12 Rβ2 chain is enhanced by IL12, IFN-γ and TNF, thus expression of the IL12 Rβ2 chain is limited to the T_H1 cell profile (Szabo *et al*, 1997). IL12 is then able to bind to its associated receptor and irreversibly activate NK cells and T cells to produce IFN-γ (a T_H1 type associated cytokine) by targeting both transcriptional (Chan *et al*, 1992a) and post transcriptional control mechanisms (Hodge *et al*, 2002).

Activation of the CD8+ T cells (also known as T cytotoxic (T_C) cells) via the MHC class I-antigen complex leads to subsequent cell differentiation into cytotoxic T lymphocytes (CTLs). CTLs have been shown to have the capacity to specifically lyse *M. bovis* infected macrophages *in vivo* (Skinner *et al*, 2003b) and to destroy mycobacteria directly *in vitro* (Stenger *et al*, 1997). Destruction of infected macrophages may occur by two methods. It has been theorised that the CTLs use extracellular ATP to induce apoptosis of infected macrophages and destroy the bacterial cell (Stober *et al*, 2001). Secondly, CTLs are able to release granulysin into the infected phagocyte to destroy both the host and bacterial cell (Stenger *et al*, 1997).

IL12 has a positive effect on the generation of CTLs and their cytotoxic functions by up-regulating the transcription of genes encoding for cytotoxic granule-associated and adhesion molecules (Trinchieri 1998). Apart from their main function of recognising and destroying infected host cells, CTLs are also able to secrete a limited range of cytokines, including IFN-γ (Schluger *et al*, 1998). It is believed that CTLs may play a part in increasing the efficiency of antigen presentation by lysing infected hosts cells and allowing more proficient APCs to ingest the released bacterial cells (Skinner *et al*, 2003b).

Granuloma formation

In addition to attacking the infection in the lymph nodes, activated CD4+ and CD8+ T lymphocytes and macrophages also migrate to the sites of initial infection (generally the lungs) through the vascular system (Flynn *et al*, 2005) via a concentration gradient supplied by

chemokines (as in innate immune response inflammatory recruitment). TNF-α and lymphotoxin-α secreted by macrophages has a controlling effect on the level of cellular influx by inducing chemokine secretion and enhancing expression of cell surface adhesion molecules (Munro *et al*, 1989). This in turn has a major effect on the size of developing granuloma (Scott Algood *et al*, 2003). Granulomas are characteristic of the cell mediated response and are formed by the influx of monocytes, CD4+ T cells, CD8+ T cells and macrophages around the infected phagocytic cell both in the lymph nodes and the lungs (Saunders and Cooper, 2000, Figure 1).

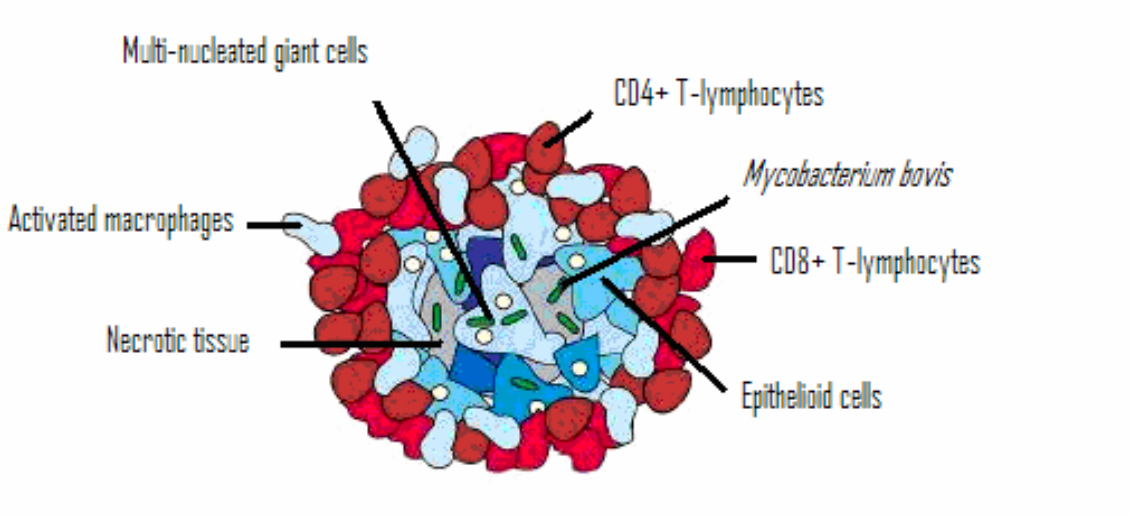

Figure 1: The structure of a mature granuloma, consisting of centralised *M. bovis* infected macrophages that have fused together to form either multi-nucleated giant cells or large epithelioid cells. The periphery of the granuloma consists of activated lymphocytes and macrophages (modification of Zahrt, 2003).

The development of granuloma have been characterised into four stages (Wangoo *et al*, 2005).

- Stage I: Un-encapsulated clusters of epithelioid macrophages with interspersed lymphocytes and a few neutrophils. Small numbers of multi-nucleated giant cells may also be present.
- Stage II: Majority of the cell types are epithelioid macrophages, with many distributed lymphocytes, neutrophils and multi-nucleated giant cells. The granuloma starts to take shape with partial or complete coverage within a thin capsule.
- Stage III: The centre of the granuloma contains necrotic areas which are caseous and mineralised, interspersed with epithelioid cells and giant cells. The periphery of the

granuloma is composed of macrophages with clusters of lymphocytes and scattered neutrophils, completely encapsulated.

- Stage IV: The granulomas are thickly encapsulated with multiple centres displaying advanced caseous necrosis and vast islands of mineralization. Epithelioid macrophages and giant cells surround the necrotic areas and lymphocytes are densely clustered around the periphery.

Essentially the granuloma is beneficial in providing an enclosed environment in which T cells and phagocytic cells can concentrate their bactericidal efforts and enhance cell to cell communication to remove the bacilli (Widdison *et al*, 2008). It also provides a mechanism of containing the bacteria locally and reducing the chances of disseminated infection. However, as the granuloma develops it inevitably becomes the pathognomic lesion characteristic of tuberculosis infection due primarily to host and bacterial cell interactions (Mustafa *et al*, 2008).
Prior to granuloma formation, *M. bovis* infected macrophages are differentiated into epithelioid cells and/or fuse together to form multi-nucleated giant cells (also known as Langhans giant cells, Wangoo *et al*, 2005, Figure 2). Little is known on this phenomenon in bovine cells; however, a human *in vitro* model of macrophage differentiation has shown this process to occur in response to endocytosis of virulent tubercle bacilli (Lay *et al*, 2007).

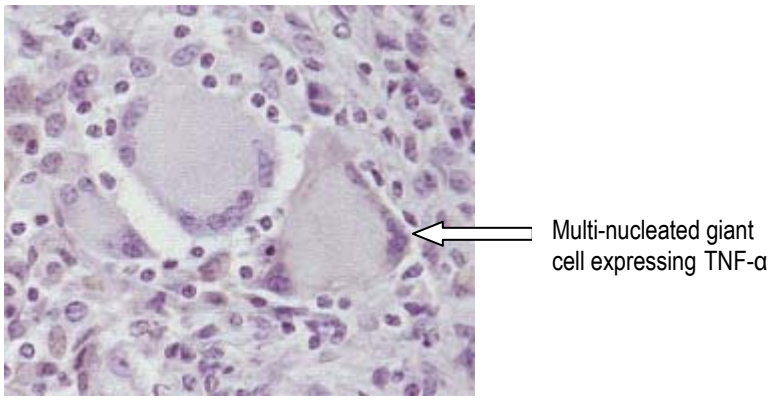

Figure 2: Immunohistochemical staining of an *M. bovis* infected bovine lymph node section. The brown stain is specific to immune cells expressing TNF-α and the blue staining (Mayers haematoxylin) allows visualisation of all cells. The section shows two large multi-nucleated giant cells, one of which is positive for TNF-α expression (photograph taken from sections used within the BCG vaccination study for this thesis).

M. tuberculosis infected human epithelioid cells express higher levels of TNF-α as compared to IFN-γ, IL10 and Transforming Growth Factor (TGF)-β and are believed to possess strong

bactericidal properties (Mustafa *et al*, 2008). These cells therefore have a small antigenic load and may act as weak APCs to T lymphocytes (Lay *et al*, 2007). In comparison, multi-nucleated giant cells (Figure 2) express increased levels of TGF-β, a strong anti-inflammatory cytokine associated with the T_H2 lymphocyte response that down-regulates expression of IFN-γ, TNF-α and IL12 (Barnes *et al*, 1994). As a consequence, the giant cells possess a much lower bactericidal ability and a larger antigenic load as compared to the epithelioid cells, therefore acting as stronger APCs (Mustafa *et al*, 2008).

Interestingly, studies on the effect of *M. tuberculosis* infection in human differentiated macrophages has shown a selective ability of infected epithelioid cells to evade apoptosis allowing subsequent fusion into giant cells (Mustafa *et al*, 2008). Mycobacteria are known to be able to inhibit apoptosis of host cells to ensure their own survival and growth within phagocytic cells (Keane *et al*, 2000). By inhibiting apoptosis of infected epithelioid cells, the bacteria ensure epithelioid differentiation into giant cells which have a much stronger APC role (Mustafa *et al*, 2008). This therefore maintains cellular recruitment and proliferation and allows the granuloma to grow substantially in size (Wangoo *et al*, 2005).

The size of the granuloma has been positively related to its' advancement through the four stages of development, as granulomas can approximately double in size between each stage (Wangoo *et al*, 2005). As the granuloma enlarges, the centre inevitably becomes necrotic due to un-infected cell apoptosis (as seen in stage III) causing subsequent loss of cell to cell interaction. Smaller granulomas are less likely to become necrotic and this could be due to cytokines such as IFN-γ, IL12 and TNF-α being able to reach the inner macrophages and maintain their activity (Orme *et al*, 1998). In response to giant cell antigen presentation and cellular recruitment, high levels of advancing cytolytic T cells may lead to uncontrolled cell destruction and granuloma liquefaction (Pratt *et al*, 2005). Protein digesting enzymes secreted by activated macrophages can weaken the granuloma wall and liquefy the necrotic tissue to produce eroding of the bronchi and extreme tissue damage. This process can expose any viable, persister bacteria to the lungs and lead to a highly infectious host (Pratt *et al*, 2005).

T lymphocyte profiles

A cell mediated response is characteristic of early tuberculosis infection. However, it has been reported that there is a shift of the immune response from a primarily T_H1 pro-inflammatory type to an anti-inflammatory, T_H2 type humoral response (Welsh *et al*, 2005) in advanced disease states. It is now understood that there is a degree of cross-regulation between cell mediated and humoral immune responses, when one is high the other is generally low. A reason for this

is the inhibitory effects of the cytokines. Interleukin 4 (IL4) is a major cytokine in the anti-inflammatory response that is essential in T_H2 type development (Seder *et al*, 1994, Abbas *et al*, 1996). It induces production of IgE antibodies, decreases expression of toll like receptors (particularly TLR2), suppresses nitric oxide synthase (Rook *et al*, 2004) and induces the generation of regulatory T cells (Pace *et al*, 2005). IL4 has also been found to exist in two splice variant forms (Waldvogel *et al*, 2004). IL4δ2 (deletion of exon 2) is able to bind to IL4 receptors and is therefore a natural antagonist of IL4 activity by inhibiting IL4 mediated T cell proliferation (Atamas *et al*, 1996). However, it also has a positive effect on collagen synthesis by fibroblasts (Atamas *et al*, 1999). In human TB studies, an increase in IL4δ2 has been described in latent infection states (Demissie *et al*, 2004) however its significance in cattle immune responses is still under debate (Widdison *et al*, 2006).

More recently the splice variant IL4δ3 (deletion of exon 3) was reported in cattle infected with *Fasciola hepatica* parasite (Waldvogel *et al*, 2004). In bTB studies, IL4δ3 appears to be expressed dominantly over IL4δ2 (Rhodes *et al*, 2007) and levels were found to increase upon both BCG vaccination and *M. bovis* challenge but were virtually non-detectable in the non-infected controls (Rhodes *et al*, 2007).

IFN-γ (T_H1) and IL4 (T_H2) are able to render T_H cells less susceptible to cytokines of the opposite T_H type (Goldsby *et al*, 2003). This is done by either down regulating or up-regulating two transcriptional factors within the T_H cells, T-Bet (required for T_H1 associated cytokine receptors) and GATA-3 (required for T_H2 associated cytokine receptors).

IL10 has been shown to be secreted by a number of cells including various T cell subsets, CD4+, CD8+ (Bendelac *et al*, 1991), T_H2 (Del Prete *et al*, 1993), T_H0 (Katsikis *et al*, 1995), CD4+ regulatory T cells type one (Tr1, Cools *et al*, 2007) and specifically for human IL10, in T_H1 (Del Prete *et al*, 1993, Rutz *et al*, 2007) as well as B lymphocytes and macrophages. It has the ability to control the expression of various cytokines, chemokines and cell surface molecules of monocytes, macrophages, dendritic and T lymphocyte cells (Moore *et al*, 2001).

As a 'suppressor' cytokine, IL10 is able to dampen the T_H1 response (Welsh *et al*, 2005) by targeting phagocytic cells. This is believed to occur via competitive IL10- and IFN-γ-induced intracellular mechanisms of the stat1 activation pathways (Ito *et al*, 1999). As the concentration of IL10 increases relative to IFN-γ, inhibition of IFN-γ induced gene expression is enhanced. IFN-γ acts to up-regulate expression of MHC class II molecules thereby increasing CD4+ T_H cell activation (Goldsby *et al*, 2003), In contrast, IL10 is able to down-regulate MHC class II molecule expression via posttranscriptional inhibition of their transport to the plasma membrane (Koppelman *et al*, 1997) subsequently reducing CD4+ T_H cell activation. IL10 is also able to

suppress the formation of nitric oxide during phagocytosis resulting in reduced expression levels of inflammatory cytokines IL1 and TNF-α as well as blocking transcription of both the p40 and p38 encoding genes of IL12.

Although IL10 may have extensive suppressor functions it has also been shown to enhance survival of human B cells by increasing expression of the anti-apoptotic protein bcl-2 (Levy and Brouet, 1994). Proliferation of B cells is also enhanced by IL10, IL2 and IL4 activity (Rousset *et al*, 1992).

Overall this has the effect of reducing the cell mediated response and increasing the antibody response (Pollock and Neill, 2002). It is not fully understood why this shift in the immune response occurs however it could be a mechanism of the host to reduce the harmful effects of the pro-inflammatory effect.

In recent years, it has been recognised that a third subset of T_H associated cells exists, termed the T_H0 type immune response (Widdison *et al*, 2006). This is characterised by the presence of both T_H1 (IFN-γ) and T_H2 (IL4 and IL5) cell types together. This type of response may be an intermediate between the pro-inflammatory and anti-inflammatory immune responses. The T_H0 type response has been reported to correlate with an increase in pathogenesis of the disease (Welsh *et al*, 2005). This could be due to the combined T_H1/T_H2 cytokine profile. TNF-α is essential for bacilli containment however in high concentrations or when the surrounding cytokines represent a T_H2 type response, typically IL4 (Rook *et al*, 2004), TNF-α can lead to extensive levels of necrosis. It therefore becomes apparent that the host immune response to *M. bovis* infection is a highly dynamic process and that there is an extremely intimate relationship between protecting the host and causing pathological tissue damage.

Epidemiology of bovine tuberculosis within Great Britain

Across Great Britain, the distributions of TB incidents within cattle herds show areas of strong clustering. These areas are located particularly to the south west and west midlands of England and to the southern and western regions of Wales (Figure 3, Reynolds, 2006). A possible reason for the concentration of bTB herd breakdowns in the south west of the country is due to its geographical location (White and Benhin, 2004). The topography and climate of the south west of England and Wales has had a substantial impact on its commercial use in agriculture and animal farming (White and Benhin, 2004). Approximately three quarters of the southwest region is utilised in farming, supporting over half a million dairy cows and 174,000 beef cows, accounting for almost a third of the country's current total cattle population (statistics from the National Farmers Union). Although the number of individual cattle herds in Great Britain have decreased since 1975 (VetNet, unpublished), there has been an increase in the average number of cattle within each herd (Goodchild and Clifton-Hadley, 2001).

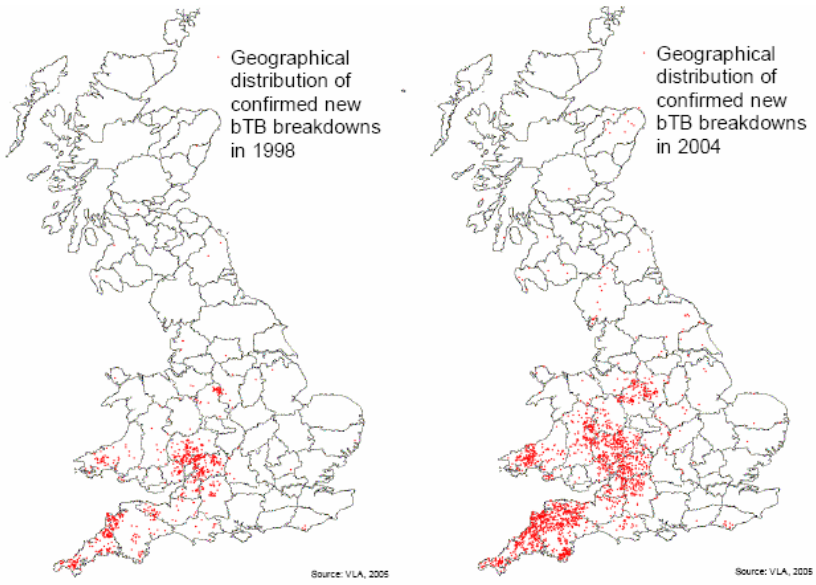

Figure 3: The geographical distribution of confirmed bTB herd breakdowns within Great Britain in 1998 and 2004. There has been a definite increase in bTB breakdowns, particularly to the west and south west of the country and the occurrence of breakdowns within previously non-infected areas (1998) such as the midlands and north east of Scotland (Veterinary Laboratory Agency, 2006).

The high density cattle farming performed within the southwest of England may therefore have an impact on the probability of cattle to cattle transmission of *M. bovis* infection (Shirima *et al*, 2003, Goodchild and Clifton-Hadley, 2001). In addition, *M. bovis* from environmental sources may contribute to bTB in cattle herds as mycobacterium bacilli have been reported to be able to survive for long periods of time within damp and warm (approximately 37^{o}C) soils (Young *et al* 2005). However, since 1993 bTB has spread into areas across the United Kingdom that previously had not shown herd incidences for many years beforehand (Figure 3). This spread in bTB has occurred in a northwardly direction from the southwest and has increased significantly in frequency since 1997 (Green and Cornell, 2005, VLA, 2006, Figure 3).

Bovine tuberculosis control within Great Britain

In response to the increasing number of bTB cases, the government developed a programme aimed at regular testing of infected animals, slaughter of those tested positive and restricted cattle movements (Reynolds 2006). This programme became compulsory in 1950 and by the mid-1960s bTB was limited to only a few isolated cases in the southwest of England. Pasteurisation of milk is now a common procedure (although it is not compulsory in the UK, Howie, 1985) and meat is regularly checked for disease at the slaughterhouses to protect against animal to human transmission (Edwards *et al*, 1997). Regardless of these beneficial control programmes, bTB cases have been increasing significantly over the last twenty years (Delahay *et al*, 2002) and the reasons behind this increase remain largely elusive. In 1997 an independent scientific review (ISR) group chaired by Professor Sir John Krebs was formed to provide a strategy for investigating the main concerns of bTB infection (Krebs *et al*, 1997). Based on the prioritised recommendations of the Krebs report, the government initiated the bTB 'Five Point Plan' aimed at:

- Protection of public health

Currently, *M. bovis* infection in humans occurs at a much lower incidence as compared to that seen at the start of the twentieth century, with approximately less than 1% of microbiologically confirmed human TB cases within the UK caused by *M. bovis* (Evans *et al*, 2007). There has, however, been some recent evidence of person to person transmission between young individuals through social contact at a local bar (Evans *et al*, 2007). This has strong implications on the control of *Mycobacterium bovis* infection in humans.

- Research into the spread of TB

Studies into the dynamics of bovine nasal shedding have revealed a dose response pattern associated with the concentration of the initial *M. bovis* inoculum. More importantly, it was found that skin test negative animals displaying no visible lesions still had the potential to secrete *M. bovis* (VLA, IAH and QUB, 2005). This highlights the value of the diagnostic test in detecting *M. bovis* during the earlier stages of infection before transmission is possible. However it also confirms the inadequacy of the current skin test method.

-Testing and control

The current bTB test is based on the intradermal injection of a purified protein derivative (PPD) produced from heat-treated *M. bovis* (termed tuberculin or PPD-B, Dickson, 1965, Lesslie *et al*, 1976). A positive response to the test is portrayed by a characteristic swelling under the skin around the injection site due to the accumulation of *M. bovis* sensitised T cells and phagocytes, termed the cell mediated delayed-type hypersensitivity (DTH) reaction (Dannenberg, 1991, Ng *et al*, 1995, Doherty *et al*, 1996). Within Britain and Europe, the test has been evolved to account for environmental infection by *Mycobacterium avium* (*M. avium*) and involves injection of both bovine and avian tuberculin (PPD-B and PPD-A), termed the single intradermal comparative tuberculin test (SICTT, Lesslie and Herbert, 1975). However, a problem associated with the skin test is its low level of sensitivity resulting in a number of infected animals being falsely labelled as negative (Monaghan *et al*, 1994). To increase sensitivity of bTB testing, an enzyme-linked immunosorbent assay (ELISA) has been developed to measure the level of IFN-γ produced in response to tuberculin stimulation of isolated bovine peripheral blood mononuclear cells (PBMCs, Rothel *et al*, 1990, Wood *et al*, 1991).

However, the use of tuberculin within the assay has limited its flexibility as a diagnostic tool, as it is unable to distinguish between cattle that have become infected and those that have been vaccinated with BCG (Doherty *et al*, 1996, Buddle *et al*, 1999, Vordermeier *et al*, 1999). This has meant that worldwide, countries including the United Kingdom are not implementing cattle BCG vaccination as part of their control policy. It is therefore an important consideration that a newly developed vaccine does not interfere with the intradermal skin test or that, alongside the new vaccine, a new diagnostic test for cattle is adopted. Studies investigating the specificity and sensitivity of antigens present within *M. bovis* but deleted from the BCG bacilli have highlighted two potential targets for developing a new bTB test. The early secretory antigenic target (ESAT)-6 kDa protein and culture filtrate protein (CFP)-10 (Van Pinxteren *et al*, 2000) are both encoded for within the RD1 region of *M. bovis* and have shown immunological activity

(Vordermeier *et al*, 2001). In addition to these, comparative genomics focused on the three genomic regions RD1, 2 and 14 (present in *M. bovis* but absent from BCG Pasteur) uncovered twenty-eight antigens that potentially could distinguish BCG vaccinated cattle from infected cattle (Cockle *et al*, 2002). Further analysis revealed three of the twenty-eight antigens (orthologues of the *M. tuberculosis* genes Rv1986, Rv3872 and Rv3878) induced immune responses within infected but not vaccinated non-infected cattle, thus may be important for future bTB detection assays (Cockle *et al*, 2006).

- Badger control

Since the mid 1970s, the Eurasian badger (*Meles meles*) has been recognised as the true maintenance host and principle reservoir of *M. bovis* infection (Muirhead *et al*, 1974). *M. bovis* can be transmitted between the two animal species via indirect aerosol inhalation from animal faeces and ingestion of grassland that had become contaminated by faeces and urine (Sweeney *et al*, 2007, Scantlebury *et al*, 2004). The Randomised Badger Culling Trial was designed to determine the effects of badger culling on the level of bTB across designated cattle herds within Britain (McDonald *et al*, 2008, Reynolds 2006). Over 10 years, three culling treatment regimes including proactive, reactive and a control (no culling) were applied within designated areas across the west and south west of England (Reynolds, 2006). The reactive regime was suspended after 5 years due to a 20% increase in bTB cases (Le Fevre *et al*, 2005). However the proactive culling produced conflicting results, as bTB cases were reported to decrease by 23% within the designated areas but increase by 24.5% in the farmlands adjacent to the trial zones (Donnelly *et al*, 2006). It has been suggested that the detrimental effect of badger culling observed in both the proactive and reactive test sites could be attributed to the social organisation of the badger population (Pope *et al*, 2007). The trial resulted in disruption of the delicate badger community by reducing the population density and removing the social limitations observed in undisturbed populations (McDonald *et al*, 2008). This allowed individual social groups to increase their movements outside of the trial areas therefore increasing the probability of *M. bovis* transmission (Pope *et al*, 2007) and placing doubt on the efficacy of wide-scale badger culling as a disease control method.

- Development of an effective cattle vaccine

The current human TB vaccine Bacillus Calmette- Guérin (BCG) was attenuated from a strain of *M. bovis* between 1908 and 1921 within the Pasteur Institute (King *et al*, 1929). Primary studies in experimental vaccination of animals reported the beneficial inhibition of the tubercle

bacilli post BCG vaccination (Smith *et al*, 1966). However, it became apparent that the use of BCG vaccination interfered with the intradermal tuberculin skin test (Hart *et al*, 1967) and was therefore abandoned for animals in favour of the diagnostic test. The vaccine has, however, been distributed worldwide to humans, traditionally via oral administration and then intradermally to over three billion people (Gagliardi *et al*, 2004). Its advantages include its safe use for children and its relatively cheap production, however an increasing number of trials over the last 70 years have shown variable results on its efficacy against TB, in particular adult pulmonary TB (Orme *et al*, 2001). Due to the extensive similarities between human and cattle TB, developmental work on TB vaccines for bovine infection has followed closely behind on an almost identical path to that of human studies (Hewinson *et al*, 2003). BCG vaccination studies in cattle have shown potential in reducing TB severity and pathological damage (Buddle *et al*, 1995, Skinner *et al*, 2003a, Wedlock *et al*, 2000, Widdison *et al*, 2006). However, the degree of protection is extremely variable and full protection was rarely seen (Francis 1947, Francis 1958, Widdison *et al*, 2006). In response to these studies, extensive research has been centred on the development of an improved TB vaccine that could be applied cattle.

Bovine tuberculosis control worldwide

M. bovis infection of cattle is a worldwide veterinary problem and is of particular importance in developing countries where *M. bovis* still remains a significant cause of human TB. The control of bTB infection in developing countries faces an extensive list of problems including the costs associated with sustainable 'test and slaughter' programs, the continuous displacement of huge numbers of humans and their animals due to wars and political instabilities as well as the lack of a suitable veterinary infrastructure (Ayele *et al*, 2004).

The main method of controlling disease spread in most developed countries such as America (Olmstead and Rhode, 2004), Australia (Radunz, 2006) and those under the European Union (Caffrey, 1994) has included a procedure of rigorous testing and subsequent slaughter of infected animals. In some cases this has been extremely successful. Following the formation of governmental strategic committees, both Austalia and the majority of American states have been awarded a 'free from bovine TB' status (Olmstead and Rhode, 2004 and Radunz, 2006). Due to this, both countries have now stopped regular testing of cattle herds and have adopted nationwide surveillance of slaughter houses as a means of disease control (Lehane, 1996). In the event that a particular animal at slaughter is found to be infected, it is possible for the

authorities to trace the livestock back to the original herd and isolate the farm for subsequent tests. This method has proved economically more viable to both the livestock keepers and the government.

Interestingly, the same 'test and slaughter' procedures applied in other areas such as Britain, New Zealand (Porphyre *et al*, 2008) or the American state of Michigan (O'Brien *et al*, 2006) have been proven unsuccessful in providing complete eradication of bTB. An important aspect of this failure is the existence of natural reservoir hosts, as described previously for the European badger in Britain (Muirhead *et al*, 1974). The bTB-free status of Australia may be in part attributed to the fact that the native Brushtail possum (*Trichosurus vulpecula*), although susceptible to *M. bovis* infection, does not appear to become naturally infected (Radunz, 2005). This is in contrast to New Zealand, where the native Brushtail possum has been of huge detriment to the national TB eradication programme (Ekdahl *et al*, 1970). This difference in disease kinetics is probably due to the extremely high possum densities inhabiting New Zealand compared to the relatively low levels in Austalia, the abundance of food and the lack of any natural predators. A similar problem has occurred in Michigan due to the endemic state of *M. bovis* infection in white-tailed deer (*Odocoileus virginianus,* Schmitt *et al*, 1997), in Canada with the Bison (*Bison bison,* Choquette *et al*, 1961) and in Spain with the European wild boar (*Sus scrofa,* Gortazar *et al*, 2003). This has meant that these countries have had to extend the traditional 'test and slaughter' methods to include the reservoir hosts, such as in Spain where serological ELISA tests are now being applied to wild boar (Aurtenetxe *et al*, 2008).

Vaccine development

It is clear from the situation within the United Kingdom and across the world that, although test and slaughter procedures remain central in the fight against *M. bovis* infection, they are an extremely expensive (both for the government as well as the farmer) and transient method of disease control. Faced with the presence of a natural reservoir host, the system is unable to cope with the continuous source of infection and acts only to maintain the threat rather than eradicate the disease altogether. Vaccination provides a low cost and extremely effective method against infection transmission. Its benefits would be extensive, as farmers would be able to retain their herd whilst ensuring productivity and trade status. Vaccination may also provide a more viable alternative in developing countries, as it would be easier to vaccinate

each animal once (or in the case of a booster, twice) rather than setting up a system in which animals would need to be tested every year.

There are a number of possible methods to improve upon the BCG vaccination procedure (Figure 4). One method is subunit vaccines involving the isolation of a small part of the *M. bovis* or *M. tuberculosis* bacterium, such as its DNA or selective proteins and utilising it with a suitable adjuvant to induce an immune response (Vordermeier *et al*, 2006). Culture filtrate proteins (CFP) from *M. tuberculosis* with the adjuvant dimethyldeoctadecyl ammonium chloride (DDA) have been shown to induce a significant level of protection in mice and guinea pigs (Hewinson *et al*, 2003). The same subunit vaccine used in cattle studies however induced an adequate antibody response but failed to produce the cellular immune response necessary to protect against bTB (Wedlock *et al*, 2002). This represents a common problem seen in protein subunit vaccines and illustrates the importance of applying experimental conditions to the host in question, as adjuvants that may work in smaller animal models will not necessarily have the same effect in cattle (Wedlock *et al*, 2000 and 2002).

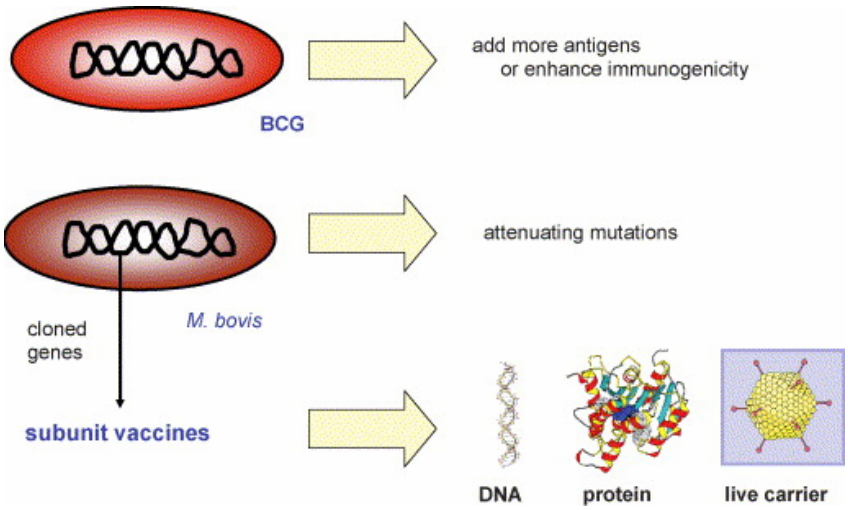

Figure 4: Strategies currently being explored to develop new bovine TB vaccines (from Vordermeier *et al*, 2006). There are three main methods of choice, improving the current BCG by genetic modification, attenuating a new *M. bovis* mutant to replace the current BCG or to selectively isolate subunits (either DNA sequences or proteins) from *M. bovis* and applying these via an adjuvant (such as attenuated recombinant viral vectors).

Another possible avenue of research is live recombinant vaccines such as Modified Vaccinia Ankara (MVA) or adenoviruses (Figure 4) which express mycobacterial antigens, for example *M. tuberculosis* Ag85A. The advantage of recombinant viral vaccines is their ability to induce a

strong cellular immune response and a long lasting T cell memory, effectively lengthening the time period of vaccine protection (Vordermeier *et al*, 2006). These have proved particularly successful in murine *M. tuberculosis* infection models, for example a recombinant adenovector-based vaccine expressing Mtb antigens Ag85A, Ag85B and TB10.4 in a single fusion protein (Radosevic *et al*, 2007) displayed strong T-cell responses, reduced bacterial lung loads and suppressed bacterial dissemination.

Other vaccines that are currently being developed include new attenuated *M. bovis* strains in which genes encoding virulent factors or proteins for metabolic pathways are specifically targeted for deletion (Figure 4). Protection against *M. bovis* in cattle was induced by an auxotrophic *M. bovis* strain, as a significantly lower number of animals developed lesions in comparison to the BCG control group (Buddle *et al*, 2002). There is also the potential of improving the BCG vaccine directly by recombination with additional antigens not expressed within the strains or to increase the expression of some of the existing antigenic proteins (Hewinson *et al*, 2003).

With extensive research being performed on vaccine development, it is becoming apparent that the most successful course of providing both *M. bovis* and *M. tuberculosis* protection in many host species has involved priming the immune system with BCG and following with a boost from one of the subunit vaccines described in figure 4 (Vordermeier *et al*, 2006). A number of combinations of heterologous prime-boost strategies have been used involving the subunit vaccines already mentioned. The vaccine combination that has shown very promising results in protection of cattle against bTB used BCG followed by modified vaccinia virus (MVA) expressing the mycobacterial antigen 85A (Vordermeier *et al*, 2004). This prime-boost strategy is currently undergoing phase I clinical trials as a vaccine in humans against *M. tuberculosis* (McShane *et al*, 2005) and so further supports the links between the human and bovine TB vaccine research developmental pathways. More recently, cattle vaccinated with an ESAT-6:CFP10 DNA vaccine alongside plasmid-encoded co-stimulatory molecules (granulocyte macrophage-colony stimulating factor (GM-CSF) and CD80/86) followed by a homologous booster dose twenty days later displayed enhanced recall responses to antigens as compared to controls (Maue *et al*, 2007). The addition of co-stimulatory molecules resulted in an increased cell-mediated response, possibly via activation of DCs whilst leaving the humoral response un-affected and lowering the degree of pathology within each animal (Maue *at al*, 2007).

Aims and Objectives

The aims of this study, in collaboration with the Veterinary Laboratories Agency (Surrey) and under the guidance of the Department of Environment, Food and Rural Agency (DEFRA, UK) are to:

- Provide a greater understanding of the bovine immune response (specifically IFN-γ, TNF-α, IL10 and IL4 expression) following *M. bovis* infection at the site of pathological disease (the thoracic lymph nodes). This was done by observing the cytokine expression within bovine bronchial lymph nodes after five, twelve and nineteen weeks of *M. bovis* infection. The ability of vaccinations to protect a host against disease is based purely on eliciting the correct immune response. The information gained from this study will therefore provide an immunological basis on which to develop novel vaccination compounds by revealing the dynamics of a successful immune response against infection.

- Apply this new immunological knowledge in assessing the protective ability of a novel BCG vaccine complement. Cattle were vaccinated with both the current BCG Pasteur and a genetically engineered alternative, followed by infection with *M. bovis* for five weeks. The comparison between the immunological profiles of cattle from the two vaccination groups provides an understanding on the most effective method of manipulating the BCG to increase its protective ability. This will contribute to the numerous vaccination developmental studies occurring across the globe with the united aim of complete *M. bovis* eradication.

Chapter 2

Methods and Materials

Methods and Materials

The infection, vaccination and post mortems of cattle were carried out by trained personnel at the Veterinary Laboratories Agency (VLA, Surrey, UK). They were approved by the local ethical review board in accordance to national U.K guidelines and undertaken with a home office licence, under the "Animals (Scientific Procedures) Act of 1986". RNA extraction and quantitative Polymerase Chain Reaction experiments were performed at the University of Hertfordshire. Immunohistochemistry was performed at the Department of Histopathology, VLA (Surrey).

Bacterial culture

Mycobacterium bovis

The *Mycobacterium bovis* (*M. bovis*) inoculum used to infect the cattle was prepared from a mid-log phase frozen seed stock of a reference strain AF2122/97 (VLA, Surrey). Seed stocks were thawed and diluted to a known titre using Middlebrook 7H9 medium (Difco Laboratories, Detroit, US) containing 0.05% Tween 80 (to prevent bacterial cell clumping). To confirm the infective dose retrospectively, the inoculum was plated in triplicate on a modified formulation of Middlebrook 7H11 agar and incubated for four weeks (37^{o}C), followed by colony counting.

Bacillus Calmette Guerin Pasteur

The BCG Pasteur strain used to vaccinate the cattle was grown in Middlebrook 7H9 medium (Difco Laboratories, Detroit, US) containing 0.05% Tween 80 (Sigma-Aldrich, US), 10% albumin-dextrose-catalase supplement (Becton Dickinson and Co, US) and 25 µg/ml Kanamycin, upon a rotating platform (37^{o}C). Bacterial BCG cultures were stored frozen (-80^{o}C) and thawed in fresh 7H9 medium when required.

Cattle experiments

Due to the extensive costs of biosecure containment facilities and the associated ethical issues surrounding *M. bovis* infection of previously healthy animals, cattle numbers in the published literature are generally low (between three and six animals in each experimental group, Thacker *et al*, 2007, Dean *et al*, 2005, Widdison *et al*, 2006). Therefore the animal numbers

employed within these studies are of a similar size (between three and five cattle within each group) and this is described in more detail within each chapter. The use of smaller animal numbers, however, has considerable implications on the statistical analysis of the data as the natural variation of the immune response is amplified. This therefore needs to be taken into consideration when interpreting the results of each study.

BCG vaccination

Friesian Holstein heifers and bullocks of approximately six months of age and with no history of tuberculosis infection were vaccinated by a subcutaneous injection of BCG Pasteur (between 5 and $6.3x10^5$ colony forming units) to the neck.

***Mycobacterium bovis* infection**

The animals were infected intratracheally with *M. bovis* strain AF2122/97 (between $6x10^3$ and $1.0x10^4$ colony forming units). This was performed by passing an endotracheal tube (80 cm) holding a fine cannula through the trachea of the anesthetised animal into the top of the left lung lobe. The infecting *M. bovis* dose was then injected through the cannula and flushed out with saline (2 ml).

Cattle post mortem

The animals were euthanized by intravenous injection of sodium pentobarbitonic at specific time points post *M. bovis* infection (the duration of infection has been outlined in the methods section of each individual study). The cattle post mortems were performed within category three containment facilities at the VLA (Surrey) and all personnel present were required to wear specialist protective clothing with fitted respirators. During the post mortems, the thoracic lymph nodes (specifically the cranial mediastinal, caudal mediastinal, cranial tracheobranochial (time course study only) and left bronchial nodes) were removed from each animal. The studies focused specifically on the thoracic lymph nodes as these have been shown to be the primary draining nodes involved in *M. bovis* infection (Liebana *et al*, 2007). It also avoids any inconsistencies that would be introduced by measuring cytokine expression in both respiratory and lymphatic systems.

Tissue samples (approximately 1 cm^3) were then taken consistently from the middle regions of visible lesions where possible for each lymph node. The samples were submerged in 10 ml of

formalin fixative for subsequent pathology analysis, total RNA extraction (time course study only) and immunohistochemistry (BCG vaccination study only). Specific for the BCG vaccination study, fresh tissue sections (approximately 0.5 cm^3) were also submerged in 5 ml of Trizol reagent (Invitrogen, Paisley, Renfrewshire, Scotland) for subsequent total RNA extraction.

Formalin fixed, paraffin embedded tissue preparation

M. bovis infected cattle lymph node tissue sections (approximately 1 cm^3) from each animal were fixed in neutral-buffered formalin (10% formaldehyde) for seven days followed by embedding within paraffin wax. For pathology analysis, the paraffin embedded samples were cut into 4 µm sections and mounted onto glass slides. For RNA extraction (time course study only), samples were cut into 10 µm sections and placed into microcentrifuge tubes.

Pathology analysis of infected lymph nodes

The slide preparation and pathology analysis was performed at the Pathology Department, VLA (Surrey) as a routine procedure. The paraffin embedded formalin fixed tissues from each lymph node sample were sectioned (4 µm) using a microtome and placed upon the surface of pre-heated water (37^{o}C) in order to stop the sections from rolling up. Microscope slides pre-treated with Vectabond (Vector Laboratories, UK) were placed underneath the tissue sections and lifted above the water surface to allow the sections to bind to the slide. The slides were dried overnight (37^{o}C) and incubated for thirty minutes (60^{o}C) before de-paraffinising the sections in xylene for five minutes, followed by incubation within absolute alcohol (five minutes) and then 70% alcohol (five minutes). The sections were stained using haematoxylin counter stain and each slide was then observed by a Veterinary Pathologist (100 x magnification). The pathology of the lymph node samples were measured using two methods; by observing the percentage area coverage of granulomatous lesions and also the developmental stage of each granuloma within the tissue sections.

- To determine percentage area coverage of granulomas within the samples, the lymph node section was first measured by counting the number of fields of view that each section covered. The granuloma lesions were also measured using the same method. It was then possible to calculate the percentage area coverage of each individual granuloma in relation to the total number of fields covered by the lymph node section.
- A scoring method developed at the VLA (Wangoo *et al,* 2005) was used to determine the developmental stage of each granuloma within the sections. Granuloma were categorised into four types based on their physiological properties. Type I granulomas were characterised as irregular, unencapsulated granulomatous inflammations composed of clustered epithelioid macrophages and peripheral lymphocytes. Type II were organised, partially or completely encapsulated and composed of primarily epithelioid macrophages with minimal necrosis. Type III was encapsulated granuloma displaying central necrosis and focal mineralization. Type IV was multilobular to irregular, large, well-encapsulated granuloma displaying prominent central necrosis with extensive mineralization. The numbers of granuloma within each stage were counted for each individual lymph node section (left bronchial, cranial mediastinal, caudal mediastinal and cranial tracheobronchial) and the results combined for each animal. The total counts for each granuloma stage were then weighted according to a

$\log_2$ scale to account for the increased size of granuloma as they advanced through the four stages.

Total RNA extraction from formalin fixed, paraffin embedded tissues (time course study only)

The published protocol for total RNA extraction from *M. bovis* infected, formalin fixed paraffin embedded lymph node tissue has been previously described (Witchell *et al*, 2008).

Diethyl pyrocarbonate (DEPC) treatment:

All glass wear, plastic and pipette tips were treated with 0.1% (v/v) DEPC solution over twenty four hours followed by autoclaving at 121^{o}C for thirty minutes to remove RNase contamination.

Table 1: Reagents and suppliers for total RNA extraction from formalin fixed, paraffin embedded lymph node tissues of cattle infected with *M. bovis* for five, twelve and nineteen weeks.

Reagent	Supplier
Ethanol (absolute)	Sigma-Alderich (Poole, Dorset, UK)
Optimum FFPE RNA Isolation kit	Ambion (Applied Biosystems, Warrington, Cheshire, UK)
Xylene	BDH (Poole, Dorset, UK)

Deparaffinisation:

Xylene (1 ml) was added to each microcentrifuge tube containing three times 10 µm sections of formalin fixed paraffin-embedded tissue. The tubes were kept at room temperature for five minutes followed by centrifugation (16,500 x *g*) at room temperature for ten minutes. The supernatant was discarded and the tissue sections dehydrated in three changes of alcohol (100%, 90% and 70%) for three minutes each. Each time the sections were centrifuged for one minute (16,500 x *g*) and the supernatant was discarded. The tissue sections were then left to air dry for ten minutes at room temperature.

Total RNA extraction:

Total RNA was extracted from the formalin fixed, paraffin embedded tissue sections according to the manufacturer's instructions for the Optimum FFPE isolation kit (Ambion, UK). Prior to

total RNA extraction, a solution of 10 µl Proteinase K (60 units/µl, Ambion, UK) and 100 µl Digestion buffer (Ambion, UK) was incubated at 37°C for ten minutes (to dissolve any precipitate). This was added to the deparaffinised tissue sections and incubated at 37°C for six hours. The samples were centrifuged for one minute (16,500 x *g*) to pellet un-dissolved tissue residue and the supernatant transferred to a new microcentrifuge tube. RNA extraction buffer (Ambion, UK) was added to the supernatant and vortexed vigorously for ten seconds. The sample was passed through a micro filter cartridge by centrifugation for one minute (16,500 x *g*) and the flow through was discarded via the micro waste collection tube. The filter cartridge was washed through by a series of centrifugation steps with the appropriate wash solutions (Ambion, UK) followed by a final centrifugation step for two minutes to remove any excess ethanol. The filter cartridge was transferred to a micro elution tube and two times 10 µl volumes of pre-heated (70°C) RNA elution solution (Ambion, UK) were added directly to the filter. This was then left at room temperature for one minute before centrifuging (16,500 x *g*) for one minute to elute the total RNA. Total RNA samples were stored at -70°C.

Total RNA isolation from freshly dissected tissues (BCG vaccination study only)

Table 2: Reagents and suppliers for total RNA extraction from *M. bovis* experimentally challenged fresh cattle lymph nodes.

Reagent	Supplier
β-Mercaptoethanol	Sigma (Poole, Dorset, UK)
Chloroform >99%	Sigma (Poole, Dorset, UK)
Ethanol (absolute)	Sigma (Poole, Dorset, UK)
Isopropanol	Sigma (Poole, Dorset, UK)
RNeasy Mini RNA Extraction kit	Qiagen (Crawley, Sussex, UK)
Trizol	Invitrogen (Paisley, Scotland)
Turbo DNA-free	Ambion (Applied Biosystems, Cheshire, UK)

Isolation was based on the single-step RNA isolation method developed by Chomczynski and Sacchi (1987) and followed per the manufacturer's instructions (Invitrogen, Scotland). All tissue manipulations were carried out in a class III cabinet (homogenisation) or a class I cabinet (RNA isolation) before washing with 70% ethanol, in which the sample was deemed safe to

remove. The tissue sections were homogenised while submerged in the Trizol reagent followed by the addition of chloroform (0.4 volumes) and vortexed vigorously. The sections were left at room temperature for five minutes before centrifugation for five minutes (5,000 x *g*) and the upper aqueous layer containing the total RNA was transferred to a new centrifuge tube. This step was repeated using chloroform (1 volume). Precipitation of the total RNA was performed using isopropanol (0.8 volumes) and sodium acetate (0.1 volumes, 3 M, pH 4.8). The sample was divided into several microcentifuge tubes and centrifuged for fifteen seconds (16,500 x *g*) to pellet the total RNA and the supernatant discarded. An equal volume of ethanol (70%) was added to the sample and the pellet gently re-suspended and washed. This was centrifuged for fifteen seconds (16,500 x *g*) and the pellet left to dry for ten minutes at room temperature. The latter part of RNA isolation was performed per the manufacturers' instructions for the RNeasy® Mini kit (Qiagen, UK) RNA cleanup protocol. The pellet was re-suspended in RNase-free water and mixed thoroughly with lysis Buffer RLT (Buffer RLT containing β-mercaptoethanol, Qiagen, UK). Absolute ethanol was added and the solution mixed gently by pipetting. This was passed through an RNeasy mini column (Qiagen, UK) by centrifugation for fifteen seconds (16,500 x *g*) and the flow through discarded. Buffer RPE (Qiagen, UK) was added to the RNeasy column and centrifuged for fifteen seconds (16,500 x *g*) to wash the column. The buffer RPE wash was repeated and the total RNA eluted in RNase-free water (50 µl total volume) by centrifugation for one minute (16,500 x *g*).

DNA digestion of total RNA samples

The total RNA sample was diluted to 200 µg/ml in a total volume of 50 µl RNase-free water. 1 µl DNase I (2 U/µl) and 1/10 the sample volume of 10x DNase buffer (Ambion, UK) were added to the eluted RNA and mixed thoroughly by pipetting. This was incubated at 37^{o}C for thirty minutes. The DNase was inactivated using DNase Inactivation Reagent (Ambion, UK) and vortexing. The reaction mixture was kept at room temperature for two minutes before centrifugation (16,500 x *g*). The treated total RNA could then be transferred to a new microcentrifuge tube and stored at -70^{o}C.

Total RNA Quantification

Individual lymph node total RNA samples were quantified using a BioPhotometer (Eppendorf, Hamburg, Germany). 200 µl of a 10^{-2} dilution of the total RNA sample (diluted using sterile distilled water) was placed within an UVette (Eppendorf, Germany) and the absorbance read at

260 nm. The BioPhotometer (Eppendorf, Germany) automatically calculated the RNA concentration in the original sample using the following equation:

(Absorbance at 260 nm x RNA coefficient) dilution factor = µg/ml of RNA

- RNA coefficient: 40 ng/µl equivalent to an absorbance reading of 1
- Dilution factor: 10^2

The BioPhotometer (Eppendorf, Germany) also gave an indication of the purity of the RNA sample by calculating the ratio between the absorbance at 260 nm (specific for nucleic acids) and 280 nm (specific for protein). A pure total RNA sample should give a ratio of between 1.7 and 2.1.

Gel electrophoresis of total RNA

Table 3: Reagents and suppliers for agarose gel electrophoresis of total RNA from *M. bovis* infected (five, twelve and nineteen weeks) formalin fixed cattle lymph node tissues.

Reagent	Supplier
Acetic Acid	Sigma (Poole, Dorset, UK)
Agarose	BDH (Poole, Dorset, UK)
Bromophenol blue	Sigma (Poole, Dorset, UK
EDTA	Invitrogen (Paisley, Renfrewshire, Scotland)
Ethidium Bromide	Sigma (Poole, Dorset, UK)
RNA Ladder (0.5-10 Kb)	Sigma (Poole, Dorset, UK)
Sucrose	Invitrogen (Paisley, Renfrewshire, Scotland)
Tris base	Sigma (Poole, Dorset, UK)
Xylene cyanol FF	Fisher (Loughborough, Leicestershire, UK)

Total RNA samples were analysed by agarose gel electrophoresis. A 1% agarose gel solution was prepared using sterile 1x Tris Acetate EDTA (TAE) buffer and poured into the gel cassette. The comb was inserted to form the sample wells and the gel left to solidify. The gel was transferred to the electrophoresis tank and submerged with sterile 1x TAE buffer. The total

RNA samples were loaded with loading buffer (TAE buffer, bromophenol blue, sucrose and xylene cyanol FF) alongside a 0.5-10 Kb RNA ladder (Sigma, Poole, Dorset, UK). The gel was run at a constant voltage (100 volts) for thirty minutes. It was then stained in ethidium bromide (1 µg/ml) for twenty minutes followed by de-staining in 1x TAE buffer for ten minutes. The total RNA samples were visualised using a UV light box (Gene Genius Bio imaging System, Syngene, Cambridge, UK) and documented with the Gene Snap program (Syngene, UK).

Quantitative Polymerase Chain Reaction

Primer and probe oligonucleotide sequences:

Table 4: Primer and dual labelled fluorescent probe oligonucleotide sequences for quantitative PCR.

Target gene	Forward primer 5'-3'	Reverse Primer 5'-3'	Fluorescent Probe
GAPDH	TGCACCACCAACTGCTTGG	GGCGTGGACAGTGGTCATCCA	HEX: ATGACCACTTTGGCATCGTGGAGGGA : BHQ-1
TNF-α	CGGTGGTGGGACTCGTATG	GCTGGTTGTCTTCCAGCTTCA	FAM: CAATGCCCTCGTGGCCAACGG: BHQ-1
IFN-γ	CAGAAAGCGGAAGAGAAGTCAGA	CAGGCAGGAGGACCATTACG	FAM: TCTCTTTCGAGGCCGGAGAGCATCA: BHQ-1
IL10	GGTGATGCCACAGGCTGAG	AGCTTCTCCCCCAGTGAGTTC	FAM: CACGGGCCTGACATCAAGGAGCA: BHQ-1
IL4	GCCACACGTGCTTGAACAAA	TCTTGCTTGCCAAGCTGTTG	FAM: TCCTGGGCGGACTTGACAGG: BHQ-1

Primer and probe sequences were designed at the VLA (Surrey) and received from Dr Shelley Rhodes. Primer and probe properties (including GC content and melting temperatures) are displayed in Appendix 1.

Table 5: Reagents and suppliers for dual labelled probe quantitative PCR.

Reagent	Supplier
Clear Seal Diamond	ABgene (Epsom, Surrey, UK)
Quantitect™ Probe RT-PCR kit	Qiagen (Crawley, Sussex, UK)
THERMO-FAST® 96 PCR Plate	ABgene (Epsom, Surrey, UK)
Primer and Probe oligonucleotides	Biomers.net (Ulm, Germany)

Real time qRT-PCR using dual labelled probes was carried out according to the manufacturers' guidelines for the Quantitect™ Probe RT-PCR kit (Qiagen, Crawley, West Sussex, UK). A standard reaction mixture (Table 6) was produced and then aliquoted (25µl) into a ninety six well plate followed by the template. All reactions were set up on ice.

Table 6: Standard Reaction mixture components for dual labelled probe quantitative RT-PCR.

Reaction mixture components	Final Concentration
2x QuantiTect Probe RT-PCR Master Mix	1x
Total RNA template	100 ng
Forward Primer	700 nmoles
Reverse Primer	700 nmoles
Probe	200 nmoles
RNase-free water	Up to 25 µl

Concentrations of primers, probes and template were optimised in previous experiments (Appendix 2).

Each lymph node sample was analysed for the expression of all four cytokines; IFN-γ, TNF-α, IL10 and IL4. The mRNA expression of the housekeeping gene glyceraldehyde-3-phosphate dehydrogenase (GAPDH) was also measured within each sample to ensure the quality of the starting template.

Standard templates:

Standard templates for each cytokine were produced to enable absolute quantification of mRNA levels within the experimental samples. The standard templates were designed based on the primer and probe sequences of each specific mRNA target with an extra ten bases on each end to provide space for oligonucleotide binding (Table 7). It was necessary to design both complimentary strands of the target sequence to ensure efficient binding of the forward and reverse primers during PCR (Table 7). Each standard template strand (Biomers.net, Ulm, Germany) was dissolved in sodium tris EDTA (STE) buffer and the complimentary strands mixed in equal molar amounts. The mixed complimentary strands were heated to 94^{o}C and then cooled gradually over three hours by 'unplugging' the heated block. This allowed the two strands to bind together. The stable double stranded product was then diluted to 5 µmoles working solution and stored at -20^{o}C.

Table 7: Standard template sequences for qPCR (produced by Biomers.net, Germany). The standards were designed to be complimentary to the relevant forward primer (blue), probe (green) and reverse primer (red) with 10 bases either end to allow space for oligonucleotide binding. Both complimentary strands of the genetic sequence were synthesised (strand 1 and 2) and then annealed together to ensure efficient binding of both the reverse and forward primer during PCR.

Target gene	Genetic sequence 5'to 3'	Total no. of base pairs after annealing
IFN-γ		
Strand 1	AATCTAACCTCAGAAAGCGGAAGAGAAGTCAGAATCTCTTTCGAGGCCGGAGAGCAT CAACGTAATGGTCCTCCTGCCTGCAATATTTGA	90
Strand 2	TCAAATATTGCAGGCAGGAGGACCATTACGTTGATGCTCTCCGGCCTCGAAAGAGAT TCTGACTTCTCTTCCGCTTTCTGAGGTTAGATT	
TNF-α		
Strand 1	GGGGCAGCTCCGGTGGTGGGACTCGTATGCCAATGCCCTCGTGGCCAACGGTGTGAA GCTGGAAGACAACCAGCTGGTGGTGCC	84
Strand 2	GGCACCACCAGCTGGTTGTCTTCCAGCTTCACACCGTTGGCCACGAGGGCATTGGCA TACGAGTCCCACCACCGGAGCTGCCCC	
IL10		
Strand 1	ACCTGGAAGAGGTGATGCCACAGGCTGAGAACCACGGGCCTGACATCAAGGAGCACGTGAACTCACT GGGGGAGAAGCTGAAGACCCT	89
Strand 2	CAGGGTCTTCAGCTTCTCCCCCAGTGAGTTCACGTGCTCCTTGATGTCAGGCCCGTGGTT CTCAGCCTGTGGCATCACCTCTTCCAGGT	
IL4		
Strand 1	ATCTACAGGAGCCACACGTGCTTGAACAAATTCCTGGGCGGACTTGACAGGAATCTC AACAGCTTGGCAAGCAAGACCTGTTCTGT	86
Strand 2	ACAGAACAGGTCTTGCTTGCCAAGCTGTTGAGATTCCTGTCAAGTCCGCCCAGGAAT TTGTTCAAGCACGTGTGGCTCCTGTAGAT	

Standard template concentrations:

From the 5 µmole working solution, a volume corresponding to 500 ng standard template was calculated and used as the starting concentration for serial dilutions. To allow for the results to be quoted in the form of copy number, the concentration (converted into g/µl) was transformed into copy number using the following calculation:

$$\text{Copy number} = \left(\frac{\text{g/µl}}{\text{(number of bases x 340 daltons/base)}} \right) \times 6.022 \times 10^{23}$$

The starting concentration was then serially diluted and the dilutions 10^{-4}, 10^{-8}, 10^{-10} and 10^{-12} were used to produce the standard curves in PCR. The corresponding copy number for each dilution was imputed into the PCR program prior to running the experimental plates (Table 8). Standard curves specific to the target cytokine gene were run on every PCR plate.

Table 8: Copy numbers of each standard template corresponding to the serial dilution of the templates. The concentrations were used to produce the standard curves and were run in every experimental plate to allow quantification of the unknown samples.

Template dilution	IFN-γ copy number	TNF-α copy number	IL10 copy number	IL4 copy number
10^{-4}	361826050	349276000	343254000	348673800
10^{-8}	36182.6	34927.6	34325.4	34867.4
10^{-10}	362	349.3	343.25	348.7
10^{-12}	3.6	3.5	3.4	3.5

Experimental reactions:

Each reaction was performed in either duplicate or triplicate. Control reactions were performed with the standard reaction mixture (Table 6) excluding the template for the no template control (to detect possible PCR product contamination). The reactions were carried out within a

Quantica Real Time Nucleic Acid Detection System (Techne, Fradley, Staffordshire, UK) to a specific program (Table 9).

Table 9: Amplification program (incubation temperatures and time periods) for dual labelled probe qRT-PCR.

qPCR Step	No. of cycles	Incubation temperature (°C)	Incubation time
Reverse Transcription	1 cycle	50°C	30 minutes
Initial Activation step	1 cycle	95°C	15 minutes
Denaturation, annealing/extension	50 cycles	94°C 60°C	15 seconds 1 minute

The real time fluorescent dye reading was taken at the annealing/extension stage (Table 9). The crossing point (CP) value was calculated for each reaction by the Quansoft program (Techne, UK) using the point at which the fluorescence of the reaction reached a set threshold level relative to the corresponding PCR cycle number. The CP values of the standard template were plotted against its known concentrations (log copy number) to produce a standard curve. This was then used to convert the CP values of the unknown samples into copy number. The CP values of the housekeeping gene were used to ensure the quality of the starting template.

Immunohistochemistry (BCG vaccination study only)

Table 10: Reagents and suppliers for immunohistochemistry (IFN-γ and TNF-α protein) of both *M. bovis* experimentally challenged and non-infected formalin fixed cattle lymph nodes.

Reagent	Supplier
Vectorbond-treatment for slides	Vector Laboratories (Peterborough, UK)
Hydrogen peroxide	Sigma (Poole, Dorset, UK)
Methanol	Sigma (Poole, Dorset, UK
Citric acid	Sigma (Poole, Dorset, UK)
Trypsin	Sigma (Poole, Dorset, UK)
α-chymotrypsin	Sigma (Poole, Dorset, UK)
Calcium chloride	Sigma (Poole, Dorset, UK)
Tris	Sigma (Poole, Dorset, UK)
Sodium Chloride	Sigma (Poole, Dorset, UK)
Tween 20	Sigma (Poole, Dorset, UK)
Normal serum block- goat	Vector Laboratories (Peterborough, UK)
Primary antibodies (IFN-γ and TNF-α)	Serotech (Oxford, Oxfordshire, UK)
Secondary antibodies (goat vs. mouse)	Vector Laboratories (Peterborough, UK)
Vector Elite Conjugate (ABC)	Vector Laboratories (Peterborough, UK)
Diaminobenzidine chromogen	Sigma (Poole, Dorset, UK)
Mayers Haemalum stain	Sigma (Poole, Dorset, UK)

During the cattle post mortems, lymph node tissue samples were collected from each animal from the five experimental groups and submerged within formalin fixative for subsequent immunohistochemistry (IHC). IHC was performed on each section primarily once for each cytokine with the addition of one negative control slide per animal. A random selection of ten slides (equating to approximately a quarter of the total number of sections) were then used to repeat IHC for each cytokine to indicate the reproducibility of the protocol. A selection of ten slides with known immunostaining profiles (VLA, Surrey) were run in parallel to the experimental sections to provide positive controls.

The formalin fixed sections were mounted upon vectorbond-treated slides (Vector Laboratories, Peterborough, UK) and the sections de-paraffinised as previously. The slides were then incubated within a solution of hydrogen peroxide (3%) and methanol (97%) for fifteen minutes to block endogenous peroxidase activity, followed by washing in tap water (3x two minutes).

Epitope de-masking:

The sections were pre-treated with antigen retrieval reagents to ensure that any protein cross-links formed by formalin fixation (obstructing antigenic sites) were broken. The IHC method for IFN-γ protein involved a heat induced epitope retrieval (HIER) system. The slides were submerged within citric buffer (0.01 M, pH 6) and heated within a microwave (100^{o}C) for six minutes (repeated three times). The sections were then cooled at room temperature for ten minutes and washed under running tap water for a further ten minutes.

The IHC method for TNF-α protein involved a proteolytic induced epitope retrieval (PIER) system. The slides were incubated within a pre-heated purified water trough (37^{o}C) for a minimum of ten minutes. A solution of trypsin (0.02 M), α-chymotrypsin (0.02 M), calcium chloride (9 mM) and purified water (pH adjusted to 7.8) was pre-heated for fifteen minutes (37^{o}C) and the slides submerged in the proteolytic solution for ten minutes (37^{o}C). This was then followed by washing under running tap water for ten minutes.

IHC staining:

After epitope retrieval, the slides were incubated for five minutes (room temperature) in TBS buffer (working concentration of x1, Table 11) for the IFN-γ protein IHC method and in TBST buffer (working concentration of x1, Table 11) for the TNF-α protein IHC method. The slides were then incubated in normal serum block from the same species used to raise the secondary link antibody (goat serum diluted 1/66 using TBS/TBST buffer) for twenty minutes at room temperature. This solution was then replaced by the primary antibody (conditions in Table 12) followed by a buffer wash (2x five minutes at room temperature). To provide negative controls, an additional lymph node section from each animal was incubated in mouse IgG antibody in place of the primary antibody to check for any non-specific binding.

The slides were incubated within the biotinylated secondary link antibody specifically targeted to the same species that was used to raise the primary antibody (goat vs. mouse, diluted 1/200 using TBS/TBST buffer) for thirty minutes (room temperature). This was followed by a buffer wash (2x five minutes).

The sections were then incubated within the Vector Elite Conjugate (ABC) solution (diluted 1/25 using TBS/TBST buffer, Vector Laboratories, UK) for thirty minutes (room temperature) followed by a buffer wash (2x five minutes).

Table 11: Reagents used to produce the immunohistochemical buffers TBS (used in the IFN-γ protocol) and TBST (used in the TNF-α protocol). The stock solution of each buffer was at a concentration of x10 and this was diluted to a working concentration of x1 for the IHC protocol.

Buffer (x10 concentration)	Reagent	Final conc.
TBST (0.85% NACL) **pH 7.6**	Sodium chloride	1.36 M
	TRIS	0.04 M
	Distilled water	Up to 1 litre
	Tween 20	0.05%
TBS (0.85% NACL) **pH 7.6**	Sodium chloride	1.36 M
	TRIS	0.04 M
	Distilled water	Up to 1 litre

Table 12: The primary antibody (IFN-γ and TNF-α) incubation conditions for immunohistochemistry.

Target cytokine	Antibody/ clone	Dilution	Incubation time	Incubation temperature
IFN-γ	Mouse anti-bovine IFN-γ / CC330	1/100 in TBS buffer	One hour	Room temperature
TNF-α	Mouse anti-bovine TNF-α / CC327	1/2000 in TBST buffer	One hour	Room temperature

Preparation of the Diaminobenzidine (DAB) chromogen solution:

The sections were incubated in diaminobenzidine (DAB) chromogen to develop the peroxidase in the ABC kit (Vector Laboratories, UK) and produce the end coloured product. The DAB solution was prepared as per the manufacturer's instructions (Sigma, Poole, Dorset, UK).

Table 13: Components and final concentrations of reagents for the two solutions (A and B) used to produce the phosphate citrate buffer needed in the preparation of the Diaminobenzidine (DAB) chromogen.

Solution	Reagent	Final concentration
Solution A	Disodium Hydrogen Orthophosphate (NA_2HPO_4)	0.16 M
	Tween 20	0.05 %
	Distilled water	Up to 1 litre
Solution B	Citric Acid	0.03 M
	Tween 20	0.05 %
	Distilled water	Up to 0.5 litre

Briefly, two solutions (A and B, Table 13) were prepared and stored at room temperature. A phosphate citrate buffer (McIlvanes) was prepared by mixing solution A (70 ml) and solution B (30 ml) using a magnetic stirrer. The pH was measured and adjusted to pH 6.4 using either solution A or B as required. The phosphate citrate buffer was then transferred (20 ml) into a plastic universal container and a DAB tablet (10 mg, Sigma, UK) added to the solution. The tablet was broken down using a magnetic stirrer and the solution mixed for five minutes. The solution was extracted from the universal container using a syringe (20 ml) and filtered through a Millipore filter (0.45 µ) into a clean plastic universal container. Hydrogen peroxide (10 µl) was added to the phosphate citrate/ DAB solution (20 ml) and mixed thoroughly using a vortex. It was then possible to check the quality of the citrate buffered DAB solution by applying a small amount to excess Vector Elite ABC conjugate solution (\Vector Laboratories, UK) therefore producing a dark brown colour change. The slides were incubated in citrate buffered DAB solution for ten minutes (room temperature). This was followed by a purified water wash for five minutes and the sections then placed under running tap water for ten minutes.

Mayers Haemalum counterstain:

The sections were counterstained with Mayers Haemalum to allow accurate visualisation of the positively stained brown cells against a blue coloured background. The protocol was followed as per the manufacturer's instructions (Sigma, UK). Briefly, sections were stained in Mayers Haemalum for fifteen minutes, followed by a wash under running tap water for fifteen minutes. The sections were placed in distilled water for thirty seconds and counter stained in Eosin Y solution for one minute. The sections were then incubated in two changes of 95% ethanol, absolute ethanol and xylene (two minutes each) before being covered in DPX mounting reagent and a cover slip placed over the slide.

Analysis of immunostained sections:

The sections were analysed semi-quantitatively based on a scoring method. Upon examination under the microscope (x100 and x400), the sections contained few granuloma which were difficult to pin-point visually. The scoring method was therefore based on the percentage of lymph node area covered by positively stained cells (the lymph node stained up as blue and the positively stained cells as brown, Figures 5 and 6). The sections were scored on a five point scale (0 to ++++) with an absence of staining represented by a 0 and maximum staining represented by ++++. The IFN-γ stained sections were scored as **+** = <5 %, **++** = 5-20%, **+++** = 21-40 % and **++++** = >40 % area coverage of positively stained cells (Figure 5). The TNF-α stained sections were scored as **+** = <1%, **++** = 1- 10 %, **+++** = 11-20% and **++++** = >20 % area coverage of positively stained cells (Figure 6).

Each slide contained approximately three-five sections of the same lymph node from the same animal and so each individual section was scored for percentage area coverage (100x magnification for IFN-γ and 400x for TNF-α). The results were then averaged to give overall percentage area coverage for that one lymph node. All of the IHC analysis was performed blindly to the experimental group that the animal came from and repeated twice.

- Score 0: no positive cells

- Score +

  Percentage area coverage of positively stained cells:

  <5 %

  Sparse staining across the section

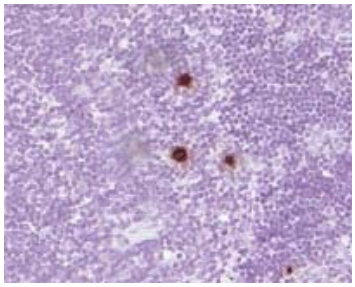

- Score ++

  Percentage area coverage of positively stained cells:

  5-20 %

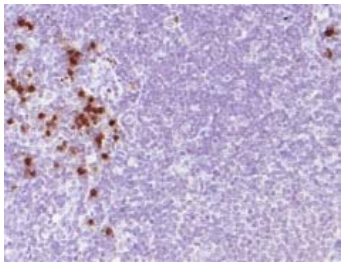

- Score +++

  Percentage area coverage of positively stained cells:

  21-40 %

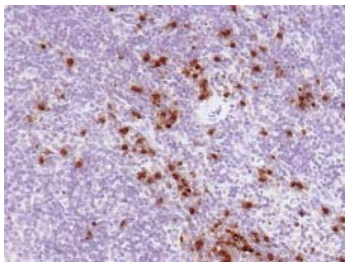

- Score ++++

  Percentage area coverage of positively stained cells:

  >40 %

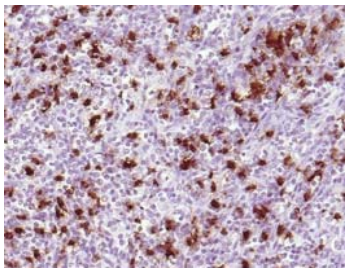

Figure 5: Immunohistochemistry scoring method of cells stained positive for IFN-γ production in the lymph node sections of cattle from five experimental groups; BCG (*sigK*) Pasteur vaccinated *M. bovis* challenged, BCG Pasteur vaccinated challenged, non-vaccinated infected, non-vaccinated non-infected and BCG Pasteur vaccinated non-infected. The positive cells were stained brown by diaminobenzidine chromogen and the background counterstained blue by Mayers haemalum. The sections were scored under a microscope magnification of 100x and analysis was performed in duplicate.

- Score 0: no positive cells

- Score +

  Percentage area coverage of positively stained cells:

  <1 %

  Very sparse staining (indicated by the arrow)

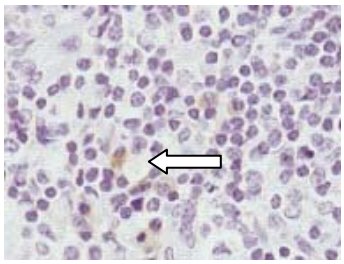

- Score ++

  Percentage area coverage of positively stained cells:

  1-10 %

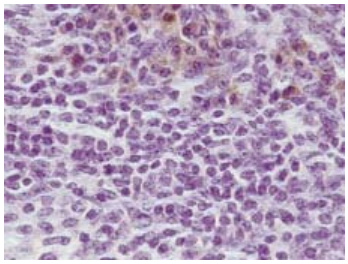

- Score +++

  Percentage area coverage of positively stained cells:

  11-20%

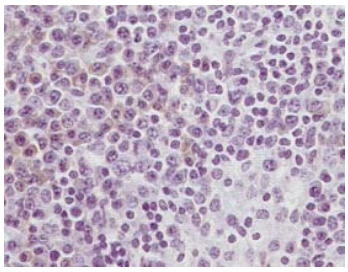

- Score ++++

  Percentage area coverage of positively stained cells:

  >20%

  Some staining present in Langhans' giant cells

  (indicated by arrow)

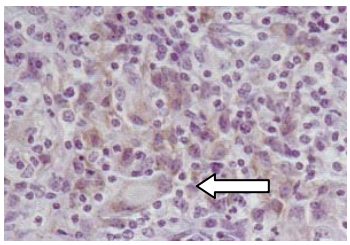

Figure 6: Immunohistochemistry scoring method of cells stained positive for TNF-α production in the lymph node sections of cattle from five experimental groups; BCG (*sigK*) Pasteur vaccinated *M. bovis* challenged, BCG Pasteur vaccinated challenged, non-vaccinated infected, non-vaccinated non-infected and BCG Pasteur vaccinated non-infected. The positive cells were stained brown by diaminobenzidine chromogen and the background counterstained blue by Mayers haemalum. The sections were scored under a microscope magnification of 400x and analysis was performed in duplicate.

Whole blood IFN-γ cultures

Whole blood cultures were collected from each animal prior to euthanisation by scientists at the VLA (Surrey). The concentration of IFN-γ protein within whole blood cultures from each animal were measured using the BOVIGAM® test (Prionics, Schlieren, Switzerland). The samples were incubated overnight (100 µl per well in a 96-well flat-bottom microtiter plates) in the presence of three different antigens (final concentration 10 µg/ml), tuberculin purified protein derivative (PPD) B, early secretory antigenic target 6-kDa (ESAT-6) and culture filtrate protein 10 (CFP-10) in 100 µl culture medium (RPMI 1640 with Glutamax (Gibco) supplemented with 5% control serum protein replacement (CSPR3, Gibco), nonessential amino acids (Gibco), 100 U/ml penicillin, 100 µg/ml streptomycin and $5x10^{-5}$ M 2-mercaptoethanol (Gibco)). The antigens stimulated lymphocytes within the blood cultures to produce IFN-γ which was then measured using a commercially available enzyme-linked immunosorbent assay kit (BOVIGAM®) according to the manufacturer's instructions. The antigen stimulated samples were transferred to microplates coated with an antibody to IFN-γ which upon incubation, bound to the IFN-γ within the blood sample. A second conjugate antibody (horseradish peroxidase labelled anti-bovine IFN-γ) was added to the reaction and bound to the primary antibody/IFN-γ complex. The conjugate antibody was labelled with an enzyme that generated a coloured signal upon IFN-γ binding. Therefore the degree of colour within the blood sample was directly proportional to the amount of IFN-γ within the sample. The colour change was measured using a spectrophotometer (450 nm) and the results given as mean optical density (OD) readings. When comparing the OD reading of a sample in the presence of antigen to the OD reading of the medium, a difference in readings of more than 0.1 was considered a positive response.

Statistical analysis

All statistical analysis was performed using a Statistical Package for the Social Sciences (SPSS, edition 15 and 16). The differences of the variances of each experimental group within the Time course and BCG vaccination studies were explored using the ANOVA one-way test (selecting Levenes F-test for homogeneity of variances). The results showed a significant difference between the variances of each experimental group. As a consequence of this and due to the relatively small number of data points with a skewed nature (descriptive statistics), it was decided to employ non-parametric tests to analyse the data.

To enable the data to be portrayed graphically, it was necessary to convert copy number into a logarithmic scale (log 2) however all statistical analysis was performed on the original data set. The means calculated from the logarithmic data are therefore geometric means whilst those calculated from the copy number data are arithmetic means.

The non-parametric Kruskal Wallis test was used to determine whether there were any statistically significant differences between more than two groups of data. Following a result of 'significant difference' with a 5% confidence interval ($p<0.05$), each experimental group was then assessed individually using the Mann Whitney test. The Bonferroni correction was applied to each Mann Whitney p value (dividing the p value by the number of comparisons made) to reduce the likelihood of identifying differences between the experimental groups by chance.

Pearsons correlation coefficient was used to determine whether there were any significant correlations between two groups of continuous data, such as copy number or percentage. Spearmans correlation coefficient was used to determine whether there were any significant correlations between two groups that contained categorical data, such as protein score.

Chapter 3

Time Course Study

Introduction

Cytokine expression studies

Mycobacterium bovis experimental studies aimed at elucidating the immunological progression of the disease have focused significantly on cytokines. As previously mentioned, cytokines are extremely important in the response to *M. bovis* infection due to the associated activation of both cell-mediated and humoral immunity. They have an extremely broad range of biological targets and processes distributed throughout the entire immunological response that can be studied at both the transcription and translational levels. Cytokine responses, in particular IFN-γ, have been used to provide a method of diagnosing *M. bovis* infection via the cell-mediated delayed-type hypersensitivity (DTH) reaction (Dickson, 1965).

Cytokine expression levels from antigen stimulated peripheral blood samples are believed to be a reliable method of determining the immunological state of *M. bovis* challenged animals throughout the infection process (Hope *et al*, 2005, Rhodes *et al*, 2000). Testing for IFN-γ levels in blood samples has therefore become a common measurement of bTB infection due to the extremely high levels of IFN-γ expression observed in response to *M. bovis* challenge (Welsh *et al*, 2005, Thacker *et al*, 2007). Thacker *et al* (2007) measured cytokine expression levels in isolated PPD stimulated bovine peripheral blood mononuclear cells (PBMCs) over a period of eighty-five days post *M. bovis* experimental infection. Levels of IFN-γ mRNA were detectable as early as fifteen days post infection and peaked at thirty days, accompanied by a peak in TNF-α and iNOS expression (Thacker *et al*, 2007). Throughout the infection period, IFN-γ, TNF-α and iNOS expression was higher within the infected as compared to the non-infected cattle. However, IL10 displayed a decrease in infected as compared to non-infected animals, with an evident trough in expression at thirty days post infection (Thacker *et al*, 2007). The authors suggest that this cytokine profile reflects a cell mediated T_H1 type response to early *M. bovis* infection with the accompanied suppression of T_H2 associated cytokine IL10. This hypothesis was supported by another similar study performed by Joardar *et al* (2002), that reported an increase in CD4+ T cells accompanied by an increase in IFN-γ expression within bovine PBMCs between four and nine weeks post *M. bovis* infection. The increase in CD4+ T cells was preceded by a dominant population of γδ+ T cells (for the first four weeks of infection)

which would support the theory of these cells being the 'first line of defence' appearing early in the infection process (Doherty *et al*, 1996, Pollock *et al*, 1996).

As the infection progresses, cytokine levels present a dynamic shift in immune profile. Welsh *et al* (2005) showed that cell mediated immunity was prominent in PPD-B stimulated bovine PBMCs through to twenty weeks post infection although the levels of IFN-γ expression showed reduced levels post twenty weeks. Similar patterns in IFN-γ expression have been reported elsewhere (Dean *et al*, 2005, Thacker *et al*, 2006) with marked reduction in levels approximately fifteen weeks following infection. Conversely, expression of IL10 was greater at twenty-six weeks as compared to the levels observed in the earlier stages of infection (Welsh *et al*, 2005). The high levels of IL10 corresponded with strong IgG1 antibody responses due to its role in the differentiation of B-cell immunoglobulin into IgG1 (Garraud and Nutman, 1996). The authors suggest that this change in profile from T_H1 to T_H2/humoral response may be a result of either the host actively suppressing the cell mediated immune response to reduce further tissue damage (Stenger and Modlin, 2002) or immunosuppressive cytokine stimulation via bacterial antigens (Dahl *et al*, 1996).

Another site for cytokine expression studies in bTB are the lymph nodes. The majority of pathological lesions in *M. bovis* naturally infected cattle are confined to the cranial and bronchial lymph nodes (Cassidy, 2006) as the primary source of infection is via aerosol delivery to the lungs (Palmer *et al*, 2002). The infection can become disseminated (travel to other bodily organs), however the 'test and slaughter' programs used in developed countries rarely allow the infection to reach this stage (Cassidy, 2006). Therefore the bronchial and cranial lymph nodes provide the most accurate visualisation of the active site of bTB infection (Liebana *et al*, 2007). Due to the logistical problems of isolating the lymph nodes and the costs of housing large numbers of cattle, the majority of studies analysing cytokine levels in bovine lymph nodes have been focused on one time point following infection (Widdison *et al*, 2006, Thacker *et al*, 2007, Liebana *et al*, 2007, Johnson *et al*, 2006). Widdison *et al* (2006) reported cytokine expression changes in the head lymph nodes of cattle infected with *M. bovis* for sixteen weeks. The levels of TNF-α, IL4 and IL10 were shown to significantly decrease post infection while there was no difference in IFN-γ or IL12 expression (Widdison *et al*, 2006). This suggests that cytokines are expressed in healthy tissue (Tanaka *et al*, 2005) and that some cytokines are preferentially suppressed in response to *M. bovis* infection. The authors conclude that the suppression of anti-inflammatory cytokines IL10 and IL4 was of a consequence of the maintaining pro-inflammatory population (Widdison *et al*, 2006). IL4 has

been shown to be suppressed following mycobacterial infection in previous studies (Rhodes *et al*, 2007, Thacker *et al*, 2007) and has also proved undetectable in some experimental models (Welsh *et al*, 2005, Aung *et al*, 2000).

Table 14: Summary of cytokine protein levels measured over different time points post *M. bovis* infection in cattle. Due to the ease with which blood samples can be taken, the time courses have all been performed on either peripheral blood mononuclear cells or whole blood cultures.

Reference	Experimental design	Cytokine	Pattern of expression
Thacker *et al*, 2007	PBMCs collected at five, fifteen, thirty, sixty and eighty-five days following infection.	IFN-γ	Detected at fifteen days post infection and peaked at thirty days, followed by a slight drop in expression at fifty days which was maintained until day eighty-five.
		TNF-α	Detected from day zero and peaked at thirty days post infection. Expression maintained fairly consistent thereafter.
		IL4	Detected at thirty days post infection and remained consistent thereafter.
		IL10	Detected from day zero and reduced dramatically at day thirty to below the level observed in the non-infected controls. The level increased after sixty days of infection but dropped again at eighty-five days.
Joardar *et al*, 2002	PBMCs collected over forty-five days of infection	IFN-γ	An increase in expression between four and nine weeks (twenty-eight and sixty-three days) post infection.
Welsh *et al*, 2005	PBMCs, collected at four, twelve, twenty, twenty-four and twenty-six weeks following infection.	IFN-γ	Expression peaked at four weeks (twenty-eight days) and declined at twelve weeks (eighty-four days) where it remained stable for the remainder of the experiment.
		IL4	Expression was undetectable for the entire experiment.
		IL10	A decrease in expression was noted in the first four weeks of infection. Levels remained consistent until twenty-six weeks, where expression increased dramatically.
Dean *et al*, 2005	Whole blood cultures collected over twenty-three weeks of infection.	IFN-γ	Protein levels increased significantly between five and fifteen weeks of infection, followed by a reduction post fifteen weeks until the end of the experiment.

Shifts in cytokine profiles are believed to affect the development of granulomatous lesions within the lymph nodes (Widdison *et al*, 2006, Thacker *et al*, 2007) and therefore pathology can also be used as an indicator of disease progression. Microscopic lesions were detected as early as fifteen days (two weeks) post *M. bovis* challenge in bovine retropharyngeal lymph nodes (Palmer *et al*, 2007). This time frame coincides exactly with the first detectable levels of IFN-γ expression (Thacker *et al*, 2007) and illustrates both the importance of the cell mediated response in producing granuloma as well as the efficient speed of lesion development. The microscopic granuloma grew in size and became gross lesion by approximately twenty-eight days (four weeks) following infection. After forty-two days (six weeks), the lesions reached a plateau in size and remained consistent thereafter (Palmer *et al*, 2007). The production of iNOS was detectable from fifteen days through to ninety days (twelve and a half weeks) of infection with a significant peak at forty-two days (Palmer *et al*, 2007). Human studies have shown a positive association between iNOS and T_H1 cytokines such as IFN-γ due to their role in inducing macrophages to produce iNOS (Munder *et al*, 1998). The production of iNOS during the early stages of infection therefore further support the theory of a strong cell mediated response.

Knowledge on the dynamics of the immune response following *M. bovis* infection is extremely important to vaccination developmental studies, as:

a) The ability of the vaccination to protect the host is dependent entirely on the immune response that it elicits. Vaccinations are therefore designed specifically to stimulate the key immune-associated cells that aid in infection control. Time course studies can be used to select those key targets.
b) A common method of assessing the efficacy of a vaccination is to measure cytokine levels (particularly IFN-γ). It is therefore important to know which cytokines are expressed at which time points before they can be used to indicate disease progression.

Within this present study, archival tissue was sourced from three separate investigations involving the infection of cattle with *M. bovis* for five, twelve and nineteen weeks. The tissue samples consisted of thoracic lymph nodes; the cranial mediastinal, caudal mediastinal, left bronchial and cranial tracheobronchial nodes. As previously mentioned, time course experiments are traditionally performed using whole blood cultures due to the ease with which they can be extracted whilst keeping the animal viable. However, the site of *M. bovis* disease

is focused specifically within the lymph nodes (Liebana *et al*, 2007) and therefore a study based on the nodes would provide more accurate information on the time-dependent expression of cytokines.

The three time points (five, twelve and nineteen weeks) were selected as they pertain to a previously un-studied area. The majority of published experiments focusing on cytokine expression within lymph nodes have been taken at later stages of infection post sixteen weeks (Widdison *et al*, 2006, Thacker *et al*, 2007, Johnson *et al*, 2006). However, cytokine expression within PBMCs has been detected as early as two to three weeks post infection (Thacker *et al*, 2007, Hanna *et al*, 1989). It was therefore decided to start the time course experiment as early as possible to provide a comparison in the lymph nodes. The shortest investigations performed on *M. bovis* infected cattle by the VLA are five weeks (as it is neither ethically or economically beneficial to infect cattle for a lesser period of time). The final time point of nineteen weeks was selected as it complemented those experiments published in the literature (Widdison *et al*, 2006, Thacker *et al*, 2007, Johnson *et al*, 2006) and thus the twelve week point provided a mid-way comparison.

RNA extraction and quantitative polymerase chain reaction

The conventional method of studying cytokine transcription levels within infected tissues samples involves tissue liquefaction and total RNA isolation, however, as technology develops this step is becoming less important (Hosokawa *et al*, 2006). There are a number of methods used to isolate total RNA although the gold standard remains to be the Chomczynski and Sacchi single step method (Chomczynski and Sacchi, 1987). RNA degradation is a major concern during isolation as it can lead to a distorted cytokine profile and it is recommended that the tissue be processed immediately after dissection (Bhudevi *et al*, 2003). Modern methods to reduce RNA degradation during tissue storage include aqueous storage compounds such as Trizol (Witchell *et al*, 2008). The standard method of storing tissue sections is to have them fixed immediately after collection in traditionally formalin (Bhudevi *et al*, 2003) but more recently zinc (Mikaelian *et al*, 2004) and Hepes glutamic acid buffer mediated organic solvent protection effect (also known as HOPE) (Olert *et al*, 2001, Witchell *et al*, 2008) prior to embedding within paraffin wax.

Post total RNA isolation, the specific cytokine mRNA population can be identified and amplified using Fluorescent Quantifiable Reverse Transcriptase Polymerase Chain Reaction or qRT-PCR (Bustin, 2002). The advantage of qRT-PCR compared to standard RT-PCR is that it has allowed complete automation of the PCR amplification and analysis stages therefore providing

a higher consistency in data reproducibility (Fleige and Pfaffl, 2006). The methodology of qRT-PCR is based on the same principle as standard RT-PCR using complimentary oligonucleotides that bind to the target sequence allowing repeated temperature dependent 'copying' of the sequence. However, qRT-PCR also involves the use of fluorescence technology to enable a computer to track target sequence amplification/fluorescence build-up in real time. The computer program sets a fluorescence threshold level and as the fluorescence within each reaction exceeds the level set, the computer calculates the number of cycles it takes for this to occur and subsequently produces numerical data. By applying a standard curve of known target sequence quantity, the computer is able to accurately quantify the target sequence within each reaction.

Aim and Objectives

It was proposed to study the immunological responses of cattle infected with *M. bovis* for three specific periods of time. The study was focused on the lymph nodes draining the bronchial region of the animals allowing a response profile to be created for the actual site of infection.

Aim: To produce a time course study of immunological responses in cattle infected with *M. bovis* for five (three animals), twelve (three animals) and nineteen weeks (four animals).

The immune response was measured using quantitative polymerase chain reaction targeting the cytokines interferon gamma (IFN-γ), tumour necrosis factor alpha (TNF-α), interleukin 10 (IL10) and interleukin 4 (IL4).

Objectives:

1. Isolation and dissection of the left bronchial, caudal mediastinal, cranial mediastinal and cranial tracheobronchial lymph nodes of each animal from the three experimental groups. The tissue samples were fixed in buffered formalin and embedded within a paraffin wax block to allow storage.
2. Pathological damage within each lymph node was measured by observing the percentage of granuloma coverage and the stage of granuloma development within mounted sections.
3. Total RNA was extracted from the formalin fixed, paraffin embedded, *M. bovis* infected lymph node tissues followed by quality checks of the extracted nucleic acid using spectrophotometry and agarose gel electrophoresis.
4. QRT-PCR was performed on the extracted total RNA from each lymph node tissue sample by firstly converting total RNA to complimentary DNA (cDNA) followed with target cytokine amplification. The housekeeping gene glyceraldehyde-3-phosphate dehydrogenase (GAPDH) was also targeted to ensure the quality of the starting template. The target mRNA sequences within each lymph node tissue sample was quantified using specifically designed standard curves and expressed in copy numbers.
5. Comparisons were made between the three experimental groups with combined data from all four types of lymph nodes to show the cytokine expression profile over time

post infection. The data was also expressed as individual lymph node types to determine differences in cytokine levels due to lymph node location.

6. To compliment the cytokine expression data within the lymph nodes, levels of IFN-γ protein were measured in cultured peripheral blood samples from each animal using enzyme linked immunosorbant assays (ELISA).

Materials and methods

Source of experimental samples

Experimental infection of large animals such as cattle involves extensive ethical consideration. Archival tissue therefore provides a source on which further experimental procedures can be performed without having to infect more animals. The scientists at the VLA (Surrey) keep an archive of all experimental tissue from each investigation performed, fixed in buffered formalin. It is therefore possible to use the archived tissue samples in numerous molecular and histological techniques many years after the initial experiments took place. To enable study of cytokine expression over different periods of *M. bovis* infection, archived lymph node tissue samples were sourced from three separate experiments in which the parameters met the aims of this study. Each of the studies involved the use of non-vaccinated Friesian Holstein heifers and bullocks of approximately six months of age (with no prior history of tuberculosis infection) which were infected intratracheally with *M. bovis* (a dose of between 0.8 and 1.0 $x10^4$ cfu's). In one study the cattle were euthanized at five weeks of infection (three animals), in another they were euthanized at twelve weeks of infection (three animals) and finally, in the last study the cattle were euthanized at nineteen weeks of infection (four animals). The cattle from all three studies were euthanized by an intravenous injection of pertobarbitonic and the bronchial lymph nodes processed according to the methods described in Chapter 2 (including pathological analysis and tissue fixation).

Archived tissues are an extremely precious source of experimental material and thus are conserved to the highest possible degree. Due to the relatively large amounts of formalin-fixed tissue needed to perform total RNA extraction and quantitative PCR, it was decided to focus this study on four specific lymph node types, the left bronchial, cranial mediastinal, caudal mediastinal and tracheobronchial nodes. Bronchial lymph nodes have been shown to display high levels of pathological development in both natural and experimental *M. bovis* infection (Cassidy *et al*, 2006, Liebana *et al*, 2007) and were therefore specifically selected for analysing immunological activity for the purpose of this study.

Total RNA extraction

Total RNA was extracted from the formalin-fixed lymph node tissues as described in Chapter 2.

Quantitative Polymerase Chain Reaction

Complimentary DNA (cDNA) synthesis:

Table 15: cDNA synthesis reaction mixture for total RNA isolated from *M. bovis* infected (five, twelve and nineteen weeks) formalin fixed lymph node tissues.

Reaction mixture components	Final concentration
ImProm-IT Reaction Buffer	1x
MgCl2	4mM
dNTP mix	0.5mM
ImProm-RT	1x

The protocol was carried out as per the manufacturers' guidelines for the ImProm RT kit (Promega, Southampton, Hampshire, UK). A concentration of 1 ug total RNA was added to a oligo(dT) solution (0.5 µg) and incubated at 70^{o}C for five minutes followed by immediate chilling on ice for five minutes. This was then added to the reaction mixture (Table 15) and vortexed gently. A negative no reverse transcriptase reaction per total RNA sample was also included to ensure that there was no contaminating DNA. The reaction mixture was then incubated at 25^{o}C for five minutes followed then by 42^{o}C for sixty minutes. The resulting cDNA product was quantified using a BioPhotometer (Eppendorf, Germany) and stored at -20^{o}C for subsequent quantitative PCR.

Quantitative PCR was performed using the Quantitect™ Probe PCR kit (Qiagen, Crawley, West Sussex) as described in Chapter 2. The qPCR experiments were designed to allow direct comparison between the three experimental groups of five, twelve and nineteen weeks *M. bovis* infection (Figure 7). Therefore each sample from the three groups had to be included in the same ninety six well PCR plate to avoid the complication of plate to plate variation. Within each PCR plate, all samples of one lymph node over the three experimental groups were analysed for one target cytokine. Each lymph node sample was analysed for the expression of all four cytokines; IFN-γ, TNF-α, IL10 and IL4. The mRNA expression of the housekeeping gene glyceraldehyde-3-phosphate dehydrogenase (GAPDH) was also measured within each sample to ensure the quality of the cDNA transcript. Lastly, each PCR plate included the

diluted standard templates specific to the target cytokine to allow construction of the standard curve (as described in Chapter 2).

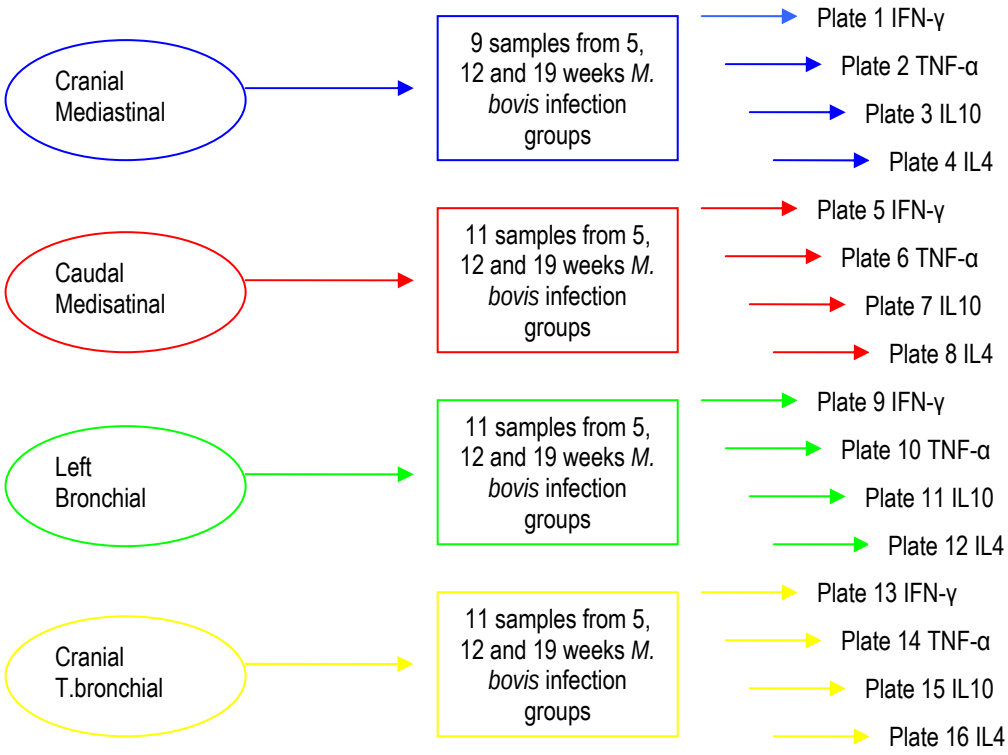

Figure 7: Quantitative PCR experimental designs for the time course study. Each 96 well plate contained reactions analysing one cytokine from all samples of one lymph node from the three experimental groups (five, twelve and nineteen weeks of infection). This allowed the direct 'in- plate' comparison of cytokine levels between the three experimental groups and reduced the potential problem of plate to plate variability. The specific standard curve for the cytokine and GAPDH were also run on each plate. Each reaction was performed either in duplicate or triplicate.

Whole blood IFN-γ cultures

Samples of heparinized whole blood were collected from each of the animals prior to euthanization by a trained scientist at the VLA (Surrey), as described in Chapter 2. The data from the BOVIGAM® tests were used to compare against the lymph node cytokine data.

Results

Total RNA extraction

The first step in the study of cytokine gene expression was to isolate total RNA from the four thoracic lymph nodes of each *M. bovis* infected cow in the three experimental groups (five, twelve and nineteen weeks post infection). The formalin fixed, paraffin embedded samples required a modified method of RNA extraction that involved deparaffinisation of the sample with xylene followed by tissue liquefaction and RNA isolation. Total RNA was quantified (Table 16) using a BioPhotometer (Eppendorf, Germany) and run on a 1% agarose electrophoresis gel (TAE buffer) to determine integrity (visualisation of the ribosomal RNA bands, Figure 8).

Table 16: Quantification (µg/ml) and purity determined by spectrophotometry of total RNA isolated from *M. bovis* infected formalin-fixed, paraffin embedded cattle lymph node tissues. The results represent averaged lymph node results of over 500 extractions in total.

Tissue type (n=500)	Total RNA (20 µl) quantification µg/ml (mean ± SD)	260/280 nm ratio (mean ± SD)
Formalin fixed paraffin embedded lymph node tissue	170.28 ± 80.3	1.8 ± 0.11

Total RNA was successfully isolated from all of the lymph node samples of cattle infected with *M. bovis* for five, twelve and nineteen weeks. The mean concentration of total RNA extracted from approximately 500 formalin fixed tissue sections was 170.28 µg/ml (or 3.4 µg/20 µl, Table 16). The large standard deviation from the mean associated with this data (80.3, Table 16) suggests that the concentration of total RNA extracted from the different lymph node samples was extremely varied (range from 44.5 to 388 µg/ml). The ratio of total RNA (OD at 260 nm) to protein (OD at 280 nm) was within the recommended range of between 1.7 and 2 (mean ratio of 1.8, Table 16) (Fleige and Pfaffl, 2006).

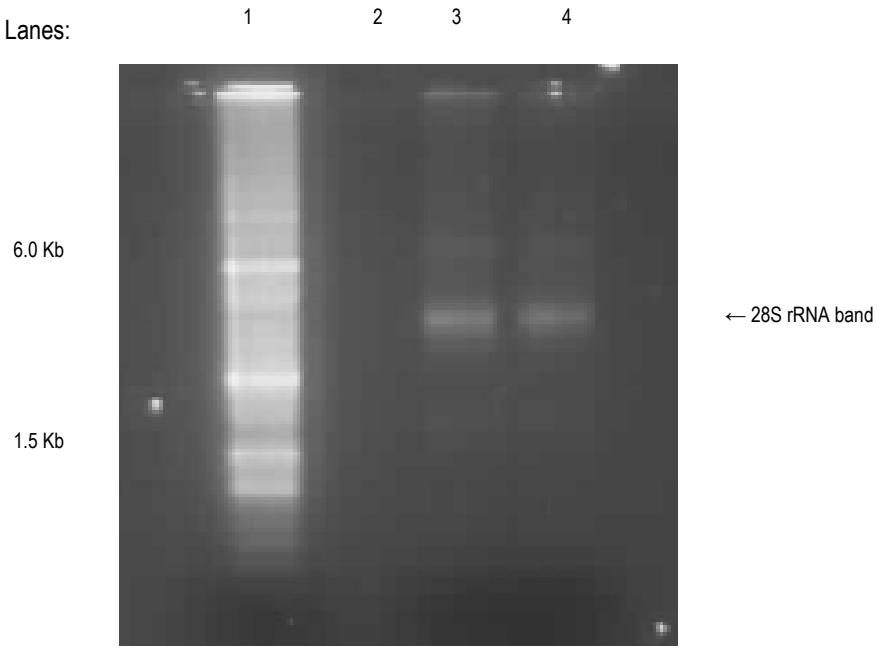

Figure 8: Agarose gel electrophoresis (1% agarose within TAE buffer and ethidium bromide staining) of total RNA samples (300 ng/ well) isolated from *M. bovis* infected formalin-fixed, paraffin embedded cattle lymph node tissues (lanes 3 and 4). Both total RNA samples displayed a 28S ribosomal RNA band of approximately 4 Kb in length. Lane 1 is a 0.5-10 Kb RNA ladder with highlighted standard RNA base pair lengths of 6 and 1.5 Kb. Lane 2 was not used. The electrophoresis experiment was repeated with different total RNA samples 10 times and displayed consistent results.

Each total RNA sample displayed a band of approximately 4 Kb in length (Figure 8). This nucleotide length corresponds to the expected length of 28S ribosomal RNA (Bradford *et al*, 2005) and gives an indication to the high level of integrity of the total RNA samples. There was little evidence of DNA contamination, which would be represented by clear bright bands nearer to the wells.

Quantitative Polymerase Chain Reaction

Standard curves

Standard templates for the cytokines IFN-γ, TNF-α, IL10 and IL4 were designed and serially diluted to produce a standard curve (Table 7 and 8). This allowed conversion of the calculated crossing point values of the unknown samples into quantitative copy number.

As can be seen from figure 9, each standard template produced a standard curve to enable quantification of the unknown samples. The line equation of each graph fulfilled the requirements of a reliable standard curve, as the slope of each line was around the ideal value of -3.32 (signifying a doubling of PCR product during each cycle), the R^2 of each graph was between 0.98-0.99 (Figure 9) suggesting an extremely tight fit/correlation of the data points and the amplification efficiency 'E' was between 2-2.1 (Figure 9) indicating 100% efficiency of each reaction.

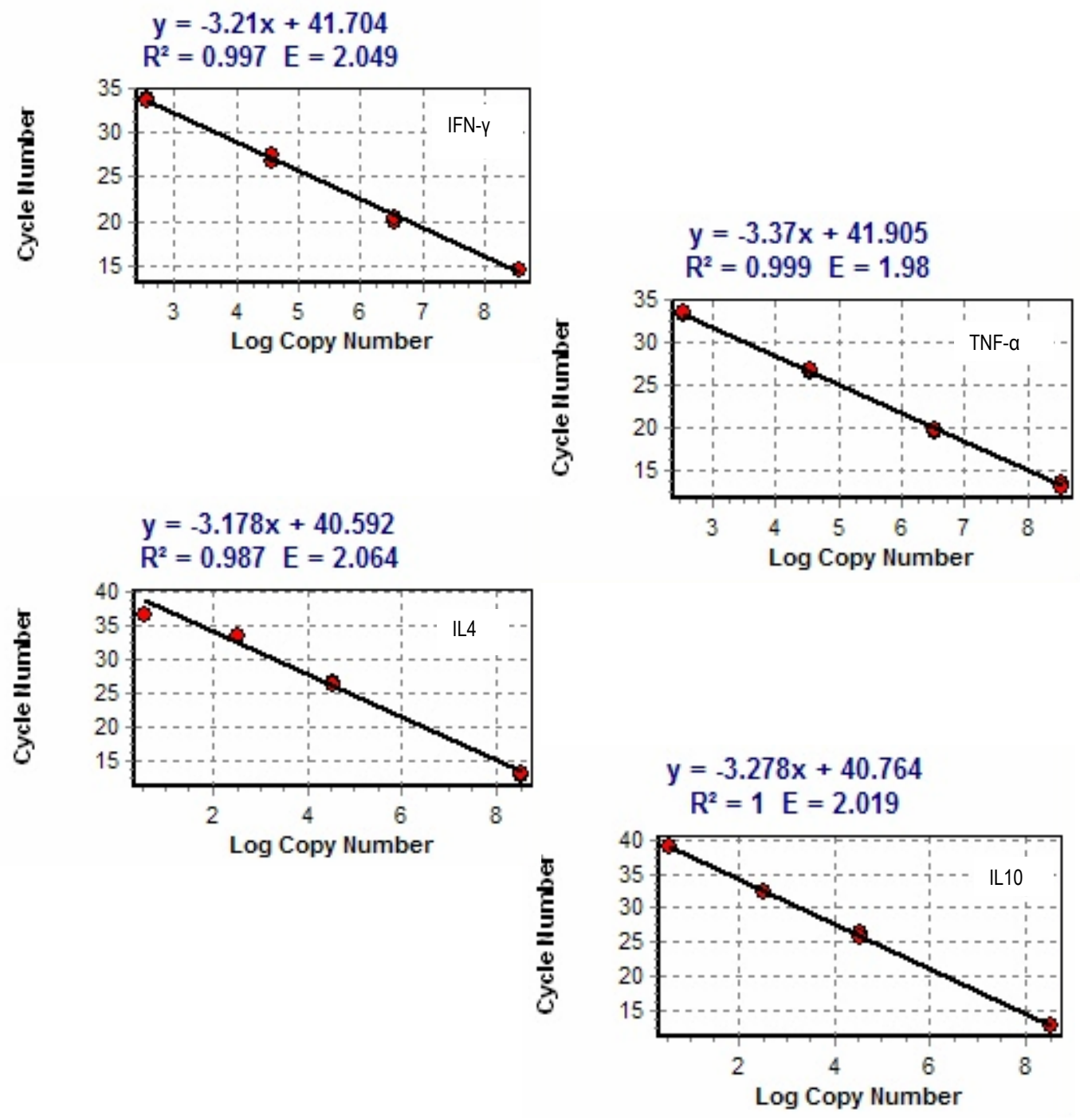

Figure 9: Quantitative PCR standard curves for IFN-γ, TNF-α, IL10 and IL4. Each standard template was designed to mimic the specific mRNA target cytokine sequence to allow sequence specific annealing of the complimentary primer and probe set during qPCR. A known concentration of the standard template was serially diluted and four of these dilutions (corresponding to $3x10^8$, $3x10^4$, $3x10^2$ and 3 copies) were run on each PCR plate. The computer program (Quantica, Techne) calculated the crossing point value for each standard template and produced a standard curve to enable quantification of the unknown samples. The equation of each graph is also displayed.

Glyceraldehyde-3-phosphate dehydrogenase (GAPDH)

The housekeeping gene GAPDH was analysed by PCR for each sample alongside each target cytokine to ensure the quality of the starting cDNA template. In the absence of a cytokine PCR product, the presence of a GAPDH PCR product ensured that the sample template was of a high quality. The mean crossing point values of GAPDH expression for each lymph node from all of the cattle within the three experimental groups was plotted within a bar chart (Figure 10).

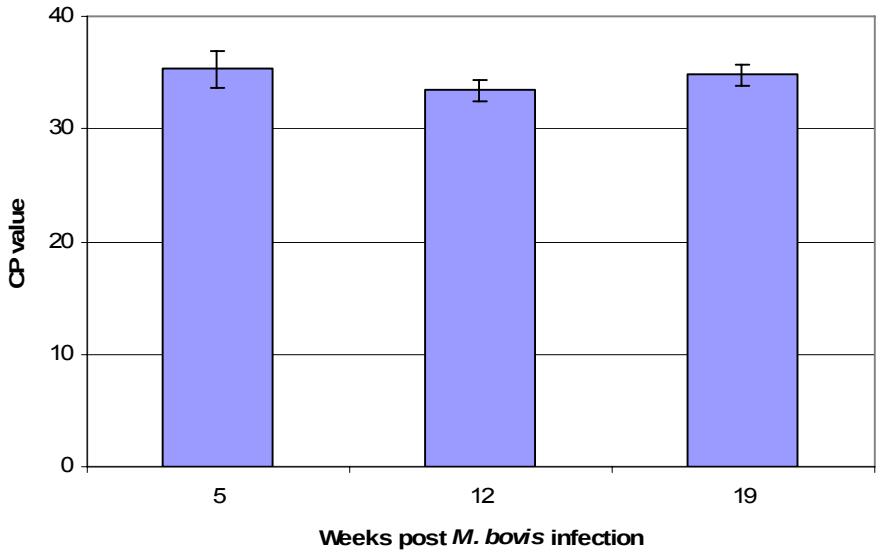

Figure 10: The crossing point (CP) values of GAPDH expression from cattle infected with *M. bovis* for five (n=3), twelve (n=3) and nineteen (n=4) weeks. The data represents the mean values from the lymph node samples of all cattle within each experimental group. The error bars represent the standard deviation (±) of the data.

There was no difference between the three experimental groups (five weeks post infection mean of 35.3, twelve weeks post infection mean of 34 and nineteen weeks post infection mean of 34.7, Figure 10) for GAPDH expression. This suggested that any potential differences in cytokine expression between the three groups were unlikely to be due to the physical condition of the template.

Cytokine mRNA expression in the combined lymph nodes

Cattle infected with *M. bovis* over three different time periods (five, twelve and nineteen weeks) were used within this study to explore the changes in cytokine mRNA expression as the infection progressed. IFN-γ, TNF-α, IL10 and IL4 mRNA levels were quantitatively measured in four different lymph nodes from each animal (left bronchial, cranial mediastinal, caudal mediastinal and cranial tracheobronchial lymph nodes). The individual lymph node results were then combined to give an overall view of cytokine expression over time.

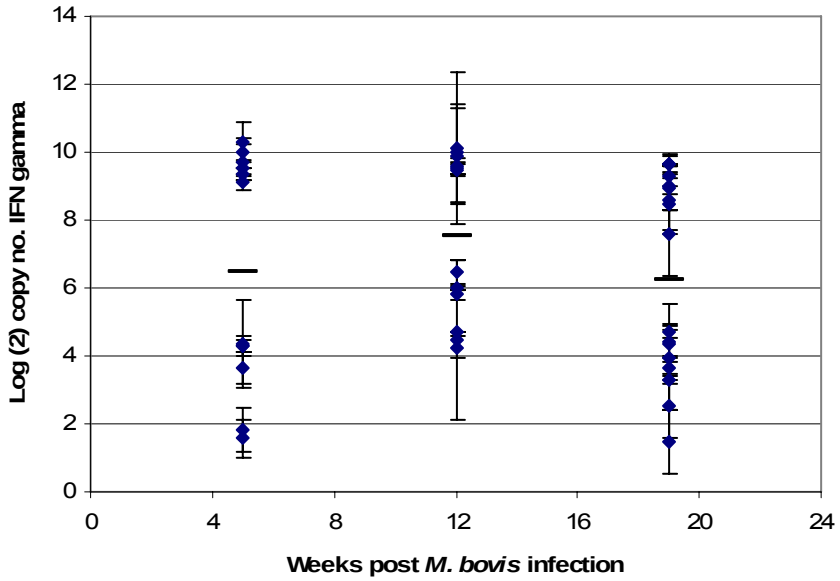

Figure 11: Quantitative PCR of IFN-γ mRNA in the lymph nodes of cattle infected with *M. bovis* for five, twelve and nineteen weeks. The data are presented in $\log_2$ copy number and each individual point represents the mean triplicate data of an individual lymph node from one animal. Four lymph node types were used from each animal (the left bronchial, cranial mediastinal, caudal mediastinal and cranial tracheobronchial) and within each group there were either three (five and twelve weeks post infection) or four (nineteen weeks post infection) animals. Error bars represent standard deviation (±) of each point and the mean of each group is shown by — symbol. There was no significant difference between the three experimental groups ($p>0.05$, Kruskal Wallis test).

At five weeks post infection, the expression levels of IFN-γ mRNA (Figure 11) were comparatively lower (mean $\log_2$ copy number of 6.50) than at twelve weeks post infection (mean $\log_2$ copy number 7.53). The IFN-γ mRNA levels then decreased between twelve and nineteen weeks post infection (mean $\log_2$ copy number 6.22, Figure 11). The expression level at nineteen weeks was slightly lower than at five weeks post infection. The differences in IFN-γ levels over time were not significant ($p> 0.05$, Kruskal Wallis test).

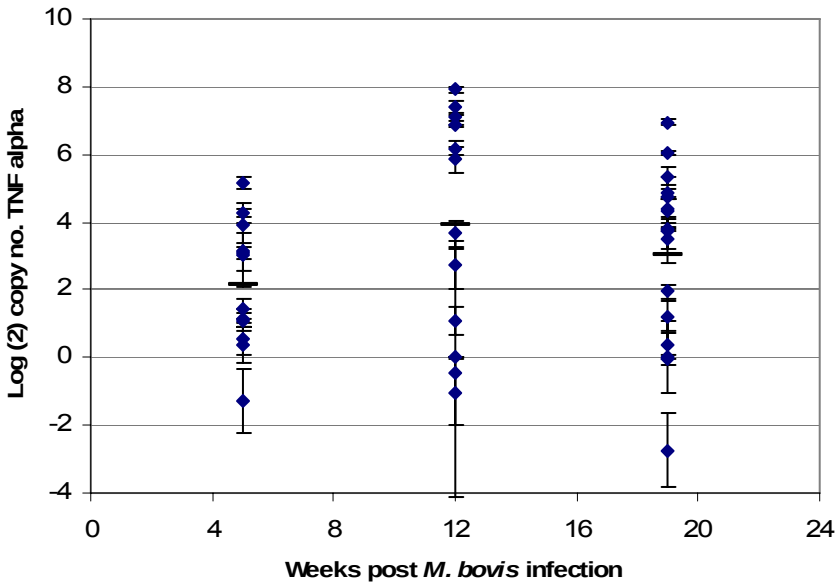

Figure 12: Quantitative PCR of TNF-α mRNA in the lymph nodes of cattle infected with *M. bovis* for five, twelve and nineteen weeks. The data are presented in log_2 copy number and each individual point represents the mean triplicate data from an individual lymph node from one animal. Four lymph node types were used from each animal (the left bronchial, cranial mediastinal, caudal mediastinal and cranial tracheobronchial) and within each group there were either three (five and twelve weeks post infection) or four (nineteen weeks post infection) animals. Error bars represent standard deviation (±) of each point and the mean of each group is shown by — symbol. There were no significant differences between the three experimental groups ($p>0.05$, Kruskal Wallis test).

The mRNA expression level of TNF-α (Figure 12) was comparatively lower at five weeks post infection (mean log_2 copy number of 2.15) as compared to twelve weeks post infection (mean log_2 copy number of 3.94). Similar to the IFN-γ profile, there was a decrease in TNF-α mRNA expression (Figure 12) between twelve and nineteen weeks post infection (mean log_2 copy number 3.02). However the level of mRNA at nineteen weeks stayed above the level measured at five weeks post infection. The changes in TNF-α mRNA expression over time were not significant ($p>0.05$, Kruskal Wallis test)

Interestingly there appeared to be a slight segregation of data points, particularly in Figure 11 but also at twelve weeks post infection in Figure 12, with a group of points positioned above the mean and a group positioned below. This suggests that the lymph node samples could be separated into two groups, those expressing considerably higher cytokine IFN-γ and those expressing lower levels. This difference is not reflected in the mean of each time point post infection and will be described in more detail at a later point.

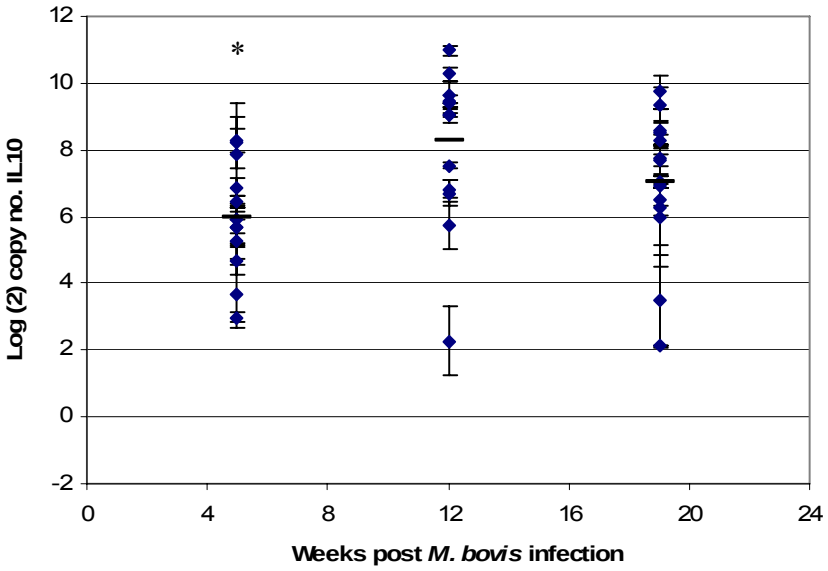

Figure 13: Quantitative PCR of IL10 mRNA in the lymph nodes of cattle infected with *M. bovis* for five, twelve and nineteen weeks. The data are presented in log_2 copy number and each individual point represents the mean triplicate data from an individual lymph node from one animal. Four lymph node types were used from each animal (the left bronchial, cranial mediastinal, caudal mediastinal and cranial tracheobronchial) and within each group there were either three (five and twelve weeks post infection) or four (nineteen weeks post infection) animals. Error bars represent standard deviation (±) of each point and the mean of each group is shown by — symbol. A significant difference between the three experimental groups is represented by * ($p<0.01$, Mann Whitney test).

IL10 mRNA expression levels (Figure 13) were significantly lower at five weeks post infection (mean log_2 copy number 5.97) compared to the expression at twelve weeks post infection (mean log_2 copy number 8.27, $p<0.01$, Mann-Whitney test and Bonferroni corrected). Between twelve and nineteen weeks post infection, there was a slight reduction in expression for IL10 (mean log_2 copy number 7.03) however this was not significant ($p>0.05$, Mann Whitney test). Though the IL10 mRNA level at nineteen weeks stayed above the level measured at five weeks post infection there was no statistical difference between the two time periods ($p>0.05$, Mann Whitney test).

Quantitative PCR of IL4 mRNA expression produced a PCR product with the same crossing point values as the negative controls consistently in all of the animal samples. It was therefore not possible to include the data as a reliable indication of IL4 mRNA within the cattle samples.

Cytokine mRNA expression in the individual lymph nodes

The cytokine mRNA expression levels of IFN-γ, TNF-α and IL10 over the three time periods were analysed within the individual lymph node types (left bronchial, caudal mediastinal, cranial mediastinal and cranial tracheobronchial). The copy numbers of IFN-γ, TNF-α and IL10 from every animal over the three different time periods (five, twelve and nineteen weeks) were grouped and divided into four categories based on the lymph node type. The four groups were then compared using the Kruskal Wallis test to determine whether there were any statistical differences in cytokine expression between the lymph node types. There was a significant difference in the cytokine levels of IFN-γ ($p<0.001$) and TNF-α ($p<0.01$) however there was no significant difference in IL10 mRNA levels ($p>0.05$, Kruskal Wallis test). The same data was then applied to the Mann Whitney test (using Bonferroni correction, Table 17) to determine specifically which lymph node types displayed a significant difference in IFN-γ and TNF-α mRNA expression.

Table 17: Statistical differences (p values determined by Mann Whitney test) of IFN-γ (top right corner) and TNF-α (bottom left corner) mRNA expression levels between the four lymph node types over the three experimental time periods (five, twelve and nineteen weeks post infection).

	LB	CM	CRM	CRT
LB		**<0.001**	0.684	**<0.001**
CM	0.529		**<0.001**	0.529
CRM	0.353	0.481		**<0.001**
CRT	0.029	0.043	**<0.001**	

Significant differences in cytokine mRNA expression levels between the four lymph node types were first ensured using the Kruskal Wallis test (IFN-γ; $p<0.001$, TNF-α; $p=0.009$ and IL10; $p=0.832$). The data for IFN-γ and TNF-α expression was then applied to the Mann-Whitney test and the p-values displayed within the table (values are deemed significant if lower than 0.008 (Bonferroni corrected) and are in bold type and underlined). LB: left bronchial; CM: caudal mediastinal; CRM: cranial mediastinal; CRT: cranial tracheobronchial lymph nodes.

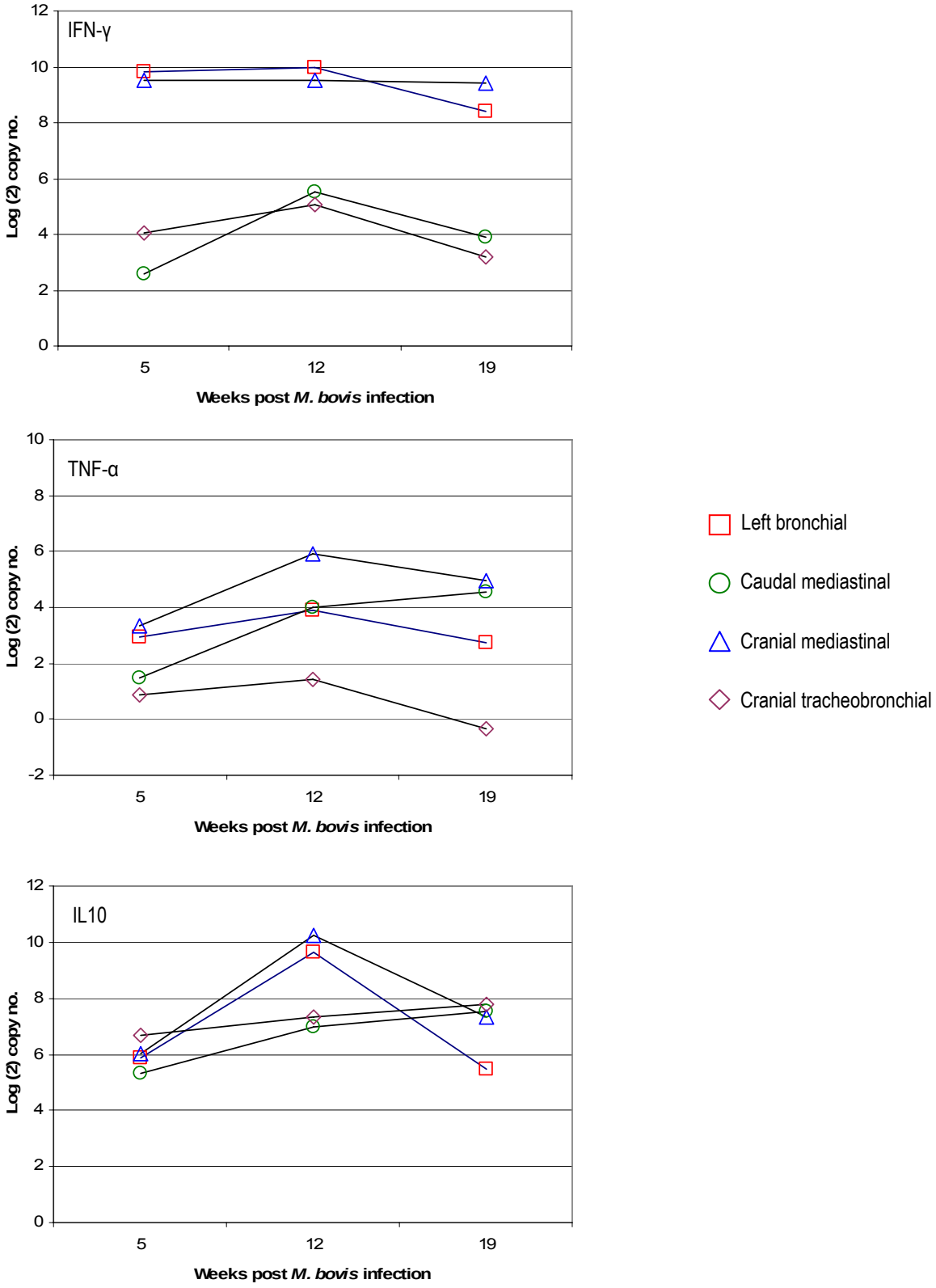

Figure 14: Quantitative PCR of IFN-γ, TNF-α and IL10 mRNA expression within the left bronchial, caudal mediastinal, cranial mediastinal and cranial tracheobronchial lymph nodes of cattle infected with *M. bovis* for five, twelve and nineteen weeks. The data are presented as $\log_2$ copy number and each data point represents the mean triplicate mRNA expression of each lymph node (at each time point) from either three (five and twelve weeks infection) or four animals (nineteen weeks infection).

The left bronchial lymph node had between 8.4 and 10 mean log_2 copies of IFN-γ mRNA over five, twelve and nineteen weeks post *M. bovis* infection (Figure 14). This was significantly higher than the IFN-γ mRNA expression levels in both the caudal mediastinal (mean log_2 copy numbers between 2.6 and 5.5, Figure 14) and the cranial tracheobronchial lymph nodes (mean log_2 copy numbers between 3.2 and 5.5, Figure 12, $p<0.001$, Mann Whitney test and Bonferroni correction, Table 17).

The cranial mediastinal lymph node had between 9.4 and 9.5 mean log_2 copy numbers of IFN-γ mRNA over five, twelve and nineteen weeks post *M. bovis* infection (Figure 14). This was significantly higher than the IFN-γ mRNA expression levels in both the caudal mediastinal and the cranial tracheobronchial lymph nodes ($p<0.001$, Mann Whitney test and Bonferroni correction, Table 17).

There was no significant difference in the level of IFN-γ mRNA expression between the left bronchial and cranial mediastinal lymph nodes ($p>0.05$, Mann Whitney test, Table 17) or between the caudal mediastinal and cranial tracheobronchial lymph nodes ($p>0.05$, Mann Whitney test, Table 17).

The cranial tracheobronchial lymph node had between -1.3 and 1.4 mean log_2 copies of TNF-α mRNA over the five, twelve and nineteen weeks post *M. bovis* infection (Figure 14). This appeared to be significantly lower than the TNF-α mRNA expression levels in the left bronchial (mean log_2 copy numbers between 2.7 and 4, Figure 14), the caudal mediastinal (mean log_2 copy numbers between 1.4 and 4, Figure 14) and the cranial mediastinal lymph nodes (mean log_2 copy number between 3.3 and 6, Figure 14, $p<0.05$, Mann Whitney test, Table 17). However, applying Bonferroni correction, the only significant difference in TNF-α expression was between the cranial tracheobronchial and cranial mediastinal lymph nodes ($p>0.001$, Mann Whitney test, Table 17).

There was no significant difference in the level of TNF-α mRNA expression between the left bronchial, cranial mediastinal and caudal mediastinal lymph nodes ($p>0.05$, Mann Whitney test, Table 17).

As previously mentioned, there was no significant difference in IL10 mRNA expression between the four lymph node types ($p>0.05$, Kruskal Wallis test). The expression of IL10 mRNA ranged between 5.5 and 10 mean log_2 copies over the five, twelve and nineteen weeks post infection for all four lymph nodes (Figure 14).

Cytokine profile of the left bronchial lymph node

Figure 15: Quantitative PCR of IFN-γ, IL10 and TNF-α mRNA expression within the left bronchial lymph node of cattle infected with *M. bovis* for five, twelve and nineteen weeks. The data are presented as log_2 copy number and each point represents the combined mean triplicate data of each left bronchial lymph node from either three animals (five and twelve weeks post infection) or four animals (nineteen weeks post infection). Differences between time periods were not significant ($p>0.016$, Mann Whitney and Bonferroni correction).

Within the left bronchial lymph node, the mRNA expression levels of IFN-γ, TNF-α and IL10 over the three time periods paralleled the results seen in combining all of the lymph nodes (Figures 11, 12 and 13).

Between five and twelve weeks post infection there was a slight increase in IFN-γ mRNA expression (mean log_2 copy number 9.81 and 10, respectively, Figure 15) and then a decrease between twelve and nineteen weeks (mean log_2 copy number 8.39). The level of IFN-γ at nineteen weeks post infection was lower than at five and twelve weeks post infection, however this was not significant ($p>0.016$, Mann Whitney test and Bonferroni correction).

IL10 mRNA levels displayed an increase between five and twelve weeks post infection (mean log_2 copy number 5.87 and 9.65, respectively, Figure 15) and a decrease between twelve and nineteen weeks (mean log_2 copy number 5.46) to that below the expression level at five weeks.

The mRNA level of TNF-α also increased between five and twelve weeks post infection (mean log_2 copy number 2.95 and 3.92, respectively) and then decreased between twelve and nineteen weeks (mean log_2 copy number 2.73).

Within the left bronchial lymph node, IFN-γ mRNA was the dominant cytokine expressed at a significantly higher level when compared to IL10 and TNF-α mRNA over the three time periods ($p=0.01$ and <0.001, respectively, Mann Whitney test and Bonferroni correction). IL10 was the second highest expressed cytokine mRNA and was higher than TNF-α mRNA expression, however this was not significant after application of the Bonferroni correction ($p=0.022$, Mann Whitney test). TNF-α was the least expressed cytokine mRNA.

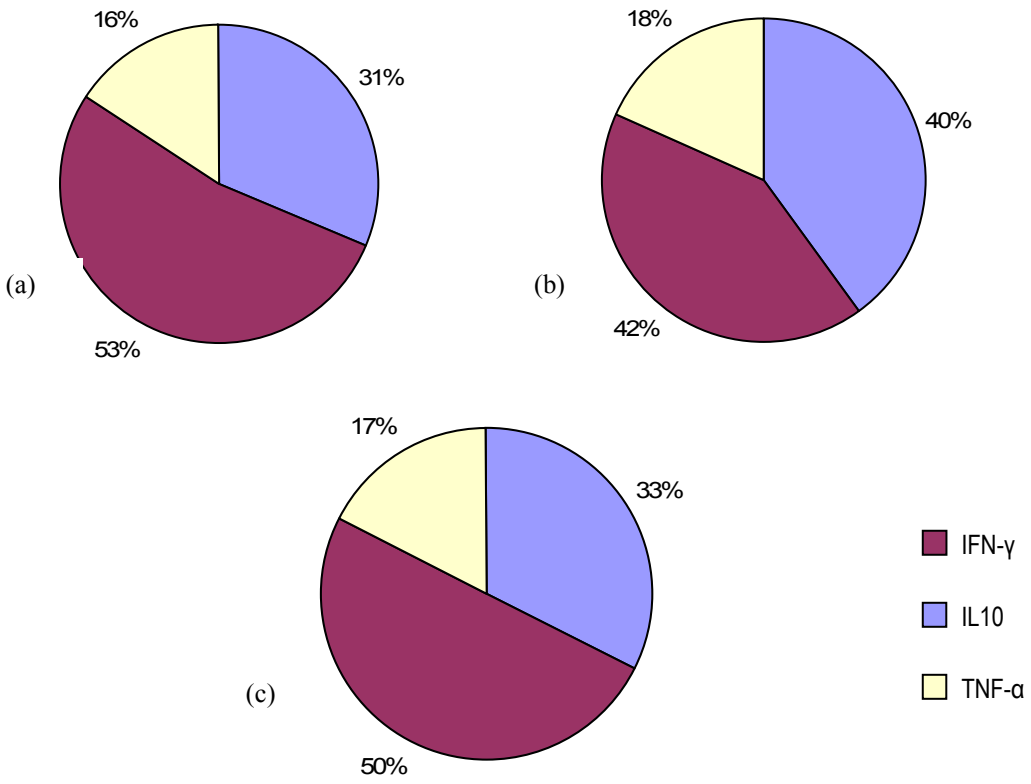

Figure 16: Percentage profile of cytokines IFN-γ, TNF-α and IL10 mRNA within the left bronchial lymph node over five (a), twelve (b) and nineteen (c) weeks post infection. The cytokine copy number data from the mean triplicate results of each left bronchial lymph node from either three (five and twelve weeks) or four (nineteen weeks) cattle were combined and each individual cytokine value calculated as a percentage of the overall expression profile.

The data in Figure 15 was used to build a profile of the percentage of each expressed cytokine within the left bronchial lymph node at each time point (Figure 16). As previously mentioned, IFN-γ mRNA was expressed at a significantly higher level (in copy number) as compared to

TNF-α and IL10 mRNA within the left bronchial lymph node (Figure 15). Similarly, when the copy number data was converted into a percentage profile, IFN-γ was the largest component over the entire nineteen week infection period (Figure 16). Between five and twelve weeks of infection, the percentage of IFN-γ as a component of the left bronchial lymph node profile decreased (from 53% to 42%) accompanied by an increase in both TNF-α (from 16% to 18%) and IL10 (from 31% to 40%, Figure 16). At nineteen weeks post infection, IFN-γ mRNA expression as a percentage of the profile increased (50%) whereas levels of TNF-α and IL10 decreased (17% and 33%, respectively, Figure 16).

Cytokine profile of the cranial mediastinal lymph node

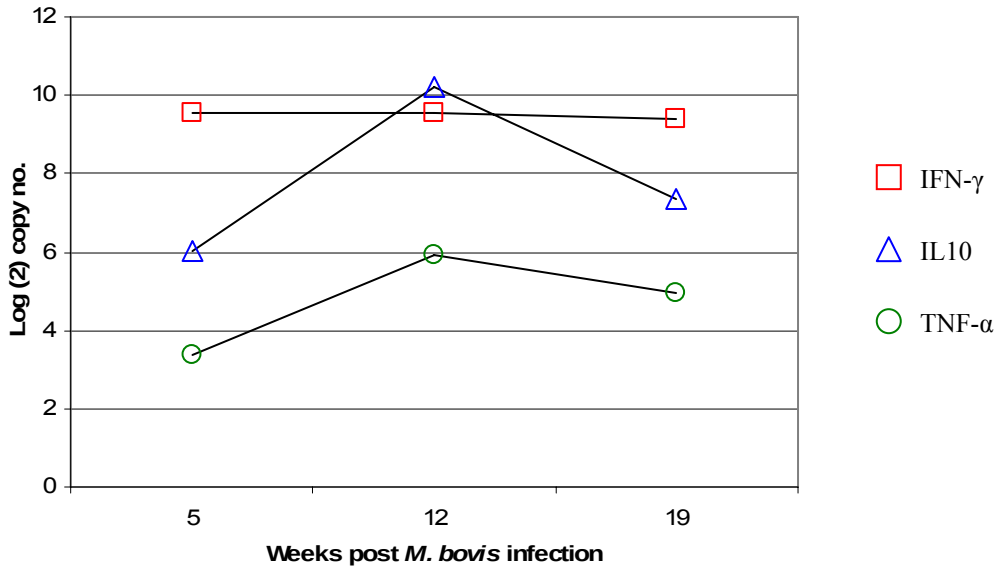

Figure 17: Quantitative PCR of IFN-γ, IL10 and TNF-α mRNA expression within the cranial mediastinal lymph node of cattle infected with *M. bovis* for five, twelve and nineteen weeks. The data are presented as $\log_2$ copy number and each point represents the combined mean triplicate data of each cranial mediastinal lymph node from either three animals (five and twelve weeks post infection) or four animals (nineteen weeks post infection). Differences between time periods were not significant ($p>0.05$, Kruskal Wallis test).

Within the cranial mediastinal lymph node, the cytokine expression levels of IL10 and TNF-α mRNA showed a similar pattern to the combined lymph node data (Figures 11, 12 and 13). Between five and twelve weeks post infection, there was an increase in IL10 mRNA levels (mean $\log_2$ copy number 6 and 10.22, respectively, Figure 17) and a decrease between twelve and nineteen weeks post infection (mean $\log_2$ copy number 7.35).

The expression levels of TNF-α mRNA increased between five and twelve weeks post infection (mean $\log_2$ copy number 3.35 and 5.91, respectively, Figure 17) and decreased between twelve and nineteen weeks post infection (mean $\log_2$ copy number 4.95).

The expression levels of IFN-γ showed a slightly different pattern over time (Figure 17). The mRNA level remained stable between five and twelve weeks post infection (mean $\log_2$ copy number 9.53, Figure 17) with a very slight decrease at nineteen weeks infection (mean $\log_2$ copy number 9.40). The changes in cytokine mRNA copy number seen within the cranial mediastinal were not significant ($p>0.05$, Kruskal Wallis test).

The cytokine mRNA copy numbers of the cranial mediastinal lymph node showed a joint dominance of IFN-γ and IL10 mRNA expression ($p>0.05$, Mann Whitney test). IFN-γ was

expressed at a significantly higher level when compared to TNF-α ($p<0.001$, Mann Whitney test). However, upon application of the Bonferroni correction, there was no significant difference between IL10 and TNF-α expression ($p>0.016$, Mann Whitney test) despite IL10 being expressed at a higher level.

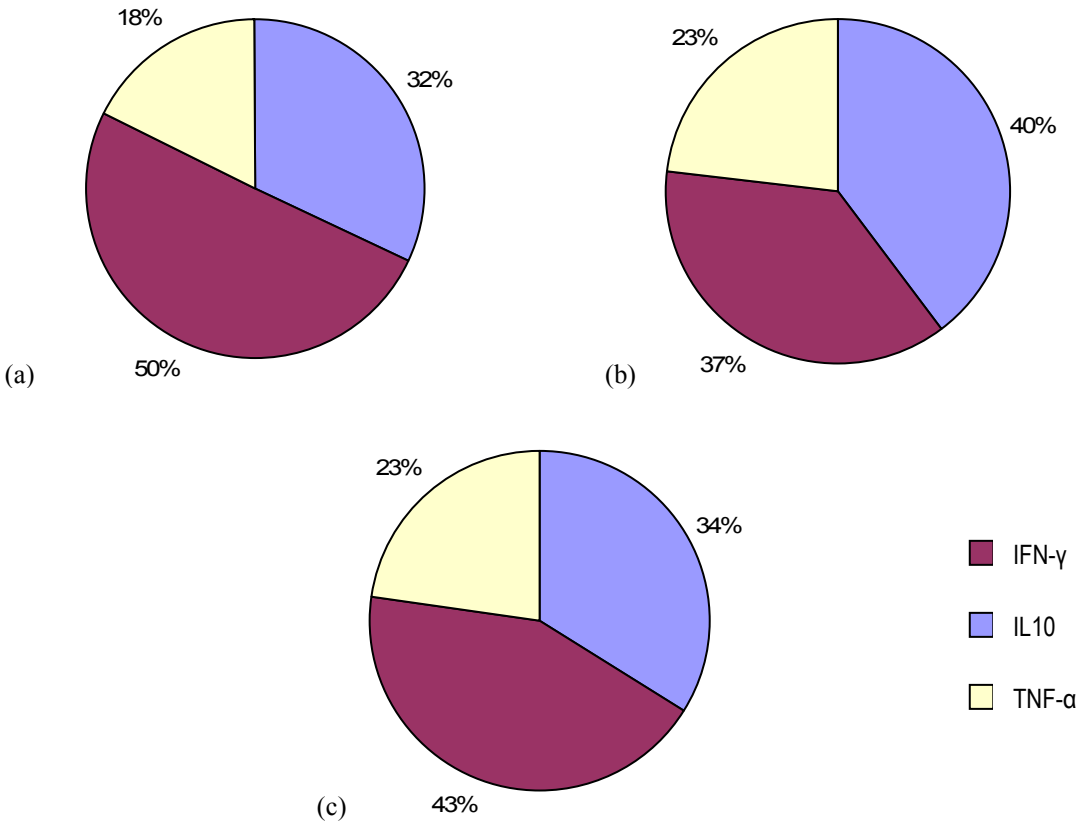

Figure 18: Percentage profile of cytokines IFN-γ, TNF-α and IL10 mRNA within the cranial mediastinal lymph node over five (a), twelve (b) and nineteen (c) weeks post infection. The cytokine copy number data from the mean triplicate results of each cranial mediastinal lymph node from either three (five and twelve weeks) or four (nineteen weeks) cattle were combined and each individual cytokine value calculated as a percentage of the overall expression profile.

The data in Figure 17 was used to build a profile of the percentage of each cytokine within the cranial mediastinal at each time point (Figure 18). As previously mentioned, IFN-γ and IL10 mRNA were both expressed at a higher level (in copy number) as compared to TNF-α mRNA within the cranial mediastinal lymph node (Figure 17). Following conversion into a percentage profile, IFN-γ mRNA is the largest expressed component in the cranial mediastinal lymph node

at five weeks post infection (IFN-γ at 50%, TNF-α at 18% and IL10 at 32%, Figure 18). At twelve weeks post infection, although IFN-γ mRNA copy number levels remained constant (Figure 17), the percentage of IFN-γ mRNA as a component of the lymph node cytokine profile decreased (37%, Figure 18). Between five and twelve weeks, the percentages of both IL10 and TNF-α mRNA increased (40% and 23%, respectively, Figure 18). As a consequence, IL10 expression replaced IFN-γ as the largest component of the cytokine profile at twelve weeks of infection. Following nineteen weeks of *M. bovis* infection, the percentage of IFN-γ mRNA within the lymph node increased (43%) however this was still lower than at five weeks post infection. The percentage of IL10 mRNA within the cranial mediastinal lymph node decreased at nineteen weeks post infection (34%) whereas levels of TNF-α mRNA remained stable (23%, Figure 18).

Cytokine profile of the cranial tracheobronchial lymph node

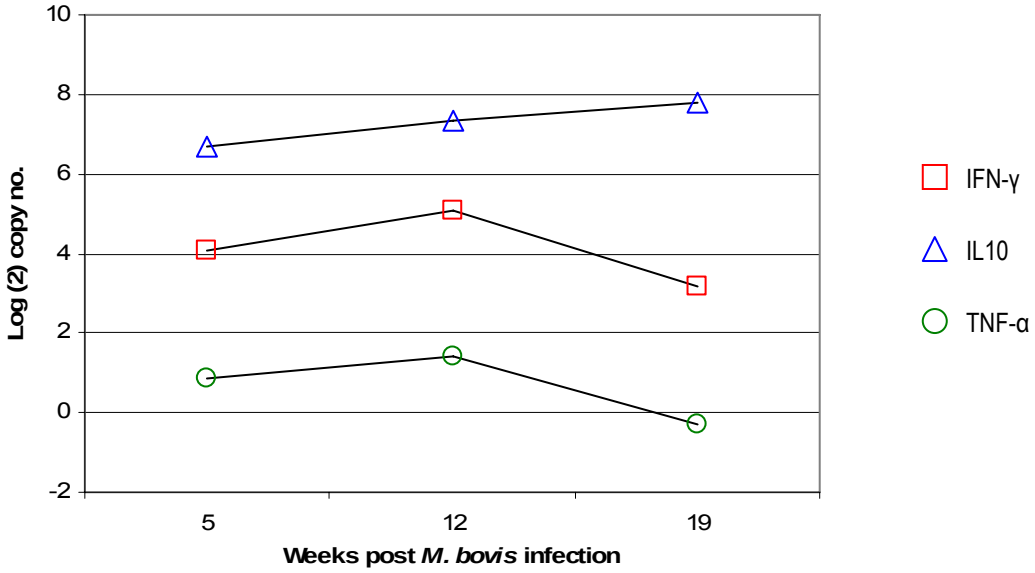

Figure 19: Quantitative PCR of IFN-γ, IL10 and TNF-α mRNA expression within the cranial tracheobronchial lymph node of cattle infected with *M. bovis* for five, twelve and nineteen weeks. The data are presented as log_2 copy number and each point represents the combined mean triplicate data of each cranial tracheobronchial lymph node from either three animals (five and twelve weeks post infection) or four animals (nineteen weeks post infection). Differences between time periods were not significant ($p>0.05$, Kruskal Wallis test)

The expression patterns of IFN-γ and TNF-α were very similar within the cranial tracheobronchial lymph node (Figure 19). IFN-γ mRNA increased between five and twelve weeks post infection (mean log_2 copy number 4.07 and 5.07, respectively, Figure 19) and decreased between twelve and nineteen weeks (mean log_2 copy number 3.19).

The level of TNF-α mRNA expression increased between five and twelve weeks post infection (mean log_2 copy number 0.85 and 1.4, respectively, Figure 19) and decreased between twelve and nineteen weeks infection (mean log_2 copy number -0.32).

The expression level of IL10 mRNA showed a slightly different pattern (Figure 19), by increasing steadily between five (mean log_2 copy number 6.68) twelve (mean log (2) copy number 7.32) and nineteen weeks post infection (mean log_2 copy number 7.78). The differences in cytokine expression between the time periods were not significant ($p>0.05$, Kruskal Wallis test).

Within the cranial tracheobronchial lymph node, IL10 mRNA was dominantly expressed above both IFN-γ and TNF-α ($p<0.001$, Mann Whitney test and Bonferroni correction). IFN-γ mRNA

was expressed at a significantly higher level as compared to TNF-α ($p<0.001$, Mann Whitney test and Bonferroni correction).

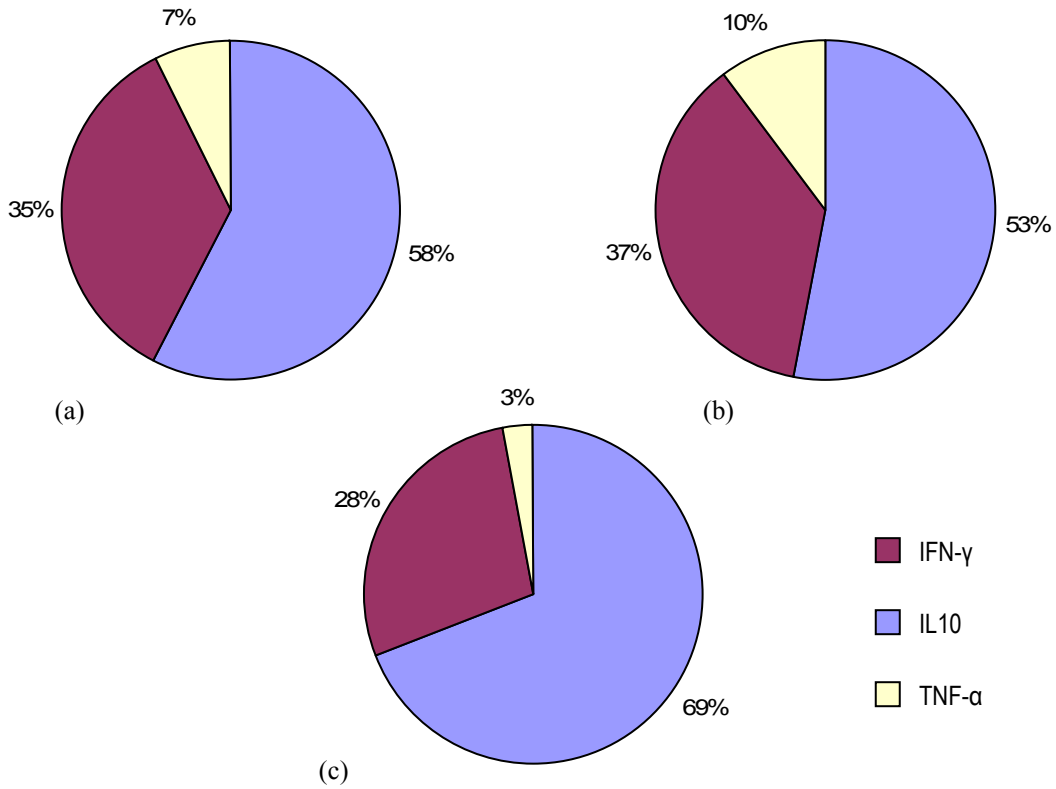

Figure 20: Percentage profile of cytokines IFN-γ, TNF-α and IL10 mRNA within the cranial tracheobronchial lymph node over five (a), twelve (b) and nineteen (c) weeks post infection. The cytokine copy number data from the mean triplicate results of each cranial tracheobronchial lymph node from either three (five and twelve weeks) or four (nineteen weeks) cattle were combined and each individual cytokine value calculated as a percentage of the overall expression profile.

The data in Figure 19 was used to build a profile of the percentage of each cytokine within the cranial tracheobronchial lymph node at each time point (Figure 20). As previously mentioned, IL10 mRNA was expressed at a significantly higher level (in copy number) as compared to IFN-γ and TNF-α mRNA within the cranial tracheobronchial lymph node (Figure 19). Similarly, when the copy number data was converted into a percentage profile, IL10 was the largest component over the entire nineteen week infection period (Figure 20). Between five and twelve weeks of infection, the percentage of IL10 as a component of the cranial tracheobronchial lymph node profile decreased (from 58% to 53%), accompanied by an increase in both IFN-γ

(from 35% to 37%) and TNF-α (from 7% to 10%, Figure 20). Nineteen weeks post infection, the percentage of IL10 mRNA expression within the profile increased to a level above that observed at five weeks of infection (69%) whereas percentage levels of both IFN-γ and TNF-α mRNA expression decreased (28% and 3%, respectively, Figure 20).

Cytokine profile of the caudal mediastinal lymph node

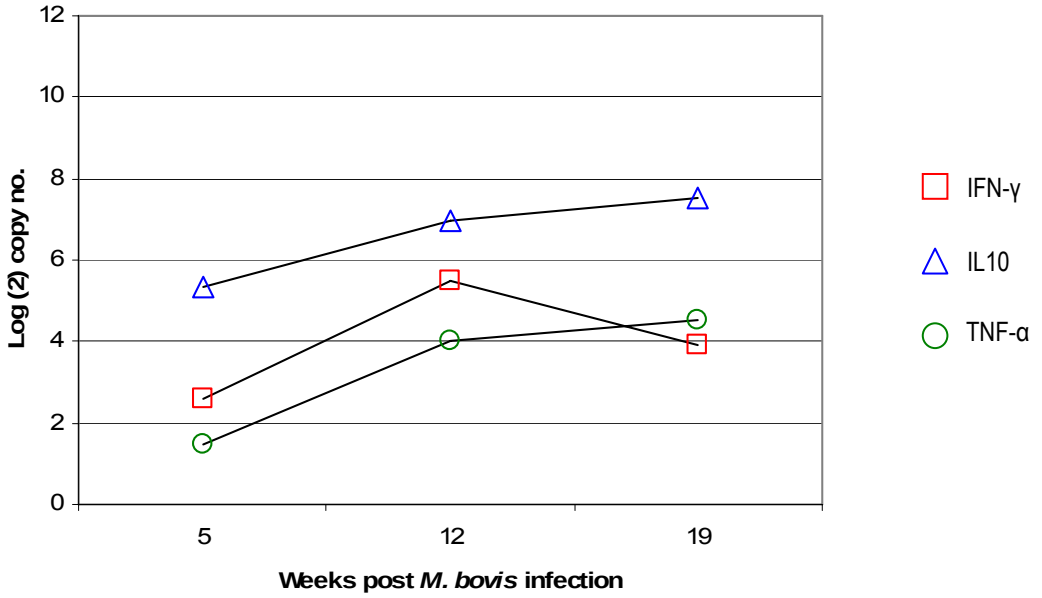

Figure 21: Quantitative PCR of IFN-γ, IL10 and TNF-α mRNA expression within the caudal mediastinal lymph node of cattle infected with *M. bovis* for five, twelve and nineteen weeks. The data are presented as log_2 copy number and each point represents the combined mean triplicate data of each caudal mediastinal lymph node from either three animals (five and twelve weeks post infection) or four animals (nineteen weeks post infection). Differences between time periods were not significant ($p>0.05$, Kruskal-Wallis test).

The expression of IFN-γ mRNA increased between five and twelve weeks (mean log_2 copy number 2.57 and 5.51, respectively, Figure 21) and decreased between twelve and nineteen weeks post infection (mean log_2 copy number 3.89).

Between five and twelve weeks post infection, TNF-α mRNA expression increased (mean log_2 copy number 1.5 and 3.9, respectively) and then increased further between twelve and nineteen weeks (mean log_2 copy number 4.5, Figure 21).

The level of IL10 mRNA expression increased steadily over five (mean log_2 copy number 5.31), twelve (mean log_2 copy number 6.99) and nineteen weeks post infection (mean log_2 copy number 7.51, Figure 21).

The cytokine profile within the caudal mediastinal lymph node showed a dominant expression of IL10 mRNA significantly higher than IFN-γ expression ($p<0.016$, Mann Whitney test and Bonferroni correction) and higher than TNF-α mRNA expression ($p<0.05$, Mann Whitney test and Bonferroni correction). IFN-γ and TNF-α were expressed at a similar level ($p>0.05$, Mann Whitney test).

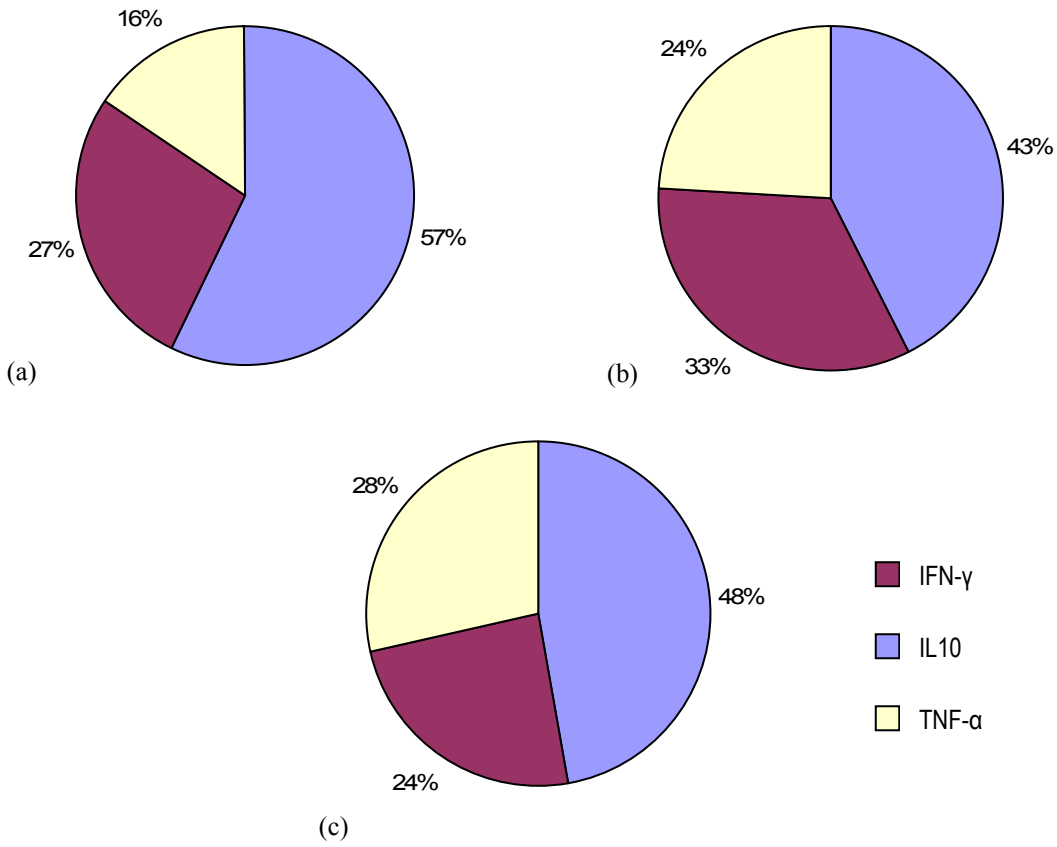

Figure 22: Percentage profile of cytokines IFN-γ, TNF-α and IL10 mRNA within the caudal mediastinal lymph node over five (a), twelve (b) and nineteen (c) weeks post infection. The cytokine copy number data from the mean triplicate results of each caudal mediastinal lymph node from either three (five and twelve weeks) or four (nineteen weeks) cattle were combined and each individual cytokine value calculated as a percentage of the overall expression profile.

The data in Figure 21 was used to build a profile of the percentage of each cytokine within the caudal mediastinal lymph node at each time point (Figure 22). As previously mentioned, IL10 mRNA was expressed at a significantly higher level (in copy number) as compared to both IFN-γ and TNF-α mRNA within the caudal mediastinal lymph node (Figure 21). Similarly, when the copy number data was converted into a percentage profile, IL10 was the largest component over the entire nineteen week infection period (Figure 22). Between five and twelve weeks of infection, the percentage of IL10 as a component of the caudal mediastinal lymph node profile decreased (from 57% to 43%), accompanied by an increase in both IFN-γ (from 27% to 33%) and TNF-α (from 16% to 24%, Figure 22). Between twelve and nineteen weeks post infection, IL10 mRNA percentage expression levels increased (48%) however the levels did not reach

those seen at five weeks post infection. At the same time, the percentage levels of IFN-γ mRNA within the profile decreased (24%). The levels of TNF-α mRNA as percentage of the profile increased slightly at nineteen weeks post infection (28%) to become the second largest component of the cytokine lymph node profile. This is in contrast to the other three lymph nodes at nineteen weeks post infection, where IFN-γ and IL10 mRNA were the two largest components of the lymph node profile (Figures 16, 18 and 20).

Correlations between cytokine mRNA expressions

The previous results shown in Figures 15, 17, 19 and 21 suggest that there may be a relationship between the expression patterns of IFN-γ, TNF-α and IL10 mRNA. This was further explored using Pearsons correlation co-efficient analysis.

(a)

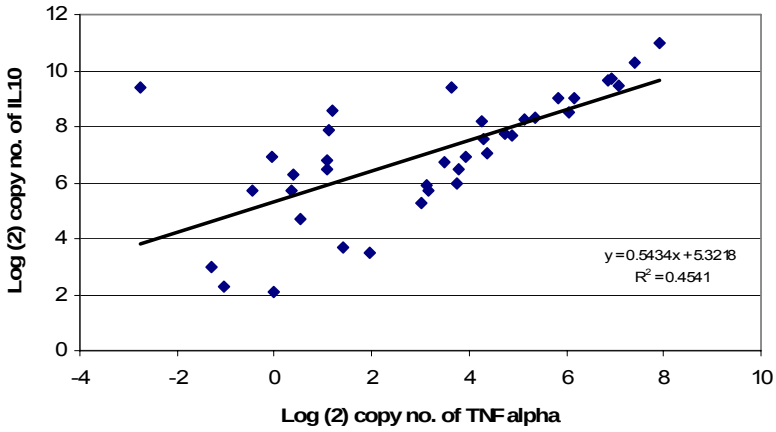

(b)

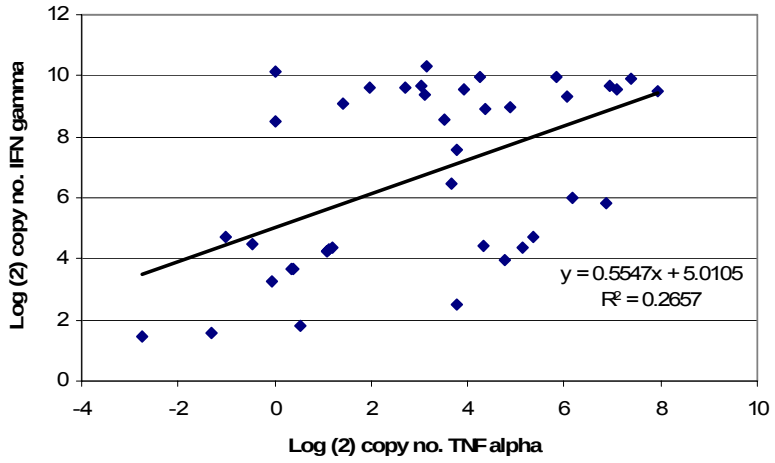

Figure 23: Correlations between (a) IL10 and TNF-α mRNA expression levels and (b) IFN-γ and TNF-α mRNA expression levels. The data are presented in $\log_2$ copy number and each individual point represents the mean triplicate data from an individual lymph node from one animal. Each graph displays the equation of the line of best fit and the R^2 value to indicate the fit of the data points.

A significant correlation was found between IL10 and TNF-α mRNA copy number expression levels ($p<0.001$, Pearsons correlation coefficient, Figure 23a) within the lymph nodes of cattle infected with *M. bovis* for five, twelve and nineteen weeks. The data presented a positive correlation (Pearsons correlation coefficient R value of 0.7) and therefore indicates that as one cytokine expression level increased, the other cytokine also experienced an increase. There was also a significant correlation between IFN-γ and TNF-α mRNA copy number expression levels ($p\leq0.001$, Pearsons correlation coefficient, Figure 23b) within the lymph nodes of cattle infected with *M. bovis* for five, twelve and nineteen weeks. The data presented a positive correlation (Pearsons correlation coefficient R value of 0.5) however this relationship was slightly weaker than the relationship between IL10 and TNF-α. This was further represented by the coefficient of determination (R^2 displayed on Figure 23) as the correlation of IL10 and TNF-α mRNA had an R^2 value of 0.45 (Figure 23a) indicating that 45% of the variance in one cytokine expression level was due to the other cytokine. The coefficient of determination for the correlation of IFN-γ and TNF-α mRNA (R^2 of 0.26, Figure 23b) suggested that 26% of the variance in one cytokine expression level was due to the other cytokine.

There was no significant correlation between IFN-γ and IL10 mRNA expression levels over the five, twelve and nineteen weeks post *M. bovis* infection ($p>0.05$, Pearsons correlation coefficient).

Lymph node pathology of cattle infected with *M. bovis* for five, twelve and nineteen weeks.

Percentage area coverage of granuloma

Granulomatous lesions within lymph nodes are a characteristic feature of *M. bovis* infection. The percentage area coverage of granulomas within individual lymph nodes can be used as an indication of the pathology caused by infection. Microscope slides of lymph node tissue were prepared for each animal infected for five, twelve and nineteen weeks. The lymph node section was first measured by counting the total fields of view that the section covered (100 x magnifications). Each individual granuloma within the section was then measured by counting the number of fields of view that the granulomas covered and the percentage area coverage calculated in respect to the entire lymph node section.

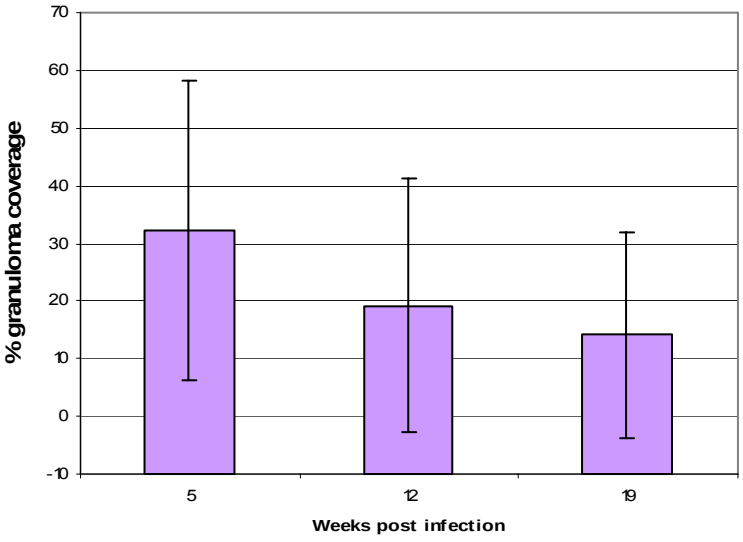

Figure 24: Percentage area coverage of granulomas (representing pathology) within cattle infected with *M. bovis* for five, twelve and nineteen weeks. The data represents the mean percentage of the combined individual lymph node results from either three cattle (five and twelve week groups) or four cattle (nineteen week group). Error bars represent standard deviation (±) of data from the mean. There was no statistically significant difference between the three groups ($p>0.05$, Kruskal Wallis test).

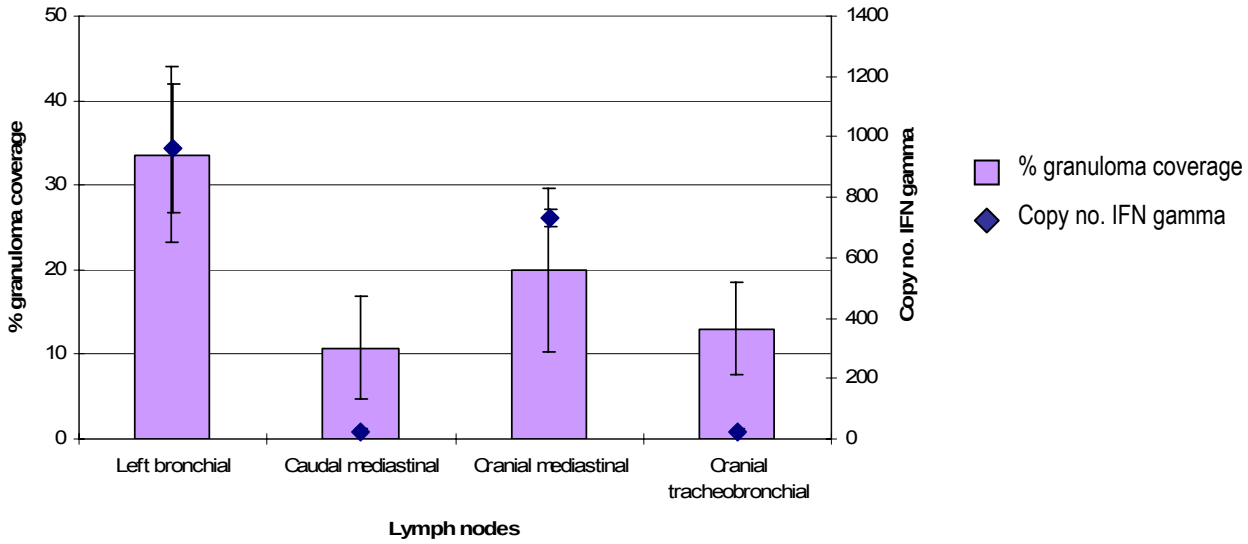

Figure 25: Percentage area coverage of granulomas (representing pathology) plotted against IFN-γ mRNA expression levels in the lymph nodes of cattle infected with *M. bovis* for five, twelve and nineteen weeks. The data represents the mean values (either percentage or copy number) for each lymph node type from a total of ten cattle (three infected for five weeks, three infected for twelve weeks and four infected for nineteen weeks). Error bars represent standard deviation (±) of data from the mean. There was no statistical significance between the four groups ($p>0.05$, Kruskal Wallis test).

The percentage area coverage of granulomas within lymph node tissues varied considerably over the nineteen week infection time period (Figure 24). The cattle infected for five weeks displayed the highest level of granuloma percentage coverage (mean 32%, Figure 24) followed by the twelve week group (mean 19.2%) and finally the nineteen week group (mean 14%). However, due to the very large variations in data within each group, these differences were not significant ($p>0.05$, Kruskal Wallis test).

There was a strong positive relationship between the level of pathology and the level of IFN-γ mRNA expression within the individual lymph nodes (Pearsons correlation coefficient R value of 0.9, Figure 25) although this was not significant ($p>0.05$, Pearsons correlation co-efficient). There was also a marked difference in the level of pathology and the level of IFN-γ expression between the different lymph nodes. The left bronchial lymph node displayed the highest level of pathology (mean of 33.6% granulomatous coverage, Figure 25) and the highest level of IFN-γ mRNA expression (mean 962.3 copies, Figure 25). The cranial mediastinal lymph node displayed the second highest level of pathology (mean of 20% granulomatous coverage, Figure 25) and the second highest level of IFN-γ mRNA expression (mean 732.44 copies). The third

highest level of pathology was found in the cranial tracheobronchial lymph node (mean of 13% granulomatous coverage) and the lowest pathology was displayed by the caudal mediastinal lymph node (mean of 10.8% granulomatous coverage, Figure 25). Both the cranial tracheobronchial and caudal mediastinal lymph nodes had similar levels of IFN-γ mRNA (mean 24.7 and 25.6 copies, respectively, Figure 25).

Granuloma developmental stage

Granulomas have been shown to progress through specific stages of development, independent of neighbouring lesions. It is therefore possible to categorise each granuloma depending on its physiological state (Wangoo *et al*, 2005) into:

- Stage I: Un-encapsulated clusters of epithelioid macrophages with interspersed lymphocytes and few neutrophils.
- Stage II: Partial or complete coverage of granuloma by a thin capsule, containing mainly epithelioid macrophages and distributed lymphocytes,
- Stage III: Completely encapsulated granuloma displaying necrotic centres and peripheral clusters of macrophages, lymphocytes and neutrophils.
- Stage IV: Thickly encapsulated with multiple centres displaying advanced caseous necrosis and vast islands of mineralisation. Epithelioid macrophages and giant cells surround the necrotic areas and lymphocytes are densely clustered around the periphery.

It was therefore possible to group the granulomas observed within the slide mounted sections of bovine lymph node into the above stages.

Table 18: Categorisation of granulomas within the lymph node sections of cattle infected with *M. bovis* for five, twelve and nineteen weeks. Granuloma specific for each of the four stages of development (I-IV) were counted within slide mounted lymph node sections. The counts were then weighted using a $\log_2$ scale to account for the larger sizes of the more advanced granuloma.

		Granuloma score (weighted score)					
Animal	*M. bovis* infection (weeks)	Stage I	Stage II	Stage III	Stage IV	Total	Mean (SEM)
8452	Five	2 (2)	4 (8)	0 (0)	1 (8)	18	
8454	Five	0 (0)	0 (0)	0 (0)	1 (8)	8	
8453	Five	3 (3)	3 (6)	3 (12)	4 (32)	53	26.3 (13.64)
8199	Twelve	13 (13)	0 (0)	0 (0)	2 (16)	29	
8197	Twelve	10 (10)	13 (26)	3 (12)	4 (32)	80	
8198	Twelve	2 (2)	1 (2)	0 (0)	0 (0)	4	37.6 (22.36)
4238	Nineteen	9 (9)	3 (6)	7 (28)	9 (72)	115	
4240	Nineteen	1 (1)	0 (0)	0 (0)	0 (0)	1	
4241	Nineteen	4 (4)	0 (0)	3 (12)	5 (40)	56	
4242	Nineteen	3 (3)	1 (2)	1 (4)	0 (0)	9	45.2 (26.22)

Weighting was applied accordingly: Stage I (x1), Stage II (x2), Stage III (x4), Stage IV (x8). Data represents the combined results from each of the four lymph nodes within each animal.

The data for the percentage area coverage of granulomatous lesions for each individual animal displayed a positive relationship with the categorised granuloma stage results ($p<0.05$, Spearmans correlation co-efficient, Table 18). Therefore as the percentage area coverage of granulomas within the lymph nodes increased, there was also an increase in the weighted total of granuloma development.

There was also a marked difference between the three experimental groups in granuloma development (Table 18) however, due to the large variations in the data sets these differences were not significant ($p>0.05$, Kruskal Wallis test). The cattle infected for five weeks showed the lowest score for granuloma development (mean 26.3, Table 18). This score increased within the lymph nodes of cattle infected for twelve weeks (mean 37.6). Finally, the nineteen week infection group displayed the highest level of granuloma development (mean 45.2, Table 18).

Focusing on the individual granuloma stage results, the five and twelve week groups had exactly the same scores for stage III (total of all three animals within each group was 12, Table 18) and stage IV (total 48) granuloma. However, the five week group had lower scores for granuloma within stages I (total 5) and II (total 14) as compared to the twelve week group (total 25 and 28, respectively).

Between twelve and nineteen weeks post infection, the number of granuloma within stages I and II decreased (total of all four animals within the nineteen week group was 17 and 8, respectively, Table 18). Alternatively, the number of granuloma within stages III and IV increased (total 44 and 112, respectively). Due to the small number of data points, these differences were not significant ($p>0.05$, Kruskal Wallis test).

Whole blood IFN-γ culture

To complement the cytokine expression studies within the lymph nodes, heparinized whole blood samples were taken from each animal prior to the cattle being euthanized for subsequent IFN-γ analysis. Three individual antigens were used to stimulate the blood culture lymphocytes to produce IFN-γ; PPD-B, ESAT-6 and CFP-10. PPD-A was also measured to ascertain previous exposure of cattle to environmental mycobacterial species (data not shown). The levels of IFN-γ were measured using a commercially available enzyme-linked immunosorbent assay kit (BOVIGAM®) and the results were expressed as mean optical density (OD at 450 nm).

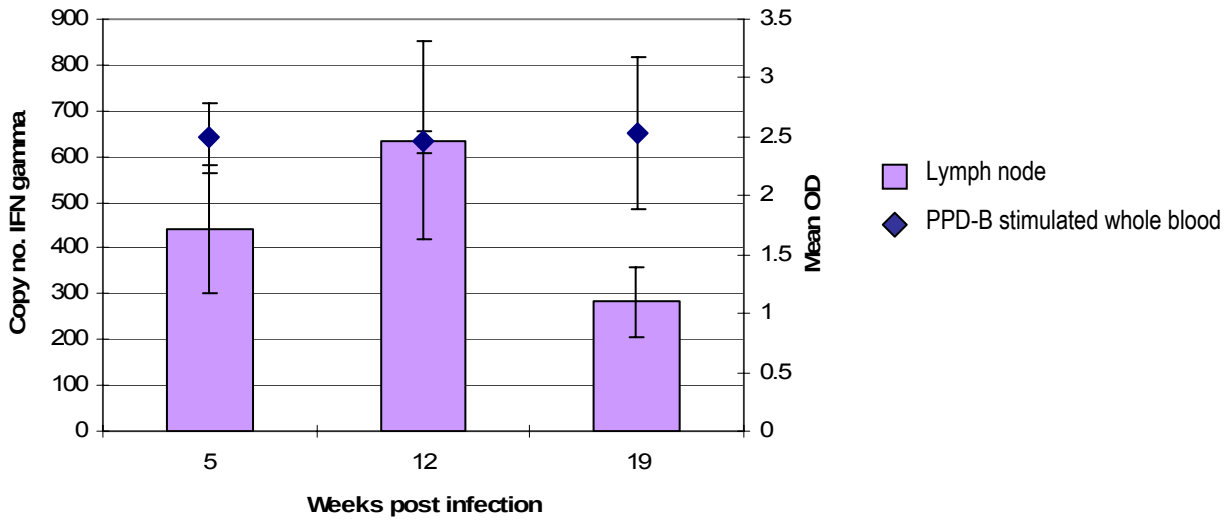

Figure 26: Expression of IFN-γ mRNA in lymph nodes and IFN-γ protein in whole blood of cattle infected with *M. bovis* for five, twelve and nineteen weeks. PBMCs were stimulated by PPD-B and the results expressed as mean optical density (OD) of the combined animal results within each group (three cattle in the five and twelve week groups and four cattle in the nineteen week group). The lymph node mRNA data represents the mean of the combined results for every animal (including all four lymph nodes examined for each animal) within each group. Error bars represent standard deviation (±) from the mean. There was no significant difference between the three groups ($p>0.05$, Kruskal Wallis test).

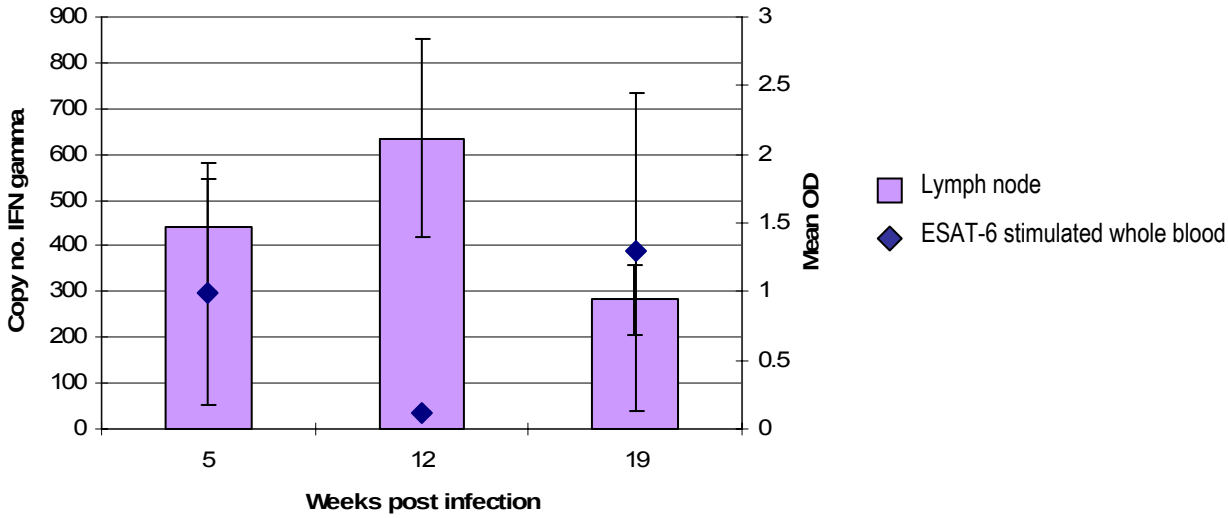

Figure 27: Expression of IFN-γ mRNA in lymph nodes and IFN-γ protein in whole blood of cattle infected with *M. bovis* for five, twelve and nineteen weeks. PBMCs were stimulated by ESAT-6 and the results expressed as mean optical density (OD) of the combined animal results within each group (three cattle in the five and twelve week groups and four cattle in the nineteen week group). The lymph node mRNA data represents the mean of the combined results for every animal (including all four lymph nodes examined for each animal) within each group. Error bars represent standard deviation (±) from the mean. There was no significant difference between the three groups ($p>0.05$, Kruskal Wallis test).

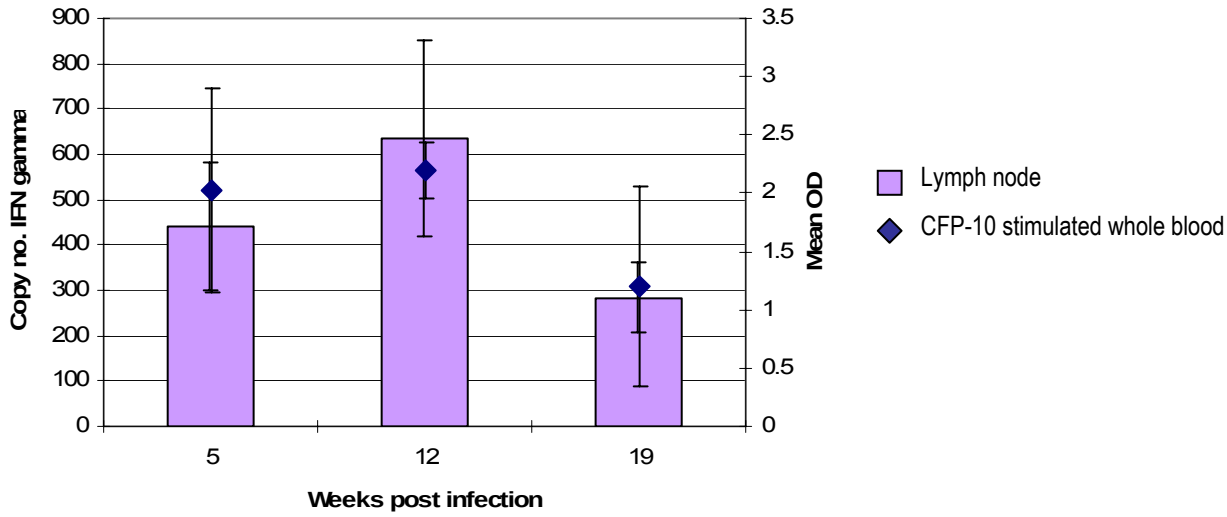

Figure 28: Expression of IFN-γ mRNA in lymph nodes and IFN-γ protein in whole blood of cattle infected with *M. bovis* for five, twelve and nineteen weeks. PBMCs were stimulated by CFP-10 and the results expressed as mean optical density (OD) of the combined animal results within each group (three cattle in the five and twelve week groups and four cattle in the nineteen week group). The lymph node mRNA data represents the mean of the combined results for every animal (including all four lymph nodes examined for each animal) within each group. Error bars represent standard deviation (±) from the mean. There was no significant difference between the three groups ($p>0.05$, Kruskal Wallis test).

Antigenic stimulation of whole blood samples isolated from cattle experimentally infected with *M. bovis* for five, twelve and nineteen weeks showed differing patterns in IFN-γ protein expression dependent on the antigen used (Figures 26, 27 and 28). Stimulation with PPD-B displayed little difference in IFN-γ protein expression over the nineteen week period (mean OD of 2.49 at five weeks, 2.45 at twelve weeks and 2.5 at nineteen weeks, Figure 26). ESAT-6 antigenic stimulation of isolated PBMCs displayed a higher level of IFN-γ protein at five weeks (mean OD of 0.99), followed by a decrease at twelve weeks (mean OD of 0.11) and a final increase at nineteen weeks (mean OD of 1.2, Figure 27) post infection. In contradiction, antigenic stimulation by CFP produced an increase in IFN-γ protein expression between five and twelve weeks (mean OD of 2 and 2.19, respectively) followed by a decrease between twelve and nineteen weeks (mean OD of 1.2, Figure 28) post infection. These differences were statistically not significant ($p>0.05$, Kruskal Wallis test).

The IFN-γ protein expression patterns of antigenic stimulated whole blood did not show a positive relationship with the IFN-γ mRNA expression patterns of the lymph nodes over the nineteen week period (Figures 26, 27 and 28). The ESAT-6 stimulated PBMCs actually displayed a negative correlation with the lymph node data ($p<0.05$, Pearsons correlation co-efficient, Figure 27). This signified that as the level of IFN-γ protein expression within the ESAT-6 stimulated blood sample increased, the IFN-γ mRNA expression levels within the lymph nodes decreased accordingly.

Discussion

Mycobacterium bovis infection of cattle is a major threat to both the global economy and healthcare state. Despite nearly sixty years of extensive control and preventative schemes, the incidence of *M. bovis* infection has been increasing significantly within Great Britain over the last twenty years (Delahay *et al*, 2002). Following the Krebs report in 1997, governmental emphasis has focused on scientific research into both the transmission of *M. bovis* and its pathogenic capabilities, with the aim of developing a more effective vaccination protocol (Krebs *et al*, 1997). A major part of this work has included detailed exploration of the bovine immune response post *M. bovis* infection to provide a greater understanding of the fine line between protection and immunopathology (Reynolds 2006). There is currently ample evidence to suggest that the cell mediated immune response is an essential component of the hosts fight against the disease (Widdison *et al*, 2006, Thacker *et al*, 2007). The study of cytokines has therefore become a useful representative of the bovine immune response to *M. bovis* infection.

The common route of *M. bovis* infection is through inhalation of the bacilli leading to pathological damage primarily within the lungs (Palmer *et al*, 2002). Murine *Mycobacterium tuberculosis* studies have revealed that transport of the bacilli from the lungs to the draining lymph nodes is essential in activating a cell mediated immune response (Chackerian *et al*, 2002). Therefore the primary site of infection and adaptive immunity occurs within the hosts' lung draining lymph nodes, thus providing the optimal site for investigation. To enable study of cytokine expression at the site of infection (lymph nodes) *in vivo* places huge limitations on the flexibility of the research study. The majority of studies focusing on immune responses within the lymph nodes, in particular within larger animals such as cattle have been restricted to one time period post infection only (Widdison *et al*, 2006, Thacker *et al*, 2007, Liebana *et al*, 2007). Alternatively, it has been suggested that the cytokine levels within the hosts peripheral blood mononuclear cells (PBMCs) could be used to provide a measure of the cell mediated response occurring within the lymph nodes (Guerkov *et al*, 2003). The ease with which PBMCs can be collected from experimentally infected animals has meant that many time course experiments based on cytokine expression have been performed on PBMCs (Thacker *et al*, 2007, Joardar *et al*, 2002). The disadvantage of this method is the reliability of the PBMCs to represent a true profile of the activated cell mediated immune response within the lymph nodes, a concept that is still under debate (Coussens *et al*, 2004, Rhodes *et al*, 2000). This study was aimed at

analysing the expression of four cytokines; interferon gamma (IFN-γ), tumour necrosis factor alpha (TNF-α), interleukin 10 and interleukin 4 directly within the lymph nodes of the bovine thorax over a nineteen week time period (five, twelve and nineteen weeks post infection). The lymph nodes of the thorax including the cranial mediastinal, caudal mediastinal, left bronchial and cranial tracheobronchial nodes have been previously shown to display pathological lesions within naturally infected cattle (Liebana *et al*, 2007) due to their direct contact via drainage from the lungs. The study of these particular four cytokines within the lymph nodes therefore allowed a greater understanding of the dynamics of the immune response, including both innate and adaptive immunity dependent on time post infection.

Total RNA extraction from formalin-fixed, paraffin embedded *M. bovis* infected bovine lymph nodes

To enable the quantification of target cytokine expression levels, total RNA was extracted from the formalin-fixed, paraffin embedded lymph node tissue samples using a previously published methodology (Witchell *et al*, 2008). The total RNA was then analysed by agarose gel electrophoresis and spectrophotometry to determine the overall integrity of the extracted samples.

Extensive debate has been focussed on the use of formalin-fixed tissues as a source of total RNA (Bustin, 2006, Castiglione *et al*, 2007, Witchell *et al*, 2008, Gilbert *et al*, 2007). Variable results have been obtained on the efficacy of RNA extraction from formalin-fixed tissues due to the formation of amino acid methylene bridges during the fixation process (Srinivasan *et al*, 2002). The cross-linked matrix formed by these bridges traps the RNA molecules thereby impeding the extraction process. However, the methodology employed to extract the RNA can have a great effect on the quality of the isolated nucleic acid (Gilbert *et al*, 2007). Extraction methods involving a proteinase K tissue digestion step have shown an enhanced ability to isolate total RNA from formalin-fixed tissues as compared to methods independent of proteinase K (Witchell *et al*, 2008). This is believed to be due to proteinase K being able to separate the RNA from its cross-linked matrix (Lewis *et al*, 2001). Also, the development of the real time polymerase chain reaction (PCR) from the conventional agarose gel PCR has established the use of comparatively shorter target amplicon sequences, thus allowing successful amplification of partially degraded RNA templates (Huggett *et al*, 2005, Castiglione *et al*, 2007).

Within this study, total RNA was extracted from formalin-fixed lymph node samples and displayed the appropriate 28S ribosomal band on the agarose gel (Figure 8). The spectrophotometry results confirmed the purity of the total RNA samples (Table 16), as the 260/280 nm ratio of 1.8 was between the expected range (Fleige and Pfaffl, 2006), thus indicating a lack of protein contamination (Bustin, 2004). As the lymph node samples produced variable quantities of total RNA (with a range of 44.5 to 388µg/ml, Table 16) it was decided to perform a two-step quantitative RT-PCR protocol to provide a cDNA pool, allowing a greater efficiency in the use of the template.

Cytokine mRNA expression in the combined lymph nodes

The total RNA extracted from the formalin-fixed, *M. bovis* experimentally infected bovine lymph nodes was reverse transcribed and applied to qPCR targeting the cytokines IFN-γ, TNF-α, IL10 and IL4, in addition to the housekeeping gene glyceraldehyde-3-phosphate dehydrogenase (GAPDH). As GAPDH is a constitutively expressed gene, it was possible to use the amplified GAPDH PCR product to determine the overall integrity of the cDNA template. The crossing point values for each GAPDH reaction displayed a consistency in mRNA expression across the three experimental groups (average of 35.3 for the five week group, 34 for the twelve week group and 34.7 for the nineteen week group, Figure 10). This suggested that any potential differences in cytokine expression between the three experimental groups were unlikely to be due to the physical condition of the template. The mRNA expression levels of IFN-γ, TNF-α, IL10 and IL4 were then measured quantitatively in four different lymph nodes from each animal; the left bronchial, cranial mediastinal, caudal mediastinal and cranial tracheobronchial lymph nodes within the three experimental groups. The crossing point values of each PCR reaction were converted to a quantitative value using the standard curve specific to each cytokine (Figure 9). The standard curves show that as the concentration of the target transcript increased, there was a related increase in the level of fluorescence observed. The resulting standard curve was therefore a straight line between the two extreme concentrations (Figure 9) and provided a means to quantify the unknown samples. The qPCR data from the individual lymph nodes was combined to produce a complete view of cytokine expression over the entire nineteen week time period (Figures 11, 12 and 13).

Five weeks post *M. bovis* infection

Upon *M. bovis* infection, the invading bacterial cells within the lungs are believed to be taken up by phagocytic cells (Fu *et al*, 1999) and disseminated to the local lymph nodes via dendritic cell movement through the draining lymphatic system (Humphreys *et al*, 2006, Bhatt *et al*, 2004) in an innate immune dependent manner. This has been shown to occur at approximately twelve to thirteen days (two weeks) post *M. tuberculosis* infection within murine models (Chackerian *et al*, 2002) and fifteen days following *M. bovis* infection within bovine models (Thacker *et al*, 2007). Murine studies have also revealed that an adaptive immune response could be initially detected (via IFN-γ expression) three to four days after the first appearance of the bacilli within the lymph node (Chackerian *et al*, 2002). This is due to the infected dendritic cells activating naïve T lymphocytes (Cella *et al*, 1997, Mellman and Steinman, 2001) and inducing a cell mediated immune response. Published bovine infection models have reported the detection of an adaptive immune response via the analysis of PBMCs (Thacker *et al*, 2007, Hanna *et al*, 1989) and directly within the draining lymph nodes (Palmer *et al*, 2007) approximately two to three weeks post *M. bovis* experimental infection. Delayed activation of the cell mediated immune response within the lymph nodes is therefore believed to be a common feature in both animal models.

Within this study, mRNA expression of IFN-γ, TNF-α and IL10 within the bovine lung draining lymph nodes was detected at the first time point analysed, five weeks after *M. bovis* infection (Figures 11, 12 and 13). This time point has been reported to coincide with a peak in the ratio of CD4+ and CD8+ T cells circulating within PBMCs of *M. bovis* infected cattle (Pollock *et al*, 1996, Joardar *et al*, 2002) created due to a significantly larger increase in CD4+ T cells in response to infection compared to CD8+ T cells (Villarreal-Ramos *et al*, 2003, Kennedy *et al*, 2002). CD4+ T cells are preferentially activated due to antigen presentation by dendritic cells occurring via the major histocompatibility complex II molecules (*Barnes et al*, 1994). In an IL12-rich environment, CD4+ T cells express high levels of IFN-γ and infected bovine PBMCs have been shown to produce a peak in IFN-γ expression at around thirty days (four weeks) post inoculation (Thacker *et al*, 2007). This was accompanied by a peak in TNF-α (due to the role of IFN-γ in phagocytic cell activation) and a decrease in IL10 expression (Thacker *et al*, 2007). This data, combined with that presented within this study supports the hypothesis that at five weeks post infection the immune response is largely cell mediated, characterised by the presence of pro-inflammatory cytokines and associated down-regulation of anti-inflammatory IL10.

Five to twelve weeks post *M. bovis* infection

Studies on cytokine expression post mycobacterial infection have shown noticeable fluctuations in mRNA expression levels over time (Thacker *et al*, 2006 and 2007, Dean *et al* 2005, Welsh *et al*, 2005). This suggests that the expression patterns of cytokines are not continuous events and are subject to numerous control mechanisms as time of infection progresses. As a result of the dynamic characteristics of the immune response, there are conflicting reports of cytokine expression in the early stages of *M. bovis* infection. PBMCs from infected bovine (Dean *et al*, 2005, Joardar *et al*, 2002) and deer (Thacker *et al*, 2006) models have been shown to produce increasing levels of IFN-γ expression between four and twelve weeks. However, infected bovine PBMC have also been shown to display decreasing levels of both IFN-γ and TNF-α expression between five and twelve weeks post inoculation, accompanied by a slight increase in IL10 expression (Thacker *et al*, 2007). Time dependent changes in cytokine expression are also evident in other animal models. A study on guinea pig lung granulomas displayed a decrease in IFN-γ expression between three and six weeks following *M. tuberculosis* infection, with little difference in TNF-α and IL10 expression levels (Ly *et al*, 2007). In comparison, a cytokine expression study within the lung granuloma of mice revealed an increase in IFN-γ and IL10 mRNA levels between three and six weeks of *M. tuberculosis* infection (Zhu *et al*, 2003). Both studies employed laser microdissection and real time PCR to analyse cytokine expression levels and therefore differences in cytokine profiles may be attributed to the different host species. Variations in cytokine expression profiles between the bovine studies may be due to the extreme difference in initial inoculation concentration, as the Thacker *et al* (2007) study utilised 10^3 CFU of *M. bovis* in comparison to the Dean *et al* (2005) study that used 1 CFU of *M. bovis*. The extreme heterogeneity of the immune response between studies and even between individual animals within the same study is therefore evident, thus making comparisons problematic. Within this study, there was an increase in mRNA expression of both IFN-γ (from a mean $\log_2$ copy number of 6.50 to 7.53, Figure 11) and TNF-α (from a mean $\log_2$ copy number of 2.15 to 3.94, Figure 12) between five and twelve weeks of *M. bovis* infection. There was also a significant increase in expression of IL10 (from a mean $\log_2$ copy number of 5.97 to 8.27, $p<0.01$, Mann Whitney test, Figure 13).

It was originally hypothesised that IL10 was produced primarily by T_H2 T cells (Fiorentino *et al*, 1989) however more recent evidence has shown IL10 to be produced by a variety of cell types, including macrophages (Katakura *et al*, 2004), dendritic cells (Corinti *et al*, 2001) and various subsets of CD4+ and CD8+ T cells (Vieira *et al*, 2004, Barrat *et al*, 2002). It is typically a

cytokine associated with immunoregulation, due to its various roles including suppression of T cell differentiation into the effector T_H1 subset by down-regulation of macrophage MHC class II molecule expression (Sendide *et al*, 2005) and direct inhibition of IL2, IL4 and IL5 production by CD4+ T cells (Joss *et al*, 2000, Schandene *et al*, 1994). IL10 also has an effect on the bactericidal properties of phagocytic cells by manipulating the phagocytic pathway and inhibiting production of toxic nitric oxide (Gazzinelli *et al*, 1992, Bogdan *et al*, 1991). An intermediate of the phagocytic process termed inducible nitric oxide synthase (iNOS) has been shown to peak in activity at forty-two days (six weeks) within cattle post *M. bovis* infection, followed by a significant reduction at sixty days (eight and a half weeks, Palmer *et al*, 2007). The reduction in iNOS observed by Palmer *et al* (2007) therefore occurred around the same time (post infection) as the significant increase in IL10 within this study.

Despite its immunosuppressive role on IFN-γ expression, levels of IL10 mRNA have been shown to increase relative to mRNA levels of IFN-γ within the lymph nodes of TB-infected patients (Lin *et al*, 1996). Further analysis of cytokine production by T cell clones derived from the bronchoalveolar lavages of *Mycobacterium tuberculosis* infected humans revealed the presence of CD4+ T cell clones producing both IFN-γ and IL10 (Gerosa *et al*, 1999). It was suggested by Gerosa *et al* (1999) that the CD4+ IFN-γ+ IL10+ cell phenotype acted as a 'self-limiting' mechanism, with IL10 regulating levels of both T_H1 and T_H2 cytokines thereby reducing the severity of pathology associated with heightened immunological activity. This hypothesis has been supported by recent studies into the T cell response towards *Leishmania major* infection in mice (Anderson *et al*, 2007). Protection against the parasite *Leishmania* is dependent upon an efficient and fast-responding T_H1 pro-inflammatory response (Locksley *et al*, 1987, Scott *et al*, 1988) comparable to infection by *M. bovis*. Analysis of chronic, localised lesions caused by the parasite revealed high levels of pro-inflammatory cytokines as well as IL10 but either low or undetectable levels of anti-inflammatory T_H2 cytokines (Melby *et al*, 1994). It was found that the antigen-specific IFN-γ+ T_H1 cells were responsible for the main production of IL10 involved in restricting pathological damage during *Leishmania* infection (Anderson *et al*, 2007). This theory may also be applied to tuberculosis infection, as the excessive amounts of pro-inflammatory cytokine IFN-γ implicated in extensive pathological damage may be controlled by simultaneous expression of IL10. Therefore the increase in expression levels of IFN-γ and TNF-α between five and twelve weeks of infection may represent the expanding population of activated T cells and phagocytic cells in response to the bacterial threat. The corresponding significant increase in IL10 expression signifies the hosts'

efforts in controlling this strong cell mediated phenotype which was activated in the earlier stages of the infection.

Conversely, as a direct consequence of down-regulating the pro-inflammatory response, IL10 expression has also been correlated with the decreased ability of the immune system to contain the mycobacterial threat (Jamil *et al*, 2007, Turner *et al*, 2002). There is evidence to suggest that mycobacteria preferentially induce IL10 expression to suppress the cell mediated immune response and therefore prolong bacterial survival (Roque *et al*, 2007). *M. tuberculosis* is able to induce dendritic cell production of IL10 via TLR-2 signalling (Jang *et al*, 2004) and IL10 production by macrophages suppresses apoptosis of *M. avium* infected cells thereby preserving bacterial proliferation (Balcewicz-Sablinska *et al*, 1999). Co-culture of human monocyte-derived dendritic cells with *M. bovis* Bacillus Calmette Guerin (BCG) has been shown to display increased levels of IL10 in a dose-dependent manner as compared to cells co-cultured with LPS (Larsen *et al*, 2007). The BCG-exposed dendritic cells were also able to induce differentiation of naïve T cells into IL10-producing populations (Larsen *et al*, 2007). This introduces a conflicting concept of the beneficial role of IL10, as it is difficult to differentiate between whether the high levels of IL10 produced during infection are the cause of or are in response to high bacterial loads (Couper *et al*, 2008). For example, early production of IL10 within *M. tuberculosis* murine models results in the inability of the host to contain the bacterial threat, leading to increased propagation of the bacilli (Roque *et al*, 2007). However in Leishmania infection, the delayed onset of CD4+ IL10+ T cells is believed to occur in response to excessive T_H1 levels produced by high bacterial burdens (Anderson *et al*, 2005, Belkaid *et al*, 2001). This results in suppression of the cell mediated response and persistence of the infection. The timing of IL10 production may have a considerable effect on its role in the development of the infection. The significant increase in IL10 expression observed within this study at twelve weeks post *M. bovis* infection may therefore have also been induced by the invading bacilli and could aid the development of pro-longed disease.

Twelve to nineteen weeks post *M. bovis* infection

Between twelve and nineteen weeks post *M. bovis* infection there was a decrease in mRNA expression of IFN-γ (mean $\log_2$ copy number of 6.22, Figure 11), TNF-α (mean $\log_2$ copy number of 3.02, Figure 12) and IL10 (mean $\log_2$ copy number of 7.03, Figure 13). The reduction in cell mediated associated cytokine activity at advanced stages of infection has been previously reported, with IFN-γ expression showing dramatic decreases between twelve and

twenty weeks post infection in bovine PBMCs (Joardar *et al*, 2002, Dean *et al*, 2005, Welsh *et al*, 2005) and sixteen weeks post infection in deer PBMCs (Thacker *et al*, 2006). Although the reductions in cytokine expression at nineteen weeks reported in this study were not significant, they do fit the general consensus that advanced stages of disease are associated with a dynamic shift from cell mediated to humoral immune responses (Welsh *et al*, 2005, Pollock *et al*, 2001, Palmer *et al*, 2000). Welsh *et al* (2005) commented on the level of cytokine expression diverging from the observed cellular activity twenty weeks after *M. bovis* infection. It was suggested that this may be due to a significant shift in the immune profile from cell mediated to humoral, as antibody levels (IgG) were shown to plateau from as early as fifteen weeks in the same animals (Welsh *et al*, 2005). Thacker *et al* (2007) also observed that cytokine gene expression diminished as the infection progressed. In support of this, bovine antibody responses measured by capture ELISA in response to MPB83 antigen have also been shown to peak between one hundred and one hundred and seventy days (fourteen and twenty-four weeks, McNair *et al*, 2001), suggesting a heightened humoral response during these time periods.

Possible mechanisms involved in the shift of cell mediated to humoral immunity are still largely unknown although there does appear to be an inverse relationship between the two profiles (Ritacco *et al*, 1991). This may be due to the inhibitory abilities of the different cytokines driving either the cell mediated (T_H1) or humoral (T_H2) responses, as both IFN-γ (cell mediated) and IL4 (humoral) have been shown to affect transcriptional factors required for T_H receptors within T lymphocytes (Goldsby *et al*, 2003). However, the results from this study do not support the development of a T_H2 immune profile, as the expression of T_H2 cytokine IL4 remained elusive throughout the nineteen weeks of infection (this will be discussed at a later point). The same lack of T_H2 development was also reported by Thacker *et al* (2007) in a bovine cytokine expression study performed during the first three months of *M. bovis* infection. However, although a T_H2 specific phenotype was not observed during this time period, the authors suggest that the conversion from pro-inflammatory to anti-inflammatory cytokine environment may occur after this time.

Interestingly, within this study although all three cytokines (IFN-γ, TNF-α and IL10) were seen to decrease between twelve and nineteen weeks post infection, only IFN-γ expression was seen to reduce to levels below that observed at five weeks (Figure 11). This may be indicative of the regulatory role of IL10 described earlier.

Absence of IL4 expression over the nineteen week infection period

Results on the expression of IL4 mRNA within the three experimental groups were deemed unreliable due to the comparative levels of expression noted within the associated negative controls. IL4 mRNA has a very short half-life (one hour or less, Ulmland *et al*, 1998) and has been shown to be exceedingly difficult to target during assays (Welsh *et al*, 2005) due to being active at very low copy numbers. The expression of IL4 has also been reported to decrease significantly following mycobacterium infection (Rhodes *et al*, 2007, Welsh *et al*, 2005, Thacker *et al*, 2007, Widdison *et al*, 2006) thus making detection even more difficult.

Cytokine mRNA expression in the individual lymph nodes

The design of the time course study allowed cytokine expression to be studied specific to four different types of lung draining lymph node; the left bronchial, cranial mediastinal, caudal mediastinal and cranial tracheobronchial. It was therefore decided to analyse the lymph node qPCR data individually to ascertain whether there were any potential differences in cytokine expression levels dependent on lymph node location. Statistical analysis revealed a striking difference in IFN-γ ($p<0.001$, Kruskal Wallis test) and TNF-α ($p=0.009$, Kruskal Wallis test) mRNA expression between the four types of lymph node (Table 17). Further tests confirmed that the four lymph node types could be grouped into two categories dependent on IFN-γ mRNA expression. The left bronchial and cranial mediastinal lymph nodes displayed comparatively similar levels of IFN-γ mRNA expression (mean $\log_2$ copies between 8.4 and 10 over the nineteen week period, Figure 14) and were significantly higher ($p<0.001$, Mann Whitney test, Table 17) as compared to the caudal mediastinal and cranial tracheobronchial lymph nodes (mean $\log_2$ copies between 2.6 and 5.5 over the nineteen week period, Figure 14). The expression of TNF-α mRNA did not differ as widely between the four lymph node types and only the cranial tracheobronchial lymph node showed some variation, with a significantly lower level of expression as compared to the cranial mediastinal node ($p<0.016$, Mann Whitney test and Bonferroni correction, Table 17). Statistically, IL10 mRNA expression levels showed no significant difference between the four lymph node types ($p>0.05$, Kruskal Wallis test, Figure 14). These results suggest that there was a location dependent effect on the immune response exhibited by each of these lymph nodes and that mRNA expression of IFN-γ was associated with this variation.

Heterogeneity of cytokine expression profiles has also been described for the lung lobes of *M. tuberculosis* infected guinea pigs (Ly *et al*, 2007). Comparisons between the peripheries of granulomas located in the upper left and lower left lung lobes at six weeks post infection revealed a large variation in the percentage of each cytokine in relation to the overall immune profile. The lower left lobes contained granulomas expressing 99.9% TNF-α, 0.1% IFN-γ and less than 0.01% IL10 (Ly *et al*, 2007) whereas the upper left lobe contained granulomas expressing 17.73 % TNF-α, 38.45% IFN-γ and 4.99% IL10, equating to a 384.5 fold difference in IFN-γ mRNA expression between the two sites. The authors suggest that haematogenous reseeding (bacterial cells returning to the lung via the vascular system, Ho *et al*, 1978) may have led to the upper left lobe containing mainly secondary (blood borne) granulomas (Ly *et al*, 2007). Murine infection models have been used to show that dissemination of bacterial cells from the infected lung lobe to the lung draining lymph nodes occurs before extrapulmonary dissemination to the contra lateral lung (Mischenka *et al*, 2002) and may produce vast differences in immune responses between the two lung cavities. Differences in bacterial burden have been shown to affect the cytokine profile, observed in the previous supplementary study (Boddu-Jasmine *et al*, 2008), as a lower level of bacilli results in fewer activated T cells and a less forceful IFN-γ response. A study performed on the intratonsilar *M. bovis* infection of cattle revealed a predominance of bacilli within the left medial retropharyngeal lymph node at twenty weeks post infection (Griffin *et al*, 2006b). This was due to the left medial retropharyngeal lymph node being the first lymphatic junction to drain the tonsils. The high number of bacilli correlated with a higher level of pathology as compared to adjacent head lymph nodes (Griffin *et al*, 2006b). From the data within this study, it is not possible to ascertain the reasons behind such a difference in IFN-γ mRNA expression between the four lymph node types. However, it may represent a possible 'route of dissemination' in which some lymph nodes are infected prior to others and therefore display a more advanced immune response.

Cytokine expression profiles within the left bronchial and cranial mediastinal lymph nodes

The individual lymph node types (Figures 15, 17, 19 and 21) displayed a similar cytokine expression pattern over the nineteen weeks of infection to that of the combined cytokine data (Figures 11, 12 and 13). Within each lymph node type, the cytokine expression levels of IFN-γ, TNF-α and IL10 displayed an increase between five and twelve weeks post infection, followed by a decrease between twelve and nineteen weeks post infection, with some exceptions

(Figures 19 and 21). However, by converting the individual cytokine expressions into a percentage of the overall profile of the three cytokines, the data reveals differences in the dynamic pattern of the response (Figures 16, 18, 20 and 22). Within the left bronchial and cranial mediastinal lymph nodes (both showing overall significantly high levels of IFN-γ mRNA, Figure 14), the level of IFN-γ mRNA expression remained consistent between five and twelve weeks post infection (mean $\log_2$ copies of 9.81 to 10 within the left bronchial and 9.53 within the cranial mediastinal lymph node, Figures 15 and 17). However as a percentage of the overall cytokine profile, IFN-γ mRNA expression within both the left bronchial and cranial mediastinal lymph nodes decreased between five and twelve weeks (from 53% to 42% and 50% to 37%, respectively, Figures 16 and 18). This decrease was accompanied by an increase in IL10 (from 31% to 40% within the left bronchial and 32% to 40% within the cranial mediastinal lymph node, Figures 16 and 18) and a very slight increase in TNF-α (from 16% to 18% in the left bronchial and 18% to 23% in the cranial mediastinal). Between twelve and nineteen weeks post infection, both the left bronchial and cranial mediastinal lymph nodes showed a decrease in IFN-γ mRNA expression (mean $\log_2$ copy of 8.39 and 9.4, respectively, Figures 15 and 17). However, the percentage of IFN-γ mRNA in the overall cytokine profile increased between twelve and nineteen weeks (from 42% to 50% within the left bronchial and 37% to 43% within the cranial mediastinal, Figures 16 and 18). This increase was accompanied by a decrease in the percentage of IL10 mRNA (from 40% to 33% in the left bronchial and 40% to 34% in the cranial mediastinal) and little change in the percentage of TNF-α mRNA (from 18% to 17% within the left bronchial and a stable 23% in the cranial mediastinal, Figures 16 and 18). These results imply that although the expression levels of IFN-γ mRNA were relatively consistent in both lymph node types over the nineteen week period, the percentage population of IFN-γ mRNA as a part of the overall immune profile did experience changes. As the percentage population of TNF-α mRNA was also fairly consistent; this suggests that a difference in IL10 mRNA expression was the main contributor to the changes seen in the immune profile. Between five and twelve weeks post infection, IL10 mRNA expression increased to such an extent that it became equal to or larger a percentage of the immune profile than IFN-γ mRNA (Figures 16 and 18). This supports the hypothesis mentioned previously, that at twelve weeks post infection the cattle exhibited a significantly increased expression of IL10 to regulate over-expression of T_H1 cytokines. However, this increase in IL10 appeared to have little impact on IFN-γ and TNF-γ mRNA expression as both either remained stable or increased (Figures 15 and 17). IL10 has been shown to have the ability to down-regulate expression of MHC class II associated molecules thereby dampening

CD4+ T_H1 cell activation (Goldsby *et al*, 2003) as well as blocking IL12 transcription and suppressing nitric oxide formation. However, murine *M. tuberculosis* models have shown that neutralising IL10 production in CD4+ populations has a negligible effect on IFN-γ production (Mason *et al*, 2007). Also, studies on IL10 in human models have suggested that the cytokine may have both inhibitory and stimulatory roles on CD8+ cells in a time dependent manner (Groux *et al*, 1998) and this may therefore compensate for any loss of IFN-γ production by CD4+ cells.

Between twelve and nineteen weeks of infection, the decrease in IL10 mRNA expression resulted in an increase in the percentage contribution of IFN-γ, despite evidence of a decrease (Figure 15) or consistent (Figure 17) expression of IFN-γ mRNA.

The comparatively large decrease in IL10 mRNA expression at nineteen weeks is surprising due to its beneficial role in controlling the cell meditated immune response and its reported up-regulation by mycobacterial antigenic/TLR-2 interaction (Jang *et al*, 2004). Interestingly, although there was an increase in the percentage of IFN-γ mRNA at nineteen weeks post infection, the level was still comparatively lower than the level at five weeks post infection and IL10 comparatively higher (Figures 16 and 18). This may support the hypothesis mentioned previously of the down-regulation of pro-inflammatory cytokines as the disease progresses.

Cytokine expression profiles within the cranial tracheobronchial and caudal mediastinal lymph nodes

The cranial tracheobronchial and caudal mediastinal lymph nodes (both showing significantly lower levels of IFN-γ expression, Figure 14) displayed a different pattern in the cytokine profile compared to the left bronchial and cranial mediastinal lymph nodes. Between five and twelve weeks post infection, there was an increase in all three cytokine mRNA levels within the cranial tracheobronchial (mean $\log_2$ copies of 4.07 to 5.07 for IFN-γ, 6.68 to 7.32 of IL10 and 0.85 to 1.4 of TNF-α, Figure 19) and caudal mediastinal lymph nodes (mean $\log_2$ copies of 2.57 to 5.51 for IFN-γ, 5.31 to 6.99 for IL10 and 1.5 to 3.9 for TNF-α, Figure 21). The same data transformed into percentages of the cytokine profile revealed an increase in the percentage of IFN-γ (from 35% to 37% for the cranial tracheobronchial and from 27% to 33% for the caudal mediastinal lymph node, Figures 20 and 22). This was accompanied by an increase in TNF-α expression (from 7% to 10% and 16% to 24%, respectively) and a decrease in IL10 expression (from 58% to 53% and 57% to 43%, respectively). However, at five and twelve weeks post infection, the percentage expression of IL10 was still comparably higher than IFN-γ.

Between twelve and nineteen weeks post infection within the cranial tracheobronchial lymph node, both IFN-γ and TNF-α mRNA expression decreased (mean log_2 copies of 3.19 and 0.32, respectively, Figure 19) while IL10 expression increased (mean log_2 copies of 7.78, Figure 19). The same data transformed into percentages of the cytokine profile revealed an increase in the percentage of IL10 to that above what was seen at five weeks of infection (from 53% to 69%, Figure 20). This was accompanied by a decrease in both IFN-γ and TNF-α expression (from 37% to 28% and 10% to 3%, respectively). The caudal mediastinal lymph node displayed a slightly different pattern between twelve and nineteen weeks, as the expression level of TNF-α and IL10 both increased (mean log_2 copies of 4.54 and 7.51, respectively, Figure 21) while IFN-γ decreased (mean log_2 copies of 3.89). This pattern was reflected in the percentage profile, as both TNF-α and IL10 increased (from 24% to 28% and 43% to 48%, respectively, Figure 22) and IFN-γ decreased in percentage (from 33% to 24%). The strong presence of IL10 expression within these two lymph nodes is therefore evident from the very beginning and throughout the entire nineteen week period of infection. This may have had a substantial impact on the development of pathological disease, as will be discussed later.

Correlations between cytokine mRNA expressions

The mRNA expression data from the three experimental groups (five, twelve and nineteen weeks post infection) displayed a positive relationship between TNF-α and both IL10 ($p<0.001$, Pearsons correlation coefficient, Figure 23a) and IFN-γ ($p=0.001$, Pearsons correlation coefficient, Figure 23b). Relationships between IFN-γ and TNF-α mRNA expression have been previously reported within the lymph nodes (Widdison *et al*, 2006) and PBMCs (Thacker *et al*, 2007) of cattle infected with *M. bovis*. IFN-γ has been found to be released by activated T lymphocytes directly into the immunological synapse formed at the interface between the T cell and APC (Huse *et al*, 2006). This allows direct communication between the two cells and induces the macrophage to produce TNF-α (Decker *et al*, 1987), thus creating a positive relationship between the two cytokines.

A relationship between TNF-α and IL10 mRNA expression has also been described previously (Widdison *et al*, 2006). However, this is slightly more difficult to explain as IL10 is known to actively down regulate TNF-α expression by inducing macrophage production of soluble TNF-α receptor type 2 (TNFR2) to form inactive TNF-α-TNFR2 complexes (Fratazzi *et al*, 1999). However, as previously mentioned T_H1 cells have the ability to produce both IFN-γ (which

stimulates macrophages to produce TNF-α) and IL10 (Gerosa *et al*, 1999), therefore providing a possible positive relationship between the expression of IL10 and TNF-α. Alternatively, IL10 is known to be heavily regulated post-transcription. Studies into the production of IL10 have revealed the importance of transcriptional regulatory factors Sp1 and Sp3 (Brightbill *et al*, 2000, Tone *et al*, 2000) in IL10 expression, which bind to the IL10 promoter within LPS-stimulated macrophages. Sp1 and Sp3 are both constitutively and ubiquitously expressed (Tone *et al*, 2000), however, it has been found that constitutively expressed IL10 mRNA is extremely unstable in non-stimulated cells and therefore is unlikely to be translated successfully (Powell *et al*, 2000), thus implying posttranscriptional regulatory controls are involved. LPS stimulation of murine macrophages has been shown to increase IL10 mRNA levels by ~2000 fold while secreted IL10 protein levels were increased by only ~10 fold (Nemeth *et al*, 2007). Thus, a positive relationship between IL10 and TNF-α mRNA expression may not reflect a positive association in protein levels. The knowledge of posttranscriptional regulation of IL10 is extremely important for this study as it would suggest that dynamic changes in IL10 mRNA expression levels may not directly represent changes in protein levels. This must therefore be taken into consideration when translating mRNA expression in terms of overall cellular responses.

Lymph node pathology of cattle infected with *M. bovis* for five, twelve and nineteen weeks

Within this study two comparable factors were used to represent the levels of pathology within the *M. bovis* infected lymph nodes; percentage area coverage of granulomas (Figure 24 and 25) and granuloma stage (Table 18). Granulomas are formed by the accumulation of T lymphocytes and antigen presenting cells around a central focus to contain bacterial spread (Saunders and Cooper, 2000). Initially a structure to protect the host, as the granuloma grows in size as a response of cellular activity it becomes associated with immunopathological harm (Mustafa *et al*, 2008). Therefore, the percentage area coverage of the granulomas within the lymph node sections can give an indication to the progression of the immune response. A study aimed at describing temporal changes in granuloma development within *M. bovis* infected cattle lymph nodes revealed that microscopic lesions could be detected within all animals as early as twenty-eight days (four weeks, Palmer *et al*, 2007) post infection. Gross lesions within the mediastinal and tracheobronchial lymph nodes were later identified at forty-

two days (six weeks) post infection (Palmer *et al*, 2007). Within this study, granulomas were observed within the bovine lymph nodes by microscopy within all three experimental groups (five, twelve and nineteen weeks post infection, Figure 24). Interestingly, the cattle at five weeks post infection showed the highest level of pathology (mean 32% granuloma coverage), followed by the twelve week (mean 19.2% granuloma coverage) and nineteen week groups (mean 14% granuloma coverage, Figure 24). These differences were not significant due to the large variation in data within each experimental group and exclusion of one particular animal from the analysis dramatically reduced the mean percentage of the five week group (mean 17% granuloma coverage, data not shown). This data would suggest therefore that differences in granuloma coverage of the lymph nodes between the three time periods (five, twelve and nineteen weeks) were negligible. Similarly, in the study performed by Palmer *et al* (2007), scoring of the granuloma within the medial retropharyngeal lymph node based on lesion size revealed little change in scores between forty-two (six weeks) and three hundred and seventy days (fifty-three weeks) post infection.

Due to the difference in cytokine expression profiles between the four types of lymph node over the nineteen week infection period, the percentage granuloma coverage for each lymph node was also examined individually (Figure 25). The mean percentage granuloma spread measured within each animal from the three experimental groups was highest within the left bronchial lymph node (33%, Figure 25). This was followed by the cranial mediastinal (20%), cranial tracheobronchial (13%) and the caudal mediastinal (10.8%, Figure 25) lymph nodes. Therefore, both of the lymph node types displaying high levels of IFN-γ expression (left bronchial 962.3 and cranial mediastinal 732.44 mean copies, Figure 25) also displayed the highest level of granuloma coverage, revealing a positive relationship between the two variables (Figure 25). A common hypothesis among many published articles on bovine tuberculosis infection is the involvement of IFN-γ in high levels of pathological damage (Villarreal-Ramos *et al*, 2003, Thacker *et al*, 2007, Dean *et al*, 2005). IFN-γ is a major contributor to the formation of granuloma due to its role in macrophage activation (Orme, 1998) and therefore increased levels of IFN-γ expression leads to enhanced granuloma formation. Within this study, those lymph node types that displayed stronger cellular activity and IFN-γ expression in response to bacterial infection also showed subsequent increased levels of pathological damage.

Immunological studies have also shown a negative relationship between IL10 mRNA expression and lesion score (based on increasing severity, Widdison *et al*, 2006). IL10 acts to down-regulate pro-inflammatory cytokines TNF-α and IFN-γ, and subsequently reduces the

formation of granulomas resulting in less pathological damage. As mentioned previously, evidence from murine *Leishmania* infection models have shown the ability of T_H1 cells to produce both IFN-γ and IL10 simultaneously with the aim of providing a 'self-regulative' mechanism (Anderson *et al*, 2007). Within this study, there were no significant differences in IL10 mRNA expression levels between the high pathology and low pathology lymph node types (Figure 14). The same consistency in IL10 expression between cattle displaying high pathological levels and those displaying lower levels was also seen within a similar study (Thacker *et al*, 2006). However, the lymph node types displaying the lower levels of IFN-γ expression (caudal mediastinal and cranial tracheobronchial) subsequently showed dominant IL10 expression (Figures 20 and 22) and the lowest level of pathology (Figure 25), therefore reinforcing the significance of IFN-γ on pathological damage. Similarly to the *Leishmania* infection model, Thacker *et al* (2006) suggested that anti-inflammatory cytokine IL10 may act to moderate IFN-γ levels to reduce pathological damage. Interestingly, only the level of IFN-γ and not that of IL10 changed in accordance with the level of pathological damage observed within this study. This implies that in environments of high IFN-γ expression, the level of IL10 produced by the T_H1 cells may be insufficient to control pathological development (Jankovic *et al*, 2007). However, as the level of IFN-γ decreases in response to other stimuli (such as decreasing bacterial load), the previously insufficient levels of IL10 may become able to control the pro-inflammatory response and subsequently the level of pathological damage. Alternatively, it has been suggested by Jankovic *et al* (2007) that high levels of IFN-γ may lead to active blocking of the activity of T_H1-produced IL10, therefore allowing an uncontrolled pro-inflammatory response. Both of these theories would explain why IL10 levels remain consistent between low pathological and high pathological groups, although it would be important to also consider the role of post-transcriptional regulation (creating differing levels of IL10 protein as compared to IL10 mRNA).

A second method of measuring pathological development within this study was based on the stage of granuloma development (Table 18). Granulomas can be categorised into four stages of development depending on their physiological and immunological status (Wangoo *et al*, 2005). The numbers of granuloma within each stage of development were counted for each lymph node sample and the data weighted to account for the larger size of the later staged granuloma (Table 18). Comparing the granuloma stage data with the percentage area coverage of granuloma for each animal revealed a statistically positive relationship ($p<0.05$, Spearmans correlation co-efficient), due to the close association between granuloma

development and granuloma spread throughout the lymph node. The cattle infected with *M. bovis* for five weeks showed the lowest score for granuloma stage (mean 26.3, Table 18), followed by the twelve week (mean 37.6) and the nineteen week groups (mean 45.2), although there was no statistical difference ($p>0.05$, Kruskal Wallis test).

Research in granuloma development has shown that granulomas are 'autonomous microenvironments' (Fenhalls *et al*, 2000) that advance physically irrespective of the state of adjacent granuloma. This therefore creates a vast heterogeneity between different granuloma within the same tissue, as different stages of lesion can exist together. This was seen within the experimentally infected cattle of this study, as cattle from each group showed a spread of granuloma of each developmental stage (Table 18). The main difference in granuloma development between five and twelve weeks post infection was the number of smaller stage I/II granuloma (Table 18). This coincided with the reported increase in cytokine expression between five and twelve weeks (Figures 11, 12 and 13) leading to increased lesion formation. Between twelve and nineteen weeks post infection, there was an increase in the number of later stage III/VI granuloma (Table 18). As previously mentioned, the expression levels of IFN-γ, TNF-α and IL10 decreased between twelve and nineteen weeks, suggesting a loss of cellular activity. However, as IFN-γ expression decreased to a level lower at nineteen weeks to that observed at five weeks of infection, the level of TNF-α and IL10 remained higher. TNF-α is crucial in the maintenance of an effective innate response and controlling cellular influx, however under the influence of IL4 in a T_H2 environment (Hernandez-Pando and Rook, 1994, Hernandez-Pando *et al*, 1997) or in excessively high levels (Bekker *et al*, 2000) TNF-α displays toxic characteristics. The action of TNF-α under these circumstances leads to increased necrosis of susceptible lymphocytes (Seah and Rook, 2001). This therefore leads to the further development of granulomas, from early stage I/II to advanced necrotic stage III/ IV, as observed within this study between twelve and nineteen weeks post infection. This further illustrates the immense sophistication of the immune response and the fine line between protection and immunopathology.

Whole blood IFN-γ cultures from cattle infected with *M. bovis* for five, twelve and nineteen weeks

The aforementioned cytokine expression studies were performed at the site of infection within the lung draining lymph nodes. However, many previous studies published by different

scientific groups have been based on cytokine expression within peripheral blood mononuclear cells (PBMC) due to the logistical problems of isolating lymph nodes. Therefore, IFN-γ protein levels from PBMCs were also measured for each animal within the three experimental groups of this study using stimulatory antigens purified protein derivative bovis (PPD-B, Figure 26), early secretory antigenic target 6-kDa (ESAT-6, Figure 27) protein and culture filtrate protein (CFP, Figure 28). Antigenic stimulation of PBMCs produces a delayed –type hypersensitivity (DTH) reaction during which activated T cells, macrophages and neutrophils converge and express high levels of IFN-γ (Pollock *et al*, 1997). This allowed study into the comparison of IFN-γ production between the periphery and actual site of infection over time post infection.

PPD-B stimulated peripheral IFN-γ expression displayed little change over the nineteen week period post infection (mean OD of 2.49 at five weeks, 2.45 at twelve weeks and 2.53 at nineteen weeks post infection, Figure 26). ESAT-6 stimulated peripheral IFN-γ expression displayed a significantly negative relationship when compared to the IFN-γ mRNA expression within the lymph nodes ($p<0.05$, Pearsons rank correlation coefficient, Figure 27). Thus the levels decreased between five and twelve weeks (mean OD 0.9 and 0.1, respectively) and increased between twelve and nineteen weeks (mean OD 1.29, Figure 27). However, CFP stimulation of PBMC expressed IFN-γ produced a very similar pattern to that observed for the IFN-γ mRNA expression within the lymph nodes, with a slight increase between five and twelve weeks (mean OD 2 and 2.2, respectively) and a decrease between twelve and nineteen weeks (mean OD 1.2, Figure 28) post infection. There were therefore clear differences in IFN-γ expression depending on the stimulatory antigen used. This phenomenon has also been reported in previously published papers, such as a time course study performed on *M. bovis* infection in cattle (Thacker *et al*, 2007) in which PPD stimulation produced a very different pattern of IFN-γ expression as compared to stimulation by an ESAT6:CFP10 recombinant fusion antigen. In contrast, bovine PBMCs infected with 1 cfu of *M. bovis* displayed very similar IFN-γ expression profiles over time post infection when stimulated by either PPD-B or ESAT-6 (Dean *et al*, 2005) although the levels were lower after ESAT-6 stimulation, as seen in this and other studies (Pollock *et al*, 2003). Interestingly, the pattern of IFN-γ expression produced within the study by Dean *et al* (2005) was very similar to the pattern seen in the lymph nodes of this study.

The difference in IFN-γ expression between the three antigenic stimulants may be due to their composition affecting differential T cell activation. A comparative study by Maue *et al* (2005) reported that in vitro stimulation of infected bovine PBMCs by PPD-B and a recombinant ESAT-6: CFP-10 protein displayed similar responses irrespective of the antigen used, except for

CD4+ proliferation. Antigenic stimulation using PPD-B produced four times the magnitude of CD4+ cell proliferation as compared to the recombinant ESAT-6: CFP-10 protein (Maue *et al*, 2005). As CD4+ T cells have been shown to be major producers of IFN-γ, this would therefore explain why PPD-B produced a comparatively higher level of IFN-γ in response to stimulation. The authors suggest that PPD-B may be more effective in producing a CD4+ response because of its composition as an extremely complex antigen (Maue *et al*, 2005).

The use of peripheral IFN-γ levels as a representative of the immune response at the site of infection is still under debate and there have been numerous studies to support (Hope *et al*, 2005, Rhodes *et al*, 2000 and Vordermeier *et al*, 2002) and refute (Barnes *et al*, 1993 and Coussens *et al*, 2004) the theory. As no significant positive relationship was revealed in IFN-γ expression between the lymph nodes and antigenic stimulated PBMCs within this study, the data suggests that peripheral cytokine levels are not representative of the site of infection. The results of the ESAT-6 stimulated PBMCs actually refute the theory, due to presenting a significantly negative relationship between the two variables (Figure 27). However, as there were no significant differences in IFN-γ expression between the three experimental groups for either lymph node data or PBMC data, then the differences seen may be due to natural heterogeneity of the immune system.

Conclusion

The bovine immune response post *M. bovis* infection is an extremely dynamic system, displaying huge heterogeneity within the host as well as between different hosts. The data from this study supports the general consensus that a strong cell mediated immune response is preferentially activated following *M. bovis* infection, leading to high levels of IFN-γ mRNA and associated TNF-α mRNA expression. As the infection progressed, the cell mediated immune response displayed a 'self-limiting' phenotype, in which IL10 was expressed at significantly higher levels to compensate for the increased expression of IFN-γ. This was followed by diminished cytokine expression levels at nineteen weeks of infection, suggesting a loss of cellular activity perhaps due to a developing humoral response. This pattern complements cytokine and antibody data reported previously by other groups (Palmer *et al*, 2007, Joardar *et al*, 2002, Dean *et al*, 2005, Thacker *et al*, 2006, Thacker *et al*, 2007, McNair *et al*, 2001) and further adds to the currently insufficient knowledge of immune responses within the actual site of infection, the lymph nodes.

This study also allowed the comparison of cytokine expression profiles of different lymph node types from the bovine lung draining area. The data showed a significant difference in IFN-γ expression between the lymph node types which may imply a specific 'route of bacterial dissemination' throughout the lymph system. Interestingly, the lymph node types displaying high levels of IFN-γ expression (left bronchial and cranial mediastinal) also displayed the highest levels of granuloma coverage, suggesting a positive relationship between IFN-γ and pathological disease. Subsequently, those lymph node types displaying lower levels of IFN-γ expression (caudal mediastinal and cranial tracheobronchial) had alternatively dominating IL10 expression profiles and lower levels of granuloma coverage. Previous reports had suggested that IL10 acted to down-regulate IFN-γ expression to control pathological disease (Thacker *et al*, 2007) and studies on *Leishmania* infection have shown the ability of T_H1 cells to produce IFN-γ and IL10 simultaneously as a 'self-limiting' mechanism (Anderson *et al*, 2007). However, there was no significant difference in IL10 expression between the four lymph node types within this study irrespective of the level of pathological damage displayed. This may suggest that the control of IL10 on the development of immunopathology may be dependent on the level of IFN-γ (Jankovic *et al*, 2007). It is also important to take into consideration that this data has been based purely on mRNA expression of the target cytokines and as mentioned previously, the presence of posttranscriptional regulatory controls on IL10 may imply that IL10 mRNA is not a true representative of protein levels.

Finally, the study of PBMC producing IFN-γ protein levels within the same cattle used to analyse lymph node IFN-γ mRNA expression levels has shown an ambiguous relationship between the two variables. As there were no significant differences between the three experimental groups (five, twelve and nineteen weeks post infection) for either the PBMC or lymph node IFN-γ levels, the data remains inconclusive as to whether PBMC immune measurements truly represent lymph node profiles. However, the significant negative correlation between ESAT-6 stimulated PBMC IFN-γ production and lymph node IFN-γ levels is an interesting result that may need further investigation.

Chapter 4

Supplementary Study 1

RNA isolation and quantitative PCR from HOPE- and formalin-fixed bovine lymph node tissues

Introduction

Archived biological material is extremely versatile as it allows analysis of parameters such as the pathological and molecular composition many years after the initial experiments were performed (Lehmann and Kreipe, 2006, Lewis *et al*, 2001, Wacharapluesadee *et al*, 2006). Buffered formalin has been widely used as a fixative as it has the capacity to conserve the morphological state of the tissue to a high level (Bhudevi and Weinstock, 2003, Srinivasan *et al*, 2002). Scientists at the VLA (Surrey) therefore routinely archive all experimental material in buffered formalin so as to keep a tissue catalogue of their research. It was therefore possible to perform total RNA extraction and quantitative PCR on tissue samples that were collected many years previously (as was done in the time course study).

There has, however, been some debate on the practical use of formalin as a fixative that conserves the integrity of nucleic acids within the tissue (Goldmann *et al*, 2006). It is believed that methylene bridges form between the amino acids within the RNA molecules thereby rendering the nucleic acid impervious to extraction procedures (Lewis *et al*, 2001, Srinivasan *et al*, 2002). A recent development in tissue fixatives has led to the production of Hepes glutamic acid buffer-mediated organic solvent protection effect (HOPE) fixative (Olert *et al*, 2001, Wiedorn *et al*, 2002) which has been shown to protect the integrity of RNA molecules within human tissues to a considerably higher level (Goldmann *et al*, 2006). This therefore increases the reliability of subsequent quantitative PCR by allowing more efficient primer/probe binding during the amplification step of the procedure. The use of HOPE fixative in the literature has so far been limited to human tissues; however it was believed that it could also prove beneficial in conserving the integrity of RNA within bovine tissue samples. It was therefore decided to perform a supplementary study to assess the quality of total RNA extracted from HOPE as compared to formalin fixed bovine lymph node samples. In addition, two different extraction methods were used, the commercial Optimum™ Formalin Fixed Paraffin Embedded (FFPE) kit and an in-house Trizol method to determine whether the type of method used provided variability in the quality of total RNA extracted. The outcome of this study provides valuable information on the use of formalin and HOPE fixative in molecular studies and aid decisions on

the most appropriate RNA extraction methods for the fixative used. It also has a considerable impact on the interpretation of the time course study results as formalin fixed tissues provided the primary source of total RNA. This work has been published (Witchell *et al*, 2008 – paper included in the appendix).

Methods

Archived bovine *Mycobacterium bovis* infected lymph node tissue (VLA, Surrey) fixed in either buffered formalin (as described in Chapter 2) or HOPE (Goldmann and Olert, 2008) were subjected to total RNA extraction. The two methods used for RNA extraction were the commercially available Optimum™ formalin-fixed, paraffin embedded (FFPE) kit (Ambion) and a Trizol method, both of which have been described in Chapter 2. Spectrophotometry and agarose gel electrophoresis were then performed to determine the overall integrity of the total RNA samples.

Quantitative reverse transcriptase polymerase chain reaction (qRT-PCR) was performed using the Quantitect™ Probe kit (Qiagen, Crawley, West Sussex) targeting the housekeeping gene glyceraldehyde-3-phosphate dehydrogenase (GAPDH) as described in Chapter 2. To enable quantification of the GAPDH transcript within the lymph node total RNA samples, a standard template was designed and manufactured (Biomers.net, Germany). The standard oligonucleotide was identical to the GAPDH-specific amplicon produced following PCR and used to produce a standard curve (as described in Chapter 2). The results were expressed as picograms of GAPDH mRNA in 100 ng of total RNA (pg/100 ng) in each tissue sample.

Results

Total RNA extracted from formalin- and HOPE-fixed, paraffin-embedded tissues using the Optimum™ FFPE kit (Ambion, UK)

The total RNA extracted from both the formalin- and HOPE-fixed bovine lymph node tissues using the Optimum™ FFPE kit produced comparative spectrophotometer results (mean of 108.1 and 96 µg/ml, respectively, $p>0.05$ Mann Whitney test, Table 19). The purity of the total RNA from each tissue sample was also within the recommended range of between 1.7 and 1.9 (Table 19).

Table 19: Quantification and purity (260/280nm ratio) of total RNA determined by spectrophotometry isolated from three formalin- and three HOPE-fixed, paraffin embedded cattle lymph node tissue sections using the Optimum™ FFPE kit (Ambion).

Fixation method and sample number	Total RNA quantification (µg/ml)	260/280 nm ratio (purity)
HOPE 1	107.9	1.8
HOPE 2	82.7	1.9
HOPE 3	97.3	1.9
Formalin 1	80.6	1.7
Formalin 2	145.7	1.8
Formalin 3	97.9	1.9

The three tissue sections from each fixative are a representative group of the isolation procedure that was repeated more than 10 times.

Following agarose gel electrophoresis, the total RNA isolated from formalin-fixed tissues using the Optimum™ kit (Ambion, UK) displayed a visible 28S rRNA band at the expected weight of approximately 4 kb (Figure 29). In comparison, the total RNA extracted from the HOPE-fixed tissues displayed both the 18S and 28S rRNA bands (2 Kb and 4 Kb, respectively, Figure 30).

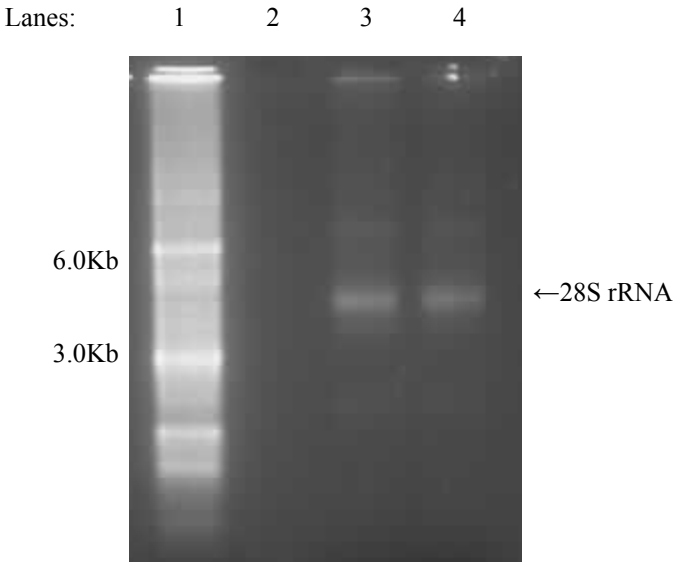

Figure 29: Agarose gel electrophoresis (ethidium bromide staining) of total RNA samples (1 µg) isolated using the Optimum™ FFPE kit (Ambion, UK) from formalin-fixed, *M. bovis* infected bovine lymph nodes (lanes 3 and 4). Lane 1 was a 0.5-10 Kb RNA ladder. Lane 2 was not used. Experiment was repeated three times.

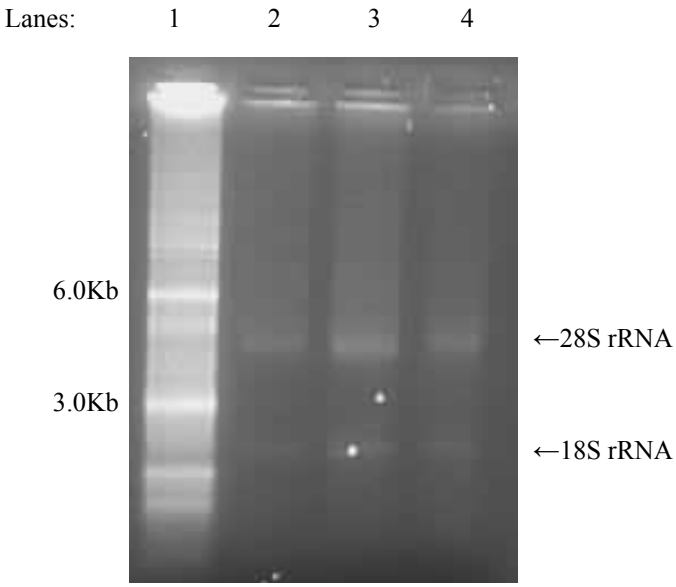

Figure 30: Agarose gel electrophoresis (ethidium bromide staining) of total RNA samples (1 µg) isolated using the Optimum™ FFPE kit (Ambion, UK) from HOPE-fixed, *M. bovis* infected bovine lymph nodes (lanes 2-4). Lane 1 was a 0.5-10 Kb RNA ladder. Experiment was repeated three times.

Total RNA extracted from formalin- and HOPE-fixed, paraffin-embedded tissues using the Trizol method

The extraction of total RNA from formalin-fixed bovine lymph node tissue using the Trizol method proved unsuccessful as confirmed by the spectrophotometry results (Table 20) and the absence of rRNA bands on the agarose gel following electrophoresis (Figure 31).

The total RNA extracted from the HOPE-fixed bovine lymph nodes using the Trizol method (mean 131.6 µg/ml, Table 20) had purity within the recommended range (Table 20) and displayed strong 18S and 28S rRNA bands at the expected molecular weights (2 Kb and 4 Kb) following agarose gel electrophoresis (Figure 31).

Table 20: Quantification and purity (as determined by 260/280nm ratio) of total RNA determined by spectrophotometry isolated from three formalin- and three HOPE-fixed, paraffin embedded cattle lymph node tissues using the Trizol method.

Fixation method and Sample number	Total RNA quantification (µg/ml)	260/280 nm ratio (purity)
HOPE 1	146.7	1.8
HOPE 2	87.0	1.8
HOPE 3	161.1	1.9
Formalin 1	Negative	Negative
Formalin 2	Negative	Negative
Formalin 3	Negative	Negative

The three tissue sections from each fixative are a representative group of the isolation procedure that was repeated more than 10 times.

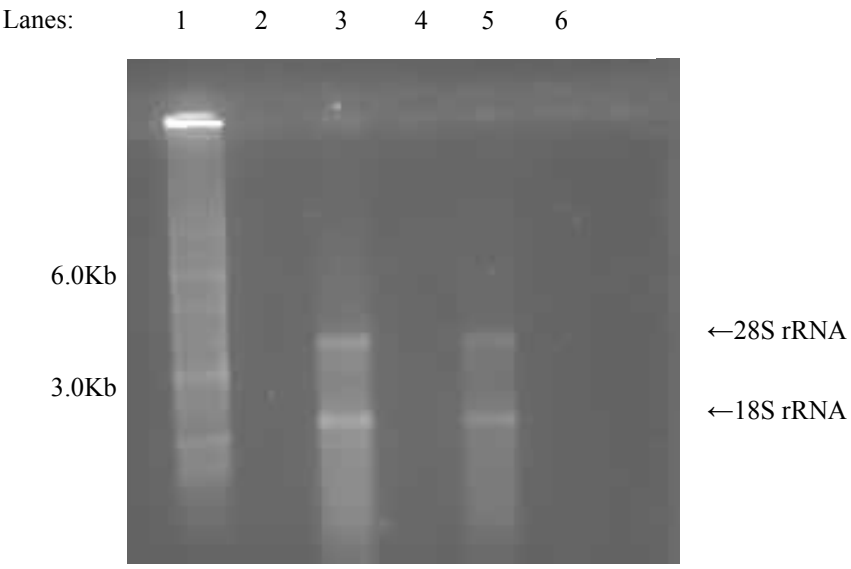

Figure 31: Agarose gel electrophoresis (ethidium bromide staining) of total RNA samples (1 µg) isolated using the Trizol method from formalin-fixed (lanes 2 and 4) and HOPE-fixed (lanes 3 and 5), *M. bovis* infected bovine lymph nodes. Lane 1 was a 0.5-10 Kb RNA ladder. Lane 6 was not used. Experiment was repeated three times.

Quantitative reverse-transcriptase polymerase chain reaction

Quantitative RT-PCR targeting the expression of GAPDH mRNA was performed on the total RNA extracted from both the formalin and HOPE-fixed, *M. bovis* infected bovine lymph node tissues. Each total RNA sample produced a quantifiable PCR product (Figure 32) with the exception of that extracted from the formalin-fixed tissues using the Trizol method.

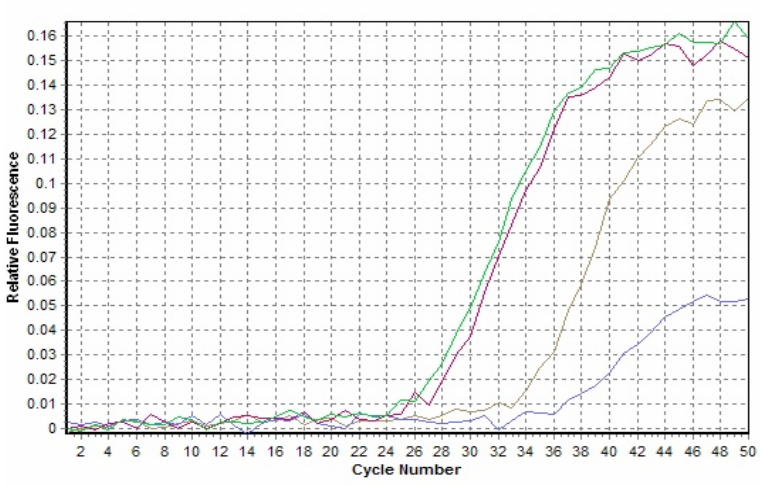

Figure 32: Quantitative RT-PCR of total RNA extracted from both the formalin- and HOPE-fixed, paraffin embedded bovine lymph node tissues using either the Optimum™ FFPE kit (brown and red lines, respectively) or the Trizol method (blue and green lines, respectively). The target sequence was an 87 base pair fragment of the bovine glyceraldehyde-3-phosphate dehydrogenase mRNA and each reaction was performed in duplicate.

A GAPDH standard template was included in each PCR plate at varying concentrations to allow the production of a standard curve. It was then possible to compare the CP values of the unknown total RNA samples to the standard curve thereby determining the exact concentration of the GAPDH template (Table 21 and Figure 32). Using the Optimum™ FFPE kit (Ambion, UK), the total RNA extracted from the formalin-fixed lymph node tissue using had a lower level of GAPDH expression (mean 5.69 $x10^{-4}$ pg/100ng) as compared to that isolated from the HOPE-fixed tissue (4.05 $x10^{-2}$ pg/100ng, Table 21). Using the Trizol method, the extract from the formalin-fixed tissues failed to produce a quantifiable product, however, the total RNA extracted from the HOPE-fixed tissues contained a GAPDH mRNA concentration of 6.45 $x10^{-2}$ pg/100 ng of total RNA (Table 21).

Table 21: QRT-PCR crossing point (CP) values for the expression of GAPDH mRNA in total RNA (100ng) extracted from formalin- and HOPE-fixed, paraffin embedded bovine lymph node samples using two methods, the Optimum™ Kit (Ambion) and a trizol method. Each reaction was performed in duplicate and the mean displayed in the table. The average CP values were then converted into quantitative values using the standard curve (data not shown) and expressed in picograms (pg) of GAPDH mRNA in 100ng total RNA.

Total RNA extraction method	Sample fixation method	Mean CP value	GAPDH mRNA concentration (pg/100ng total RNA)
Optimum™ Kit (Ambion)	Formalin	34.71	$5.69 x10^{-4}$
	HOPE	28.19	$4.05 x10^{-2}$
Trizol	Formalin	Negative	Negative
	HOPE	27.39	$6.45 x10^{-2}$

Discussion

The quality of total RNA extracted from archived tissue samples has a considerable affect on the outcome of subsequent molecular techniques (Bustin, 2002, Bustin and Mueller, 2006). It has been suggested in the literature that formalin fixation compromises the integrity of the nucleic acids within the tissue samples thus reducing the efficacy of extraction procedures (Bustin and Mueller, 2006, Srinivasan *et al*, 2002, Lewis *et al*, 2001). This supplementary study aimed to determine the quality of total RNA extracted from formalin-fixed, bovine lymph node samples as compared to novel fixative HOPE. This also included the use of two different extraction methods, a commercial kit from Ambion (UK) and a Trizol method developed in-house. The results showed that, although the total RNA extracted from both the formalin- and HOPE-fixed tissues using the Optimum™ kit was of a comparable concentration (Table 19), there was a difference in the level of GAPDH mRNA expression between the two fixative types (Figure 32 and Table 21). The total RNA extracted from the formalin-fixed bovine lymph node tissues displayed a lower level of GAPDH expression following qRT-PCR as compared to that observed in the HOPE-fixed derived total RNA (a concentration of approximately 70x less mRNA, Table 21). This suggests that HOPE fixative conserved the integrity of the bovine RNA to a much higher degree, as suggested by Wiedorn *et al* (2002) in human tissues. This was further supported by the agarose gel electrophoresis results, as the total RNA extracted from the HOPE-fixed tissues displayed both rRNA bands compared to that extracted from the formalin-fixed tissue which displayed only the 28S rRNA band (Figures 29 and 30). The ability of HOPE fixative to preserve both morphological and molecular composition may be due to the increased rate of tissue dehydration, enabled by the diffusion of a protective solution of amino acids into the tissue section (Srinivasan *et al*, 2002).

The total RNA extracted from the HOPE-fixed tissues using the trizol method produced very similar spectrophotometry and qRT-PCR results to that extracted using the Optimum™ kit (Tables 20 and 21). Interestingly, it was not possible to extract quantifiable total RNA from the formalin-fixed tissues using the trizol method (Table 20 and Figure 31). The ability of the Optimum™ kit (Ambion) but not the trizol method to isolate the total RNA from the formalin-fixed tissues may be attributed to the use of proteinase K. Proteinase K is efficient at separating the RNA from the cross-linked matrix formed as a result of the reactive ability of

formaldehyde (Srinivasan *et al*, 2002). Therefore, with the absence of a proteinase k step, the trizol method was not able to successfully isolate total RNA from the formalin-fixed tissues.

In conclusion, this study supports a strong consensus that HOPE fixative is a more appropriate fixative for tissue sections that will be used in molecular methods. This is because HOPE fixative is able to conserve the integrity of total RNA to a much higher level as compared to formalin fixative. This is the first study to explore HOPE fixation in *M. bovis* infected bovine lymph node tissues. Since this study, the scientists at the VLA have started to routinely fix tissues in HOPE as well as formalin to allow more versatile use of the archived samples. In addition, these results highlight the importance of selecting the appropriate extraction method dependent on the fixative used to enable the most efficient isolation of total RNA.

It is also important to consider these findings when analysing the time course study described previously. As the total RNA templates for the time course study were extracted from formalin fixed *M. bovis* infected lymph node tissues, it would be appropriate to assume that the cytokine expression levels observed were relatively low due to partial RNA degradation. The conclusions drawn from the time course study still provide some valid theories on the role of cytokines in *M. bovis* infection, however, the exact quantification of the expression levels may be compromised as a result of using a template extracted from formalin fixed tissues.

Chapter 5

Supplementary Study 2

Cytokine mRNA expression in cattle infected with different dosages of *Mycobacterium bovis*

Introduction

An important feature of experimental *M. bovis* models is their relevance and applicability to natural *M. bovis* bovine infection. In previous years, cattle have been experimentally infected with relatively large doses of infectious *M. bovis* to ensure that the animals successfully presented disease (for example, 10^6 cfu's in Johnson *et al*, 2006 and Joardar *et al*, 2002 or 10^4 cfu's in Widdison *et al*, 2006 and Villarreal-Ramos *et al*, 2003). Studies have shown, however, that a host need only inhale one or two bacterial cells to become naturally infected (Schafer *et al*, 1999). To determine the possible effects of different infecting dosages, Dean *et al* (2005) experimentally inoculated cattle with 1, 10, 100 and 1,000 cfu's of *M. bovis* and described the pathological state of the lymph nodes as well as the profile of whole blood IFN-γ and IL4 proteins after twenty-six weeks. Surprisingly, there did not appear to be any difference in the pathology scores of the lymph nodes for the skin test-positive calves between the different groups. This suggests that 1 cfu of bacteria created a level of pathological disease similar to that produced by 1,000 cfu (Dean *et al*, 2005). The group also found that there were no significant differences in whole blood IFN-γ or IL4 protein between the animals infected with different dosages of *M. bovis*.

The concentrations of *M. bovis* used within the time course (10^4 cfu's) and BCG vaccination (10^3 cfu's) studies were either at the higher end or supra-threshold to those concentrations used in Dean *et al* (2005). Therefore to supplement the studies within this thesis and to determine their relevance to natural *M. bovis* infection, it was decided that the molecular methods developed and described in chapter 2 would be applied to the same experimental samples used by Dean *et al* (2005). This new information provides an insight into the immunological state of the lymph nodes and determines whether the concentration of the starting inoculum provided any variation in cytokine response. This work was carried out entirely by an MSc student using the RNA extraction and quantitative PCR methods that were developed for this thesis (Boddu-Jasmine *et al*, 2008 - paper included in the appendix).

Methods

Sixteen six month old Friesian Holstein heifers were intratracheally infected with 1, 10, 100 or 1,000 cfu's of *M. bovis* (strain AF 2122/97, four cattle within each group) as described in Dean *et al* (2005). The animals were then euthanized at twenty-six weeks post infection by an intravenous injection of sodium pentobarbitone and the lymph nodes (cranial mediastinal, caudal mediastinal and left bronchial) dissected. Following on from Supplementary study 1, it was decided to fix the lymph node tissue samples in HOPE to provide optimum preservation of the nucleic acid (fixation method described in Boddu-Jasmine *et al*, 2008). The trizol method (Witchell *et al*, 2008) was used to extract total RNA from each HOPE-fixed bovine sample. Quantitative PCR targeting the expression of IFN-γ, TNF-α, IL10 and IL4 were performed on each lymph node sample using the Quantitect™ Probe kit (Qiagen, UK) as described in Chapter 2.

Results

The expression of IFN-γ, TNF-α, IL10 and IL4 mRNA measured using quantitative RT-PCR displayed a significant difference in response to varying concentrations of *M. bovis* infecting inoculum ($p<0.05$, Kruskal Wallis test, Table 22). As the starting dosage of *M. bovis* inoculum increased, there was a related increase in the level of cytokine gene expression (Table 22).

IFN-γ expression increased over 1, 10, 100 and 1,000 cfu's of infecting *M. bovis* (2.1×10^5, 2.3×10^5, 4.2×10^5 and 9.0×10^5 copies, respectively, Table 22). There was a significant difference in IFN-γ expression between 1 and 1,000 cfu's (4.23 fold increase) and between 10 and 1,000 cfu's (3.88 fold increase, $p<0.05$, Mann Whitney test).

TNF-α expression displayed a slight decrease between 1 and 10 cfu's of *M. bovis* infecting dosage (2.5×10^5 and 2.6×10^5, respectively, Table 22) although this was not significant ($p>0.05$, Mann Whitney test). Between 10, 100 and 1,000 cfu's there was an increase in TNF-α expression (2.6×10^5, 5.6×10^5 and 7.1×10^5 copies, respectively) however these differences were not significant ($p>0.05$, Mann Whitney test).

IL4 expression increased over 1, 10, 100 and 1,000 cfu's of infecting *M. bovis* concentration (2.0×10^5, 2.2×10^5, 4.5×10^5 and 6.3×10^5 copies, respectively, Table 22). There was a significant difference in IL4 expression between 1 and 1,000 cfu's (3.15 fold increase) and also 10 and 1,000 cfu's (2.86 fold increase, $p<0.05$, Mann Whitney test).

The expression of IL10 increased significantly between 1 and 100 cfu's of *M. bovis* (9.3×10^4 and 4.5×10^5, respectively, Table 22). There was also a significant increase in IL10 expression between 1 and 1,000 cfu's of *M. bovis* (9.3×10^4 and 5.1×10^5, respectively, 5.5 fold increase, Table 22).

Table 22: The mean copy numbers of cytokine (IFN-γ, TNF-α, IL10 and IL4) mRNA within the lymph nodes of cattle infected with either 1, 10, 100 or 1,000 cfu's of M. bovis (measured using quantitative RT-PCR).

	Cytokine expression (molecules/µl) at different experimental *M. bovis* dosages			
Cytokines	1 cfu	10 cfu	100 cfu	1,000 cfu
IFN-γ	213,500	234,665	425,825	904,750
TNF-α	252,450	260,675	565,000	715,125
IL10	200,875	221,125	449,250	633,000
IL4	93,850	288,975	450,000	510,750

Discussion

In the study performed by Dean *et al* (2005), no significant difference in pathological score was noted in the lymph nodes of cattle infected with either 1, 10, 100 or 1,000 cfu's of *M. bovis*. In addition, there were no significant differences in whole blood IFN-γ or IL4 protein between the four experimental groups (Dean *et al*, 2005). The same bovine lymph node samples were used to investigate the expression of IFN-γ, TNF-α, IL10 and IL4 within this study, and interestingly, significant differences between the four experimental groups were revealed ($p<0.05$, Mann Whitney test). As the concentration of *M. bovis* inoculum increased, there was a simultaneous increase in the expression of the four target cytokines. This is believed to be due to the increased antigenic stimulation associated with higher levels of bacterial infection thereby producing a stronger cytokine immune response. The largest increases were in IFN-γ (fold increase of 4.23 between 1 and 1,000 cfu's) and IL10 expression (fold increase of 5.5 between 1 and 1,000 cfu's, Table 22). IFN-γ, as mentioned previously, is an extremely important part of the immune response following *M. bovis* infection and is strongly activated via the T_H1 pro-inflammatory profile. It is therefore not surprising that IFN-γ expression experienced such a large increase with increased infective dose. IFN-γ has also been shown to be heavily involved

in the pathological development of the disease. However, the data from these animals show that increasing IFN-γ expression did not have any effect on the level of pathology and this may be as a consequence of the time point post infection the samples were taken. In a bovine *M. bovis* infection study performed by Palmer *et al* (2007), little difference was seen in lesion coverage of lymph nodes between six and fifty three weeks following inoculation. This suggests that for any difference in pathological state to be observed as a result of increasing *M .bovis* dose, it would be necessary to take lymph node samples at a much earlier time point pre-twenty-six weeks.

A reoccurring theme in both the time course and BCG vaccination studies was the role of IL10 in limiting the damage of pro-inflammatory cytokine IFN-γ. As noted from the results of this study, IFN-γ and IL10 expression have been shown to increase relative to one another (Lin et al, 1996) as both are produced by CD4+ T cell clones (Gerosa et al, 1999). Gerosa et al (1999) suggested that this may be a mechanism of 'self-limiting' to control the destructive properties of TH1 and TH2 associated cytokines. This would explain why both IFN-γ and IL10 displayed the largest increase in expression as response to increasing *M. bovis* dosage.

Interestingly, expression of IL4 was evident in all of the lymph node samples from each of the four experimental groups (Table 22). IL4 is associated with the T_H2 anti-inflammatory response that develops late in bTB infection (Welsh *et al*, 2005). It was not possible to detect IL4 mRNA expression in any of the *M .bovis* infected lymph nodes of the time course or BCG vaccination studies and again, this may be due to the time points post infection that were used. IL4 was not detected at five, twelve or nineteen weeks following infection; however, in this specific study it was detectable at twenty-six weeks. This represents the importance of IL4 in the later stages of bTB infection when the cell mediated response is actively dominated by the developing humoral response (Welsh *et al*, 2005).

Lastly, TNF-α was the only cytokine to not show a significant increase in expression as the M. bovis inoculation concentration increased (Table 22). These results reflect those seen in the time course and BCG vaccination studies, as expression of TNF-α shows little variation to differing conditions as compared to the other cytokines. This may be due to the role of posttranscriptional regulation. Therefore the lack of significant differences in TNF-α expression may not be representational of the pattern in TNF-α protein production.

In conclusion, although there were no apparent differences in pathology of the bovine lymph nodes as a result of increasing the inoculation concentration of *M. bovis*, the expression levels of IFN-γ, IL10 and IL4 did show significant changes. The increasing concentrations of *M. bovis*

led to enhanced antigenic stimulation and subsequently an enhanced rate of cytokine expression. This therefore suggests that the cytokine expression levels observed in experimental bovine models that use relatively high concentrations of *M. bovis* may not necessarily represent those that would be observed in natural infection conditions. However it is important to note that as all of the cytokines increased in expression relative to each other, the patterns observed at high *M. bovis* concentrations may still be relevant to lower *M. bovis* concentrations. This supports the use of experimental bovine models in exploring bTB infection but also shows that it is possible to use smaller doses of infecting inoculums to produce immune profiles that more resemble natural infection.

Chapter 6

BCG Vaccination Study

Introduction

Developing a new and improved BCG vaccine

BCG bacterium evolution

A critical step in the development of an improved BCG is the understanding of where and why the current BCG may be failing to induce sufficient and consistent protection against tuberculosis. The BCG vaccine used today is extremely different genomically to the BCG that was first produced at the beginning of the twentieth century and this is partly due to the lack of production standardisation (Charlet *et al*, 2005). Although the attenuated form of the BCG bacterium was produced in 1921, the technology used to store bacterial stocks (freezing or lyophilisation) was not developed until 1961. This meant 53 years passed between the production of the vaccine and the ability to store it in a metabolically inactive state. In this time the BCG bacterium underwent an estimated 1,173 passages under laboratory selective pressures, equating to around 15,000 generations (Mostowy *et al*, 2003). Current legislation recommends that bacterial stocks for vaccine production undergo a maximum of 12 passages to ensure the consistency of each vaccine batch (Brosch *et al*, 2007).

A pivotal step in understanding the evolutionary path of the BCG has been the complete mapping of the genome for *M. bovis* (Garnier *et al*, 2003), *M. tuberculosis* (Cole *et al*, 1998) and BCG Pasteur (Brosch *et al*, 2007). This, in combination with advances in modern comparative tools such as genome microarrays, has made it possible to determine the genetic basis of the original attenuation of BCG and the sequence polymorphisms experienced post 1921 (Charlet *et al*, 2005). Amazingly, in the comparatively short time of 53 years (between BCG production and immortalisation), the average BCG bacterium lost more genomic DNA than isolated clinical strains of *M. tuberculosis* had over centuries (Kato-Maeda *et al*, 2001). A large percentage of these deletions are due to the loss of the RD1 group, representing genes encoding mostly antigenic proteins (Behr, 2002). A possible reason for these particular deletions could be due to the redundancy of antigenic proteins under laboratory growth conditions (Mostowy *et al*, 2003). Bovine TB pathogenesis relies heavily on the action of antigenic proteins and the loss of the RD1 region including ESAT-6 during attenuation of BCG was one of the major factors in its development. It has been suggested that further losses of

antigenic proteins between 1921 and 1961 could have rendered BCG less able to mimic the *in vivo* disease and reduced its immunising properties (Charlet *et al*, 2005).

Antigenic proteins MPB70 and MPB83

There are a number of antigenic proteins that are differentially expressed between *M. tuberculosis*, *M. bovis* and BCG. Two of the more well-known are MPB70 and MPB83 (MPT in *M. tuberculosis,* Said-Salim *et al*, 2006). Both of these proteins are antigenic, are believed to play a role in determining the host preference of the bacteria (Hewinson *et al*, 2006) and are well known for their ability to induce cellular and humoral immune responses (Lyashchenko *et al*, 2001). The expression of these proteins is controlled by the extracytoplasmic alternative sigma factor K (SigK) which is in turn regulated post-translationally by the anti-sigma factor RskA (Said-Salim *et al*, 2006). Within *M. tuberculosis*, RskA binds to SigK thus preventing the transcription of both *mpt70* and *mpt83* (Husson, 2006). In response to the appropriate environmental stimuli and in particular during phagosomal containment (Schnappinger *et al*, 2003), RskA releases SigK and allows it to bind to the promoter of *mpt70* and *mpt83,* up-regulating the expression of these antigenic proteins (Said-Salim *et al*, 2006). Genetic studies based on the sequenced genomes of *M. tuberculosis* and *M. bovis* have shown that there is no variation in the sequences of *mpt*/*mpb*70, *mpt*/*mbp*83 or *sigK* between the two mycobacterial species (Charlet *et al*, 2005). However within *M. bovis*, the gene sequence encoding for RskA (*Rv0444c*) displayed two single nucleotide polymorphisms (SNPs) and therefore a distorted ability to repress SigK resulting in over-production of the antigenic proteins. MPB/MPT70 and MPB/MPT83 are therefore produced in an inducible manner by *M. tuberculosis* but are constitutively expressed by *M. bovis* species (Said-Salim *et al*, 2006). In murine infection models *M. bovis* has been shown to produce increased levels of pathological disease and extensive dissemination as compared to *M. tuberculosis* (Medina *et al*, 2006), however the effect of the inactivated anti-sigma factor RskA on this enhanced level of virulence is as yet unknown.

MPB70 and MPB83 are produced by the *M. bovis* derivative BCG *in vitro* although the expression levels vary dramatically between different sub-strains (Charlet *et al*, 2005). Based on the production of MPB70, it is possible to separate BCG strains (Harboe and Nagai, 1984) into those derived from the parental BCG strain before 1929, termed high producers of MPB70 and those derived after 1931, termed low producers of MPB70. The MPB83 protein also seems to follow the same pattern although not as consistently as MPB70 (Wiker *et al*, 1996).

Extensive research has been performed on these two proteins to elucidate this difference in expression profiles. There is a detectable difference in *mpb70* transcription between the two BCG strains Tokyo (high producer) and Pasteur (low producer), however when complementing BCG Pasteur with *mpb70* from BCG Tokyo there was no significant increase in the level of MPB70 (Matsuo *et al*, 1995, Matsumoto *et al*, 1995). These results therefore indicate a possible difference in the control of *mpb70* transcription by regulatory proteins in addition to the mutation described for the gene *Rv0444c*. The gene responsible for encoding SigK (*Rv0445c*) has been shown to be down-regulated in the low producing BCG strains and subsequent sequence analysis of *Rv0445c* revealed a polymorphism in its associated start codon (Charlet *et al*, 2005). The high producer strains of BCG (and all members of the mycobacterium family) contained an AUG start codon whereas the low producers contained an AUA start codon due to a G→A single nucleotide polymorphism in the third nucleotide (Table 23). Both start codons are functional however the AUA codon (also detected in *Escherichia coli* and *Salmonella* spp.) results in significantly lower translational levels of SigK. This in turn leads to a significantly lower level of MPB70 and MPB83.

Table 23: Genetic comparison of different BCG strains on the level of MPB70 and MPB83 production and the sequence of the *sigK* start codon (adapted from Charlet *et al*, 2005). The species highlighted in blue (including *M. bovis*) are termed high producers of MPB70 and MPB83 whereas those highlighted in red are low producers following a mutation in the *sigK* start codon.

Strains	High / low producers of MPB70 and MPB83	Third nucleotide of 3 bp start codon
M. bovis	High	G
BCG Russia	High	G
BCG Moreau	High	G
BCG Japan	High	G
BCG Sweden	High	G
BCG Birkhaug	High	G
BCG Prague	Low	A
BCG Glaxo	Low	A
BCG Denmark	Low	A
BCG Tice	Low	A
BCG Connaught	Low	A
BCG Frappier	Low	A
BCG Phipps	Low	A
BCG Pasteur	Low	A

The protective properties of MPT83 have been explored in DNA and RNA vaccine trials and have been shown to induce protection against *M. tuberculosis* infection in mice (Xue *et al*, 2004). However in cattle, DNA vaccines expressing MPB70 and MPB83 when used individually or as a MPB70 DNA prime- protein boost strategy showed no evidence of significant protection against *M. bovis* infection (Wedlock *et al*, 2003). Both DNA vaccines failed to induce a cell mediated immune response (characterised by IFN-γ and IL-12) and the DNA prime-protein boost preferentially activated a strong antibody response with minimal IFN-γ production. Interestingly, the vaccines did not produce a DTH reaction in response to the PPD tuberculin test which is a huge advantage in the development of a vaccine/diagnostic testing strategy for infected cattle. The authors suggest that these vaccines may provide a basis for future vaccine development and that improvements in inducing an appropriate cell mediated response may be possible by subunit modification (Wedlock *et al*, 2003).

Although comparative genomics have provided a greater understanding of the genetic basis and evolution of MPB70 and MPB83 expression across the different BCG sub-strains (Mostowy *et al*, 2003, Brosch *et al*, 2007), an area that has received less attention is that of standardising the actual levels of MPB70 and MPB83 production. A study involving the comparison of these protein expression profiles in high and low BCG producers would provide much more insight into their importance on the protective efficacy of the vaccine (Charlet *et al*, 2005). Vaccination studies on human infants has suggested that BCG Japan (a high producer) provides a higher level of protection as compared to BCG Denmark (low producer) by inducing significantly higher levels of T_H1 cytokines and T cells (both CD4 and CD8, Davids *et al*, 2006). Although the contribution of MPB70 and MPB83 to this increased immunological ability is unknown, evidence of the immunogenic properties of these proteins in related studies (Liu *et al*, 2007, Vordermeier *et al*, 2000, Rhodes *et al*, 2000) provides a compelling idea on their importance in vaccine efficacy.

Experiments based on the complementation of BCG Pasteur with wild-type *sigK* have significantly increased levels of *mpb70* and *mpb83* transcription and as a result levels of MPB70 and MPB83 protein were comparable to those of high producer BCG strains (Charlet *et al*, 2005). However to date there has been a lack of studies aimed at investigating whether a genetically modified BCG Pasteur complemented with a wild-type *sigK* would improve its immunological ability and therefore its protective efficacy as a vaccine against tuberculosis.

Aims and Objectives

It was proposed to study the immunological responses of cattle vaccinated with either BCG Pasteur or a genetically modified BCG Pasteur and challenged with *M. bovis*. The genetically modified BCG Pasteur was complemented with a wild-type copy of the *sigK* gene from BCG Russia in order to up-regulate expression of MPB83 and MPB70. The study also included three control groups of cattle, non-vaccinated *M. bovis* infected, non-vaccinated non-infected and BCG Pasteur vaccinated non-infected. This aided in determining the dynamics of the immune response to infection and vaccination.

Aim 1: To compare the immunological responses of BCG Pasteur vaccinated challenged cattle to the three control groups.

Aim 2: To compare the immunological responses of genetically modified *sigK* BCG Pasteur vaccinated challenged cattle to the three control groups.

The study focused on the lymph nodes draining the bronchial region of the animals therefore allowing a response profile to be created for the actual site of infection. The immune response was measured using quantitative polymerase chain reaction targeting the cytokines interferon gamma (IFN-γ), tumour necrosis factor alpha (TNF-α), interleukin 10 (IL10) and interleukin 4 (IL4). This was followed up by studying the protein expression of IFN-γ and TNF-α within the same samples using immunohistochemistry.

Objectives:

1. The left bronchial, caudal mediastinal and cranial mediastinal lymph nodes of each animal from the five experimental groups were isolated and dissected. The dissected tissue samples were then either incubated in Trizol and prepared for immediate extraction of total RNA or fixed in buffered formalin and embedded within a paraffin wax block for subsequent immunohistochemistry (IHC).
2. Pathological damage within each lymph node was measured by observing the percentage of granuloma coverage and the developmental stage of each lesion within the mounted sections.

3. Total RNA was extracted from the freshly dissected lymph node tissues and quality checked using spectrophotometry and agarose gel electrophoresis.
4. QRT-PCR was performed on the extracted total RNA from each lymph node tissue sample targeting the four cytokines as well as the housekeeping gene glyceraldehyde-3-phosphate dehydrogenase (GAPDH) to ensure the quality of the starting template. The target mRNA sequences from each of the lymph node tissue samples were quantified using specifically designed standard curves and expressed in copy numbers.
5. The formalin fixed, paraffin embedded tissue samples were sectioned and mounted onto slides for IHC. This was performed for both IFN-γ and TNF-α protein analysis on all of the lymph node tissues from each animal. The results were expressed semi-quantitatively by using a scoring method based on the percentage coverage of positively stained cells over the lymph node section.
6. To compliment the cytokine expression data within the lymph nodes, levels of IFN-γ protein were measured in cultured peripheral blood samples from each animal using enzyme linked immunosorbant assays (ELISA).

Materials and Methods

Experimental design

Twenty Friesian Holstein heifers and bullocks of approximately six months of age and with no history of tuberculosis infection were divided into five experimental groups. Cattle from group one (three animals) and group five (four animals) were vaccinated by subcutaneous injection of standard BCG Pasteur ($6.3x10^5$ colony forming units of BCG). Cattle from group two (four animals) were vaccinated by subcutaneous injection of genetically modified *sigK* BCG Pasteur ($5x10^5$ colony forming units of BCG). The BCG Pasteur::pRUSS (*sigK* complemented) construct was provided by Marcel Behr (University of McGill, Montreal, Canada). The construct consisted of a BCG Pasteur strain containing a copy of the *sigK* gene from a BCG Russia strain (Charlet *et al*, 2005). Cattle from group three (four animals) and group four (five animals) were left unvaccinated. Each animal within groups one, two and three were challenged intratracheally with *M. bovis* (strain AF2122/97, $6x10^3$ cfu) ten weeks following vaccination, as described in Chapter 2. Groups four and five were non-infected controls.

Table 24: Combinations of experimental vaccination (BCG Pasteur or BCG (*sigK*) Pasteur) and *M. bovis* challenge in the five cattle groups.

Animal group	Vaccination	Challenge	No. cattle
1	BCG Pasteur	*M. bovis*	3
2	BCG (*sigK*) Pasteur	*M. bovis*	4
3	None	*M. bovis*	4
4	None	None	5
5	BCG Pasteur	None	4

Post mortems and lymph node tissue preparation

The *M. bovis* challenged cattle (groups one, two and three) were euthanized at five weeks post infection (fifteen weeks after the start of the experiment). Cattle within groups four and five (the non-infected animals) were euthanized at fourteen and sixteen weeks after the experimental start date due to logistical restraints (limited category three space and resources). The cattle were euthanised as per the method described in Chapter 2. Tissue sections were dissected

from the lymph nodes (left bronchial, cranial mediastinal and caudal mediastinal nodes) and submerged in both trizol for subsequent total RNA extraction and buffered formalin for immunohistochemistry (as described in Chapter 2).

Quantitative reverse transcriptase polymerase chain reaction

Quantitative PCR was performed using the Quantitect™ Probe RT-PCR kit (Qiagen, Crawley, West Sussex) as described in Chapter 2. The qRT-PCR experiments were designed to allow direct comparison between the five experimental cattle groups (Figure 33). Therefore each sample from the five groups had to be included in the same ninety six well PCR plate to avoid the complication of plate to plate variation. Within each PCR plate, all samples of one lymph node over the five experimental groups were analysed for one target cytokine. Each lymph node sample was analysed for the expression of all four cytokines; IFN-γ, TNF-α, IL10 and IL4. The mRNA expression of the housekeeping gene GAPDH was also measured within each sample to ensure the quality of the total RNA transcript. Lastly, each PCR plate included the diluted standard templates specific to the target cytokine to allow construction of the standard curve (as described in Chapter 2).

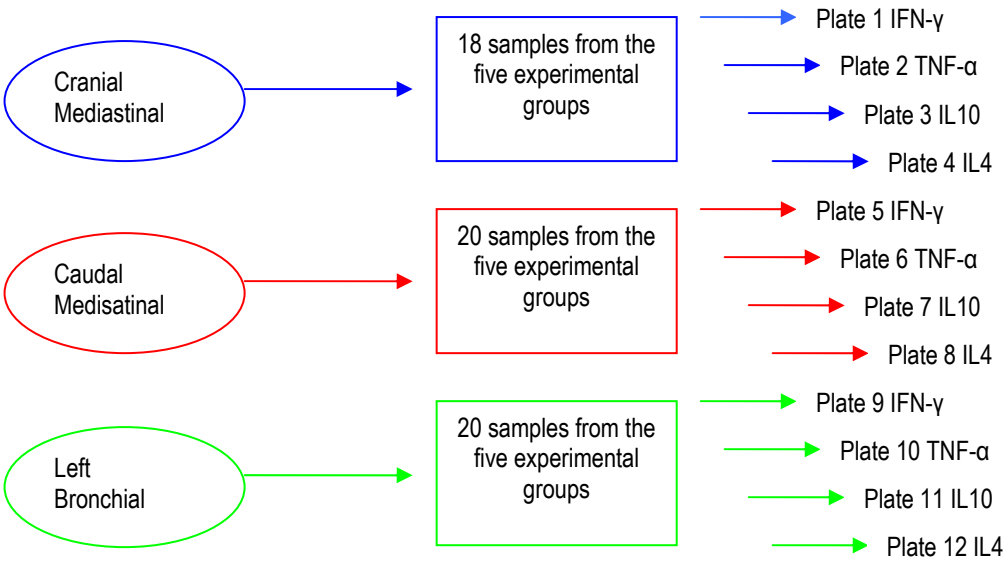

Figure 33: Quantitative RT-PCR experimental designs for the BCG vaccination study. Each 96 well plate contained reactions analysing one cytokine from all samples of one lymph node from the five experimental groups (BCG Pasteur vaccinated challenged, BCG (*sigK*) Pasteur vaccinated challenged, non-vaccinated infected, non-vaccinated non-infected and BCG Pasteur vaccinated non-infected). This allowed the direct 'in- plate' comparison of cytokine levels between the five experimental groups and reduced the potential problem of plate to plate variability. The specific standard curve for the cytokine and a GAPDH for each sample were also run on each plate. Each reaction was performed either in duplicate or triplicate.

Immunohistochemistry

The formalin-fixed lymph node tissue samples were used for immunohistochemistry to detect cells positive for IFN-γ and TNF-α protein secretion, as described in Chapter 2.

Whole blood IFN-γ cultures

Samples of heparinized whole blood were collected from each of the animals prior to euthanization (Surrey), as described in Chapter 2. The data from the BOVIGAM® tests were used to compare against the lymph node cytokine data.

Results

Total RNA extraction

The first step in the study of cytokine gene expression was to isolate total RNA from the three thoracic lymph nodes of each animal in the five experimental groups (BCG Pasteur vaccinated challenged, BCG (*sigK*) Pasteur vaccinated challenged, non-vaccinated infected, non-vaccinated non-infected and BCG Pasteur vaccinated non-infected). The freshly sectioned lymph node samples were homogenised while submerged in trizol and the total RNA was extracted using chloroform – isopropanol. Total RNA was quantified (Table 25) using a BioPhotometer (Eppendorf, Germany) and run on a 1% agarose electrophoresis gel (TAE buffer) to determine sample integrity (visualisation of the ribosomal RNA bands, Figure 34).

Table 25: Quantification (µg/ml) and purity determined by spectrophotometry of total RNA isolated from the lymph nodes of *M. bovis* infected and non-infected cattle. The data represents averaged lymph node results of approximately 50 extractions in total.

Tissue type (n=50)	Total RNA (50 µl) quantification µg/ml (mean ± SD)	260/280 nm ratio (mean ± SD)
Freshly dissected lymph node tissue	781.92 ± 451.78	1.9 ± 0.11

Total RNA was successfully isolated from all of the lymph node samples of cattle from the five experimental groups. The mean concentration of total RNA extracted from approximately 50 freshly dissected tissue sections was 781.92 µg/ml (in a 50 µl total volume, Table 25). The large standard deviation of the mean associated with this data (451.78, Table 25) suggests that the concentration of total RNA extracted from the different lymph node samples was extremely varied (range from 170 to 1,952 µg/ml). The ratio of total RNA (OD at 260 nm) to protein (OD at 280 nm) was within the recommended range (mean 1.9, Table 25) (Fleige and Pfaffl, 2006).

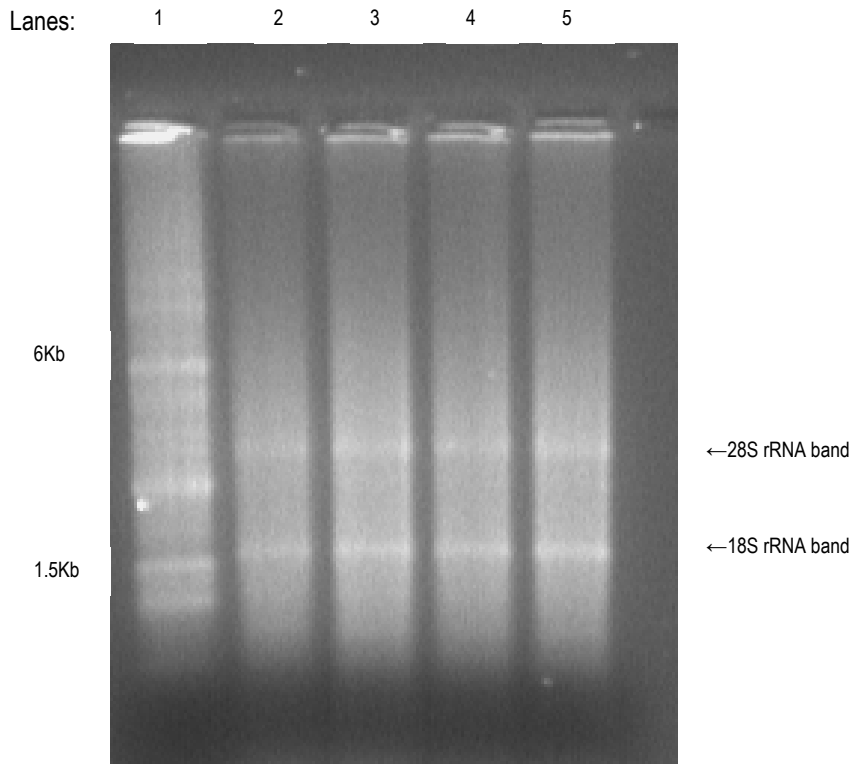

Figure 34: Agarose gel electrophoresis (1% agarose within TAE buffer and ethidium bromide staining) of total RNA samples (300 ng/ well) isolated from *M. bovis* challenged and non-challenged cattle lymph node tissues (lanes 2 to 5). All total RNA samples displayed a 28S ribosomal RNA band of approximately 4 Kb in length and an 18S ribosomal band of approximately 2 Kb. Lane 1 is a 0.5-10 Kb RNA ladder with highlighted standard RNA base pair lengths of 6 and 1.5 Kb. The electrophoresis experiment was repeated with different total RNA samples 10 times and displayed consistent results.

Each total RNA sample displayed bands of approximately 4 Kb and 2 Kb in length (Figure 34). These nucleotide lengths correspond to the expected lengths of 28S and 18S ribosomal RNA (Bradford *et al*, 2005) and give an indication to the high level of integrity of the total RNA samples. There was little evidence of DNA contamination, which would be represented by clear bright bands nearer to the wells (Figure 34). The total RNA samples extracted from the freshly dissected cattle lymph nodes showed high levels of messenger RNA when run on the agarose gels, represented by the localised smearing seen on the gel (Bradford *et al*, 2005).

Quantitative Reverse Transcriptase Polymerase Chain Reaction

Standard curves

Standard templates for the cytokines IFN-γ, TNF-α, IL10 and IL4 were designed and serially diluted to produce a standard curve. This allowed conversion of the calculated crossing point values of the unknown samples into quantitative copy number. The results of the standard curves were as previously described for the Time course study.

Glyceraldehyde-3-phosphate dehydrogenase (GAPDH)

The housekeeping gene GAPDH was analysed by qRT-PCR for each sample alongside each target cytokine to ensure the quality of the starting total RNA template. In the absence of a cytokine PCR product, the presence of a GAPDH PCR product ensured that the sample template was of a high quality.

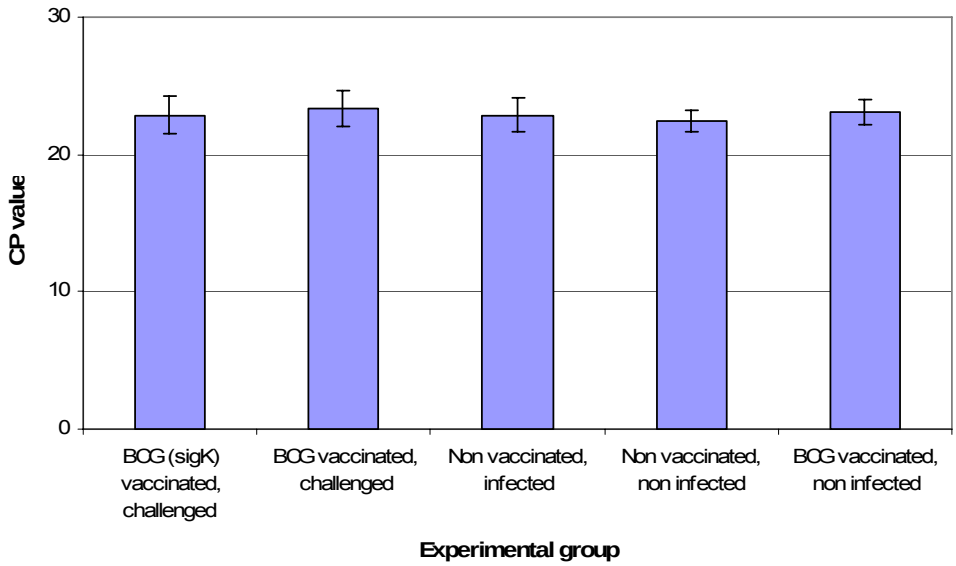

Figure 35: The crossing point (CP) values of GAPDH expression within the thoracic lymph nodes of cattle either vaccinated with BCG (*sigK*) Pasteur prior to *M. bovis* challenge (n=4), vaccinated with BCG Pasteur prior to challenge (n=3), non-vaccinated infected (n=4), non-vaccinated non-infected (n=5) or BCG Pasteur vaccinated non-infected (n=4). The data represents the mean triplicate values from the lymph nodes (left bronchial, cranial mediastinal and caudal mediastinal) of all cattle within each experimental group. Error bars represent the standard deviation (±) of the data.

There was no difference in GAPDH crossing point (CP) values (Figure 35) between the cattle BCG vaccinated *M. bovis* challenged (average CP of 22.8), BCG (*sigK*) vaccinated *M. bovis* challenged (average CP of 23.3), non-vaccinated *M. bovis* infected (average CP of 22.8), non-vaccinated non-infected (average CP of 22.4) and BCG vaccinated non-infected (average CP of 23). This suggested that any potential differences in cytokine expression between the five groups were unlikely to be due to the physical condition of the template.

Cytokine mRNA expression in the combined lymph nodes

Five experimental groups of cattle, each displaying a different combination of vaccination and *M. bovis* infection were analysed for cytokine mRNA expression levels. IFN-γ, TNF-α, IL10 and IL4 mRNA levels were quantitatively measured in three lymph nodes from each animal (left bronchial, cranial mediastinal and caudal mediastinal lymph nodes). The individual lymph node results were then combined for each animal to give an overall view of cytokine expression within each experimental group.

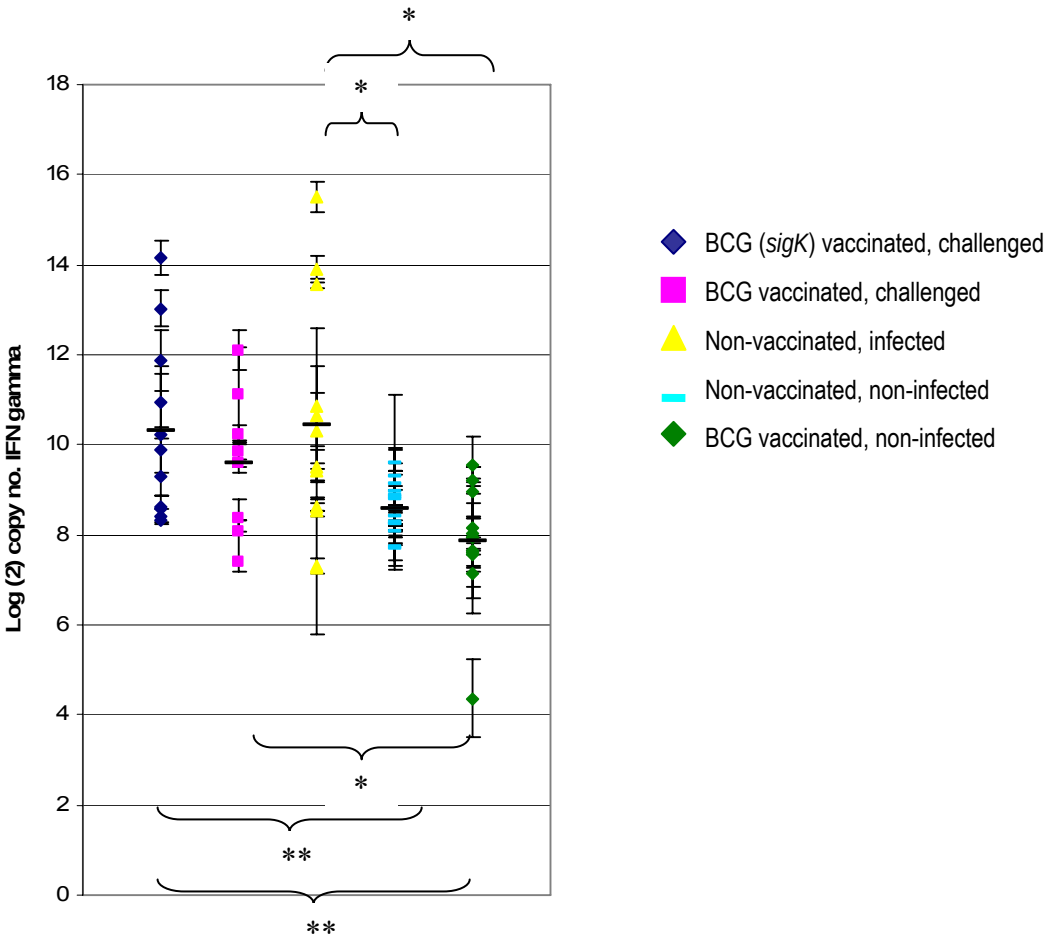

Figure 36: Quantitative RT-PCR of IFN-γ mRNA in the lymph nodes of cattle from five experimental groups; BCG (*sigK*) vaccinated followed by *M. bovis* challenge (n=4), BCG vaccinated followed by *M. bovis* challenge (n=3), non-vaccinated *M. bovis* infected (n=4), non-vaccinated non-infected (n=5) and BCG vaccinated non-infected (n=4). The data are presented in $\log_2$ copy number and each individual point represents the mean triplicate data from an individual lymph node from one animal. Three lymph nodes were used from each animal (left bronchial, cranial mediastinal and caudal mediastinal). Error bars represent standard deviation (±) of each point and the mean of each group is shown by — symbol. Significant differences between groups are displayed as * ($p<0.05$) and ** ($p<0.005$, Mann Whitney test).

There were significant differences in IFN-γ mRNA expression between the five experimental groups ($p<0.005$, Kruskal Wallis test, Figure 36). The non-vaccinated *M. bovis* infected cattle showed the highest level of IFN-γ mRNA expression (mean $\log_2$ copy number of 10.5, Figure 36) and was significantly higher than both the non-vaccinated non-infected group (mean $\log_2$ copy number 8.58, $p<0.05$, Mann Whitney Test and Bonferroni corrected) and the BCG vaccinated non-infected group (mean $\log_2$ copy number 7.84, $p<0.01$, Mann Whitney test and Bonferroni corrected).

Prior vaccination with either BCG (*sigK*) Pasteur or BCG Pasteur caused a slight reduction in IFN-γ mRNA levels (mean $\log_2$ copy number of 10.3 and 9.6, respectively) as compared to the animals that were non-vaccinated prior to infection (Figure 36) however this was not significant.

The BCG (*sigK*) Pasteur vaccinated challenged animals showed a significantly higher level of IFN-γ mRNA as compared to the non-vaccinated non-infected group ($p<0.005$, Mann Whitney test and Bonferroni corrected) and the BCG vaccinated non-infected group ($p<0.005$, Mann Whitney test and Bonferroni corrected). Whereas the BCG Pasteur vaccinated challenged group showed a significantly higher level of IFN-γ mRNA expression only when compared to the BCG vaccinated non-infected group ($p<0.05$, Mann Whitney test and Bonferroni corrected). There was no significant difference between the non-vaccinated non-infected and BCG vaccinated non-infected groups ($p>0.05$, Mann Whitney test, Figure 36).

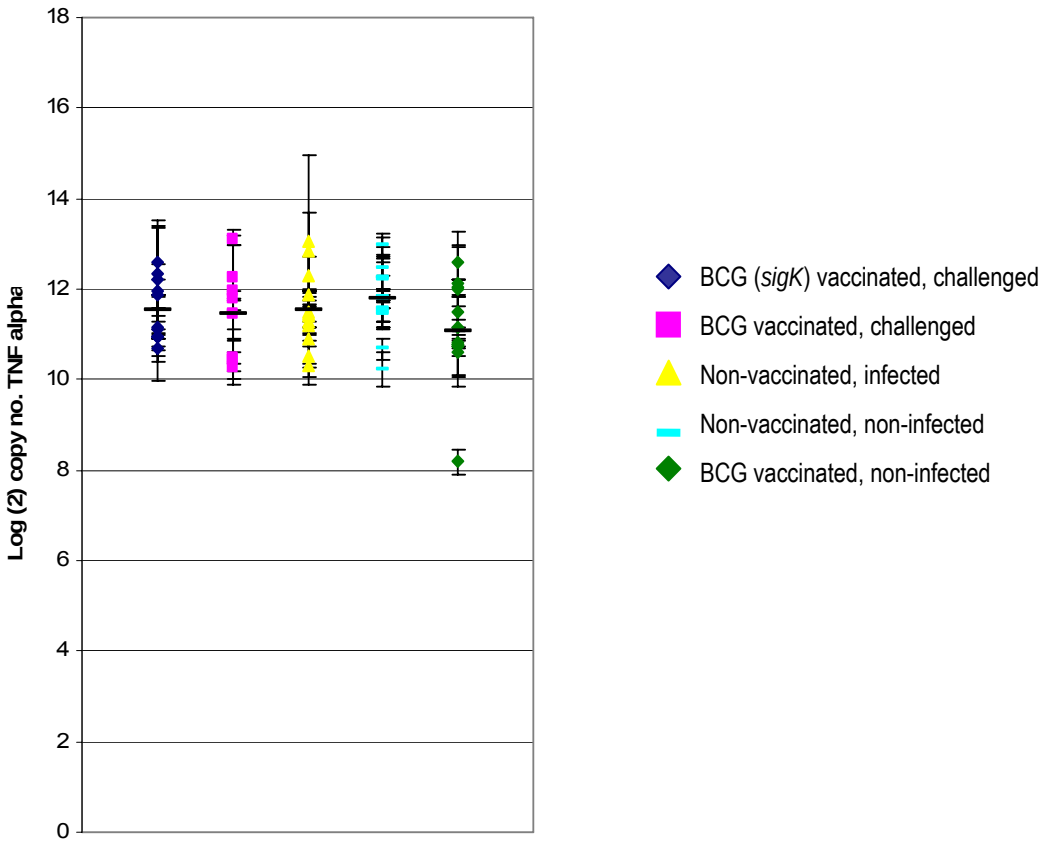

Figure 37: Quantitative RT-PCR of TNF-α mRNA in the lymph nodes of cattle from five experimental groups; BCG (*sigK*) vaccinated followed by *M. bovis* challenge (n=4), BCG vaccinated followed by *M. bovis* challenge (n=3), non-vaccinated *M. bovis* infected (n=4), non-vaccinated non-infected (n=5) and BCG vaccinated non-infected (n=4). The data are presented in $\log_2$ copy number and each individual point represents the mean triplicate data from an individual lymph node from one animal. Three lymph nodes were used from each animal (the left bronchial, cranial mediastinal and caudal mediastinal). Error bars represent standard deviation (±) of each point and the mean of each group is shown by — symbol. There was no significant difference between the five experimental groups ($p>0.05$, Kruskal Wallis test).

There were no significant differences in TNF-α mRNA expression levels between the five experimental groups ($p>0.05$, Kruskal Wallis test, Figure 37). The non-vaccinated non-infected group showed the highest level of TNF-α mRNA expression (mean $\log_2$ copy number 11.8, Figure 37). The BCG vaccinated non-infected group showed the lowest level of TNF-α mRNA expression (mean $\log_2$ copy number 11.06, Figure 37). The three *M. bovis* infected groups (BCG (*sigK*) Pasteur vaccinated, BCG Pasteur vaccinated and non-vaccinated) showed extremely similar TNF-α mRNA expression levels (mean $\log_2$ copy numbers of 11.53, 11.47 and 11.55, respectively, Figure 37).

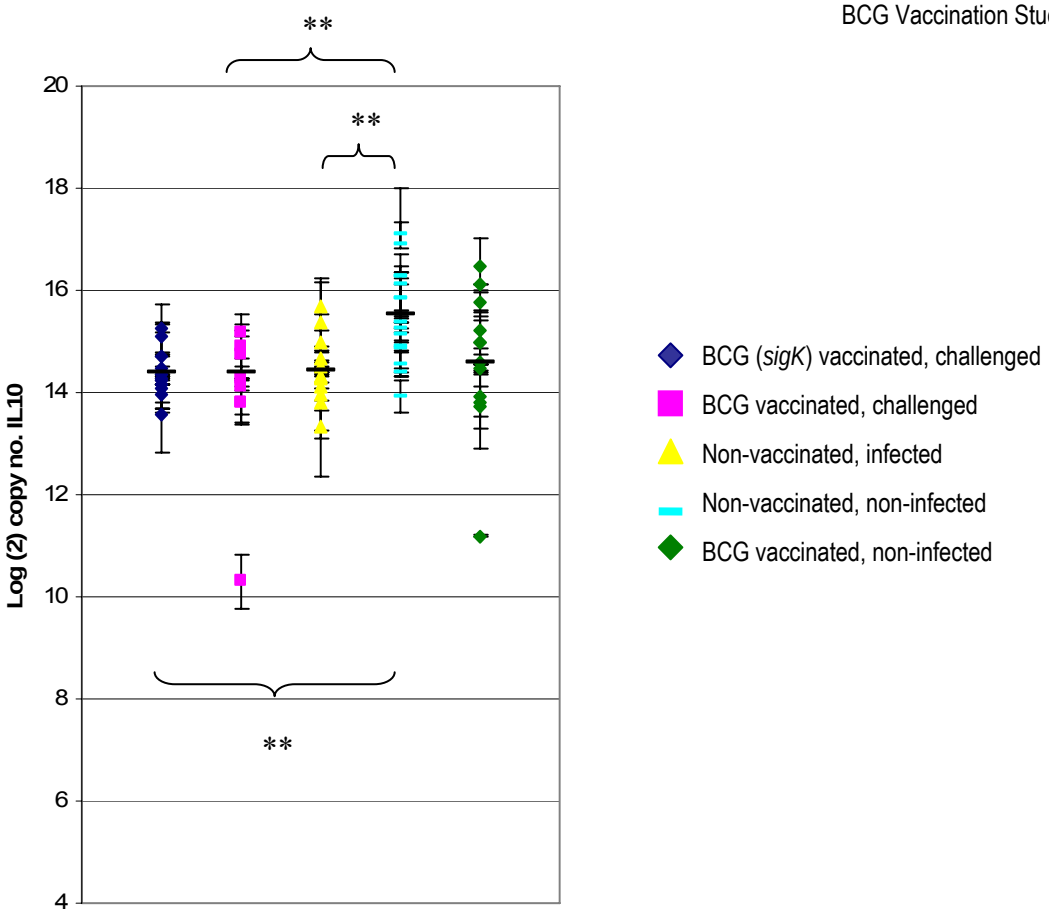

Figure 38: Quantitative RT-PCR of IL10 mRNA in the lymph nodes of cattle from five experimental groups; BCG (*sigK*) vaccinated followed by *M. bovis* challenge (n=4), BCG vaccinated followed by *M. bovis* challenge (n=3), non-vaccinated *M. bovis* infected (n=4), non-vaccinated non-infected (n=5) and BCG vaccinated non-infected (n=4). The data are presented in $\log_2$ copy number and each individual point represents the mean triplicate data from an individual lymph node from one animal. Three lymph nodes were used from each animal (the left bronchial, cranial mediastinal and caudal mediastinal). Error bars represent standard deviation (±) of each point and the mean of each group is shown by — symbol. Significant differences between groups are displayed as ** ($p<0.005$, Mann Whitney test).

There were significant differences in IL10 mRNA expression levels between the five experimental groups ($p=0.005$, Kruskal Wallis test, Figure 38). The non-vaccinated non-infected group showed the highest level of IL10 mRNA expression (mean $\log_2$ copy number 15.5, Figure 38) and was statistically higher ($p<0.005$, Mann Whitney test and Bonferroni corrected) than the three *M. bovis* infected groups; BCG (*sigK*) Pasteur vaccinated, BCG Pasteur vaccinated and non-vaccinated (mean $\log_2$ copy number of 14.4, 14.4 and 14.44, respectively, Figure 38). There were no significant differences between the three *M. bovis* infected groups ($p>0.05$, Mann Whitney test) and no significant difference between the BCG vaccinated non-infected group (mean log (2) copy number 14.6, Figure 38) and the non-vaccinated non-infected group ($p>0.05$, Mann Whitney test).

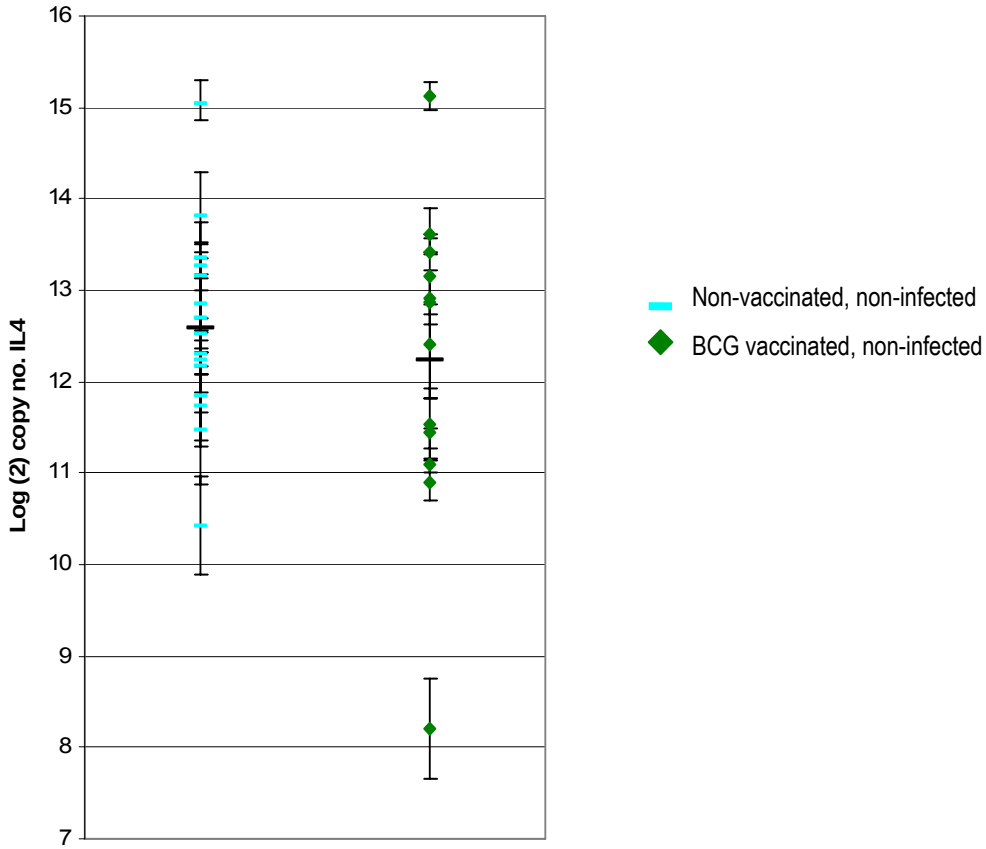

Figure 39: Quantitative RT-PCR of IL4 mRNA in the lymph nodes of cattle from two experimental groups; non-vaccinated non-infected (n=5) and BCG vaccinated non-infected (n=4). The data are presented in log_2 copy number and each individual point represents the mean triplicate data from an individual lymph node from one animal. Three lymph nodes were used from each animal (the left bronchial, cranial mediastinal and caudal mediastinal). Error bars represent standard deviation (±) of each point and the mean of each group is shown by — symbol. There was no significant difference between the two groups ($p>0.05$, Kruskal Wallis test).

Expression of IL4 mRNA was found only within the two non-infected groups; non-vaccinated non-infected and BCG vaccinated non-infected (Figure 39). The crossing point values obtained for IL4 mRNA within the three *M. bovis* infected groups (BCG (*sigK*) Pasteur vaccinated, BCG Pasteur vaccinated and the non-vaccinated) were extremely similar to those of the negative controls for each sample (reactions excluding the reverse transcriptase enzyme) and therefore were not considered reliable data.

There was no significant difference in IL4 mRNA expression levels between the two experimental groups ($p>0.05$, Kruskal Wallis test). The non-vaccinated non-infected group showed a slightly higher level of IL4 mRNA expression (mean log_2 copy number of 12.6, Figure 39) as compared to the BCG vaccinated non-infected group (mean log_2 copy number of 12.2, Figure 39).

Correlations between cytokine mRNA expression levels

Previous work on expression profiles over different time periods of *M. bovis* infection revealed relationships between different cytokines. The expression levels of cytokines IFN-γ, TNF-α, IL10 and IL4 from the combined lymph node data of all five experimental groups (BCG (*sigK*) Pasteur vaccinated challenged, BCG Pasteur vaccinated challenged, non-vaccinated infected, non-vaccinated non-infected and BCG vaccinated non-infected) were analysed using Pearsons correlation coefficient (Table 26).

Table 26: Statistically tested correlations (p values determined by Pearsons correlation coefficient) between IFN-γ, TNF-α, IL10 and IL4 mRNA expression levels. Data represents the combined lymph node results of all five experimental groups; BCG (*sigK*) vaccinated *M. bovis* challenged, BCG vaccinated challenged, non-vaccinated infected, non-vaccinated non-infected and BCG vaccinated non-infected animals.

	IFN-γ	TNF-α	IL10	IL4
IFN-γ		0.111	0.518	**0.006**
TNF-α	0.111		**0.008**	**0.002**
IL10	0.518	**0.008**		**0.002**
IL4	**0.006**	**0.002**	**0.002**	

Significant correlations ($p<0.05$, Pearsons correlation coefficient) highlighted in bold and underlined.

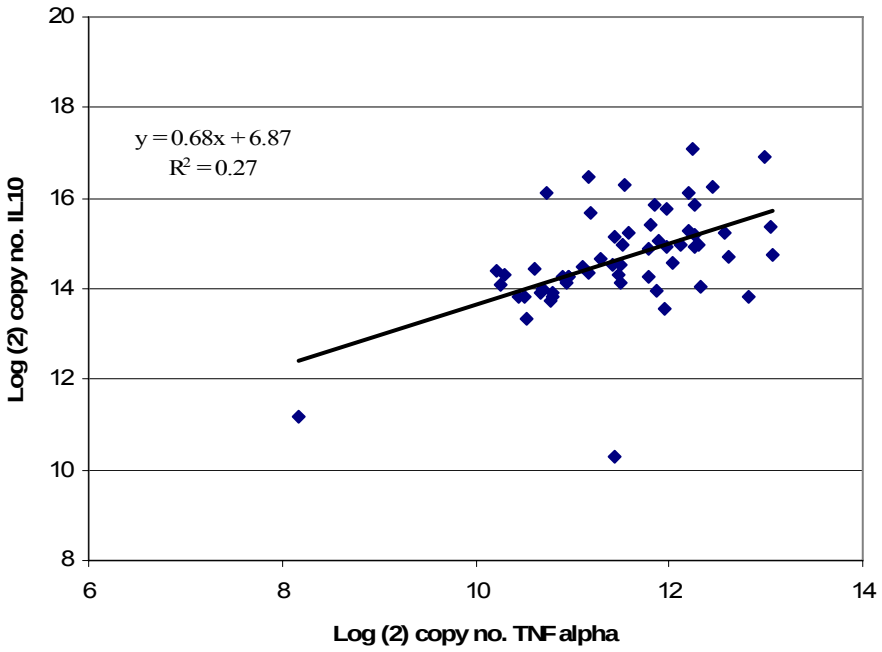

Figure 40: Correlation between IL10 and TNF-α mRNA expression levels in the lymph nodes of cattle either BCG (*sigK*) Pasteur vaccinated *M. bovis* challenged, BCG Pasteur vaccinated challenged, non-vaccinated infected, non-vaccinated non-infected or BCG Pasteur vaccinated non-infected. The data are presented in $\log_2$ copy number and each individual point represents the mean triplicate data from an individual lymph node from one animal. The graph displays the equation of the line of best fit and the R^2 value to indicate the fit of the data points.

There was a significant correlation between IL10 and TNF-α mRNA expression levels within cattle from the five experimental groups; BCG (*sigK*) Pasteur vaccinated *M. bovis* challenged, BCG Pasteur challenged, non-vaccinated infected, non-vaccinated non-infected and BCG Pasteur vaccinated non-infected (p=0.008, Pearsons correlation coefficient, Table 26). The data showed a positive correlation (Pearsons correlation coefficient R value of 0.5) and therefore indicated that as one cytokine increased in expression, the other cytokine also increased in expression. The coefficient of determination (R^2 of 0.2697 (multiplied by 100 to give as a percentage), Figure 40) suggested that 26.9% of the variance in one cytokine expression level was due to the other cytokine. This also gave an indication of the fit of the data points to the linear trend line, as the further R^2 from the value of 1, the larger the variation in data around the trend line.

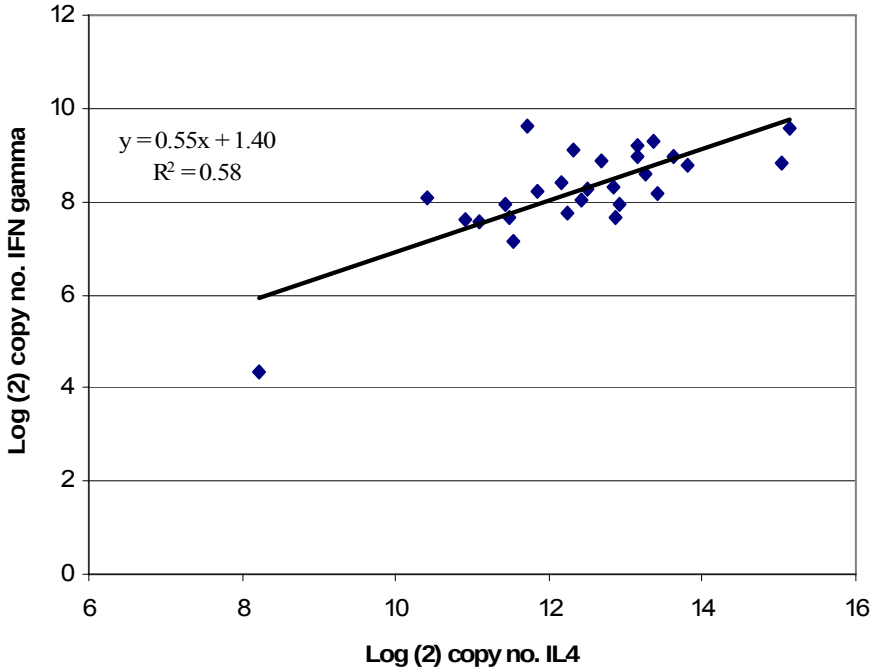

Figure 41: Correlation between IL4 and IFN-γ mRNA expression levels in the lymph nodes of cattle either non-vaccinated non-infected or BCG Pasteur vaccinated non-infected. The data are presented in log_2 copy number and each individual point represents the mean triplicate data from an individual lymph node from one animal. The graph displays the equation of the line of best fit and the R^2 value to indicate the fit of the data points.

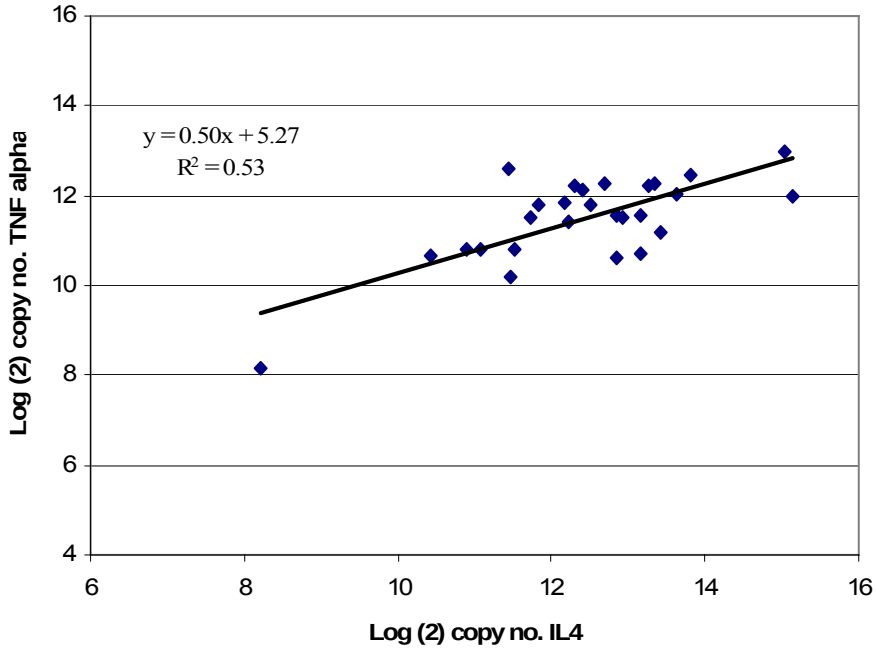

Figure 42: Correlation between IL4 and TNF-α mRNA expression levels in the lymph nodes of cattle either non-vaccinated non-infected or BCG Pasteur vaccinated non-infected. The data are presented in log_2 copy number and each individual point represents the mean triplicate data from an individual lymph node from one animal. The graph displays the equation of the line of best fit and the R^2 value to indicate the fit of the data points.

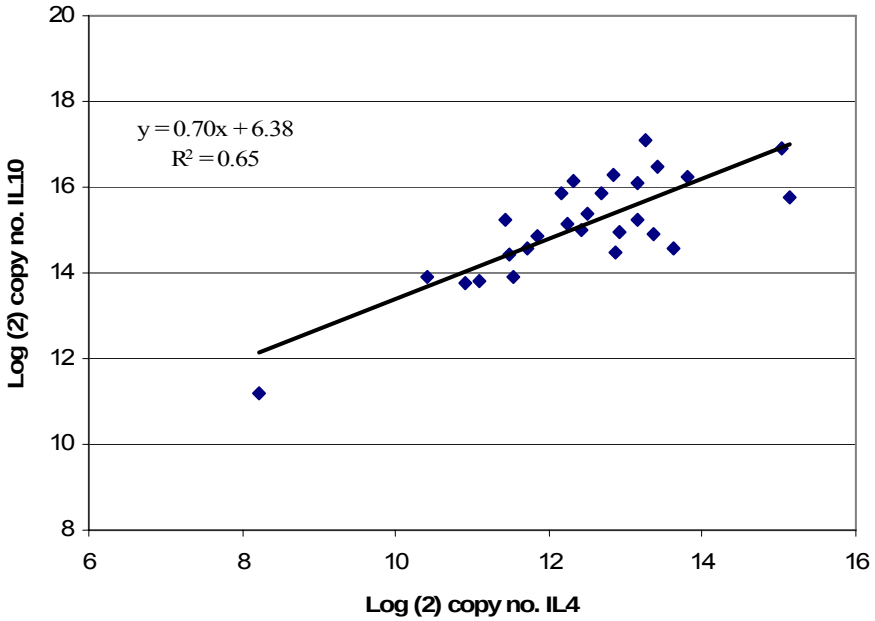

Figure 43: Correlation between IL4 and IL10 mRNA expression levels in the lymph nodes of cattle either non-vaccinated non-infected or BCG Pasteur vaccinated non-infected. The data are presented in log_2 copy number and each individual point represents the mean triplicate data from an individual lymph node from one animal. The graph displays the equation of the line of best fit and the R^2 value to indicate the fit of the data points.

There was a significant correlation between IL4 mRNA expression levels and IFN-γ, TNF-α and IL10 mRNA levels within cattle from two of the five experimental groups; non-vaccinated non-infected and BCG vaccinated non-infected (p=0.006, 0.002 and 0.002, respectively, Pearsons correlation coefficient, Table 26). The data showed a positive correlation for all three relationships (Pearsons correlation coefficient R values of 0.76, 0.73 and 0.8, respectively, Figures 41, 42 and 43) therefore indicating that an increase in IL4 mRNA expression level was paralleled by an increase in IFN-γ, TNF-α and IL10 mRNA expression within these two experimental groups. The correlations were relatively strong, shown by the coefficient of determination for each relationship (R^2 multiplied by 100 to give a percentage, Figures 41, 42 and 43). The correlation between IL4 and IFN-γ mRNA expression showed a relationship of 58% (Figure 41), between IL4 and TNF-α mRNA expression the relationship was 53% (Figure 42) and between IL4 and IL10 mRNA expression the relationship was 65% (Figure 43). This also indicated the fit of the data to the linear trend line, as the relationship between IL4 and IL10 showed a tighter fit of data (R^2 closer to a value of 1).

Immunohistochemistry

Quantitative RT-PCR allowed the quantification of IFN-γ, TNF-α, IL10 and IL4 mRNA templates within the lymph node samples of cattle either BCG (modified *sigK*) Pasteur vaccinated *M. bovis* challenged, BCG Pasteur vaccinated *M. bovis* challenged, non-vaccinated *M. bovis* infected, non-vaccinated non-infected or BCG Pasteur vaccinated non-infected. This gave an indication of the genetic expression profile of the animal's immune response at five weeks post *M. bovis* challenge. This work was followed by exploring the level of IFN-γ and TNF-α protein production within the same lymph node samples at the same time point using immunohistochemistry. The results were expressed as a scoring method based on the percentage area coverage of positively identified cells expressing IFN-γ and TNF-α.

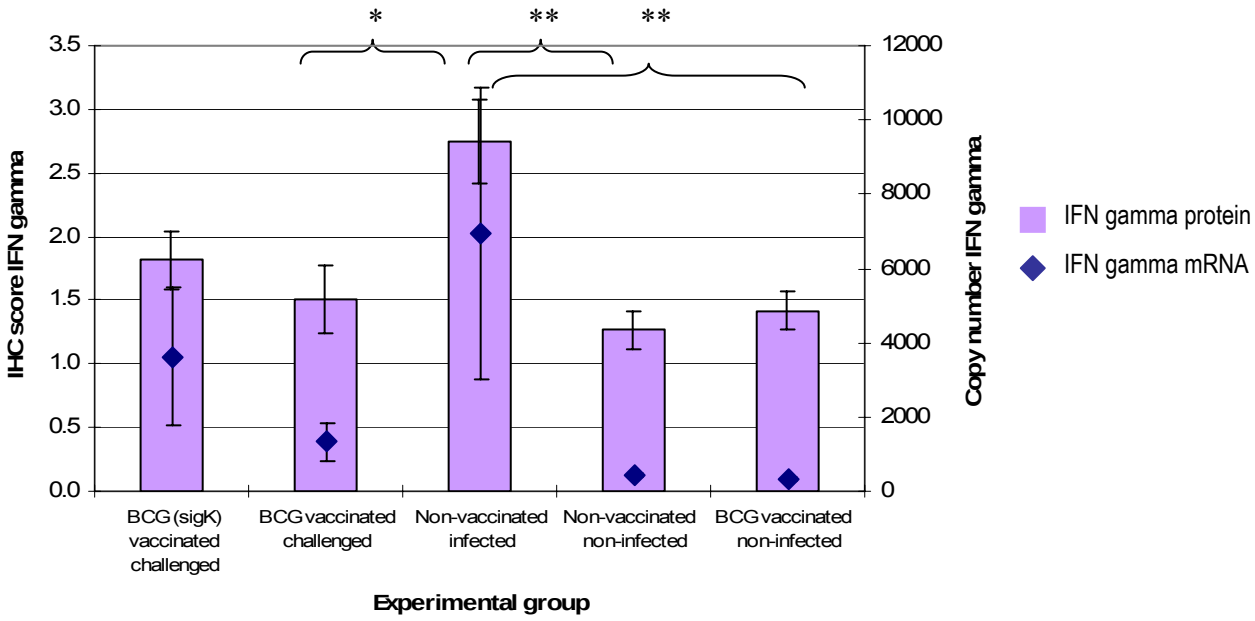

Figure 44: Protein and mRNA expression of IFN-γ within cattle either BCG (*sigK*) Pasteur vaccinated *M. bovis* challenged (n=4), BCG Pasteur vaccinated challenged (n=3), non-vaccinated infected (n=4), non-vaccinated non-infected (n=5) and BCG Pasteur vaccinated non-infected (n=4). Protein data are expressed as a score of percentage area coverage of cells expressing IFN-γ (IHC) based on the scale of 0 = no positive cells, 1 = <5% area coverage, 2 = between 5-20 % area coverage, 3 = between 21-40% area coverage and 4 = over 40% area coverage (100x magnification). The mRNA IFN-γ data are expressed as actual copy number (qRT-PCR). Data represents the mean triplicate results from three different lymph nodes (caudal mediastinal, cranial mediastinal and left bronchial) from every animal within each group. Error bars represent standard deviation (±) of the mean. Statistical differences between levels of protein were displayed as * ($p<0.05$) and ** ($p<0.005$, Mann Whitney test).

The immunohistochemistry studies on cells expressing IFN-γ protein within cattle from the five experimental groups (mean of all animals within each group) showed a similar pattern to the IFN-γ mRNA expression profiles observed using qRT-PCR (Figure 44). This trend was also shown when analysing the three individual lymph nodes (left bronchial, caudal mediastinal and cranial mediastinal) data separately (Figure 45). Statistically, using the data from the individual lymph nodes (Figure 45), there was a significant correlation between IFN-γ protein and IFN-γ mRNA expression levels ($p<0.001$, Spearmans correlation coefficient).

There was also a significant difference in the number of cells expressing IFN-γ protein between each group ($p<0.005$, Kruskal Wallis test, Figure 44). The non-vaccinated *M. bovis* infected group had a significantly higher level of IFN-γ protein expressing cells (mean score of 2.75, Figure 44) as compared to the BCG Pasteur challenged group (mean score of 1.5, $p<0.05$, Mann Whitney test and Bonferroni corrected). The non-vaccinated infected group also had significantly higher levels of IFN-γ protein expressing cells as compared to the non-vaccinated non-infected group (mean score of 1.27) and the BCG vaccinated non-infected group (mean score of 1.42, $p\leq0.005$, Mann Whitney test and Bonferroni corrected, Figure 44). Cattle that received BCG (*sigK*) Pasteur vaccination prior to challenge had slightly lower levels of IFN-γ protein expressing cells (mean score of 1.8, Figure 44) as compared to the non-vaccinated infected group and higher levels compared to the BCG Pasteur vaccinated group, however this was not a significant difference.

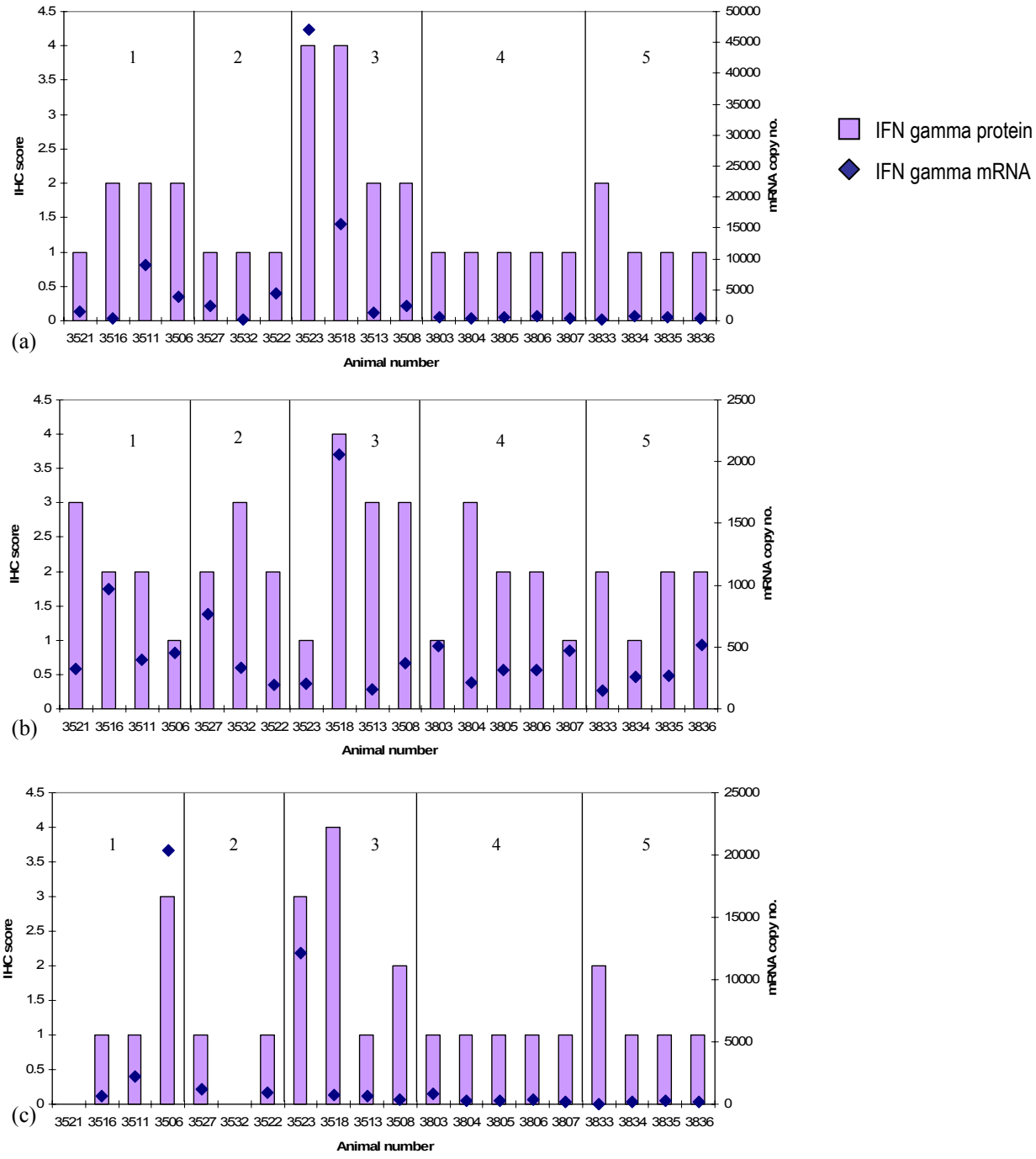

Figure 45: Protein and mRNA expression of IFN-γ within the (a) left bronchial, (b) caudal mediastinal and (c) cranial mediastinal lymph nodes of cattle either BCG (*sigK*) Pasteur vaccinated *M. bovis* challenged (group 1), BCG Pasteur vaccinated challenged (group 2), non-vaccinated infected (group 3), non-vaccinated non-infected (group 4) and BCG vaccinated non-infected (group 5). Protein data are expressed as a score of percentage area coverage of cells expressing IFN-γ (IHC) based on the scale of 0 = no positive cells, 1 = <5% area coverage, 2 = 5-20 % area coverage, 3 = 21-40% area coverage and 4 = over 40% area coverage (100x magnification). The mRNA IFN-γ data are expressed as actual copy number (qRT-PCR). Data represents the averaged triplicate results from each lymph node.

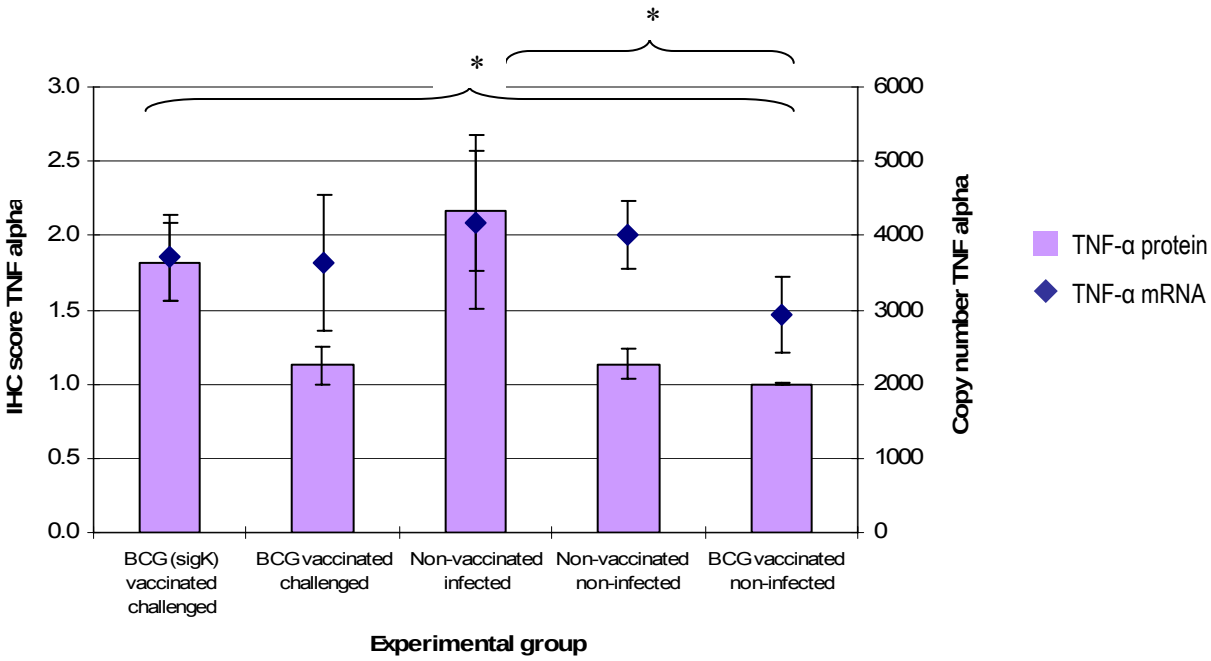

Figure 46: Protein and mRNA expression of TNF-α within cattle either BCG (*sigK*) vaccinated *M. bovis* challenged (n=4), BCG vaccinated challenged (n=3), non-vaccinated infected (n=4), non-vaccinated non-infected (n=5) and BCG vaccinated non-infected (n=4). Protein data are expressed as a score of percentage area coverage of cells expressing TNF-α (immunohistochemistry) based on the scale of 0 = no positive cells, 1 = <1% area coverage, 2 = between 2-10% area coverage, 3 = between 11-20% area coverage and 4 = over 20% area coverage (400x magnification). The mRNA TNF-α data are expressed as actual copy number (qRT-PCR). Data represents the mean results from three different lymph nodes (caudal mediastinal, cranial mediastinal and left bronchial) from every animal within each group. Statistical differences between levels of protein were displayed as * ($p<0.05$, Mann Whitney test).

The immunohistochemistry studies on cells expressing TNF-α protein within cattle from the five experimental groups (averaged data from all animals within each group) showed a slightly different pattern to the TNF-α mRNA expression profiles observed during qRT-PCR (Figure 46). This was also shown when analysing the three different lymph nodes (left bronchial, caudal mediastinal and cranial mediastinal) data separately (Figure 47). Statistically, using the data from the individual lymph nodes (Figure 47), there was no significant correlation between TNF-α protein and TNF-α mRNA expression levels ($p>0.05$, Spearmans correlation coefficient).

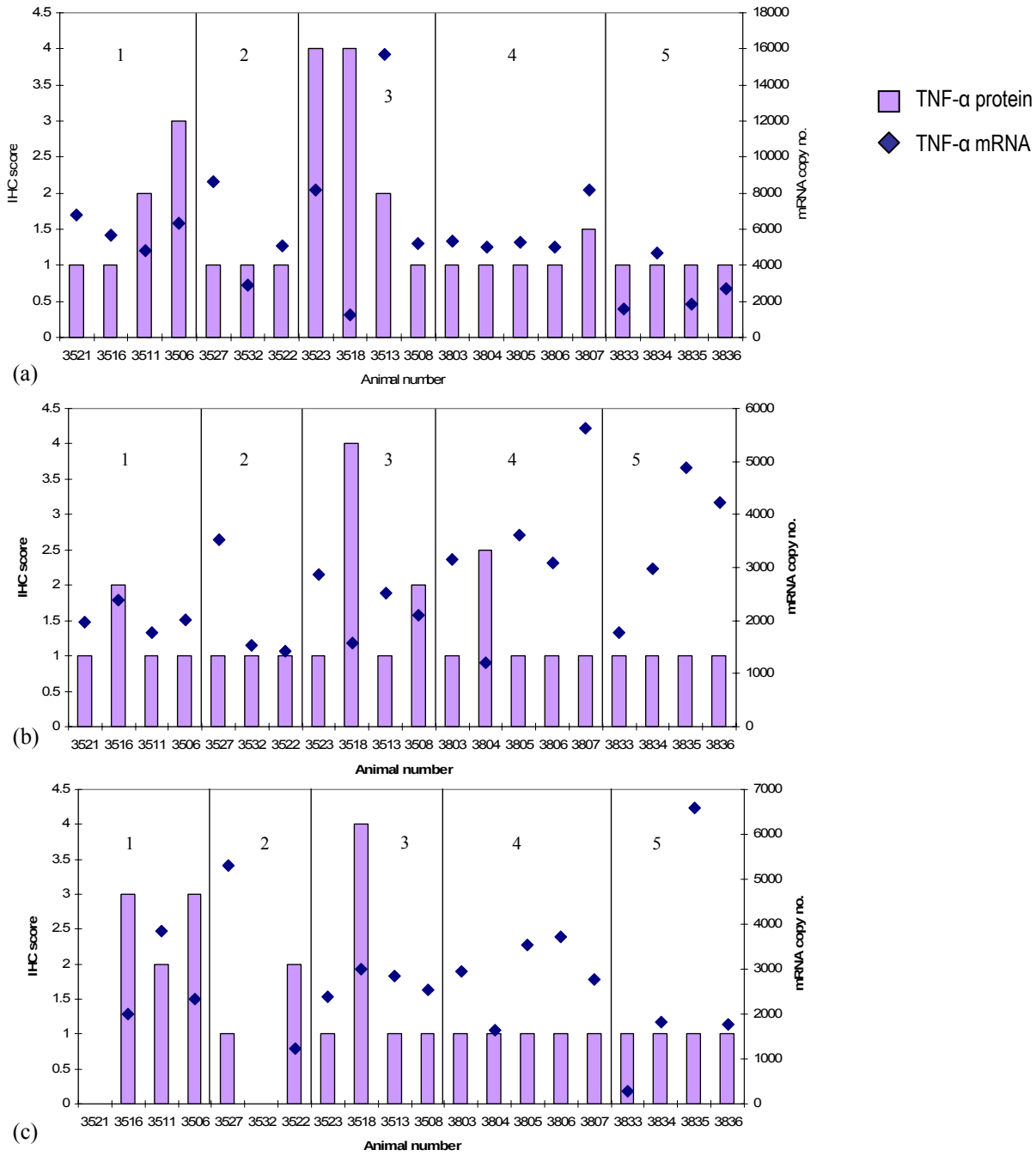

Figure 47: Protein and mRNA expression of TNF-α within (a) the left bronchial, (b) caudal mediastinal and (c) cranial mediastinal lymph nodes of cattle either BCG (*sigK*) vaccinated *M. bovis* challenged (group 1), BCG vaccinated challenged (group 2), non-vaccinated infected (group 3), non-vaccinated non-infected (group 4) and BCG vaccinated non-infected (group 5). Protein data are expressed as a score of percentage area coverage of cells expressing TNF-α (IHC) based on the scale of 0 = no positive cells, 1 = <1% area coverage, 2 = 2-10 % area coverage, 3 = 11-20% area coverage and 4 = over 20% area coverage (400x magnification). The mRNA TNF-α data are expressed as actual copy number (qRT-PCR). Data represents the mean triplicate results from each lymph node.

There was a significant difference in the number of cells expressing TNF-α protein between each group ($p<0.005$, Kruskal Wallis test, Figure 46). The non-vaccinated *M. bovis* infected group had the highest level of cells expressing TNF-α protein (mean score of 2.17, Figure 46) and this was statistically higher than the BCG vaccinated non-infected group (mean score of 1, $p<0.05$, Mann Whitney test and Bonferroni corrected). The BCG (*sigK*) Pasteur vaccinated challenged group had a significantly higher number of cells expressing TNF-α protein (mean score of 1.82, $p<0.05$, Mann Whitney test and Bonferroni corrected) as compared to the BCG vaccinated non-infected group (Figure 46). The BCG vaccinated challenged group and the non-vaccinated non-infected group had the same level of cells expressing TNF-α protein (mean score of 1.13, Figure 46).

The TNF-α mRNA expression data of the five experimental groups showed a slightly different pattern when expressed as copy number (Figure 46) compared to when expressed as $\log_2$ copy number (Figure 37). Both forms of the data represented the average of the total data set for each experimental group. However, the average of the data in copy number format was the arithmetic mean whereas the average of the data in $\log_2$ copy number format was the geometric mean. This produced slightly different expression profiles although this difference was not significant ($p>0.05$, Mann Whitney test).

There was also a significant correlation between the levels of IFN-γ protein and TNF-α protein in the five experimental groups ($p<0.001$, Spearmans correlation coefficient).

Lymph node pathology of *M. bovis* challenged cattle

Percentage granuloma coverage

Granulomatous lesions within lymph nodes are a characteristic feature of *M. bovis* infection. The percentage area coverage of granulomas within individual lymph nodes can be used to indicate the extent of pathology caused by infection. Microscope slides of lymph node tissue were prepared for each animal from three of the five experimental groups; BCG (*sigK*) Pasteur vaccinated *M. bovis* challenged, BCG Pasteur vaccinated challenged and non-vaccinated infected. There was no gross pathology data for the non-vaccinated non-infected and BCG Pasteur vaccinated non-infected groups due to the absence of granulomas in non-infected animals. The lymph node section was first measured by counting the total fields of view that the section covered (100 x magnifications). Each individual granuloma within the section was then measured by counting the number of fields of view that the granulomas covered and the percentage area coverage calculated in respect to the entire lymph node section.

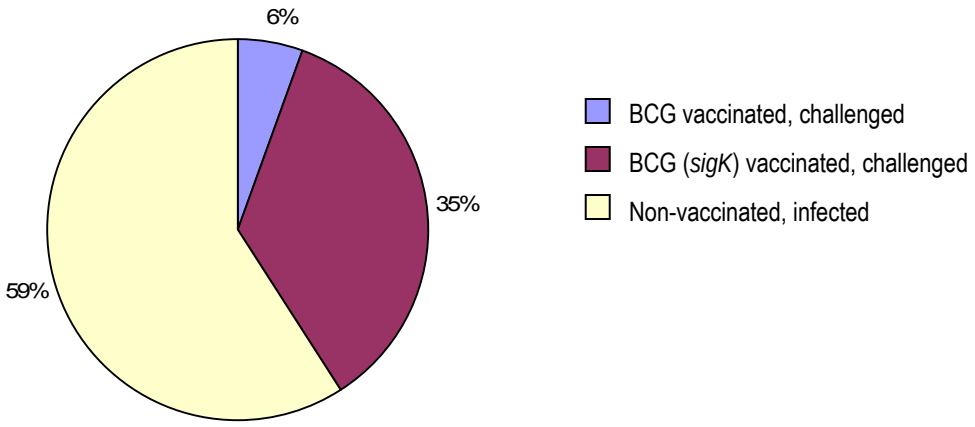

Figure 48: Percentage area coverage of granulomas within the lymph nodes of cattle either vaccinated with BCG (*sigK*) Pasteur prior to *M. bovis* challenge (n=4), vaccinated with BCG Pasteur prior to challenge (n=3) or non-vaccinated and infected (n=4). The combined total area of granuloma coverage for each lymph node (left bronchial, caudal mediastinal and cranial mediastinal) of each animal was calculated. This data was then transformed into a percentage of the total area of granuloma coverage in all three experimental groups.

(a)

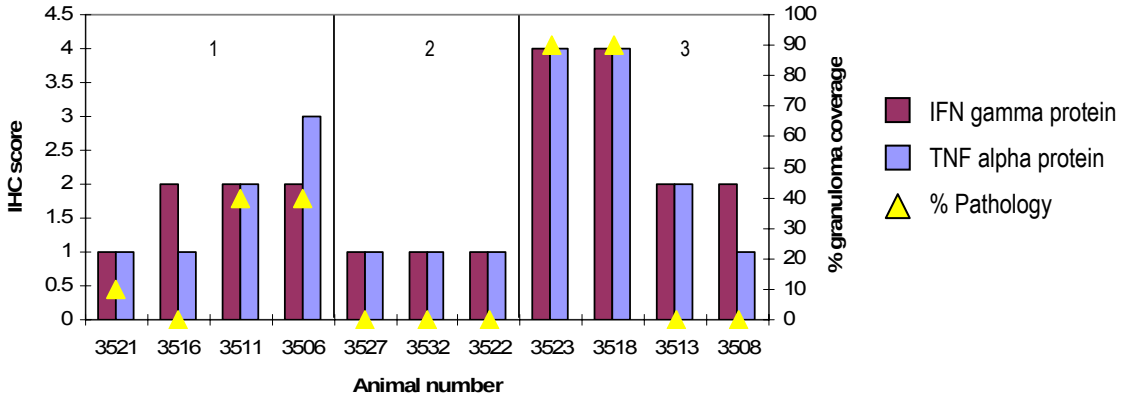

(b)

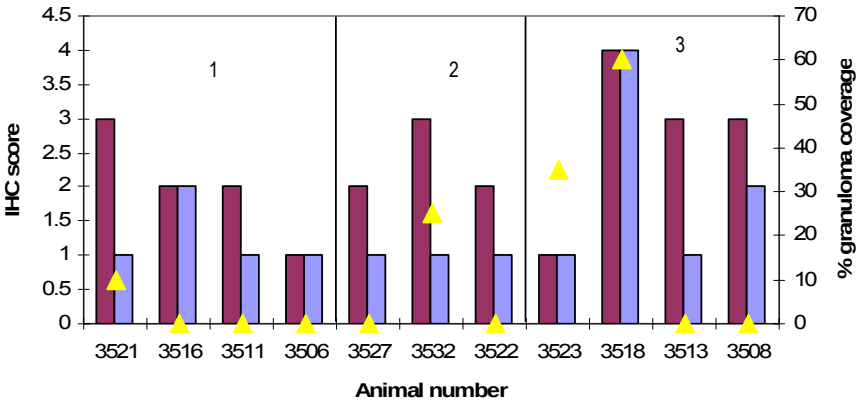

(c)

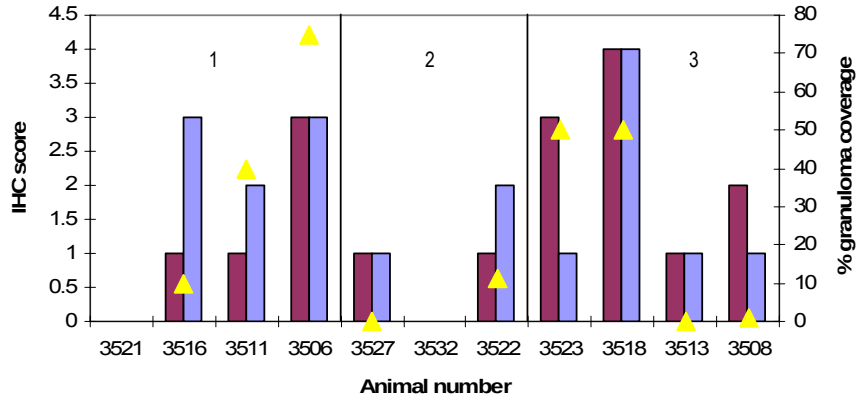

Figure 49: Protein expression (IFN-γ and TNF-α) and extent of pathological disease within (a) the left bronchial, (b) caudal mediastinal and (c) cranial mediastinal lymph nodes of cattle either vaccinated with BCG (*sigK*) Pasteur prior to *M. bovis* challenge (group 1), vaccinated with BCG Pasteur prior to *M. bovis* challenge (group 2) or non-vaccinated infected (group 3). Protein data are expressed as a score of percentage area coverage of cells expressing TNF-α and IFN-γ (IHC) based on the scale 1 (lowest percentage coverage) to 4 (highest percentage coverage). Pathological data are expressed as percentage area coverage of granulomas within the infected lymph nodes. Data represents the mean duplicate results for each lymph node from each animal.

Overall, there appeared to be a difference in the percentage of granuloma coverage between the three *M. bovis* experimentally infected animals, however this was not significant ($p>0.05$, Kruskal-Wallis test, Figure 48). The non-vaccinated *M. bovis* infected cattle group (combined lymph node data) showed the highest level of pathological disease (total of 59% area coverage of granulomatous lesions over the lymph node section, Figure 48). Vaccination prior to *M. bovis* challenge lessened the degree of pathology noted within the selected lymph nodes. However, the BCG (*sigK*) Pasteur vaccinated animals had a higher level of pathology (total of 35% area coverage of granulomatous lesions over the lymph node section, Figure 48) as compared to the BCG Pasteur vaccinated animals (total of 6% area coverage, Figure 48).

The individual lymph node data (Figure 49) showed the same trend as seen in the combined lymph node data (Figure 48). The non-vaccinated *M. bovis* infected cattle lymph nodes generally had a higher level of pathology as compared to the vaccinated cattle. The non-vaccinated infected animals had between 0 and 90% granuloma coverage in the left bronchial (Figure 49a), between 0 and 60% granuloma coverage in the caudal mediastinal (Figure 49b) and between 0 and 50% granuloma coverage in the cranial mediastinal lymph node (Figure 49c). The BCG (*sigK*) Pasteur vaccinated challenged animals had between 0 and 40% granuloma coverage in the left bronchial (Figure 49a) and between 0 and 10% granuloma coverage in the caudal mediastinal lymph node (Figure 49b). The exception to the rule was the BCG (*sigK*) vaccinated animal 3506 (cranial mediastinal lymph node) which had a higher level of pathology as compared to the same lymph nodes in the non-vaccinated animals (75% granuloma coverage, Figure 49c). The BCG Pasteur vaccinated challenged animals had 0% granuloma coverage in the left bronchial (Figure 49a), between 0 and 25% granuloma coverage in the caudal mediastinal (Figure 49b) and between 0 and 11% granuloma coverage in the cranial mediastinal lymph node (Figure 49c).

The BCG (*sigK*) vaccinated animals had higher levels of pathology as compared to the BCG vaccinated animals, with the exception of animal 3532 (caudal mediastinal lymph node) which had a higher level of granuloma coverage at 25% (Figure 49b).

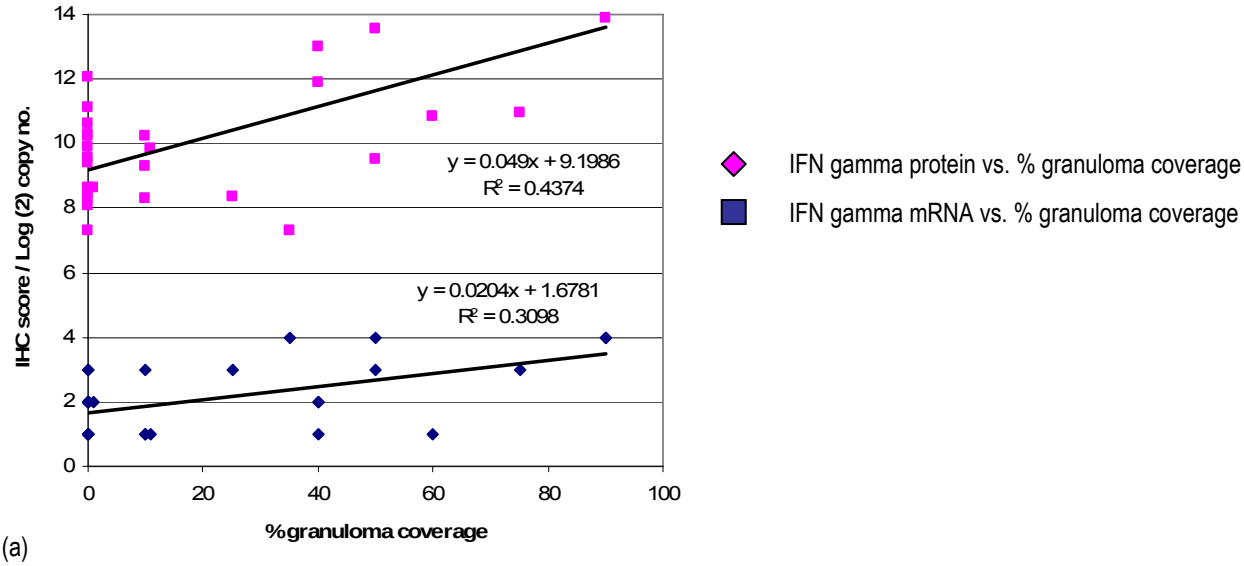

(a)

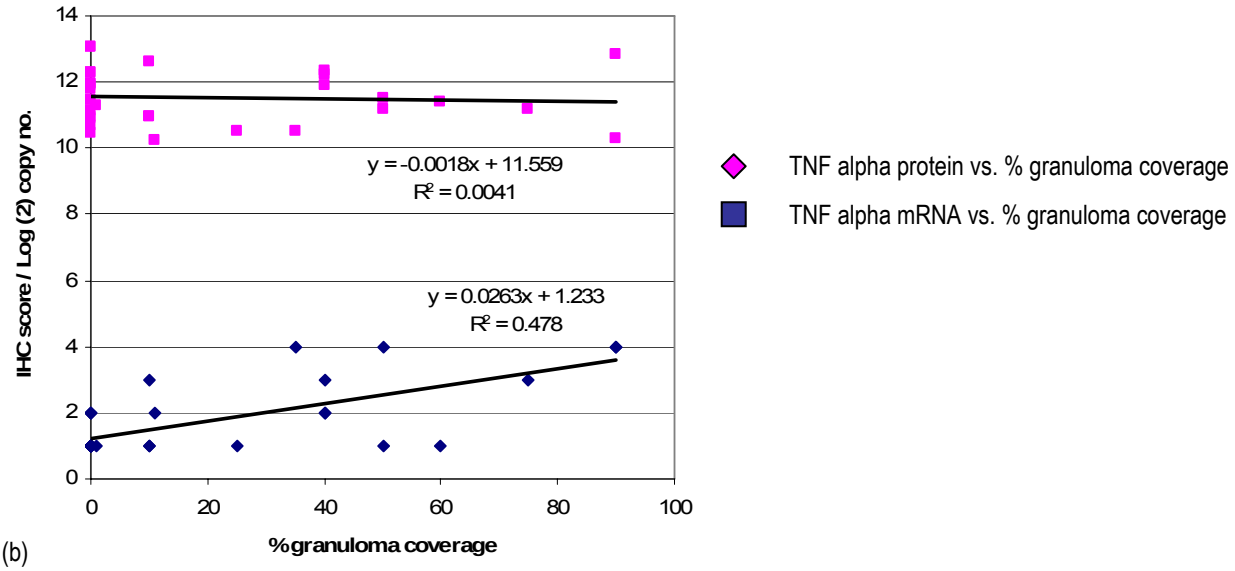

(b)

Figure 50: Correlations between the percentage area coverage of granuloma and both (a) IFN-γ and (b) TNF-α. The graphs display both mRNA (log_2 copy number) and protein (IHC score) data for the thoracic lymph nodes of cattle either vaccinated with BCG (*sigK*) Pasteur prior to *M. bovis* challenge (n=4), vaccinated with BCG Pasteur prior to challenge (n=3) or non-vaccinated infected (n=4). The lymph node IFN-γ protein data are expressed as a score of percentage area coverage of cells expressing IFN-γ (IHC) based on the scale 1 (lowest percentage coverage) to 4 (highest percentage coverage). The IFN-γ mRNA data are expressed in log_2 copies obtained from the qRT-PCR experiments. Each data point represents one animal. The graph also displays both equations of the line including the R^2 value.

The individual lymph node data (Figure 49) suggested a relationship between the levels of IFN-γ and TNF-α protein expression with the percentage of granuloma coverage within each lymph node section. Statistically, there was a significant positive correlation between the percentage coverage of granuloma and both IFN-γ protein expression ($p<0.05$, Spearmans correlation co-efficient, Figure 50a) and TNF-α protein expression ($p<0.001$, Spearmans correlation co-efficient, Figure 50b). There was also a significant positive correlation between levels of pathology and the level of IFN-γ mRNA expression within each lymph node ($p<0.001$, Pearsons correlation coefficient, Figure 50a) but not with TNF-α or IL10 (graph not shown) mRNA expression levels ($p>0.05$, Pearsons correlation coefficient, Figure 50b).

Granuloma score

An additional method used to indicate the extent of pathology caused by *M. bovis* infection based on the score of each individual granuloma within the lymph node samples was also performed. A scoring scale developed by Wangoo *et al* (2005) was used to organise each granuloma into one of four stages based on their morphological and physiological state. The slides used previously for granuloma percentage coverage were used to determine the number of granuloma that corresponded with each stage (Table 27). As granuloma advancement through the stages is coupled with an increase in size the counts were weighted using a $\log_2$ scale, this allowed compensation for the larger sizes of the later stage granulomas.

Table 27: Categorisation of granulomas within the lymph node sections of cattle infected with *M. bovis* and either non-vaccinated, BCG Pasteur vaccinated or BCG (*sigK*) Pasteur vaccinated. Granuloma specific for each of the four stages of development (I-IV) were counted within slide mounted lymph node sections.

		Granuloma score (weighted score)					
Animal	Treatment	Stage I	Stage II	Stage III	Stage IV	Total	Mean (SEM)
3523	Non-vaccinated	11 (11)	10 (20)	2 (8)	4 (32)	71	
3518	Non-vaccinated	5 (5)	6 (12)	0 (0)	3 (24)	41	
3513	Non-vaccinated	7 (7)	3 (6)	0 (0)	4 (32)	45	
3508	Non-vaccinated	9 (9)	10 (20)	0 (0)	1 (8)	37	48.5 (7.67)
3527	BCG vaccinated	0 (0)	0 (0)	0 (0)	0 (0)	0	
3532	BCG vaccinated	12 (12)	7 (14)	1 (4)	0 (0)	30	
3522	BCG vaccinated	1 (1)	7 (14)	0 (0)	0 (0)	15	15 (8.66)
3521	BCG (*sigK*) vaccinated	5 (5)	0 (0)	0 (0)	0 (0)	5	
3516	BCG (*sigK*) vaccinated	6 (6)	0 (0)	0 (0)	0 (0)	6	
3511	BCG (*sigK*) vaccinated	16 (16)	36 (72)	6 (24)	0 (0)	112	
3506	BCG (*sigK*) vaccinated	5 (5)	46 (92)	14 (56)	0 (0)	153	69 (37.6)

The granuloma counts were weighted (in brackets) on a $\log_2$ scale to account for the increased size of the advanced stage granuloma. Therefore, the count for stage I was multiplied by 1, stage II multiplied by 2, stage III multiplied by 4 and stage IV multiplied by 8. The sum of the weighted scores for each animal was then calculated and the mean of the total sum (including the standard error of the mean) for each experimental group displayed in the final column.

The data for the percentage area coverage of granulomatous lesions (Figure 49) for each individual animal displayed a positive relationship with the categorised granuloma stage results ($p<0.001$, Spearmans correlation co-efficient, Table 27). Therefore as the percentage area coverage of granulomas within the lymph nodes increased, there was also an increase in the weighted total of granuloma development.

There was also a marked difference between the three experimental groups in granuloma development (Table 27) however, due to the large variations in the data sets these differences were not significant within the animals studied ($p>0.05$, Kruskal Wallis test). The BCG Pasteur vaccinated challenged group showed the lowest score for granuloma development (mean 15, Table 27). This score increased within the lymph nodes of cattle non-vaccinated infected (mean 48.5). Finally, the BCG (*sigK*) Pasteur vaccinated challenged group displayed the highest level of granuloma development (mean 69, Table 27).

Focusing on the individual granuloma stage results, stage IV granuloma were found within the non-vaccinated infected group only (scores of 32, 32 and 24 for the three animals within the non-vaccinated infected group, Table 27). Both the non-vaccinated and BCG (sigK) Pasteur vaccinated challenged groups displayed the same total score for stage I granuloma (sum of 32). For the stage II and III granuloma, the BCG (*sigK*) Pasteur vaccinated group showed the highest scores (sum of 164 and 80, respectively, Table 27), followed by the non-vaccinated infected group (sum of 58 and 8, respectively, Table 27). The BCG Pasteur vaccinated challenged group displayed the lowest scores for granuloma across the three stages of development I, II and III (13, 28 and 4, respectively, Table 27).

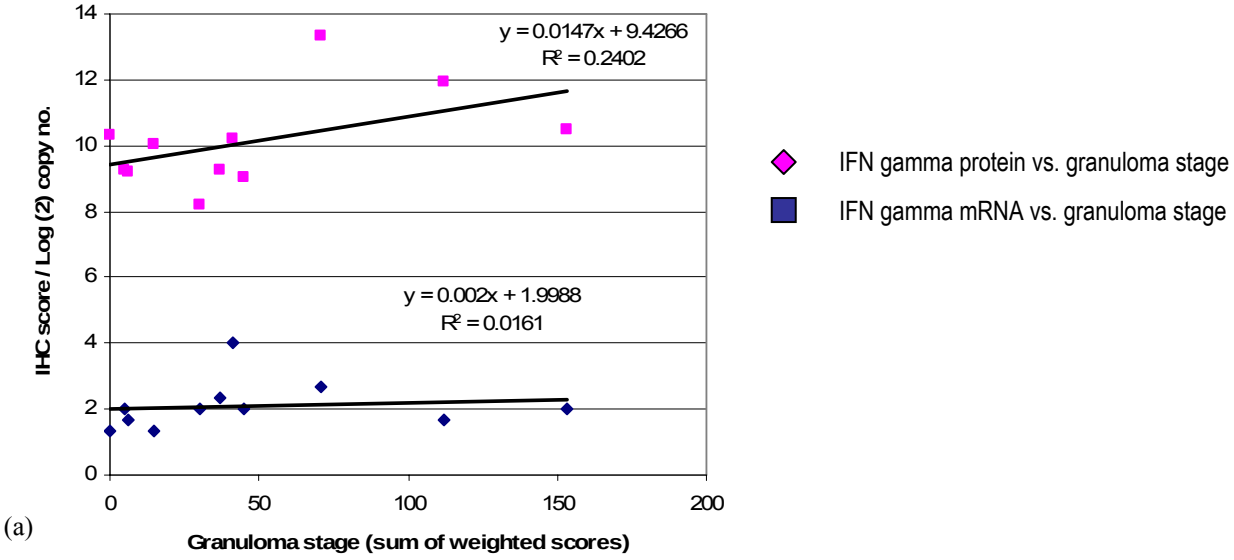

(a)

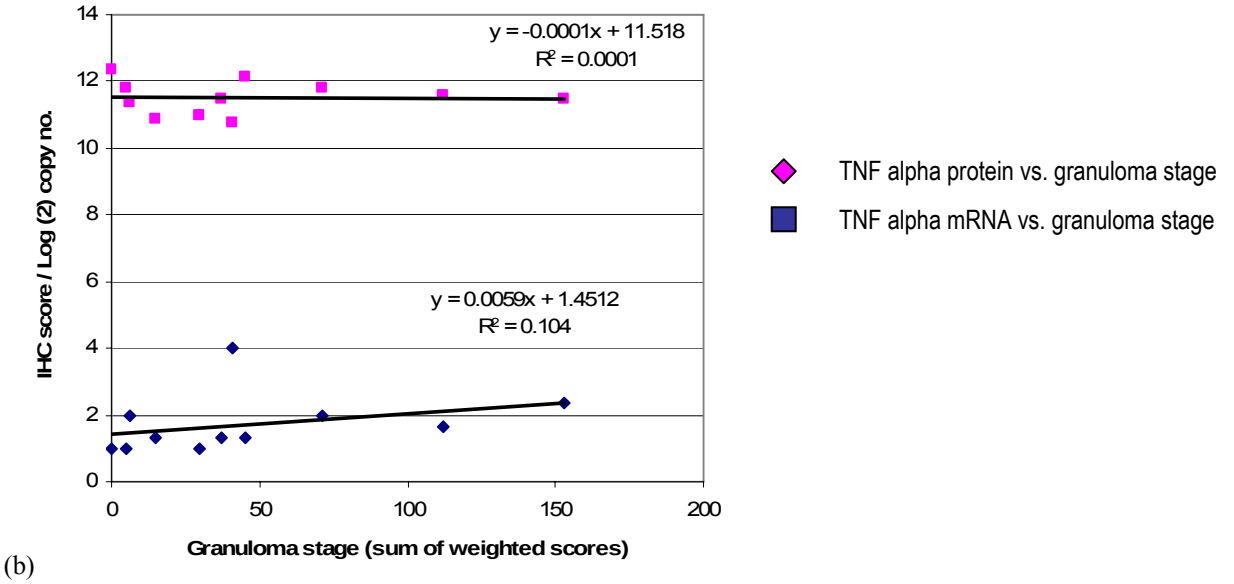

(b)

Figure 51: Correlations between granuloma stage (sum of weighted scores) and both (a) IFN-γ and (b) TNF-α. The graphs display both mRNA (log_2 copy number) and protein (IHC score) data for the thoracic lymph nodes of cattle either vaccinated with BCG (*sigK*) Pasteur prior to *M. bovis* challenge (n=4), vaccinated with BCG Pasteur prior to challenge (n=3) or non-vaccinated infected (n=4). The lymph node IFN-γ protein data are expressed as a score of percentage area coverage of cells expressing IFN-γ (IHC) based on the scale 1 (lowest percentage coverage) to 4 (highest percentage coverage). The IFN-γ mRNA data are expressed in log_2 copies obtained from the qRT-PCR experiments. Each data point represents one animal. The graph also displays both equations of the line including the R^2 value.

There was no significant relationship between IFN-γ mRNA or protein data and the granuloma developmental score for each animal ($p>0.05$, Spearmans correlation coefficient, Figure 51a). There was also no significant relationship between TNF-α (Figure 51b) or IL10 mRNA (graph not shown) and the granuloma developmental score ($p>0.05$, Spearmans correlation coefficient). There was however, a significant positive correlation for TNF-α protein levels ($p<0.05$, Spearmans correlation coefficient, Figure 51b).

Whole blood IFN-γ cultures

Whole blood samples were taken from each animal within the *M. bovis* infected groups (BCG (*sigK*) Pasteur vaccinated, BCG Pasteur vaccinated and non-vaccinated) at five weeks post infection (prior to euthanisation). The samples were incubated with tuberculin purified protein derivative (PPD) B to stimulate lymphocytes present within the blood to subsequently produce IFN-γ protein. Using an enzyme-linked immunosorbent assay (ELISA), IFN-γ protein was detected via spectrophotometry (450 nm) and the results expressed as mean optical density (OD) for each animal. The blood IFN-γ protein levels were compared to lymph node IFN-γ protein levels obtained by IHC.

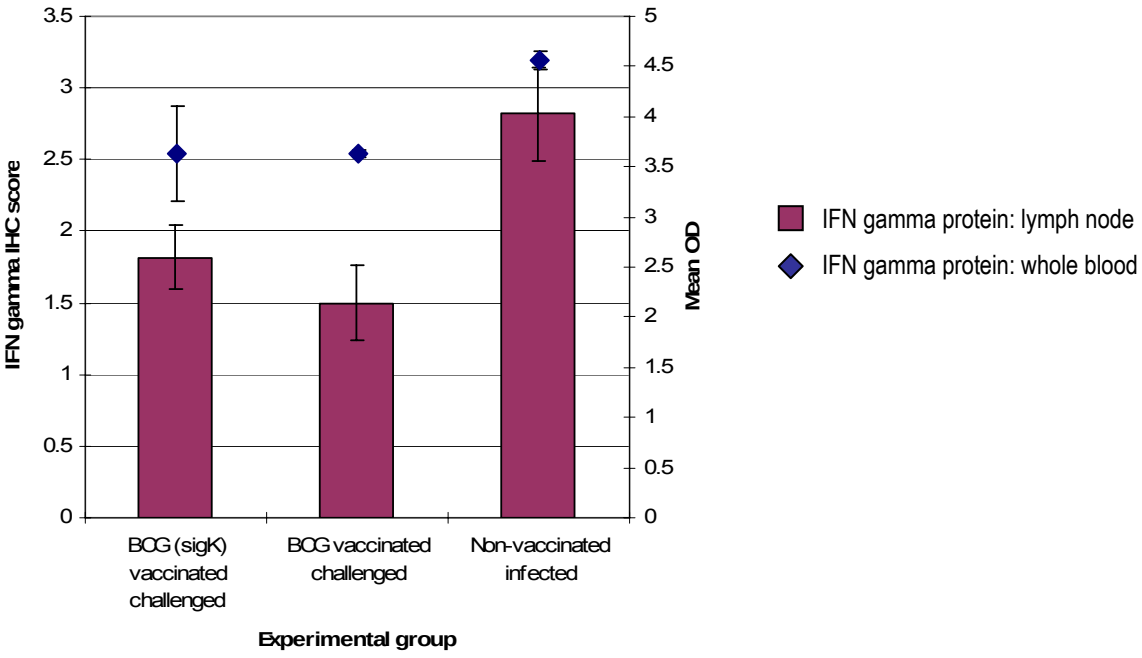

Figure 52: IFN-γ protein levels in the blood and lymph nodes of cattle either vaccinated with BCG (*sigK*) Pasteur prior to *M. bovis* challenge (n=4), vaccinated with BCG Pasteur prior to challenge (n=3) or non-vaccinated infected (n=4). The lymph node IFN-γ protein data are expressed as a score of percentage area coverage of cells expressing IFN-γ (IHC) based on the scale 1 (lowest percentage coverage) to 4 (highest percentage coverage). The data represents the mean of triplicate values from three lymph nodes (left bronchial, caudal mediastinal and cranial mediastinal) from every animal in each group. The whole blood IFN-γ protein data are expressed as mean optical density (OD) readings obtained from ELISA's of samples from each animal within each experimental group (performed in duplicate). Error bars indicate the standard deviation (±) from the mean.

Comparing the level of IFN-γ protein within whole blood cultures of cattle from the three experimental groups, the non-vaccinated *M. bovis* infected animals had the highest level of IFN-γ protein (mean OD reading of 4.57, Figure 52). Vaccination prior to challenge produced a decrease in the levels of blood IFN-γ protein, as both the BCG (*sigK*) Pasteur vaccinated and BCG Pasteur vaccinated cattle had lower levels of IFN-γ protein as compared to the non-vaccinated group (mean OD reading of 3.63, Figure 52).

The trend in IFN-γ protein levels within whole blood cultures was very similar to the trend in IFN-γ protein and mRNA levels within the thoracic lymph nodes (Figure 52). Statistically, there was a positive correlation (R value of 0.62) between lymph node IFN-γ protein and whole blood IFN-γ ($p<0.05$, Spearmans correlation coefficient, Figure 53).

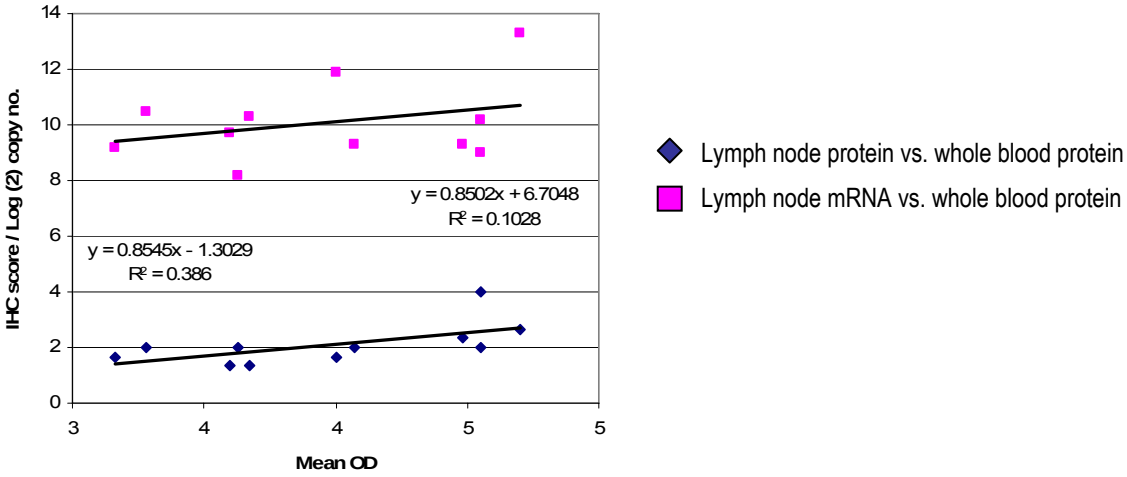

Figure 53: Correlation between IFN-γ protein in whole blood cultures and both IFN-γ mRNA (log_2 copy number) and protein (IHC score) in thoracic lymph nodes of cattle either vaccinated with BCG (*sigK*) Pasteur prior to *M. bovis* challenge (n=4), vaccinated with BCG Pasteur prior to challenge (n=3) or non-vaccinated infected (n=4). The lymph node IFN-γ protein data are expressed as a score of percentage area coverage of cells expressing IFN-γ (IHC) based on the scale 1 (lowest percentage coverage) to 4 (highest percentage coverage). The whole blood IFN-γ protein data are expressed as mean optical density (OD) readings obtained from ELISA's from each animal (performed in duplicate). The IFN-γ mRNA data are expressed in log_2 copies obtained from the qRT-PCR experiments. Each point represents one animal. The graph also displays both equations of the line including the R^2 value.

The non-vaccinated infected group had the highest level of both IFN-γ protein in the blood and IFN-γ protein in the thoracic lymph nodes (IHC score of 2.75, Figure 52). Prior vaccination reduced both IFN-γ protein in the blood and IFN-γ protein in the thoracic lymph nodes (IHC scores of 1.84 and 1.55, respectively, Figure 52). There was no difference in IFN-γ protein blood levels between the two vaccinated groups however there was a slight difference in IFN-γ protein lymph node levels between the two vaccinated groups (BCG (*sigK*) vaccinated group had an IHC score of 1.84 and the BCG vaccinated group had an IHC score of 1.55, Figure 52).

Discussion

The Bacillus Calmette Guérin (BCG) vaccination is the 'Gold standard' in protection against TB infection (Buddle *et al*, 2005) to which all new vaccines are measured against. Attenuated from a strain of *M. bovis*, BCG vaccination displays the ability to induce an immune response (Watanabe *et al*, 2006, Whelan *et al*, 2008, Huang *et al*, 2007) with reduced virulence (Junqueira-Kipnis *et al*, 2006). The vaccination has been shown to protect against mycobacterial infection in a variety of species, including bovine (Vordermeier *et al*, 2002) and murine (Giri *et al*, 2006) models, however rarely been shown to completely eradicate the bacteria (Buddle *et al*, 2005, Orme *et al*, 2001). In response to the growing need for a reliable bovine vaccination, the Krebs report (Krebs *et al*, 1997) highlighted the importance of creating a greater understanding of protective immunity. It is widely accepted that an essential component of the immune response to TB infection is cell mediated and this therefore may represent a potential correlate of protective immunity (Endsley *et al*, 2007). IFN-γ production and lymphocyte proliferation have been shown to be biomarkers of the cell mediated response although there are conflicting reports on their ability to indicate protection post vaccination (Wedlock *et al*, 2007, Buddle *et al*, 2003, Mittrucker *et al*, 2007). In addition to this, those correlates that have been shown to successfully predict vaccine induced protection in smaller animal models have been less successful in human infection (Buddle *et al*, 2003, Hoft *et al*, 2002). The added complications associated with cattle challenge experiments (high costs and limited availability of appropriate holding facilities) increases the need for a reliable correlate of protection that can be measured post vaccination but prior to challenge (Vordermeier *et al*, 2006). This further emphasises the importance of an improved understanding on the host's immune system in response to BCG Pasteur vaccination and *M. bovis* challenge (Endsley *et al*, 2007).

Modern molecular techniques have enabled genome sequencing of *M. bovis* (Garnier *et al*, 2003), *M. tuberculosis* (Cole *et al*, 1998) and BCG Pasteur (Brosch *et al*, 2007), thus allowing extensive genomic comparisons between the different mycobacterial species. A critical step in the attenuation of all BCG sub-types from *M. bovis* was the loss of the region of difference (RD) 1 (Pym *et al*, 2002, Lewis *et al*, 2003). However, genomic studies have also revealed apparent deletions, insertions and single nucleotide polymorphisms that differ between the BCG sub-types, effectively dividing them into early (including BCG Russia, Japan and Sweden) and late

(including BCG Pasteur, Danish and Glaxo) strains (Brosch *et al*, 2005). One such dividing factor is the production of antigenic proteins MPB70 and MPB83, which are produced in high levels by the earlier BCG strains and in low levels by late BCG strains (Harboe and Nagai, 1984) due to a polymorphism in the gene encoding for the regulatory factor *sigK* (Charlet *et al*, 2005). Comparative vaccination studies of human infants using both BCG Japan and BCG Pasteur (Davids *et al*, 2006) have indicated a stronger protective ability of BCG Japan. The difference in protective efficacy may be linked to the comparatively higher level of production of antigenic proteins MPB70 and MPB83, though there are no reports in the literature to support this hypothesis.

Complementation of BCG Pasteur with a wild-type *sigK* (BCG (*sigK*) Pasteur) has been shown to produce increased levels of MPB70 and MPB83 (Charlet *et al*, 2005) and so it was possible within this study to apply the genetically modified vaccine in bovine *M. bovis* challenge experiments. The immune response of cattle challenged with *M. bovis* post BCG Pasteur or BCG (*sigK*) Pasteur vaccination were analysed to provide an understanding of their protective efficacy. Recombinant vaccines with enhanced antigenic capabilities have been shown to induce an increased cell mediated immune response post vaccination (Shi *et al*, 2007, Qie *et al*, 2008, Ryan *et al*, 2007). Therefore by increasing the levels of MPB70 and MPB83, the BCG (*sigK*) Pasteur vaccine may induce a stronger immune response within the experimental cattle. The study also involved cattle from three control groups, non-vaccinated *M. bovis* infected, non-vaccinated non-infected and BCG Pasteur vaccinated non-infected to allow a more comprehensive overview of the immune system in response to different stimuli.

Total RNA extraction

To enable the quantification of target cytokine expression levels, total RNA was extracted from the freshly dissected bovine lymph node tissue samples using a Trizol/chloroform method (modified from Chomczynski and Sacchi, 1987). The total RNA was then analysed by agarose gel electrophoresis and spectrophotometry to determine the overall integrity of the extracted samples.

Reagents that have been developed to sequester RNA before the onset of degradation have proved extremely valuable for subsequent genetic analysis (Blow *et al*, 2008, Ahmed *et al*, 2004, Müller *et al*, 2002). Within this study, total RNA was extracted from freshly dissected lymph node samples and following agarose gel electrophoresis, both the 28S and 18S ribosomal bands were observed (Figure 34). The spectrophotometry results confirmed the

purity of the total RNA samples (Table 25), as the 260/280 nm ratio of 1.9 was in the expected range (Fleige and Pfaffl, 2006), thus indicating a lack of protein contamination (Bustin, 2004). Finally, the lymph node samples produced variable quantities of total RNA (with an approximate range of 170 to 1,952 µg/ml, Table 25) and this may be due to the individual extraction processes and the quality of each sample. The trizol/chloroform method resulted in a large quantity of total RNA from each sample (mean of 781.92 ug/ml, Table 25) and therefore it was decided to apply a one-step reverse transcriptase PCR method in which total RNA is added directly to the PCR reaction. This has the advantage of reducing potential contamination that may be introduced between the reverse transcriptase and PCR steps (Wacker and Godard, 2005).

Cytokine mRNA expression in the combined lymph nodes

The total RNA extracted from the five experimental cattle group lymph nodes (BCG Pasteur vaccinated *M. bovis* challenged, BCG (*sigK*) Pasteur vaccinated *M. bovis* challenged, non-vaccinated infected, non-vaccinated non-infected and BCG Pasteur vaccinated non-infected) were applied to qRT-PCR targeting the cytokines IFN-γ, TNF-α, IL10 and IL4, in addition to the housekeeping gene glyceraldehyde-3-phosphate dehydrogenase (GAPDH). As GAPDH is a constitutively expressed gene, it was therefore possible to use the amplified GAPDH PCR product to determine the overall integrity of the total RNA template. The crossing point values for each GAPDH reaction displayed a consistency in mRNA expression across the five experimental groups (mean CP of 22.8 for the BCG Pasteur vaccinated challenged group, 23.3 for the BCG (*sigK*) vaccinated challenged group, 22.8 for the non-vaccinated infected group, 22.4 for the non-vaccinated non-infected group and 23 for the BCG vaccinated non-infected group, Figure 35). This suggested that any potential differences in cytokine expression between the five experimental groups were unlikely to be due to the physical condition of the template. The mRNA expression levels of IFN-γ, TNF-α, IL10 and IL4 were then measured quantitatively in three different lymph nodes (left bronchial, cranial mediastinal and caudal mediastinal) from each animal within the five experimental groups. The qRT-PCR data from the individual lymph nodes was combined to produce a complete view of cytokine expression in response to BCG Pasteur/BCG (*sigK*) Pasteur vaccination and *M. bovis* infection (Figures 36 - 39). Cytokine expression was detected within all of the lymph node samples from every animal within each of the five experimental groups, including the non-vaccinated non-infected animals.

These results show that it is possible to detect cytokine expression within healthy cattle tissues and this has also been reported previously (Widdison *et al*, 2005).

Immune response to BCG Pasteur vaccination

The BCG Pasteur vaccinated non-challenged cattle displayed no significant change in cytokine expression as compared to the non-vaccinated non-infected cattle ($p>0.05$, Mann Whitney test, Figures 36 - 39) between fourteen and sixteen weeks post vaccination. All four cytokines displayed slightly lower expression levels in response to BCG vaccination (mean $\log_2$ copies of 7.84 for IFN-γ, 11.06 for TNF-α, 14.6 for IL10 and 12.2 for IL4, Figures 36 - 39) as compared to non-vaccinated non-infected cattle (mean $\log_2$ copies of 8.58 for IFN-γ, 11.8 for TNF-α, 15.5 for IL10 and 12.6 for IL4, Figures 36 - 39). Therefore, in the non-stimulated thoracic lymph node tissues, BCG Pasteur vaccination did not appear to produce an immune response that was apparent fourteen to sixteen weeks after vaccination.

A similar study performed by Widdison *et al* (2006) investigated cytokine expression levels in bovine parotid, submandibular and retropharyngeal lymph nodes. Comparisons of BCG vaccinated non-infected and non-vaccinated non-infected cattle also revealed no significant differences in IFN-γ, TNF-α or IL4 mRNA expression. However the study did show a significant increase in IL10 in response to vaccination (Widdison *et al*, 2006) which has also been reported in vaccination studies using human monocyte-derived dendritic cells (Gagliardi *et al*, 2005, Larsen *et al*, 2007). Analysis of the effects of BCG vaccination revealed the ability of dendritic cells to induce differentiation of naïve T cells into IL10 producing T regulatory (Tr1) cells (Larsen *et al*, 2007). The authors suggest that the Tr1 cells contribute to the immune response by regulating excessive T_H1 and T_H2 responses. This hypothesis is further supported by studies in IL10-deficient mice, which showed significantly enhanced levels of IL12 and TNF-α accompanied by numerous advanced granulomas following BCG vaccination (Jacobs *et al*, 2002). The IL10-deficient mice quickly eradicated the bacilli however the granulomatous lesions remained in a destructive state even after bacterial cell clearance, leading to irreversible tissue damage (Jacobs *et al*, 2002). This highlights the importance of IL10 as a regulatory cytokine and therefore the increase in expression post vaccination may represent the host's efforts to limit pathological disease.

Within this study, IL10 expression levels did not differ significantly in response to BCG Pasteur vaccination (Figure 38) and this may be due to the lymph nodes studied. The parotid lymph node is present within the neck/head region of the cow (Whipple *et al*, 1996) and thus would directly drain lymph from the site of BCG vaccination. A study observing the dissemination of

BCG Pasteur forty-two days post vaccination via subcutaneous injection to the neck of mice showed that very small numbers of bacilli reached the mediastinal lymph nodes (<5 cfu) in comparison to the spleen (between 90 to 110 cfu, Irwin *et al*, 2008). Assuming that this data would be applicable to larger animals as well, the lymph nodes of the bovine thorax may have been less likely to be directly affected by BCG vaccination.

The results from Widdison *et al* (2006) would suggest that BCG vaccination has a minimal affect on the bovine immune response as no significant difference was seen in pro-inflammatory cytokine expression. However, prior antigenic stimulation of whole blood bovine cultures isolated six weeks post BCG vaccination have been shown to produce significantly higher levels of IFN-γ as compared to non-stimulated vaccinated cultures (Endsley *et al*, 2007). Following BCG vaccination, naïve T cells are activated by antigen-presenting dendritic cells within the lymph nodes (Cella *et al*, 1997, Mellman and Steinman, 2001). The naïve cells differentiate into primary effector T cells and migrate to the initial site of infection to eliminate the bacterial threat. The majority of these effector T cells undergo apoptosis to maintain homeostasis and prevent the development of autoimmunity (Lin *et al*, 2000). However a small population of primary effector T cells maintain their antigen specificity for the rest of the hosts lifetime and are termed long lasting 'memory' T cells (Zinkernagel, 2000, Sprent and Surh, 2001). Two types of memory cell have been described, T effector-memory (T_{EM}) and T central-memory (T_{CM}) cells (Sallusto *et al*, 1999) which are recognised based on the expression of cell markers CD62L and CCR7 (T_{EM} express both whereas T_{CM} express neither, Campbell *et al*, 2001). Upon re-stimulation with the appropriate antigen, T_{EM} cells provide immediate protection against the bacterial threat at the site of infection by producing IFN-γ (Masopust *et al*, 2001). In contrast, T_{CM} cells are located primarily within the lymph nodes and following antigenic stimulation produce IL2 and IL10 (Sallusto *et al*, 1999). The T_{CM} cells are also able to stimulate dendritic cells via CD40 to produce IL12 (Sallusto *et al*, 1999), thus aiding differentiation of naïve T cells into primary T_H1 effector T cells. Therefore the lack of IFN-γ expression post BCG vaccination observed within Widdison *et al* (2006) and this study may be linked to the absence of *in vitro* antigenic stimulation needed to activate both subsets of memory T cells.

Isolated bovine PBMC CD4+ T cell populations also revealed a significant increase of both IFN-γ and perforin expression in antigenic stimulated compared to non-stimulated cultures (Endsley *et al*, 2007). In contrast, IFN-γ and perforin levels were not increased upon antigenic stimulation of non-vaccinated cattle (Endsley *et al*, 2007) implying that BCG vaccination

successfully primed the immune response. In addition to this, the IFN-γ+ and perforin+ CD4+ cells were shown to express memory cell markers (CD45RA-,CD45RO+ and CD62L+), enabling future detection of *M. bovis* infection (Endsley *et al*, 2007). It is important however, to be aware that *in vitro* stimulation can change cell phenotypes and therefore these results may not represent which memory cells were present *in vivo*.

Vaccination protocols inducing a strong cell mediated immunity, characterised by IFN-γ and IL2 expression (with a peak around two to four weeks post vaccination) have been shown to be suggestive of a protective ability if the host were to be challenged (Wedlock *et al*, 2007, Buddle *et al*, 1995, Skinner *et al*, 2003a, Vordermeier *et al*, 2002). However there are several studies that provide conflicting results, such as reports of high levels of IFN-γ expression induced in vaccination protocols that did not show the capacity to protect the host post experimental challenge (Waters *et al*, 2007). This was further illustrated in a recent study performed by Wedlock *et al* (2008) in which a prime-boost vaccination protocol involving BCG and CFP was employed in cattle alongside different combinations of adjuvants and immunostimulators. The results showed a significant increase in protection when BCG was applied in combination with a CFP adjuvant system, as opposed to BCG vaccination alone (Wedlock *et al*, 2008). Interestingly, application of BCG followed by an adjuvant combination without CFP acted to decrease protection as compared to sole BCG vaccination. Extensive analysis of the immune response post vaccination (including IFN-γ, IL10, IL4 and IL12) revealed no significant differences between the cattle vaccinated with BCG alone and those vaccinated with BCG followed by adjuvant (Wedlock *et al*, 2008).

Nevertheless, where the cell mediated response was absent or slow to evolve, the vaccine inevitably failed to induce significant protection (Wedlock *et al*, 2003, Buddle 2001). Therefore IFN-γ expression and the cell mediated immune response may be a valuable tool to prioritise protocols post vaccination but is limited in its usefulness as a correlate of protection (Vordermeier *et al*, 2006).

Immune response to *M. bovis* infection

In response to five weeks of *M. bovis* infection without prior vaccination, IFN-γ expression increased (from mean $\log_2$ copies of 8.58 in non-vaccinated non-infected cattle to 10.5 in non-vaccinated infected cattle, Figure 36) however this was not significant due to the large spread of data. This increase was accompanied by little change in TNF-α expression between the non-vaccinated infected and non-vaccinated non-infected groups (mean $\log_2$ copies of 11.8 and 11.55, respectively, Figure 37) but a significant decrease in IL10 expression (mean $\log_2$

copies of 15.5 and 14.44, respectively, Figure 38). Interestingly IL4 was not detected post *M. bovis* infection (Figure 39) whereas it was detected within non-infected cattle, suggesting that infection dramatically reduced the expression of IL4 at this time point.

It is widely accepted that a cell mediated immune response (T_H1 T cell type), supported by high levels of IFN-γ expression is the dominant profile induced early in infection (Welsh *et al*, 2005, Thacker *et al*, 2007). The time course study described previously provided evidence that this occurs around five weeks post infection, the same time point used within this study.

The competitive nature of the T cell profiles T_H1 (pro-inflammatory) and T_H2 (anti-inflammatory) denote that when one is highly expressed, the other is generally suppressed (Welsh *et al*, 2005). Therefore in environments of high IFN-γ expression, expression of T_H2 cytokines such as IL4 is low (Sanders *et al*, 1995), as seen within this data.

The study performed by Widdison *et al* (2006) also described a not significant change in IFN-γ expression in response to *M. bovis* infection. However the mean IFN-γ expression level was lower for the non-vaccinated infected animals as compared to the non-vaccinated non-infected animals; in contrast to the observed increase in IFN-γ expression within this study. This variation may be due to the time point post infection explored, as this study examined immune responses at five weeks as compared to at sixteen weeks post infection in the study by Widdison *et al* (2006). Research on progression of the bovine (Thacker *et al*, 2007, Welsh *et al*, 2005) and murine (Zhu *et al*, 2003) immune response post *M. bovis* infection has shown the system to be extremely dynamic. The time course study described previously produced data that suggested a mixed IFN-γ and IL10 profile at twelve weeks of infection. This is believed to represent the 'self-limiting' ability of T_H1 cells and the subsequent reduction in IFN-γ expression as observed at nineteen weeks post infection. Therefore at sixteen weeks (the time point used in Widdison *et al*, 2006) IFN-γ expression may be at a lower level as compared to earlier time points due to the suppressive role of T_H1-produced IL10. Interestingly, Widdison *et al* (2006) also revealed significant reductions in TNF-α and IL4 expression in response to infection, mirroring the changes observed within this study.

Immune response to vaccination and *M. bovis* challenge

Vaccinated challenged cattle displayed an increase in IFN-γ expression as compared to the vaccinated non-infected group (mean $\log_2$ copies of 9.6 in BCG Pasteur vaccinated and 10.3 in BCG (*sigK*) Pasteur vaccinated challenged cattle, Figure 36). This reflects the increase in cell mediated immunity observed post experimental challenge. However, the level of IFN-γ

expression remained lower in the vaccinated challenged groups to that observed within the non-vaccinated infected animals, suggesting that prior vaccination modified the cell mediated response. There was no significant difference in IFN-γ expression between the two BCG Pasteur vaccines (Figure 36). However, the BCG Pasteur vaccinated animals displayed a lower level of IFN-γ than that shown by the BCG (*sigK*) Pasteur vaccinated animals, when compared to the non-vaccinated infected cattle. Interestingly, the BCG (*sigK*) Pasteur vaccinated challenged animals displayed significantly higher levels of IFN-γ expression as compared to the BCG Pasteur vaccinated non-infected group, whereas the BCG Pasteur vaccinated challenged group did not. This would suggest that at five weeks post challenge, cattle vaccinated with BCG Pasteur vaccination displayed levels of IFN-γ expression levels similar to those observed prior to challenge.

Decreases in IFN-γ expression post challenge as compared to non-vaccinated animals have been reported previously in BCG vaccinated cattle (Vordermeier *et al*, 2002, Widdison *et al*, 2006, Waters *et al*, 2007, Buddle *et al*, 1995) and have been associated with limited disease dissemination and severity (Waters *et al*, 2007). Vordermeier *et al* (2002) observed the immune responses of BCG Pasteur vaccinated cattle infected with *M. bovis* over an eighteen week time period. *In vitro,* rapid T cell proliferation within both ESAT-6 and PPD-B stimulated PBMCs isolated from the non-vaccinated infected controls was detectable three weeks post challenge and remained strong throughout the eighteen week period (Vordermeier *et al*, 2002). In comparison, PBMCs isolated from BCG Pasteur vaccinated cattle displayed levels of T cell proliferation towards PPD-B that were similar to those observed pre-challenge (Vordermeier *et al*, 2002). These results were mirrored in the data obtained by IFN-γ assays (measured using both the BOVIGAM enzyme immunoassay and Direct enzyme-linked immunspots) as the levels were significantly lower in response to ESAT-6 within the BCG vaccinated cattle as compared to the non-vaccinated control animals (Vordermeier *et al*, 2002). Similar results were obtained by Hope *et al* (2005) in a study aimed at measuring the immune response within *in vitro* stimulated PBMC from vaccinated and challenged neonatal calves over a sixteen week period. The BCG vaccinated cattle produced high levels of IFN-γ for the first two weeks immediately following challenge which remained consistent for the remainder of the sixteen weeks (Hope *et al*, 2005). In contrast, the non-vaccinated bovine PBMC induced IFN-γ was produced at comparatively lower levels until four weeks after challenge, at which point the levels increased dramatically to almost double that seen in the vaccinated animals (Hope *et al*, 2005). The authors suggest that this delay in cell mediated immunity allowed the bacterial cells to replicate

freely leading to a hyper-potent IFN-γ response and extensive lesion development (Hope *et al*, 2005). In comparison, the vaccinated animals were able to effectively remove the bacterial threat from the early stages of infection resulting in a decreased effector T cell population, lower levels of IFN-γ and less tissue damage (Vordermeier *et al*, 2002, Hope *et al*, 2005).

Waters *et al* (2007) reported no significant difference in TNF-α expression post challenge in vaccinated cattle as compared to non-vaccinated infected cattle and this was paralleled within this study (mean $\log_2$ copies of 11.47 in BCG Pasteur and 11.53 in BCG (*sigK*) Pasteur vaccinated challenged, as compared to 11.55 for the non-vaccinated infected group, Figure 37). TNF-α is an essential cytokine of the innate immune response and is up-regulated in the presence of IFN-γ (Ding *et al*, 1988). The lack of any significant differences between the five experimental groups in TNF-α expression would imply that there may be posttranscriptional controls regulating protein translation (Baseggio *et al*, 2002, Kruys *et al*, 1993). This point will be discussed in further detail in relation to the immunohistochemistry data.

Similarly, there was no significant difference in IL10 expression in vaccinated compared to non-vaccinated cattle five weeks post *M. bovis* challenge (mean $\log_2$ copies of 14.4 for the BCG Pasteur vaccinated challenged, 14.44 for the BCG (*sigK*) vaccinated challenged and 14.44 for the non-vaccinated infected groups, Figure 38). In contrast to this data, Widdison *et al* (2006) reported a significant increase in IL10 mRNA expression in BCG Pasteur vaccinated compared to non-vaccinated cattle following sixteen weeks of *M. bovis* infection. The authors suggested that the increase in IL10 expression was in part due to the dampened IFN-γ response within the vaccinated animals, caused by a decreased bacterial load (Widdison *et al*, 2006). Human T cells have been reported to be able to produce both IFN-γ and IL10 (Gerosa *et al*, 1999) and as previously mentioned in the time course study, it is believed that the ratio of IFN-γ/IL10 may have a huge impact on whether the T cell displays anti-inflammatory characteristics (Katsikis *et al*, 1995). The increase in IL10 observed by Widdison *et al* (2006) may therefore be due to the 'self-limiting' nature of the T_H1 response, in which reduced antigenic loads result in down-modulation of IFN-γ expression. A probable explanation for the inconsistency in IL10 expression between Widdison *et al* (2006) and this study may again be due to the differing time points of sample collection (sixteen and five weeks, respectively). Interestingly, a study performed on BCG Pasteur vaccination of neonatal calves sixteen weeks post *M. bovis* challenge reported no significant difference in PBMC stimulated IL10 protein levels between vaccinated and non-vaccinated animals (Hope *et al*, 2005). As previously mentioned within the time course study, translation of IL10 protein is also controlled by numerous posttranscriptional

regulatory elements (Powell *et al*, 2000, Nemeth *et al*, 2007), thus mRNA expression levels may not be representational of protein levels.

As observed within the non-vaccinated infected group, IL4 expression was undetectable in both the BCG Pasteur and BCG (*sigK*) Pasteur vaccinated challenged groups (Figure 39). The neonatal calf study by Hope *et al* (2005) also reported that IL4 protein was undetectable at sixteen weeks after challenge in both vaccinated and non-vaccinated animals. IL4 mRNA is known to be extremely unstable (Dokter *et al*, 1993, Umland *et al*, 1998) and has been shown to be down-regulated in response to *M. bovis* infection (Rhodes *et al*, 2007, Welsh *et al*, 2005), thus making it even more difficult to detect. In reference to the Widdison *et al* (2006) study, IL4 mRNA was detected sixteen weeks post challenge in both vaccinated and non-vaccinated animals. In addition to this, the vaccinated animals displayed significantly higher levels of IL4 as compared to the non-vaccinated animals, due to the dampened IFN-γ response (Widdison *et al*, 2006). These three studies (this study, Widdison *et al*, 2006 and Hope *et al*, 2005) illustrate the extreme heterogeneity in the immune response to vaccination and challenge, aggravated by differing sampling time points, vaccination protocols (intratracheal or intranasal) and target sample tissues (lymph nodes or PBMCs/ mRNA or protein).

Correlations between cytokine mRNA expression levels

The qRT-PCR data displayed significant positive relationships between IL10 and TNF-α (Table 26 and Figure 40) as well as between IL4 and each of the other three cytokines ($p<0.01$ Pearsons correlation co-efficient, Table 26 and Figures 41, 42 and 43).

As IL4 expression was found within the two control groups only (non-vaccinated non-infected and BCG vaccinated non-infected) it is not surprising that a significant correlation was found between IL4 and each of the other three cytokines. All four cytokines displayed a slight decrease in expression in the BCG Pasteur vaccinated non-infected group compared to the non-infected non-vaccinated group (Figure 39). The data from these two groups would therefore produce a strong correlation between all of the four cytokines studied but would not represent a true relationship due to the small number of data points.

A relationship between TNF-α and IL10 mRNA expression has been previously reported in published studies (Widdison *et al*, 2006). Focusing on the mRNA expression data from this study (Figures 37 and 38); it is evident that the non-vaccinated non-infected group displayed the highest level of both TNF-α and IL10 mRNA. However the differences in TNF-α expression

between the five experimental groups were insignificant and as both TNF-α and IL10 have been reported to experience posttranscriptional control (Powell *et al*, 2000, Nemeth *et al*, 2007), the relationship in mRNA expression may not reflect a true relationship in protein production.

Immunohistochemistry

An important factor in the study of mRNA expression is the degree to which it represents protein production levels. Therefore, analysis of the levels of IFN-γ and TNF-α protein were analysed in the selected lymph nodes of each animal within the five experimental groups using immunohistochemistry. This allowed a direct comparison between the mRNA and protein levels within the same bovine samples and also a deeper understanding of the immune response occurring within each experimental group.

There was a significant positive relationship between the level of IFN-γ mRNA expression and the level of IFN-γ protein ($p<0.001$, Spearmans correlation coefficient, Figures 44 and 45). This would suggest that the expression of IFN-γ mRNA is in direct relation to the production of IFN-γ protein (Thacker *et al*, 2007). Analysing the IHC data in experimental groups, the non-vaccinated infected group had the highest level of IFN-γ protein (mean score of 2.75, Figure 44). This was statistically higher than both of the control groups, non-vaccinated non-infected (mean score of 1.27) and the BCG Pasteur vaccinated non-infected group (mean score of 1.42, $p\leq0.005$, Figure 44). Vaccination with either BCG Pasteur or BCG (*sigK*) Pasteur prior to challenge displayed an increase in IFN-γ protein post challenge as compared to the non-infected groups (mean score of 1.5 and 1.8, Figure 44), however the level was not as high as in the non-vaccinated infected group. This strongly resembles the mRNA expression data and reflects the variability of the IFN-γ response depending on the infection scenario.

In contrast, there was no significant relationship between the level of TNF-α mRNA expression and the level of TNF-α protein ($p>0.05$, Spearmans correlation coefficient, Figures 46 and 47). This would suggest that the expression of TNF-α mRNA is not in direct relation to the production of TNF-α protein and that one or more forms of posttranscriptional regulation are in place. Comparing the mRNA and protein data (Figure 46), posttranscriptional control is most evident in the non-vaccinated non-infected and BCG vaccinated non-infected groups, as the protein levels are lower than that displayed by the mRNA data (mean score 1.13 and 1,

respectively, Figure 46). As previously mentioned, it is not unusual to detect TNF-α mRNA expression in non-infected tissues (Widdison *et al*, 2006) however, studies have found the TNF-α mRNA to be unstable and translation of TNF-α protein repressed in healthy tissues (Kruys *et al*, 1993, Beutler and Cerami, 1989, Geppert *et al*, 1994). Therefore, as observed, the mRNA expression measured within the two control groups did not reliably represent protein levels due to repression of the translational process. Following stimulation by lipopolysaccharide, the stability of TNF-α mRNA has been shown to be enhanced (Baseggio *et al*, 2002) and translation un-repressed (Skinner *et al*, 2008). *M. tuberculosis* (Yang *et al*, 2005) and *M. bovis* BCG (Mendez-Samperio *et al*, 2004) have also displayed the ability to trigger intracellular signalling processes essential in TNF-α translation, such as the phosphatidylinositol 3-kinase (PI 3-K) cascade and the extracellular regulated kinase (ERK) pathway 1/2 in human monocyte-derived macrophages. The role of *M. bovis* in up-regulating TNF-α translation would therefore support the data observed within this study, as the non-vaccinated infected group had the highest level of TNF-α protein (mean score 2.17, Figure 46). Vaccination with BCG (*sigK*) Pasteur prior to challenge had a negligible effect on TNF-α protein levels (mean score 1.82) whereas prior vaccination with BCG Pasteur reduced TNF-α protein to pre-challenge levels (mean score 1.13, Figure 46). A study performed on the bronchoalveolar lavage cells of guinea pigs revealed that, prior to *M. tuberculosis* challenge both non-vaccinated and BCG Tokyo vaccinated animals displayed a lower level of non-antigenically stimulated TNF-α protein with little difference between the two groups (Yamamoto *et al*, 2007). Three weeks after *M. tuberculosis* challenge; the non-vaccinated animals displayed relatively lower levels of TNF-α production. However, by five weeks, non-vaccinated animals displayed significantly higher levels of PPD-B stimulated TNF-α protein as compared to pre-challenge levels and four fold greater levels than the BCG Tokyo vaccinated animals. In contrast, the BCG Tokyo vaccinated animals displayed similar PPD-B stimulated TNF-α protein levels pre and post *M. tuberculosis* challenge (Yamamoto *et al*, 2007). The authors suggest that BCG vaccination acts to modulate TNF-α production subsequently reducing immunopathological harm associated with increased TNF-α concentrations (Bekker *et al*, 2000). In contrast, the non-vaccinated animals did not control the infection in the early stages (low TNF-α level at three weeks post challenge). Therefore, the increasing bacillary loads exasperated the immune response, leading to an uncontrolled TNF-α production at five weeks of challenge.

Lymph node pathology

Percentage granuloma coverage

Within this study two comparable factors were used to represent the levels of pathology within the *M. bovis* infected lymph nodes; percentage area coverage of granulomas (Figures 48 and 49) and granuloma stage (Table 27). As previously mentioned, the granuloma is initially a structure formed to protect the host, however as it grows in size as a response of cellular activity it becomes associated with immunopathological harm (Mustafa *et al*, 2008). Therefore, the percentage area coverage of the granulomas within the lymph node sections can give an indication to the progression of the immune response.

The percentage area of granuloma coverage for the three *M. bovis* challenged groups revealed differences between the vaccinated and non-vaccinated cattle, however due to the large variations in data these differences were not significant ($p>0.05$, Kruskal Wallis test, Figure 48). The non-vaccinated infected group showed the largest percentage area of granuloma coverage (mean of 59%) as compared to the BCG (*sigK*) Pasteur vaccinated challenged (mean of 35%) and BCG Pasteur vaccinated challenged (mean of 6%) groups (Figure 48).

There are numerous studies reporting the beneficial effects of BCG vaccination on host disease pathology as compared to non-vaccinated infected controls (Widdison *et al*, 2006, Wedlock *et al*, 2007, Hope *et al*, 2005, Vordermeier *et al*, 2002, Ng *et al*, 1995). A study by Johnson *et al* (2006) showed a significant reduction in percentage area of granulomatous inflammation within BCG vaccinated cattle lymph nodes (14.9%) as compared to non-vaccinated infected controls (65.6%). This suggests that BCG vaccination does provide a considerable degree of protection against pathological damage due to the limited immune response. However, vaccination was not able to rid the host of disease entirely.

The degree of granuloma growth and pathological disease displayed a positive correlation with both IFN-γ protein and mRNA expression ($p<0.05$, Spearmans correlation coefficient, Figure 50a). The non-vaccinated infected group had the highest level of IFN-γ expression, coinciding with the highest level of granuloma percentage coverage (Figure 48). However at the time point studied, prior vaccination resulted in a lower level of IFN-γ and also a lower level of granulomatous coverage (Figure 48). The association between high levels of IFN-γ post challenge and high levels of pathological damage have been described in similar studies (Wedlock *et al*, 2007, Vordermeier *et al*, 2006, Vordermeier *et al*, 2002). IFN-γ is a potent pro-

inflammatory cytokine that induces production of macrophage cytocidal compounds (such as reactive oxygen and nitric oxide synthesis) and bacterial phagocytosis (Ding *et al*, 1988). Activation of macrophages and enhancement of their antigen presenting ability leads to increased T cell maturation and subsequently increased IFN-γ production (Barnes *et al*, 1994). Bacterial cell load has been shown to be a significant factor in the number of T effector cells recruited to the infection site (Lalvani, 2004) and as a result, also the level of IFN-γ production (Lyashchenko *et al*, 2004, Vordermeier *et al*, 2002, Skinner *et al*, 2003a). Non-vaccinated cattle have been reported to harbour significantly higher numbers of bacilli within lymph node granulomas as compared to BCG Pasteur vaccinated cattle at eighteen weeks post infection (Johnson *et al*, 2006). It therefore seems probable that vaccination prior to challenge allows the host to eradicate the bacterial threat more efficiently and quickly, leading to a lower expression of IFN-γ at the time point these parameters were measured for this study and ultimately a lower level of granulomatous spread. As previously mentioned, the same theory has also been applied to TNF-α and BCG vaccination (Yamamoto *et al*, 2007) and this is not surprising due to the role of IFN-γ in enhancing TNF-α production (Ding *et al*, 1988). In addition, both TNF-α and IFN-γ have been shown to enhance expression of cell surface adhesion molecules thus aiding monocyte migration (Munro *et al*, 1989) and granuloma growth. A positive correlation was also revealed between granuloma growth and TNF-α protein ($p<0.001$) but not with TNF-α mRNA ($p>0.05$, Spearmans correlation coefficient, Figure 50b) due to the posttranscriptional regulation of the TNF-α transcript.

Granuloma score

A second method of measuring pathological development within this study was based on the stage of granuloma development (Table 27). Granulomas can be categorised into four stages of development depending on their physiological and immunological status (Wangoo *et al*, 2005). The numbers of granuloma within each stage of development were counted for each lymph node sample and the data weighted to account for the larger size of the later staged granuloma (Table 27). Comparison of the granuloma developmental stage results (Table 27) with the data for granuloma percentage area coverage (Figure 49) for each individual animal revealed a statistically positive relationship ($p<0.001$, Spearmans correlation co-efficient) between the two variables. Granulomas have been reported to double in size (mean lesion size measured in millimetres) between each developmental stage (Wangoo *et al*, 2005) due to the accumulation of T cells and macrophages that both directly and indirectly (through cytokines and necrosis) mark the advancement through each stage.

The BCG (*sigK*) Pasteur vaccinated challenged cattle displayed the highest score for granuloma development (mean 69, Table 27), followed by the non-vaccinated infected group (mean 48.5, Table 27). The lowest score for granuloma development was shown by the BCG Pasteur vaccinated challenged group (mean 15, Table 27) although these differences were not significant due to the small number of data points and large data variation. Interestingly, the mean score for the BCG (*sigK*) Pasteur vaccinated challenged group was increased dramatically by two particular animals, identification numbers of 3511 and 3506 (scores of 112 and 153, respectively, Table 27). This suggests a large variability in both the ability of the vaccine to protect each individual host and the immune profile of each animal in response to challenge.

As described for the time course study, there was a spread of granuloma developmental stages within each animal (Table 27), illustrating the vast heterogeneity between individual granulomas. The main difference in granuloma development between the vaccinated and non-vaccinated animals was the presence of stage IV lesions, as neither vaccinated group showed such advancement in lesions. However, each of the four animals within the non-vaccinated infected group displayed advanced granuloma development (total IV granuloma score of 96, Table 27). Johnson *et al* (2006) described granulomas within BCG vaccinated cattle to be much smaller and less advanced as compared to non-vaccinated controls after eighteen weeks of challenge. The BCG vaccinated cattle also displayed higher levels of T and B cells with fewer macrophages and Langhans giant cells (Johnson *et al*, 2006). The authors suggested that this immune profile enhanced the interaction between the cells, allowing the activity of infected macrophages to be maintained thereby reducing the development of caseous necrotic lesions (Johnson *et al*, 2006, Ulrichs *et al*, 2004). The lower levels of IFN-γ and TNF-α observed within the BCG vaccinated animals of this study would support this theory, as both have been connected to the development of advanced necrosis (Hernandez-Pando and Rook, 1994), characterising stage IV granuloma (Wangoo *et al*, 2005).

Over the first three stages of granuloma development (stage I, II and III), the BCG Pasteur vaccinated group displayed the lowest scores (total of 13, 28 and 4, respectively, Table 27). Conversely, The BCG (*sigK*) Pasteur vaccinated group displayed the same score for stage I granuloma as compared to the non-vaccinated infected group (total of 32, Table 27). The BCG (*sigK*) Pasteur vaccinated group also displayed a higher score for the stage II granuloma (total of 164 as compared to 58 for the non-vaccinated group) and a tenfold higher number of stage

III granuloma (total of 80 as compared to 8 for the non-vaccinated group, Table 27). This would suggest that although the levels of IFN-γ and TNF-α were low enough to suppress the development of necrotic lesions (stage IV); the immune response had not removed the bacterial threat as efficiently as the BCG vaccinated animals, leading to increased numbers of early staged granuloma. It seems probable that the reason behind the BCG (*sigK*) Pasteur vaccinated group showing a higher total granuloma development score than the non-vaccinated infected animals is connected to the nature of the granulomas within each stage. As previously mentioned the stage IV granuloma can be considerably larger in size as compared to the smaller stage II and III (Wangoo *et al*, 2005) and therefore leaves limited lymph node surface area for new granuloma development. In addition to this, the extensive necrosis associated with stage IV granuloma may obscure smaller granulomas situated adjacent to stage IV lesions, therefore lowering their total count. This is supported by the results of the percentage area coverage of granuloma within each experimental group, as the non-vaccinated infected animals displayed a considerably higher percentage as compared to the BCG (*sigK*) Pasteur vaccinated group.

Interestingly, TNF-α protein and not IFN-γ displayed a positive relationship with the granuloma developmental score ($p<0.05$, Spearmans correlation coefficient, Figure 51A and B). Three of the main grouping factors used to characterise the granuloma into the four stages were the presence of necrosis, epithelioid macrophages and multi-nucleated giant cells (Wangoo *et al*, 2005). TNF-α has been shown to correlate positively with necrosis in human TB lesions (Fenhalls *et al*, 2000 and 2002) due to its destructive properties when present in either excessive levels (Bekker *et al*, 2000) or dominant T_H2 environments (Hernandez-Pando and Rook, 1994). In addition, *M. bovis* infected macrophage differentiation into epithelioid or giant multi-nucleated cells is believed to be connected to bacterial cell endocytosis (Lay *et al*, 2007), a process which also induces macrophage-produced TNF-α (Goldsby *et al*, 2003).

Whole blood IFN-γ cultures

The aforementioned cytokine expression studies were performed at the site of infection within the lung draining lymph nodes. However, peripheral or whole blood mononuclear cells are frequently used to measure IFN-γ expression post vaccination due to the logistical problems of isolating lymph nodes. Therefore, IFN-γ protein levels from PBMCs were also measured for

each animal within the BCG Pasteur vaccinated challenged, BCG (*sigK*) Pasteur vaccinated challenged and non-vaccinated infected groups of this study using stimulatory antigen purified protein derivative bovis (PPD-B, Figure 52). Antigenic stimulation of PBMCs express high levels of IFN-γ and produce a delayed –type hypersensitivity (DTH) reaction during which activated T cells, macrophages and neutrophils converge (Pollock *et al*, 1997). It was therefore possible to compare the levels of IFN-γ expression between the peripheral blood and at the actual site of infection within the lymph nodes.

The non-vaccinated infected group displayed the highest level of whole blood stimulated IFN-γ (mean OD reading of 4.57, Figure 52) as compared to the level displayed by both vaccinated groups (mean OD reading of 3.63, Figure 52). Although there was no statistical significance between the vaccinated and non-vaccinated groups, the results revealed a significantly positive correlation with the lymph node IFN-γ protein levels ($p<0.05$, Spearmans correlation coefficient, Figure 53). This would suggest that, post challenge, the analysis of whole blood stimulated IFN-γ from this study was an accurate representation of the immune response at the site of infection. Although there are studies that dispute this idea (Barnes *et al*, 2003), there are also some that provide evidence to support the relationship between whole blood and lymph node IFN-γ levels (Hope *et al*, 2005, Rhodes *et al*, 2000).

These results show that IFN-γ levels both within the lymph nodes and whole blood were expressed at a lower level in BCG Pasteur vaccinated challenged cattle, similarly described in Wedlock *et al* (2007). Interestingly, the whole blood stimulated IFN-γ levels did not differentiate between the two vaccination types as was found for the lymph node IFN-γ levels. This suggests that the more subtle differences in cytokine expression observed within the lymph nodes that led to enhanced levels of pathological damage may not be mirrored within the whole blood immune profile.

Conclusion

The results of this study have reinforced those previously published by other groups (Vordermeier *et al*, 2002, Widdison *et al*, 2006, Waters *et al*, 2007, Buddle *et al*, 1995) on the benefits of BCG vaccination in reducing immunopathological development. The *M. bovis* challenged non-vaccinated cattle displayed increased levels of IFN-γ (mRNA and protein) and TNF-α (protein) expression coinciding with significantly reduced IL10 and undetectable IL4

levels as compared to the non-infected animals. This immune profile is characteristic of a strong cell mediated response and led to high levels of pathological damage. BCG vaccination (both BCG Pasteur and BCG (*sigK*) Pasteur) resulted in lower levels of both IFN-γ and TNF-α expression but had little impact on either IL10 or IL4 levels post challenge as compared to the non-vaccinated cattle. Vaccination acts to induce a cell mediated immune response via TB specific antigenic stimulation, leading to a population of both effector and memory CD4+ and CD8+ T cells (Irwin *et al*, 2008). Future infection with *M. bovis* triggers the memory T cell population and therefore initiates a faster cell mediated and IFN-γ response, enabling more efficient eradication of the bacterial threat (Waters *et al*, 2007). This protective memory response takes place early post challenge (approximately two to three weeks, Vordermeier *et al*, 2006 and 2002) and then declines, possibly in parallel with a decreased bacterial load. This would explain the decreased IFN-γ expression found in this study measured at five weeks post challenge, in the vaccinated compared to non-vaccinated controls.

However, experimental BCG vaccination of cattle has shown varying levels of protective efficacy (Buddle *et al*, 2005, Orme *et al*, 2001) and is currently impracticable for wide-scale use due to its interference with the tuberculin diagnostic skin test (Doherty *et al*, 1995). With the number of bovine TB cases increasing annually (Reynolds, 2006) the need for an improved and more reliable vaccination protocol has become a priority of the veterinary scientific community. BCG vaccination is still considered the 'gold standard' (Buddle *et al*, 2005) against TB infection and therefore the majority of newly developed protocols have included its use. A potential pathway in increasing the efficacy of BCG vaccination has been to introduce antigenic genes that have been either deleted or repressed during its attenuation (Vordermeier *et al*, 2006). This study included analysis of the bovine immune response to vaccination with a recombinant BCG Pasteur expressing a wild-type *sigK* gene from BCG Russia (Charlet *et al*, 2005). The recombinant BCG Pasteur has been shown to produce increased levels of antigenic proteins MPB70 and MPB83 (Charlet *et al*, 2005) and therefore presented itself as an ideal candidate for vaccination studies. It was hypothesised that by increasing the strength of the antigenic stimulation, the vaccine would be able to induce a stronger cell mediated response and thus a higher level of protection against challenge. However, the results from this study did not support this hypothesis. BCG (*sigK*) Pasteur was shown to induce protection against *M. bovis* by reducing IFN-γ and TNF-α expression as well as immunopathological disease in respect to the non-vaccinated infected animals. However, the BCG (*sigK*) Pasteur vaccinated cattle displayed higher levels of pathology as well as increased expression of IFN-γ

and TNF-α as compared to the BCG Pasteur vaccinated cattle post challenge. This suggests that increasing the MPB70 and MPB83-specific antigenic properties of the vaccine actually proved detrimental to the hosts' protection against *M. bovis* challenge. A possible reason for the reduced ability of the recombinant BCG vaccine could be linked to development of the central memory response. The level of protection induced post challenge is dependent upon the strength and duration of antigenic stimulation as well as the level of co-stimulation induced by vaccination (Seder and Ahmed, 2003). These factors combine to affect both T cell distribution and function following vaccination and subsequently the effectiveness of memory T cells to detect future infection (Seder and Ahmed, 2003). It has been suggested that by increasing the immunogenicity of the vaccine, the host is able to mount a stronger immune response and eradicate the bacterial threat more quickly, thus reducing the duration of antigenic stimulation (Orme *et al*, 2006). The cattle vaccinated with BCG (*sigk*) Pasteur were therefore not able to mount a sufficient memory response upon re-stimulation by *M. bovis* challenge, leading to a larger persistent bacterial load and a heightened IFN-γ response. The increased pathological damage observed within the BCG (*sigK*) Pasteur vaccinated cattle may also imply involvement of the MPB83 and MPB70 proteins in pathogenesis of the disease. Structural studies of both MPB70 and MPB83 have revealed a potential ability of the antigens for binding to cell surface host proteins via specific interaction sites (Carr *et al*, 2003). The authors suggest that this may represent a role for these antigens in modulating host cell behaviour by intercepting signalling pathways to the advantage of the pathogen (Carr *et al*, 2003). This may skew the hosts' immune response and lead to increased immuno-pathological harm.

Other studies have also shown vaccines expressing enhanced antigenic properties to be less effective in providing protection against infection as compared to BCG (Rao *et al*, 2005). Murine vaccination models of different BCG sub-strains have shown that increased antigenic properties did not increase protective efficacy against *M. tuberculosis* infection (Irwin *et al*, 2008). BCG Pasteur, BCG Sweden and BCG Connaught (lower antigenic level) induced differing levels of IFN-γ post vaccination in mice, with BCG Connaught inducing the highest response (Irwin *et al*, 2008). Post challenge, there was no difference in protection between the different sub-strains, further illustrating the inadequacy of IFN-γ as a correlate of protection (Mittrucker *et al*, 2007).

A potential solution to the problem of duration and strength of antigenic stimulation would be to vaccinate the same host twice in a prime-boost protocol using either BCG alone (homologous,

Griffin *et al*, 2006a) or in conjunction with a subunit vaccine (heterologous, Skinner *et al*, 2003a, Wedlock *et al*, 2005). This would enable the use of highly immunogenic vaccines and still lengthen the duration of antigenic stimulation. Various vaccine candidates are currently being applied in this manner with some very encouraging results (Vordermeier *et al*, 2006). An example of this is the ESAT-6:CFP10+GM-CSF+CD80/CD86 DNA vaccine in combination with BCG (Maue *et al*, 2007). The DNA vaccine alone was able to induce a cell mediated immune response due to its ability to induce DC maturation and increase T cell stimulation; however the addition of a BCG boost significantly reduced bacterial loads and pathological damage (Maue *et al*, 2007). Increased pathology has been directly related to the potential for the host to transmit the disease (McCorry *et al*, 2005) and thus vaccination also has the benefit of not only protecting the host but also suppressing transmission of the infection.

In 2005 the government announced a ten year strategy to produce a sustainable reduction in bovine TB across the United Kingdom (DEFRA, 2005b). A major part of this plan is the development of an improved bTB vaccine, to which over £4 million have been invested (Reynolds, 2006). Of the approximate sixty candidate vaccines developed, ten have been trialled in experimental bovine models and those that have shown the most promising results are based on prime-boost protocols involving BCG (Haile *et al*, 2005, Hope *et al*, 2005, Vordermeier *et al*, 2004). The results of this study further support the beneficial uses of BCG in bovine protection against *M. bovis* and the disadvantages of applying vaccines of high immunogenic capacities without a prime-boost protocol. It has also highlighted the importance of the cell mediated response and in particular IFN-γ at the site of infection within the lymph nodes, illustrating the fine balance between protection and immunopathological harm.

Chapter 7

Conclusions and Future Work

The steady increase in cases of bovine tuberculosis over the past twenty years within the United Kingdom reflects the extensive threat *M. bovis* is currently posing on a global scale. Whilst the traditional test and slaughter method, developed in the beginning of the twentieth century, has performed exceptionally well at decreasing levels of bTB across the world, the increasing importance of wild animals as natural disease reservoirs has continually undermined control efforts. Vaccination would provide a cost effective and reliable method of protection against bTB. However, as the only vaccination currently available against *M. bovis*, BCG has provided extremely variable results on its efficacy and cannot be used successfully alongside the current intradermal tests. Development of improved bTB vaccination protocols have been continually hindered by the absence of protection-specific immunological correlates (Elias *et al*, 2005, Leal *et al*, 2001).

The central aims of this study, in collaboration with the VLA (Surrey) and under the guidance of DEFRA (UK), were to:

- Provide a greater understanding of the bovine immune response (in particular IFN-γ, TNF-α, IL10 and IL4 expression) to *M. bovis* infection in a time dependent manner. This would greatly aid vaccination developmental studies as the key to an effective vaccination is in the immune profile that it elicits. However, before we use immunological status as a marker of vaccination success, it is essential that we understand which immune profiles afford the most protection against disease in the bovine model.
- Apply this new knowledge on the immune response to assess the potential protective ability of a novel BCG Pasteur vaccination. BCG Pasteur is believed to possess reduced antigenic properties due to the loss of genetic information during its production. A BCG Pasteur complement containing a *sigK* transcript from BCG Russia has been shown to display enhanced antigenic properties and therefore may provide a relatively higher level of protection against *M. bovis* as compared to the original BCG Pasteur strain.

The key findings that have emerged from this present study are:

- The influential role of IL10 as a constituent of the bovine immune response to *M. bovis* infection. The significant decrease in IL10 expression observed five weeks post infection (within the BCG vaccination study) has been reported previously (Thacker *et al*, 2007). However, by analysing the expression over five, twelve and nineteen weeks

of infection, this study has provided a novel view of IL10 at the site of *M. bovis* infection. The significant increase in IL10 expression after twelve weeks of infection in parallel to a sustained level of IFN-γ expression reflects the hosts endeavour to reduce the pathological damage associated with intense pro-inflammatory immune profiles.

Thus the two lymph node types (caudal mediastinal and cranial tracheobronchial) that displayed significantly lower levels of IFN-γ and as a result, IL10 represented a larger component of the immune profile, also had the lowest levels of pathology.

The ability of CD4+ T cells to produce both IFN-γ and IL10 has been described in human tuberculosis (Gerosa *et al*, 1999) and more recently for *Leishmania* infection in mice (Anderson *et al*, 2007). However, this study is the first to reveal the 'self-limiting' mechanism in cattle, particularly in association with *M. bovis* infection. IFN-γ levels are routinely measured as a correlate of infection and to predict the protective efficacy of vaccination, although the reliability of this has been questioned. These results indicate the importance of IL10 in the progression of the disease and therefore suggest that, if measured alongside IFN-γ, IL10 would provide much more detail on *M. bovis* infection.

- This study is the first to assess the protective efficacy of a *sigK* complemented BCG Pasteur in a bovine vaccination and *M. bovis* infection model. As previously mentioned, the ability of a vaccine to protect a host against infection is based entirely on the immune response and resultant memory T cell population that it elicits. Therefore, it was hypothesised that by enhancing the antigenic properties of the vaccine, the heightened immune response induced would result in a higher level of protection against subsequent infection. The data from this study did not support the hypothesis, as the cattle vaccinated with the modified sigK vaccination displayed increased IFN-γ expression levels and higher levels of lymph node pathology as compared to the animals vaccinated with the standard BCG. It was suggested that a heightened immune profile in response to vaccination may prove detrimental to the host, as the host acts to remove the foreign bodies at a much faster rate, affecting the size of the memory T cell population. Following infection, the smaller memory T cell population is not able to react as quickly and therefore the disease is able to progress further. This study supports the development of prime-boost vaccination protocols, in which the immune responses are stimulated twice to enhance the memory T cell population.

The comprehensive nature of this thesis was enhanced by the number of similarities between both the time course and BCG vaccination studies. Analysis was focused on the same lymph node types within cattle infected with similar concentrations of *M. bovis* for five weeks (in addition to twelve and nineteen weeks for the time course study). The same primer sets and standard curves were also applied to each of the studies targeting IFN-γ, TNF-α, IL10 and IL4 expression levels. The major difference between the two studies was the use of formalin fixed tissues (time course study) and freshly dissected tissues (BCG vaccination study) however due to tissue availability this was an unavoidable aspect of this thesis. Nevertheless, both studies produced some very interesting and comparable themes.

Cytokine analysis of cattle lymph nodes within both the time course and the BCG vaccination studies displayed a prominent cell mediated immune response five weeks following infection. There was a significantly lower level of IL10 expression at five weeks post infection compared to twelve weeks within the time course study, suggestive of the suppressive influence of IFN-γ. This data set was complimented by the significant reduction in IL10 expression and significant increase in IFN-γ in the infected compared to the non-infected group of the BCG vaccination study, also taken after five weeks of infection. In addition, IL4 expression was undetectable in both studies within the infected cattle, as compared to the detectable levels obtained from the non-infected cattle within the BCG vaccination study. Collectively, this data presents a strong case for the dominance of a cell mediated immune profile in response to infection, displaying characteristically high levels of pro-inflammatory T_H1 type cytokines such as IFN-γ and subsequent suppression of anti-inflammatory T_H2 associated cytokines such as IL4. This immune profile has been described previously (Welsh *et al*, 2005, Widdison *et al*, 2006).

Another common theme in the cytokine analysis was the positive relationships revealed between IL10 and TNF-α expression as well as between TNF-α and IFN-γ levels (Figures 23 and 40). The relationship between IL10 and TNF-α was difficult to explain as IL10 is believed to have a negative effect on TNF-α production (Fratazzi *et al*, 1999) and therefore this data may be reflective of the posttranscriptional regulation of both of these cytokines. This was further supported by the lack of difference in TNF-α mRNA expression between the two pathologically distinct lymph node types of the time course study (high vs. low pathology) and also between the five treatment groups of the BCG vaccination investigation. Consequently, comparison of the TNF-α mRNA and protein data of the BCG vaccination study yielded a non-significant correlation (Figures 46 and 47). These results highlight the importance of posttranscriptional regulation of cytokines and should be taken into consideration when solely analysing mRNA expression.

The comparison between the whole blood IFN-γ and the lymph node IFN-γ data also revealed some interesting similarities between the two studies. The whole blood IFN-γ results did not reflect the differences in expression between the experimental groups to the same extent as was seen within the lymph nodes. The time course whole blood stimulated with PPD-B results showed no difference in IFN-γ expression over the nineteen week period whereas the lymph node results suggested a change over time (Figure 26). Similarly, the BCG vaccination whole blood stimulated with PPD-B results did not show any difference between the two vaccination types, although did show an increase in the non-vaccinated infected cattle (Figure 52). This would suggest that the precise changes observed within the lymph nodes were not reflected in the whole blood of the host, as has been suggested by others (Barnes *et al*, 1993 and Coussens *et al*, 2004). In addition to this, the time course study displayed a lack of correlation between the whole blood IFN-γ protein and lymph node IFN-γ mRNA expression levels and this was also seen for the BCG vaccination study. However, the BCG vaccination study did display a positive correlation between the whole blood and lymph node IFN-γ protein levels, reiterating the potential consequences of analysing mRNA levels separate to protein.

When interpreting the data from the time course and BCG vaccination studies, it is extremely important to consider the knowledge gained from the two supplementary studies (chapters 4 and 5). The time course study used lymph node tissues fixed in formalin from the experimental archives at the VLA (Surrey). Unfortunately it took an extremely large quantity of tissue samples to obtain sufficient concentrations of total RNA for the subsequent qPCR experiments, thus severely depleting the archival sources. A novel fixative, HOPE, was compared for its ability to preserve total RNA to a higher quality and the results indicated that its performance was superior to that of formalin fixative (chapter 4). By conserving the integrity of the nucleic acid, smaller quantities of the starting tissue could be used to produce sufficient concentrations of RNA for qPCR. The VLA has now started to routinely fix tissue samples in HOPE due to these results. The impact that this supplementary study has on the time course is evident, as it confirmed that formalin does lead to RNA degradation and therefore the cytokine expression levels observed may differ from that which may have been observed if fresh lymph node tissue was used. However, this does not mean that the key concepts revealed by the time course study should be dismissed, as many of the themes observed were also reflected in the BCG vaccination study using fresh tissue. It would suggest that the quantified cytokine expression levels measured may be lower than the natural system due to the influence of the formalin

fixative and therefore further studies would need to be performed on either HOPE-fixed or fresh lymph node tissues.

The second supplementary study (chapter 5) was performed to investigate the affect of *M. bovis* infecting dose on the cytokine expression levels within the bovine lymph nodes. In the past, bovine infection models have regularly used considerably larger doses of *M. bovis* so as to ensure that the animal successfully displayed pathological disease. However, studies have shown that a host need only inhale one to two bacterial cells to become infected (Schafer *et al*, 1999) and that maybe experimental models are not true representatives of natural disease. By measuring cytokine expression in cattle infected with increasing doses of *M. bovis*, it was revealed that the immune response increased as infecting dose increased (chapter 5, Table 22). This would suggest that the cytokines levels observed within experimental infection models do not truly reflect the natural disease, as they are likely to be higher in expression level. However, the patterns in cytokine expression were very similar between the different dosages. The conclusion from this study is that, although the cytokine levels may be higher, the immune profiles remain unchanged and thus experimental bovine models are still able to provide extremely useful data that would not be available from naturally infected cattle. Considering the immense costs associated with the infection and accommodation of larger animals such as cattle and also the ethical issues, it is probably more viable to use higher doses of *M. bovis* as this ensures that cattle display pathological disease. The risk of using smaller doses is that the cattle will effectively eradicate the infection and therefore not provide useful experimental data. This would then require a larger number of cattle to be infected to ensure that the investigation could be completed and thus larger doses of *M. bovis* would be justified.

Finally, the dominant theme repeated throughout both the time course study and the BCG vaccination study was the powerful influence and importance of IFN-γ in the immune response against *M. bovis*. Levels of IFN-γ expression displayed a significant division between the lymph node types displaying high levels of pathology (high IFN-γ) and those displaying low pathology (low IFN-γ) within the time course study. Similarly, the BCG Pasteur vaccinated animals produced a dampened IFN-γ response post challenge and simultaneously displayed lower levels of pathological disease as compared to the non-vaccinated infected animals. The varying levels of IFN-γ observed are believed to be a consequence of differing bacterial burdens, as portrayed within the supplementary study 2 (Boddu-Jasmine *et al*, 2008). Previous studies (Ly *et al*, 2007, Griffin *et al*, 2006b, Mischenka *et al*, 2002) have suggested that higher

levels of bacterial burden in the hosts lungs and lymph nodes were due to the specific route of bacilli dissemination. It may therefore be hypothesised that the contrasting levels of IFN-γ observed within the different lymph node types may be due to some lymph nodes becoming infected before others and thereby displaying increased bacterial loads. Similarly, BCG vaccinated challenged cattle have been shown to display reduced levels of bacterial load as compared to non-vaccinated infected animals (Lyashchenko, *et al*, 2004, Johnson *et al*, 2006) alongside decreased levels of IFN-γ expression (Widdison *et al*, 2006, Waters *et al*, 2007, Buddle *et al*, 1995). This has been directly linked to a reduction in both disease severity and bacterial dissemination (Waters *et al*, 2007). Both of these studies therefore highlight the fine line between immune-induced protection and immune-induced pathology. Vaccination prior to challenge allows the cell mediated immune response to react quickly to the invading bacilli, subsequently controlling both the infection and level of IFN-γ (Hope *et al*, 2005). Unfortunately, despite the integral role of IFN-γ in the infection process and its potential use as a correlate of protection, numerous studies have shown that it is an unreliable indicator of the effectiveness of vaccination pre-challenge (Elias *et al*, 2005, Leal *et al*, 2001). The discovery of new potential correlates of protection, such as CD4+ T cells specific to the *M. tuberculosis* antigen TB10.4 (Hervas-Stubbs *et al*, 2006) will better aid future vaccination studies. Until a more effective correlate is found, IFN-γ expression remains a crucial immunological marker of the activated cell mediated response post vaccination and a useful method to prioritise further challenge experiments (Vordermeier *et al*, 2006).

Future work

As previously mentioned the immune response to *M. bovis* infection is extremely dynamic and involves numerous different molecular components. The four cytokines studied (IFN-γ, TNF-α, IL10 and IL4) are particularly useful in representing various immunological profiles (pro- and anti-inflammatory, regulatory T cells). However, the work could be extended to include additional immunological markers to better enhance the knowledge gained on *M. bovis* infection and BCG vaccination. Analysis of the cytokine IL12 would further support the hypothesis of a strong cell mediated response early in infection (Trinchieri, 2003, Szabo *et al*, 1997) accompanied by the study of tumour growth factor (TGF-) β which has been shown to be dominantly expressed in advanced stages of infection (Bai *et al*, 2004). Analysis of cell types such as macrophages, T cells and dendritic cells coupled with cytokine protein levels in a multiplex immune-staining method would allow an understanding of which cells dominate in expressing IFN-γ post challenge and vaccination. An inclusive and comprehensive picture of the host immune response post BCG vaccination and *M. bovis* challenge would be invaluable for future vaccination experiments.

An important aspect of cytokine analysis highlighted by both studies is the need to take into consideration posttranscriptional controls. The expression levels of mRNA may not be directly representational of the levels of cytokine protein. Therefore studying mRNA expression exclusively may not reflect significant changes in protein levels and would not correlate with immunological features such as associated pathology. In future studies, it would be advantageous to include both mRNA and protein analysis accompanied by the study of *M. bovis* bacterial loads within the isolated lymph nodes.

To improve upon the time course study, it may be beneficial to include time points prior to five weeks of infection. Published studies have shown the immune response to be detectable as early as two-three weeks post infection (Thacker *et al*, 2007, Hanna *et al*, 1989, Palmer *et al*, 2007) and an early cell mediated immune response (prior to four weeks following challenge) to be particular effective in vaccinated animals (Hope *et al*, 2005). Thacker *et al* (2007) found cytokine levels to significantly correlate with pathological levels at thirty days post infection however this relationship was not detected at later time points. The authors suggested that infected cattle should be studied during the first four to six weeks following infection to provide the most useful information.

The BCG Pasteur vaccination study confirmed previous reports on its protective efficacy against *M. bovis* infection (Widdison *et al*, 2006, Wedlock *et al*, 2007, Hope *et al*, 2005, Vordermeier *et al*, 2002, Ng *et al*, 1995). However, the genetically recombinant BCG (*sigK*) Pasteur vaccine displaying a broader antigen repertoire did not perform to the same standard as the wild-type BCG Pasteur. It was hypothesised that this drop in protection may be linked to a lower number of differentiated memory T cells. Future studies could extend this work by analysing memory T cell populations post vaccination with the recombinant BCG (*sigK*) Pasteur to confirm this hypothesis.

Ultimately it is becoming more apparent that the main method of future vaccinations against tuberculosis will be based on heterologous prime-boost protocols involving BCG (Wedlock *et al*, 2005, Vordermeier *et al*, 2006). Increasing the antigen repertoire of the vaccination protocol to increase immune stimulation may play a crucial role in this.

References

Abbas, A. K., Murphy, K. M., Sher, A. (1996) Functional diversity of helper T lymphocytes. *Nature.* **383**: 787

Ahmed, F. E., James, S. I., Lysle, D. T., Dobbs, L. J. Jr., Johnke, R. M., Flake, G., Stockton, P., Sinar, D. R., Naziri, W., Evans, M. J., Kovacs, C. J., Allison, R. R. (2004) Improved methods for extracting RNA from exfoliated human colonocytes in stool and RT-PCR analysis. *Digestive Diseases and Science*. **49** (11-12): 1889-98

Akbari, O., DeKruyff, R. H., Umetsu, D. T. (2001) Pulmonary dendritic cells producing IL10 mediate tolerance induced by respiratory exposure to antigen. *Natural Immunology*. **2** (8): 725-31

Algood, H. M., Chan, J., Flynn, J. L. (2003) Chemokines and tuberculosis. *Cytokine Growth Factor Review*. **14** (6): 467-77

Anderson, C. F., Mendez, S., Sacks, D. L. (2005) Nonhealing infection despite Th1 polarization produced by a strain of *Leishmania major* in C57BL/6 mice. *Journal of Immunology*. **174** (5): 2934-41

Anderson, C. F., Oukka, M., Kuchroo, V. J., Sacks, D. (2007) CD4(+) CD25(-) Foxp3(-) Th1 cells are the source of IL10 mediated immune suppression in chronic cutaneous leishmaniasis. *Journal of Experimental Medicine*. **204** (2): 285-97

Aranaz, A., Liebana, E., Gomez-Mampaso, E., Galan,J. C., Cousins, D., Ortega, A., Blazquez, ,J., Baquero, F., Mateos, A., Suarez, G., Dominquez, L. (1999) *Mycobacterium tuberculosis* subsp. *caprae* subsp. nov.: a taxonomic study of a new member of the *Mycobacterium tuberculosis* complex isolated from goats in Spain. *International Journal of Systematic Bacteriology*. **49**: 1263-73

Armstrong, J. A., Hart, P. D. (1971) Response of cultured macrophages to *Mycobacterium tuberculosis*, with observations on fusion of lysosomes with phagosomes. *Journal of Experimental Medicine*. **134** (3): 713-740

Armstrong, J. A., Hart, P. D. (1975) Phagosome-lysosome interactions in cultured macrophages infected with virulent tubercle bacilli. Reversal of the usual nonfusion pattern and observations on bacterial survival. *Journal of Experimental Medicine*. **142** (1): 1-16

Asselineau, J., Lederer, E. (1950) Structure of the mycolic acids of Mycobacteria. *Nature*. **166** (4227): 782-3

Atamas, S. P., Choi, J., Yurovsky, V. V., White, B. (1996) An alternative splice variant of human IL4, IL4 delta 2, inhibits IL4 stimulated T cell proliferation. *Journal of Immunology*. **156** (2): 435-41

Atamas, S. P., Yurovsky, V. V., Wise, R., Wigley, F. M., Goter Robinson, C. J., Henry, P., Alms, W. J., White, B. (1999) Production of type 2 cytokines by CD8+ lung cells is associated with greater decline in pulmonary function in patients with systemic sclerosis. *Arthritis and rheumatism*. **42** (6): 1168-78

Aung, H., Toossi, Z., McKenna, S. M., Gogate, P., Sierra, J., Sada, E., Rich, E. A. (2000) Expression of transforming growth factor beta but not tumour necrosis factor alpha, interferon gamma and interleukin 4 in granulomatous lung lesions in tuberculosis. *Tubercle and Lung Disease: the official journal of the International Union against Tuberculosis and Lung disease*. **80** (2): 61-7

Aurtenetxe, O., Barral, M., Vicente, J., la Fuente, J., Gortazar, C., Juste, R. A. (2008) Development and validation of an enzyme-linked immunosorbent assay for antibodies against *Mycobacterium bovis* in European Wild boar. *BMC Veterinary Research*. **4**: 43

Ayele, W. Y., Neill, S. D., Zinsstag. J., Weiss, M. J., Pavlik, I. (2004) Bovine tuberculosis: an old disease but a new threat to Africa. *Tubercle and Lung Disease*. **8**: 924-937

Bai, X., Wilson, S. E., Chmura, K., Feldman, N. E., Chan, E. D. (2004) Morphometric analysis of Th (1) and Th (2) cytokine expression in human pulmonary tuberculosis. *Tuberculosis (Edinb)*. **84** (6): 375-85

Balcewicz-Sablinska, M. K., Gan, H., Remold, H. G. (1999) Interleukin 10 produced by macrophages inoculated with *Mycobacterium avium* attenuates mycobacteria-induced apoptosis by reduction of TNF-alpha activity. *The Journal of Infectious Diseases*. **180** (4): 1230-7

Balcewicz-Sablinska, M. K., Keane, J., Kornfeld, H., Remold, H. G. (1998) Pathogenic *Mycobacterium tuberculosis* evades apoptosis of host macrophages by release of TNF-R2, resulting in inactivation of TNF-alpha. *Journal of Immunology*. **161** (5): 2636-41

Barnes, P. F., Lu, S., Abrams, J. S., Wang, E., Yamamura, M., Modlin, R. L. (1993) Cytokine production at the site of disease in human tuberculosis. *Infection and Immunity*. **61**: 3482-9

Barnes, P. F., Modlin, R. L., Ellner, J. J. (1994) T-cell responses and cytokines. In Tuberculosis: Pathogenesis, Protection and Control. Ed. Bloom. B.R. *American Society for Microbiology*, Washington, D. pp. 417

Barrat, F. J., Cua, D. J., Boonstra, A., Richards, D. F., Crain, C., Savelkoul, H. F., de Waal-Malefyt, R., Coffman, R. L., Hawrylowicz, C. M. (2002) In vitro generation of interleukin 10-producing regulatory CD4(+) T cells is induced by immunosuppressive drugs and inhibited by T helper type 1 (Th1) and Th2-inducing cytokines. *The Journal of Experimental Medicine*. **195** (5): 603-16

Baseggio, L. Charlot, C., Bienvenu, J., Felman, P., Salles, G. (2002) Tumour necrosis factor-alpha mRNA stability in human peripheral blood cells after lipopolysaccharide stimulation. *European Cytokine Network*. **13** (1): 92-8

Behr, M. A. (2002) BCG - different strains, different vaccines? *Lancet Infection and Disease*. **2**: 86-92

Bekker, L. G., Moreira, A. L., Bergtold, A., Freeman, S., Ryffel, B., Kaplan, G. (2000) Immunopathologic effects of tumour necrosis factor alpha in murine mycobacterial infection are dose dependent. *Infection and Immunity*. **68** (12): 6954-61

Belkaid, Y., Hoffmann, K. F., Mendez, S., Kamhawi, S., Udey, M. C., Wynn, T. A., Sacks, D. L. (2001) The role of interleukin (IL) 10 in the persistence of *Leishmania major* in the skin after healing and the therapeutic potential of anti-IL10 receptor antibody for sterile cure. *The Journal of Experimental Medicine*. **194** (10): 1497-506

Bendelac, A., Schwartz, R. H. (1991) CD4+ and CD8+ T cells acquire specific lymphokine secretion potentials during thymic maturation. *Nature*. **353** (6339): 68-71

Beutler, B., Cerami, A. (1989) The biology of cachectin/TNF-a primary mediator of the host response. *Annual Review of Immunology*. **7**: 625-55

Bhatt, K., Hickman, S. P., Salgame, P. (2004) Cutting edge: a new approach to modelling early lung immunity in murine tuberculosis. *Journal of Immunology*. **172** (5): 2748-51

Bhudevi, B, Weinstock, D. (2003) Detection of bovine viral diarrhoea virus in formalin fixed paraffin embedded tissue sections by real time RT-PCR (taqman). *Journal of Virology Methods*. **109** (1): 25-30

Black, R. A., Rauch, C. T., Kozlosky, C. J., Peschon, J. J., Slack, J. L., Wolfson, M. F., Castner, B. J., Stocking, K. L., Reddy, P., Srinivasan, S., Nelson, N., Boiani, N., Schooley, K. A., Gerhart, M., Davis, R., Fitzner, J. N., Johnson, R. S., Paxton, R. J., March, C. J., Cerretti, D. P. (1997) A metalloproteinase disintegrin that releases tumour-necrosis factor-alpha from cells. *Nature*. **385** (6618): 729-33

Blow, J. A., Mores, C. N., Dyer, J., Dohm, D. J. (2008) Viral nucleic acid stabilization by RNA extraction reagent. *Journal of Virological Methods*. **150** (1-2): 41-4

Boddu-Jasmine, H. C., Witchell, J., Vordermeier, M., Wangoo, A., Goyal, M. (2008) Cytokine mRNA expression in cattle infected with different dosages of *Mycobacterium bovis*. *Tuberculosis*. **88** (6): 610-5

Bodnar, K. A., Serbina, N. V., Flynn, J. L. (2001) Fate of *Mycobacterium tuberculosis* within murine dendritic cells. *Infection and Immunity*. **69** (2): 800-9

Bogdan, C., Vodovotz, Y., Nathan, C. (1991) Macrophages deactivation by interleukin 10. *The Journal of Experimental Medicine*. **174** (6): 1549-55

Brightbill, H. D., Libraty, D. H., Krutzik, S. R., Yang, R. B., Belisle, J. T., Bleharski, J. R., Maitland, M., Norgard, M. V., Plevy, S. E., Smale, S. T., Brennan, P. J., Bloom, B. R., Godowski, P. J., Modlin, R. L. (1999) Host defence mechanisms triggered by microbial lipoproteins through toll-like receptors. *Science*. **285** (5428): 732-6

Brightbill, H. D., Plevy, S. E., Modlin, R. L., Smale, S. T. (2000) A prominent role for Sp1 during lipopolysaccharide-mediated induction of the IL-10 promoter in macrophages. *Journal of Immunology*. **164** (4): 1940-51

Brosch, R., Gordon, S. V., Garnier, T., Eiglmeier, K., Frigui, W., Valenti, P., Dos Santos, S., Duthoy, S., Lacroix, C., Garcia-Pelayo, C., Inwlad, J. K., Golby, P., Garcia, J. N., Hewinson, R. G., Behr, M. A., Quail, M. A., Churcher, C., Barrell, B. G., Parkhill, J., Cole, S.T. (2007) Genome plasticity of BCG and impact on vaccine efficacy. *Proceedings of the National Academy of Sciences of the USA.* **104** (13): 5596-601

Brosch, R., Gordon, S. V., Marmiesse, M., Brodin, P., Buchrieser, C., Eiglmeier, K., Garnier, T., Gutierrez, C., Hewinson, G., Kremer, K., Parsons, L. M., Pym, A. S., Samper, S., van Soolingen, D., Cole, S. T. (2002) A new evolutionary scenario for the *Mycobacterium tuberculosis* complex. *Proceedings of the National Academy of Sciences of the USA*. **99** (6): 3684-9

Brosch, R., Pym, A. S., Gordon, S. V., Cole, S. T (2001) The evolution of mycobacterial pathogenicity: clues from comparative genomics. *Trends in Microbiology*. **9** (9): 452-8

Buddle, B. M. (2001) Vaccination of cattle against *Mycobacterium bovis*. *Tuberculosis (Edinb).* **81** (1-2): 125-32

Buddle, B. M., de Lisle, G. W., Pfeffer, A., Aldwell, F. E. (1995) Immunological responses and protection against *Mycobacterium bovis* in calves vaccinated with a low does of BCG. *Vaccine*. **13** (12): 1123-30

Buddle, B. M., McCarthy, A. R., Ryan, T. J., Pollock, J. M., Vordermeier, H. M., Hewinson, R. G., Andersen, P., de Lisle, G. W. (2003) Use of mycobacterial peptides and recombinant proteins for the diagnosis of bovine tuberculosis in skin test-positive cattle. *The Veterinary Record*. **153** (20): 615-20

Buddle, B. M., Parlane, N. A., Keen, D. L., Aldwell, F. E., Pollock, J. M., Lightbody, K., Andersen, P. (1999) Differentiation between *Mycobacterium bovis* BCG-vaccinated and *M. bovis*-infected cattle by using recombinant mycobacterial antigens. *Clinical and Diagnostic Laboratory Immunology*. **6** (1): 1-5

Buddle, B. M., Wedlock, D. N., Denis, M., Skinner, M. A. (2005) Identification of immune response correlates for protection against bovine tuberculosis. *Veterinary Immunology and Immunopathology*. **108** (1-2): 45-51

Bustin, S. A. (2002) Quantification of mRNA using real time reverse transcription PCR (RT-PCR): trends and problems. *Journal of Molecular Endocrinology*. **29**: 23-29

Bustin, S. A., Mueller, R. (2006) Real-time reverse transcription PCR and the detection of occult disease in colorectal cancer. *Molecular Aspects of Medicine*. **27** (2): 192-223

Bustin, S. A., Nolan, T. (2004) Pitfalls of quantitative real-time reverse-transcription polymerase chain reaction. *Journal of Biomolecular Techniques*. **15** (3): 155-66

Caffrey, J. P. (1994) Status of bovine tuberculosis eradication programmes in Europe. *Veterinary Microbiology*. **40** (1-2): 1-4

Campbell, J. J., Murphy, K. E., Kunkel, E. J., Brightling, C. E., Soler, D., Shen, Z., Boisvert, J., Greenberg, H. B., Vierra, M. A., Goodman, S. B., Genovese, M. C., Wardlaw, A. J., Butcher, E. C., Wu, L. (2001) CCR7 expression and memory T cell diversity in humans. *Journal of Immunology*. **166** (2): 877-84

Carr, M. D., Bloemink, M. J., Dentten, E., Whelan, A. O., Gordon, S. V., Kelly, G., Frenkiel, T. A., Hewinson, R. G., Williamson, R. A. (2003) Solution structure of the *Mycobacterium tuberculosis* complex protein MPB70: from tuberculosis pathogenesis to inherited human corneal disease. *The Journal of Biological Chemistry*. **278** (44): 43736-43

Cassidy, J. P., Bryson, D. G., Pollock, J. M., Evans, R. T., Forster, F., Neill, S. D. (1998) Early lesion formation in cattle experimentally infected with *Mycobacterium bovis*. *Journal of Comparative Pathology*. **119**: 27-44

Cassidy, J. P. (2006) The pathogenesis and pathology of bovine tuberculosis with insights from studies of tuberculosis in humans and laboratory animal models. *Veterinary Microbiology*. **112** (2-4): 151-61

Cassidy, J. P., Bryson, D. G., Gutierrez, Cancela, M. M., Forster, F., Pollock, J. M., Neill, S. D. (2001) Lymphocyte subtypes in experimentally induced early-stage bovine tuberculous lesions. *Journal of Comparative Pathology*. **124** (1): 46-51

Castiglione, F., Degl'Innocenti, D. R., Taddei, A., Garbini, F., Buccoliero, A. M., Raspollini, M. R., Pepi, M., Paqlierani, M., Asirelli, G., Freschi, G., Bechi, P., Taddei, G. L. (2007) Real-time PCR analysis of RNA extracted formlin-fixed and paraffin-embedded tissues: effects of the fixation on outcome reliability. *Applied Immunohistochemistry and Molecular Morphology*. **15** (3): 338-42

Cella, M., Engering, A., Pinet, V., Pieters, J., Lanzavecchia, A. (1997) Inflammatory stimuli induce accumulation of MHC class II complexes on dendritic cells. *Nature*. **388** (6644): 782-7

Chackerian, A. A., Alt, J. M., Perera, T. V., Dascher, C. C., Behar, S. M. (2002) Dissemination of *Mycobacterium tuberculosis* is influenced by host factors and precedes the initiation of T cell immunity. *Infection and Immunity*. **70** (8): 4501-9

Chan, S. H., Kobayashi, M., Santoli, D., Perussia, B., Trinchieri, G. (1992a) Mechanisms of IFN-gamma induction by natural killer cell stimulatory factor (NKSF/IL-12). Role of transcription and mRNA stability in the synergistic interaction between NKSF and IL-2. *Journal of Immunology*. **148** (1): 92-8

Chan, J., Xing, Y., Magliozzo, R. S., Bloom, B. R. (1992b) Killing of virulent *Mycobacterium tuberculosis* by reactive nitrogen intermediates produced by activated murine macrophages. *The Journal of Experimental Medicine*. **175** (4): 1111-22

Chan, J., Kauffmann, S. H. E. (1994) Immune mechanisms of protection. In Tuberculosis: Pathogenesis, Protection and Control. Ed. Bloom. B.R. *American Society for Microbiology*, Washington, D. pp. 389

Charlet, D., Mostowy, S., Alexander, D., Sit, L., Wiker, H. G., Behr, M. A. (2005) Reduced expression of antigenic proteins MPB70 and MPB83 in *Mycobacterium bovis* BCG strains due to a start codon mutation in *sigK*. *Molecular Microbiology*. **56**: 1302-1313

Cho, H., Laso, T. M., Allen, S. S., Yoshimura, T., McMurray, D. N. (2005) Recombinant guinea pig tumour necrosis alpha stimulates the expression of interleukin 12 and the inhibition of *Mycobacterium tuberculosis* growth in macrophages. *Infection and Immunity*. **73** (3): 1367-76

Chomczynski, P., Sacchi, N. (1987) Single-step method of RNA isolation by acid guanidinium thiocyanate-phenol-chloroform extraction. *Analytical Biochemistry*. **162** (1): 156-9

Choquette, L. P., Gallivan, J. F., Byrne, J. L., Pilipavicius, J. (1961) Parasites and diseases of Bison in Canada: Tuberculosis and some other pathological conditions in Bison at Wood buffalo and Elk island national parks in the fall and winter of 1959-60. *Canadian Veterinary Journal*. **2**: 168-174

Clevers, H., MacHugh, N. D., Bensaid, A., Dunlap, S., Baldwin, C. L., Kaushal, A., Iams, K., Howard, C. J., Morrison, W. I. (1990) Identification of a bovine surface antigen uniquely expressed on CD4-CD8- T cell receptor gamma/delta+ T lymphocytes. *European Journal of Immunology.* **20** (4): 809-17

Cockle, P. J., Gordon, S. V., Hewinson, R. G., Vordermeier, H. M. (2006) Field evaluation of a novel differential diagnostic reagent for detection of *Mycobacterium bovis* in cattle. *Clinical and Vaccine Immunology*. **13** (10): 1119-1124

Cockle, P. J., Gordon, S. V., Lalvani, A., Buddle, B. M., Hewinson, R. G., Vordermeier, H. M. (2002) Identification of novel *Mycobacterium tuberculosis* antigens with potential as diagnostic reagents or subunit vaccine candidates by comparative genomics. *Infection and Immunity*. **70** (12): 6996-7003

Cole, S. T, Barrell, B. G. (1998) Anaylsis of the genome of *Mycobacterium tuberculosis* H37Rv. *Novartis Foundation Symposium*. **217**: 160-72

Cools, N., Ponsaerts, P., Van Tendeloo, V. F., Berneman, Z. N. (2007) Regulatory T cells and human disease. *Clinical and Developmental Immunology*. **2007**: 89195

Corinti, S., Albanesi, C., la Sala, A., Pastore, S., Girolomoni, G. (2001) Regulatory activity of autocrine IL10 on dendritic cell functions. *Journal of Immunology*. **166** (7): 4312-8

Couper, K. N., Blount, D. G., Riley, E. M. (2008) IL10: The master regulator of immunity to infection. *The Journal of Immunology*. **180**: 5771-5777

Coussens, P. M., Verman, N., Coussens, M. A., Elftman, M. D., McNulty, A. M. (2004) Cytokine gene expression in peripheral blood mononuclear cells and tissues of cattle infected with *Mycobacterium avium* subsp. *paratuberculosis*: evidence for an inherent pro-inflammatory gene expression pattern. *Infection and Immunity*. **7**:1409-22

Dahl, K. E., Shiratsuchi, H., Hamilton, B. D., Ellner, J. J., Toossi, Z. (1996) Selective induction of transforming growth factor beta in human monocytes by lipoarabinomannan of *Mycobacterium tuberculosis*. *Infection and Immunity*. **64** (2): 399-405

Dannenberg, A. M. Jr. (1991) Delayed-type hypersensitivity and cell mediated immunity in the pathogenesis of tuberculosis. *Immunology Today*. **12**: 228-32

Davids, V., Hanekom, W. A., Mansoor, N., Gamieldien, H., Gelderbloem, S. J., Hawkridge, A., Hussey, G. D., Hughes, E. J., Soler, J., Murray, R. A., Ress, S. R., Kaplan, G. (2006) The effect of bacilli Calmette-Guérin vaccine strain and route of administration on induced immune responses in vaccinated infants. *The Journal of Infectious Diseases*. **193** (4): 531-6

Dawson, D.J. (1971) Potential pathogens among strains of mycobacteria isolated from house-dusts. *The Medical Journal of Australia*. **1** (13): 679-81

Dean, G. S., Rhodes, S. G., Coad, M., Whelan, A. O., Cockle, P. J., Clifford, D. J., Hewinson, R. G., Vordermeier, H. M. (2005) Minimum effective dose of *Mycobacterium bovis* in cattle. *Infection and Immunity*. **73** (10) 6467-71

Decker, T., Lohmann-Matthes, M. L. Gifford, G. E. (1987) Cell-associated tumour necrosis factor (TNF) as a killing mechanism of activated cytotoxic macrophages. *Journal of Immunology*. **138** (3): 957-62

DEFRA (2005a) Animal health 2004- The report of the Chief Veterinary Officer. DEFRA publications, London.

DEFRA (2005b) Government strategic framework for the sustainable control of bovine tuberculosis (bTB) in Great Britain. DEFRA publications, London

DEFRA (accessed January 2008) Animal health database (Vetnet); Detailed TB statistics for 1 January to 30 November 2007 (GB): http://www.defra.gov.uk/animalh/tb/stats/07/2007gb.pdf

Del Prete, G., De Carli, M., Almerigogna, F., Giudizi, M. G., Biagiotti, R., Romagnani, S. (1993) Human IL10 is produced by both type 1 helper (Th1) and type 2 helper (Th2) T cell clones and inhibits their antigen-specific proliferation and cytokine production. *Journal of Immunology*. **150** (2): 353-60

Delahay, R. J., Leeuw, A. N., Barlow, A. M., Clifton-Hadley, R. S., Cheeseman, C. L. (2002) The status of *Mycobacterium bovis* infection in UK wild mammals: a review. *Veterinary Journal*. **164** (2): 90-105

Demissie, A., Abebe, M., Aseffe, A., Rook, G., Fletcher, H., Zumla, A., Weldingh, K., Brock, I., Andersen, P., Doherty, T. M. (2004) Healthy individuals that control a latent infection with *Mycobacterium tuberculosis* express high levels of Th1 cytokines and the IL4 antagonist IL4delta2. *Journal of Immunology*. **172** (11): 6938-43

Denis, M., Keen, D. L., Parlane, N. A., Storset, A. K., Buddle, B. M. (2007) Bovine natural killer cells restrict the replication of *Mycobacterium bovis* in bovine macrophages and enhance IL12 release by infected macrophages. *Tuberculosis*. **87** (1): 53-62

Dick, T., Lee, B. H., Murugasu-Oei, B. (1998) Oxygen depletion induced dormancy in *Mycobacterium smegmatis*. *FEMS Microbiology Letters*. **163** (2) 159-64

Dickson, R. C. (1965) The tuberculin test. *Canadian Medical Association Journal*. **92**: 25-29

Dieu, M. C., Vanbervliet, B., Vicari, A., Bridon, J. M., Oldham, E., Ait-Yahia, S., Briere, F., Zlotnik, A., Lebecque, A., Caux, C. (1998) Selective recruitment of immature and mature dendritic cells by distinct chemokines expressed in different anatomic sites. *The Journal of Experimental Medicine*. **188** (2): 373-86

Ding, A. H., Nathan, C. F., Stuehr, D. J. (1988) Release of reactive nitrogen intermediates and reactive oxygen intermediates from mouse peritoneal macrophages. Comparison of activating cytokines and evidence for independent production. *Journal of Immunology*. **141** (7): 2407-12

Doherty, M. L., Bassett, H. F., Quinn, P. J., Davis, W. C., Kelly, A. P., Monaghan, M. L. (1996) A sequential study of the bovine tuberculin reaction. *Immunology*. **87** (1): 9-14

Doherty, M. L., Monaghan, M. L., Bassett, H. F., Quinn, P. J., Davies, W. C. (1995) Effect of dietary restriction on cell mediated immune responses in cattle infected with *Mycobacterium bovis. Veterinary Immunology and Immunopathology*. **49**: 307-20

Dokter , W. H., Esselink, M. T., Sierdsema, S. J., Halie, M. R., Vellenga, E. (1993) Transcriptional and posttranscriptional regulation of the interleukin-4 and interleukin-3 genes in human T cells. *Blood.* **81** (1): 35-40

Donnelly, C. A., Woodroffe, R., Cox, D. R., Bourne, F. J., Cheeseman, C. L., Clifton-Hadley, R. S., Wei, G., Gettinby, G., Gilks, P., Jenkins, H., Johnston, W. T., Le Fevre, A. M., McInerney, J. P., Morrison, W. I. (2006) Positive and negative effects of widespread badger culling on tuberculosis in cattle. *Nature.* **439** (7078): 843-6

Ducati, R. G., Ruffino-Netto, A., Basso, L. A., Santos, D. S. (2006) The resumption of consumption – a review on tuberculosis. *Memórias do Instituto Oswaldo Cruz*. **101** (7): 697-714

Dunn, P. L., North, R. J. (1995) Virulence ranking of some *Mycobacterium tuberculosis* and *Mycobacterium bovis* strains according to their ability to multiply in the lungs, induce pathology and cause mortality in mice. *Infection and Immunity*. **63** (9): 3428-37

Edwards, D. S., Johnston, A. M., Mead, G. C. (1997) Meat inspection: an overview of present practices and future trends. *The Veterinary Journal*. **154** (2): 135-47

Elias, D., Akuffo, H., Britton, S. (2005) PPD induced in vitro interferon gamma production is not a reliable correlate of protection against *Mycobacterium tuberculosis*. *Transactions of the Royal Society of Tropical Medicine and Hygiene*. **99** (5): 363-8

Ekdahl, M., Smith, B., Money, D. (1970) Tuberculosis in some wild and feral animals in New Zealand. *New Zealand Veterinary Journal.* **18**: 44-45

Endsley, J. J., Hogg, A., Shell, L. J., McAulay, M., Coffey, T., Howard, C., Capinos Scherer, C. F., Waters, W. R., Nonnecke, B., Estes, D. M., Villarreal-Ramos, B. (2007) *Mycobacterium bovis* BCG vaccination induces memory CD4+ T cells characterised by effector biomarker expression and anti-mycobacterial activity. *Vaccine*. **25** (50): 8384-94

Essey, M. A., Koller, M. A. (1994) Status of bovine tuberculosis in North America. *Veterinary Microbiology*. **40** (1-2): 15-22

Evans, J. T., Smith, E. G., Banerjee, A., Smith, R. M., Dale, J., Innes, J. A., Hunt, D., Tweddell, A., Wood, A., Anderson, C., Hewinson, R. G., Smith, N. H., Hawkey, P. M., Sonnenberg, P. (2007) Cluster of human tuberculosis caused by *Mycobacterium bovis*: evidence for person-to-person transmission in the UK. *Lancet.* **369** (9569): 1270-6

Fenhalls, G., Stevens, L., Bezuidenhout, J., Amphlett, G. E., Duncan, K., Bardin, P., Lukey, P. T. (2002) Distribution of IFN-gamma, IL4 and TNF-alpha protein and CD8 T cells producing IL12p40 mRNA in human lung tuberculous granulomas. *Immunology.* **105** (3): 325-35

Fenhalls, G., Wong, A., Bezuidenhout, J., van Helden, P., Bardin, P., Lukey, P. T. (2000) *In situ* production of gamma interferon, interleukin 4 and tumour necrosis factor alpha mRNA in human lung tuberculous granulomas. *Infection and Immunity*. **68** (5): 2827-36

Fiorentino, D. F., Bond, M. W., Mosmann, T. R. (1989) Two types of mouse T helper cell IV. Th2 clones secrete a factor that inhibits cytokine production by Th1 clones. *The Journal of Experimental Medicine*. **170** (6): 2081-95

Fleige, S., Pfaffl, M. W. (2006) RNA integrity and the effect on the real-time qRT-PCR performance. *Molecular Aspects of Medicine.* **27**: 126-139

Fleming, A. (1922) On a remarkable bacteriolytic element found in tissues and secretions. *Proceedings of the Royal Society of London. Series B, containing papers of a Biological character. Royal Society (Great Britain).* **93**: 306-317

Flynn, J. L., Chan, J. (2001) Immunology of tuberculosis. *Annual Review of Immunology*. **19**: 93-129

Flynn, J. L., Chan, J. (2005) What's good for the host is good for the bug. *Trends in Microbiology*. **13** (3): 98-102

Francis, J. (1947) Bovine tuberculosis. Staples Press, London.

Francis, J. (1958) A study of Tuberculosis in animals and man. Cassell, London.

Fratazzi, C., Arbeit, R. D., Carini, C., Balcewicz-Sablinska, M. K., Keane, J., Kornfeld, H., Remold, H. G. (1999) Macrophage apoptosis in mycobacterial infections. *Journal of Leukocyte Biology*. **66** (5): 763-4

Frothingham, R., Hills, H. G., Wilson,K. H. (1994) Extensive DNA sequence conservation throughout the *Mycobacterium tuberculosis* complex. *Journal of Clinical Microbiology*. **32** (7): 1639-43

Fu, Y., Chaplin, D. D. (1999) Development and maturation of secondary lymphoid tissues. *Annual Review of Immunology*. **17**: 399-433

Gagliardi, M. C., Teloni, R., Giannoni, F., Pardini, M., Sargentini, V., Brunori, L., Fattorini, L., Nisini, R. (2005) *Mycobacterium bovis* Bacillus Calmette-Guerin infects DC-SIGN dendritic cell and causes the inhibition of IL-12 and the enhancement of IL-10 production. *Journal of Leukocyte Biology*. **78** (1): 106-13

Gagliardi, M. C., Teloni, R., Mariotti, S., Iona, E., Pardini, M., Fattorini, L., Orefici, G., Nisini, R. (2004) Bacillus Calmette-Guérin shares with virulent *Mycobacterium tuberculosis* the capacity to subvert monocyte differentiation into dendritic cell: implication for its efficacy as a vaccine preventing tuberculosis. *Vaccine*. **22** (29-30): 3848-57

Gannon, B. W., Hayes, C. M., Roe, J. M. (2007) Survival rate of airborne *Mycobacterium bovis*. *Research in Veterinary Science*. **82** (2): 169-172

Ganz, T. (2002) Epithelia: Not just physical barriers. *Proceedings of the National Academy of Sciences of the USA*. **99** (6): 3357-3358

Garnier, T., Eiglmeier, K., Camus, J. C., Medina, N., Mansoor, H., Pryor, M., Duthoy, S., Grondin, S., Lacroix, C., Monsempe, C., Simon, S., Harris, B., Atkin, R., Doggett, J., Mayes, R., Keating, L., Wheeler, P. P., Parkhill, J., Barrell, B. G., Cole, S. T., Gordon, S. V., Hewinson, R. G. (2003) The complete genome sequence of *Mycobacterium bovis*. *Proceedings of the National Academy of Sciences of the USA*. **100** (3): 7877-82

Garraud, O., Nkenfou, C., Bradley, J. E., Nutman, T. B. (1996) Differential regulation of antigen-specific IgG4 and IgE antibodies in response to recombinant filarial proteins. *International Immunology*. **8** (12): 1841-8

Gazzinelli, R. T., Oswald, I. P., James, S. L., Sher, A. (1992) IL10 inhibits parasite killing and nitrogen oxide production by IFN gamma activated macrophages. *Journal of Immunology*. **148** (6): 1792-6

Gazzinelli, R. T., Wysocka, M., Hayashi, S., Denkers, E. Y., Hieny, S., Caspar, P., Trinchieri, G., Sher, A. (1994) Parasite-induced IL-12 stimulates early IFN-gamma synthesis and resistance during acute infection with *Toxoplasma gondii*. *Journal of Immunology*. **153** (6): 2533-43

Geppert, T. D., Whitehurst, C. E., Thompson, P., Beutler, B. (1994) Lipopolysaccharide signals activation of tumour necrosis factor biosynthesis through the ras/raf-1/MEK/MAPK pathway. *Molecular Medicine*. **1** (1): 93-103

Gerosa, F., Nisii, C., Righetti, S., Micciolo, R., Marchesini, M., Cazzadori, A., Trinchieri, G. (1999) CD4(+) T cell clones producing both interferon gamma and interleukin 10 pre-dominate in bronchoalveolar lavages of active pulmonary tuberculosis patients. *Clinical Immunology*. **92** (3): 224-34

Gilbert, M.T., Haselkom, T., Bunce, M., Sanchez, J.J., Lucas, S.B., Jewell, L.D., Van Marck, E., Worobey, M. (2007) The isolation of nucleic acids from fixed, paraffin embedded tissues – which methods are useful when? *PLoS ONE*. **2** (6): 537

Gilleron, M., Nigou, J., Nicolle, D., Quesniaux, V., Puzo, G. (2006) The acylation state of mycobacterial lipomannans modulates innate immunity response through toll-like receptor 2. *Chemistry and Biology*. **13**: 39-47

Giri, P. K., Verma, I., Khuller, G. K. (2006) Protective efficacy of intranasal vaccination with *Mycobacterium bovis* BCG against airway *Mycobacterium tuberculosis* challenge in mice. *The Journal of Infection*. **53** (5): 350-6

Goldmann, T., Burgemeister, R., Sauer, U., Loeschke, S., Lang, D. S., Branscheid, D., Zabel, P., Vollmer, E. (2006) Enhanced molecular analyses by combination of the HOPE- technique and laser microdissection. *Diagnostic Pathology*. **1**: 2

Goldmann, T., Olert, J. (Accessed 2008) Welcome to HOPE fixation: www.hope-fixation.com/index.html

Goldsby, R. A., Kindt, T. J., Kuby, B. A., Osborne, B. A. (2003) Immunology: fifth edition. WH Freeman and Co.

Gonzalez-Juarrero, M., Orme, I. M. (2001) Characterisation of murine lung dendritic cells infected with *Mycobacterium tuberculosis. Infection and Immunity*. **69** (2): 1127-33

Goodchild, A. V., Clifton-Hadley, R. S. (2001) Cattle-to-cattle transmission of *Mycobacterium bovis*. *Tuberculosis*. **81** (1/2): 23-41

Gortazar, C., Vicente, J., Gavier-Widen, D. (2003) Pathology of bovine tuberculosis in the European wild boar (*Sus scrofa*). *Veterinary Record*. **152** (25): 779-80

Goslee, S., Wolinsky, E. (1976) Water as a source of potentially pathogenic mycobacteria. *The American Review of Respiratory Disease*. **113** (3): 287-92

Grange, J. M. (1987) Infection and disease due to the environmental mycobacteria. *Transactions of the Royal Society of Tropical Medicine and Hygiene*. **81** (2):179-82

Green, L. E., Cornell, S. J. (2005) Investigations of cattle herd breakdowns with bovine tuberculosis in four counties of England and Wales using VETNET data. *Preventive Veterinary Medicine*. **70** (3-4): 293-311

Griffin, J. F., Mackintosh, C. G., Rodgers, C. R. (2006a) Factors influencing the protective efficacy of a BCG homologous prime-boost vaccination regime against tuberculosis. *Vaccine*. **24** (6): 835-45

Griffin, J. F., Rodgers, C. R., Liggett, S., Mackintosh, C. G. (2006b) Tuberculosis in ruminants: characteristic of intra-tonsilar *Mycobacterium bovis* infection models in cattle and deer. *Tuberculosis (Edinb).* **86** (6): 404-18

Grohmann, U., Belladonna, M. L., Bianchi, R., Orabona, C., Ayroldi, E., Fioretti, M. C., Puccetti, P. (1998) IL-12 acts directly on DC to promote nuclear localisation of NF-kappaB and primes DC for IL-12 production. *Immunity*. **9** (3): 315-23

Groux, H., Bigler, M., de Vries, J. E., Roncarolo, M. G. (1998) Inhibitory and stimulatory effects of IL-10 on human CD8+ T cells. *Journal of Immunology*. **160** (7): 3188-93

Guerkov, R. E., Tarqoni, O. S., Kreher, C. R., Boehm, B. O., Herrera, M. T., Tary-Lehmann, M., Lehmann, P. V., Schwander, S. K. (2003) Detection of low-frequency antigen-specific IL10- producing CD4(+) T cells via ELISPOT in PBMC: cognate vs. non-specific production of the cytokine. *Journal of Immunological Methods*. **279** (1-2): 111-21

Haile, M., Hamasur, B., Jaxmar, T., Gavier-Widen, D., Chambers, M. A., Sanchez, B., Schroder, U., Kallenius, G., Svenson, S. B., Pawlowski, A. (2005) Nasal boosting with adjuvanted heat-killed BCG or arabinomannan-protein conjugate improves BCG-induced protection in C57BL/6 mice. *Tuberculosis (Edinb).* **85** (1-2): 107-14

Hamerman, J. A., Ogasawara, K., Lanier, L. L. (2005) NK cells in innate immunity. *Current Opinion in Immunology*. **17** (1): 29-35

Hanna, J., Neill, S. D., O'Brien, J. J. (1989) Use of PPD and phosphatide antigens in an ELISA to detect the serological response in experimental bovine tuberculosis. *Research in Veterinary Science*. **47** (1): 43-7

Harboe, M., Nagai, S. (1984) MPB70, a unique antigen of *Mycobacterium bovis* BCG. *The American Review of Respiratory Disease.* **129**: 444-452

Hart, P. D., Sunderland, I., Thomas, J. (1967) The immunity conferred by effective BCG and vole bacillus vaccines, in relation to individual variations in induced tuberculin sensitivity and to technical variations in the vaccines. *Tubercle.* **48**: 201-210

Hein, W. R., Mackay, C. R. (1991) Prominence of gamma delta T cells in the ruminant immune system. *Immunology Today*. **12** (1): 30-4

Hernandez-Pando, R., Orozco, H., Arriaga, K., Sampieri, A., Larriva-Sahd, J., Madrid-Marina, V. (1997) Analysis of the local kinetics and localisation of interleukin-1 alpha, tumour necrosis factor-alpha and transforming growth factor-beta, during the course of experimental pulmonary tuberculosis. *Immunology*. **90** (4): 607-17

Hernandez-Pando, R., Rook, G. A. (1994) The role of TNF-alpha in T cell mediated inflammation depends on the Th1/Th2 cytokine balance. *Immunology*. **82** (4): 591-5

Hervas-Stubbs, S., Majlessi, L., Simsova, M., Morova, J., Rojas, M. J., Nouze, C., Brodin, P., Sebo, P., Leclerc, C. (2006) High frequency of CD4+ T cells specific for the TH10.4 protein correlates with protection against *Mycobacterium tuberculosis* infection. *Infection and Immunity*. **74** (6): 3396-407

Hestvik, A. L. K., Hmama, Z., Av-Gay, Y. (2005) Mycobacterial manipulation of the host cell. *FEMS Microbiology Reviews*. **29** (5): 1041-1050

Hewinson, R. G., Vordermeier, H. M., Buddle, B. M. (2003) Use of the bovine model of tuberculosis for the development of improved vaccines and diagnostics. *Tuberculosis (Edinb).* **83** (1-3): 119-30

Hewinson, R. G., Vordermeier, H. M., Smith, N. H., Gordon, S. V. (2006) Recent advances in our knowledge of *Mycobacterium bovis*: a feeling for the organism. *Veterinary Microbiology*. **112** (2-4): 127-139

Hickman, S. P., Chan, J., Salgame, P. (2002) *Mycobacterium tuberculosis* induces differential cytokine production from dendritic cells and macrophages with divergent effects on naïve T cell polarization. *Journal of Immunology*. **168** (9): 4636-42

Ho, R. S., Fok, J. S., Harding, G. E., Smith, D. W. (1978) Host-parasite relationships in experimental airborne tuberculosis. VII. Fate of *Mycobacterium tuberculosis* in primary lung lesions and in primary lesion-free lung tissue infected as a result of bacillemia. *The Journal of Infectious Diseases*. **138** (2): 237-41

Hodge, D. L., Martinez, A., Julias, J. G., Taylor, L. S., Young, H. A. (2002) Regulation of nuclear gamma interferon gene expression by interleukin 12 (IL-12) and IL-2 represents a novel form of posttranscriptional control. *Molecular Cell Biology*. **22** (6): 1742-53

Hoft, D. F., Worku, S., Kampmann, B., Whalen, C. C., Ellner, J. J., Hirsch, C. S., Brown, R. B., Larkin, R., Li, Q., Yun, H., Silver, R. F. (2002) Investigation of the relationships between immune-mediated inhibition of mycobacterial growth and other potential surrogate markers of protective *Mycobacterium tuberculosis* immunity. *The Journal of Infectious Diseases*. **186** (10): 1148-57

Hope, J. C., Thom, M. L., Villarreal-Ramos, B., Vordermeier, H. M., Hewinson, R. G., Howard, C. J. (2005) Vaccination of neonatal calves with *Mycobacterium bovis* BCG induces protection against intransal challenge with virulent *M. bovis*. *Clinical and Experimental Immunology*. **139** (1): 48-56

Hosokawa, Y., Hosokawa, I., Ozaki, K., Nakae, H., Matsuo, T. (2006) Increase of CCL20 expression by human gingival fibroblasts upon stimulation with cytokines and bacterial endotoxin. *Clinical and Experimental Immunology*. **142** (2): 285-91

Howie, J. (1985) The case for compulsory pasteurisation. *British Medical Journal (Clinical Research ed.).* **291** (6493): 422-3

Huang, D., Qiu, L., Wang, R., Lai, X., Du, G., Seghal, P., Shen, Y., Shao, L., Halliday, L., Fortman, J., Shen, L., Letvin, N. L., Chen, Z. W. (2007) Immune gene networks of mycobacterial vaccine-elicited cellular responses and immunity. *The Journal of Infectious Diseases.* **195** (1): 55-69

Huard, R. C., Fabre, M., de Haas, P., Lazzarini, L. C., van Soolingen, D., Cousins, D., Ho, J. L. (2006) Novel genetic polymorphisms that further delineate the phylogeny of the *Mycobacterium tuberculosis* complex. *Journal of Bacteriology*. **188** (12): 4271-87

Huggett, J., Dheda, K., Bustin, S., Zumla, A. (2005) Real-time RT-PCR normalisation; strategies and considerations. *Genes and Immunity*. **6** (4): 279-84

Humphreys, I, R., Stewart, G. R., Turner, D. J., Patel, J., Karamanou, D., Snelgrove, R. J., Young, D. B. (2006) A role for dendritic cells in the dissemination of mycobacterial infection. *Microbes and Infection*. **8** (5): 1339-46

Huse, M., Lillemeier, B. F., Kuhns, M. S., Chen, D. S., Davis, M. M. (2006) T cells use two directionally distinct pathways for cytokine secretion. *Nature Immunology*. **7** (3): 247-55

Husson, R. N. (2006) Leaving on the lights: host-specific derepression of *Mycobacterium tuberculosis* gene expression by anti-sigma factor gene mutations. *Molecular Microbiology*. **62** (5): 1217-9

Irwin, S. M., Goodyear, A., Keyser, A., Christensen, R., Troudt, J. M., Taylor, J. L., Bohsali, A., Briken, V., Izzo, A. A. (2008) Immune response induced by three *Mycobacterium bovis* BCG substrains with diverse regions of deletion in a C57BL/6 mouse model. *Clinical and Vaccine Immunology*. **15** (5): 750-6

Ito, S., Ansari, P., Sakatsume, M., Dickensheets, H., Vazquez, N., Donnelly, R. P., Larner, A. C., Finbloom, D. S. (1999) Interleukin-10 inhibits expression of both interferon alpha and interferon gamma- induced genes by suppressing tyrosine phosphorylation of STAT1. *Blood*. **93** (5): 1456-63

Jacobs, M., Fick, L., Allie, N., Brown, N., Ryffel, B. (2002) Enhanced immune response in *Mycobacterium bovis* bacille calmette guerin (BCG)-infected IL10-deficient mice. *Clinical Chemistry and Laboratory Medicine*. **40** (9): 893-902

Jalava, K., Jones, J. A., Goodchild, T., Clifton-Hadley, R., Mitchell, A., Story, A., Watson, J. M. (2007) No increase in human cases of *Mycobacterium bovis* disease despite resurgence of infections in cattle in the United Kingdom. *Epidemiology and Infection*. **135** (1): 40-5

Jamil, B., Shahid, F., Hasan, Z., Nasir, N., Razzaki, T., Dawood, G., Hussain, R. (2007) Interferon gamma/IL10 ratio defines the disease severity in pulmonary and extra pulmonary tuberculosis. *Tuberculosis (Edinb).* **87** (4): 279-87

Jang, S., Uematsu, S., Akira, S., Salgame, P. (2004) IL6 and IL10 induction from dendritic cells in response to *Mycobacterium tuberculosis* is predominantly dependent on TLR2-mediated recognition. *Journal of Immunology*. **173** (5): 3392-7

Jankovic, D., Kullberg, M. C., Feng, C. G., Goldszmid, R. S., Collazo, C. M., Wilson, M., Wynn, T. A., Kamanak, M., Flavell, R. A., Sher, A. (2007) Conventional T-bet(+)Foxp3(-) Th1 cells are the major source of host-protective regulatory IL10 during intracellular protozoan infection. *The Journal of Experimental Medicine*. **204** (2): 273-83

Joardar, S. N., Ram, G. C., Goswami, T. (2002) Dynamic changes in cellular immune responses in experimental bovine tuberculosis. *Medical Science Monitor: international medical journal of experimental and clinical research*. **8** (11): 471-80

Johnson, L., Gough, J., Spencer, Y., Hewinson, G., Vordermeier, M., Wangoo, A. (2006) Immunohistochemical markers augment evaluation of vaccine efficacy and disease severity in bacillus Calmette-Guerin (BCG) vaccinated cattle challenged with *Mycobacterium bovis*. *Veterinary Immunology and Immunopathology*. **111** (3-4): 219-29

Jones, R. J., Jenkins, D. E. (1965) Mycobacteria isolated from soil. *Canadian Journal of Microbiology*. **11**: 127-33

Joss, C. L., Akdis, M., faith, A., Blaser, K., Akdis, C. A. (2000) IL10 directly acts on T cells by specifically altering the CD28 co-stimulation pathway. *The European Journal of Immunology*. **30** (6): 1683-90

Junqueira-Kipnis, A. P., Basaraba, R. J., Gruppo, V., Palanisamy, G., Turner, O. C., Hsu, T., Jacobs, W. R. Jr., Fulton, S. A., Reba, S. M., Boom, W. H., Orme, I. M. (2006) Mycobacteria lacking the RD1 region do not induce necrosis in the lungs of mice lacking interferon-gamma. *Immunology*. **119** (2): 224-31

Kaneda, K., Imaizumi, S., Mizuno, S., Baba, T., Tsukamura, M., Yano, I. (1988) Structure and molecular species composition of the three homologous series of alpha-mycolic acids from *Mycobacterium* spp. *Journal of General Microbiology*. **134** (8): 2213-29

Katakura, T., Miyazaki, M., Kobayashi, M., Herndon, D. N., Suzuki, F. (2004) CCL17 and IL10 as effectors that enable alternatively activated macrophages to inhibit the generation of classically activated macrophages. *Journal of Immunology*. **172** (3): 1407-13

Kato-Maeda, M., Rhee, J. T., Gingeras, T. R. (2001) Comparing genomes within the species *Mycobacterium tuberculosis*. *Genome Research*. **11**: 547-54

Katsikis, P. D., Choen, S. B., Murison, J. G., Uren, J., Hibbart, L. M., Callard, R. E., Di Padova, F., Feldmann, M., Londei, M. (1995) Human alpha beta T-cell receptor CD4-CD8 T cell clones are predominantly Th0-like. *Immunology*. **84** (4): 501-4

Katsikis, P. D., Cohen, S. B., Londei, M., Feldmann, M. (1995) Are CD4+ Th1 cells pro-inflammatory or anti-inflammatory? The ratio of IL10 to IFN gamma or IL2 determines their function. *International Immunology*. **7** (8): 1287-94

Keane, J., Balcewicz-Sablinska, M. K., Remold, H. G., Chupp, G. L., Meek, B. B., Fenton, M. J., Kornfeld, H. (1997) Infection by *Mycobacterium tuberculosis* promotes human alveolar macrophage apoptosis. *Infection and Immunity*. **65** (1): 298-304

Keane, J., Remold, H. G., Kornfield, H. (2000) Virulent *Mycobacterium tuberculosis* strains evade apoptosis of infected alveolar macrophages. *Journal of Immunology*. **164** (4): 2016-20

Kennedy, H. E., Welsh, M. D., Bryson, D. G., Cassidy, J. P., Forster, F. I., Howard, C. J., Collins, R. A., Pollock, J. M. (2002) Modulation of immune responses to *Mycobacterium bovis* in cattle depleted of WC1(+) gamma delta T cells. *Infection and Immunity*. **70** (3): 1488-500

King, M. J., Park, W. H. (1929) Effect of Calmette's BCG vaccine on experimental animals. *American Journal of Publics health and the Nations health*. **19** (2): 179-92

Klenk. (accessed January 2008) DSMZ: German collection of micro organisms and cell cultures. http://www.dsmz.de/microorganisms/bacterial_nomenclature_info.php?genus=Mycobacterium&species=bovis&bnu_no=1940#1940

Kopp, E., Medzhitov, R. (2003) Recognition of microbial infection by Toll-like receptors. *Current Opinion in Immunology*. **15**: 396-401

Koppelman, B., Neefjes, J. J., de Vries, J. E., de Waal Malefyt. R. (1997) Interleukin-10 down regulates MHC class II alphabeta peptide complexes at the plasma membrane of monocytes by affecting arrival and recycling. *Immunity*. **7** (6): 861-71

Krebs, J., Anderson, R. M., Clutton-Brock, T., Donnelly, C. A., Frost, S., Morrison, W. I., Woodroffe, R., Young, D. (1998) Badgers and bovine TB: conflicts between conservation and health. *Science*. **279**: 817-818

Krebs, J., Anderson, R., Clutton-Brock, T., Morrison, I., Young, D., Donnelly, C. (1997) Bovine tuberculosis in cattle and badgers – report by the Independent Scientific Review Group. Ministry of Agriculture, Fisheries and Food Publications, London.

Kruys, V., Thompson, P., Beutler, B. (1993) Extinction of the tumour necrosis factor locus, and of genes encoding the lipopolysaccharide signalling pathway. *The Journal of Experimental Medicine*. **177** (5): 1383-90

Lalvani, A., (2004) Counting antigen-specific T cells: a new approach for monitoring response to tuberculosis treatment? *Clinical and Infectious Diseases*. **38** (5): 757-9

Larsen, C. P., Ritchie, S. C., Hendrix, R., Linsley, P. S., Hathcock, K. S., Hodes, R. J., Lowry, R. P., Pearson, T. C. (1994) Regulation of immunostimulatory function and costimulatory molecule (B7-1 and B7-2) expression on murine dendritic cells. *Journal of Immunology*. **152** (11): 5208-19

Larsen, C. P., Ritchie, S. C., Pearson, T. C., Linsley, P. S., Lowry, R. P. (1992) Functional expression of the costimulatory molecule, B7/BB1, on murine dendritic cell populations. *The Journal of Experimental Medicine*. **176** (4): 1215-20

Larsen, J. M., Benn, C. S., Fillie, Y., van der Klejj, D., Aaby, P., Yazdanbakhsh, M. (2007) BCG stimulated dendritic cells induce an interleukin 10 producing T cell population with no T helper 1 or T helper 2 bais *in vitro*. *Immunology*. **121**: 276-282

Lasunskaia, E. B., Campos, M. N., de Andrade, M. R., Damatta, R. A., Kipnis, T. L., Einicker-Lamas, M., de Silva, W. D. (2006) Mycobacteria directly induce cytoskeletal rearrangements for macrophage spreading and polarization through TLR2- dependent PI3K signalling. *Journal of Leukocyte Biology*. **80** (6): 1480-90

Lay, G., Poquet, Y., Salek-Peyron, P., Puissegur, M. P., Botanch, C., Bon, H., Levillain, F., Duteyrat, J. L., Emile, J. F., Altare, F. (2007) Langhans giant cells from *M. tuberculosis*-induced human granulomas can not mediate mycobacterial uptake. *Journal of Pathology*. **211** (1): 76-85

Le Fevre, A. M., Donnelly, C. A., Cox, D. R., Bourne, J., Clifton-Hadley, R. S., Gettinby, G., Johnston, T., McInerney, J. P., Morrison, W. I., Woodroffe, R. (2005) The impact of localised badger culling versus no culling on TB incidence in British cattle: a randomised trial. ISG Publications, DEFRA: http://www.defra.gov.uk/animalh/tb/isg/isgpublications.htm

Leal, I. S., Smedegard, B., Andersen, P., Appelberg, R. (2001) Failure to induce enhanced protection against tuberculosis by increasing T cell-dependent interferon-gamma generation. *Immunology.* **104** (2): 157-61

Lehmann, U., Kreipe, H. (2006) Real-time PCR analysis of DNA and RNA extracted from formalin-fixed and paraffin-embedded biopsies. *Methods.* **25**: 409

Lehane, R. (1996) Beating the odds in a big country, The eradication of bovine Brucellosis and Tuberculosis in Australia, CSIRO Rub, Collingwood, Victoria.

Lesslie, I. W., Hbert, C. N., Frerichs, G. N. (1976) Practical application of bovine tuberculin PPD in testing cattle in Great Britain. *The Veterinary Record*. **98** (9): 170-2

Lesslie, I. W., Herbert, C. N. (1975) Comparison of the specificity of human and bovine tuberculin PPF for cattle testing. 3. National trial in Great Britain. *The Veterinary Record*. **96** (15): 338-41

Levy, Y., Brouet, J. C. (1994) Interleukin-10 prevents spontaneous death of germinal center B cells by induction of the bcl-2 protein. *The Journal of Clinical Investigation*. **93** (1): 424-8

Lewis, F., Maughan, N.J., Smith, V., Hillan, K., Quirke, P. (2001) Unlocking the archive – gene expression in paraffin embedded tissue. *Journal of Pathology*. **195**: 66

Lewis, K. N., Liao, R., Guinn, K. M., Hickey, M. J., Smith, S., Behr, M. A., Sherman, D. R. (2003) Deletion of RD1 from *Mycobacterium tuberculosis* mimics bacilli Calmette-Guérin attenuation. *Journal of Infectious Diseases*. **187** (1): 117-23

Liebana, E., Marsh, S., Gough, J., Nunez, A., Vordermeier, H. M., Whelan, A., Spencer, Y., Clifton-Hardley, R., Hewinson, G. (2007) Distribution and activation of T lymphocyte subsets in tuberculosis bovine lymph node granulomas. *Veterinary Pathology*. **44** (3): 366-72

Lim, A., Eleuterio, M., Hutter, B., Muruqasu-Oei, B., Dick, T. (1999) Oxygen depletion-induced dormancy in *Mycobacterium bovis* BCG. *Journal of Bacteriology*. **181** (7): 2252-6

Lin, M. Y., Selin, L. K., Welsh, R. M. (2000) Evolution of the CD8 T cell repertoire during infections. *Microbes and Infection*. **2** (9): 1025-39

Lin, T., Zhang, M., Hofman, F. M., Gong, J., Barnes, P. F. (1996) Absence of a prominent Th2 cytokine response in human tuberculosis. *Infection and Immunity*. **64** (4): 1351-6

Liu, S., Guo, S., Wang, C.m Shao, M., Zhang, X., Guo, Y., Gong, Q. (2007) A novel fusion protein-based indirect enzyme-linked immunosorbent assay for the detection of bovine tuberculosis. *Tuberculosis (Edinb).* **87** (3): 212-7

Locksley, R. M., Heinzel, F. P., Sadick, M. D., Holaday, B. J., Gardner, K. D. Jr. (1987) Murine cutaneous leishmaniasis: susceptibility correlates with differential expansion of helper T cell subsets. *Annales de l'Institut Pasteur Immunologie*. **138** (5): 744-9

Louden, R. G., Roberts, R. M. (1968) Singing and the dissemination of tuberculosis. *The American Review of Respiratory Disease.* **98**: 297-300

Louden, R. G., Spohn, S. K. (1969) Cough frequency and infectivity in patients with pulmonary tuberculosis. *The American Review of Respiration Disease*. **99**: 109-111

Lukacs, G. L., Rotstein, O. D., Grinstein, S. (1990) Phagosomal acidification is mediated by a vacuolar-type H+ -ATPase in murine macrophages. *The Journal of Biological Chemistry*. **265** (34): 21099-21107

Ly, L. H., Russell, M. I., McMurray, D. N. (2007) Microdissection of the cytokine milieu of pulmonary granulomas from tuberculous guinea pigs. *Cellular Microbiology*. **9** (5): 1127-36

Lyashchenko, K. P., Wiker, H. G., Harboe, M., McNair, J., Komissarenko, S. V., Pollock, J. M. (2001) Novel monoclonal antibodies against major antigens of *Mycobacterium bovis*. *Scandinavian Journal of Immunology*. **53**: 498-502

Lyashchenko, K., Whelan, A. O., Greenwald, R., Pollock, J. M., Andersen, P., Hewinson, R. G., Vordermeier, H. M. (2004) Association of tuberculin-boosted antibody responses with pathology and cell mediated immunity in cattle vaccinated with *Mycobacterium bovis* BCG and infected with *M. bovis*. *Infection and Immunity*. **72** (5): 2462-7

MacHugh, N. D., Mburu, J. K., Carol, M. J. Wyatt, C. R., Orden, J. A., Davis, W. V. (1997) Identification of two distinct subsets of bovine gamma delta cells with unique cell surface phenotypes and tissue distribution. *Immunology*. **92** (3): 340-5

Mason, C. M., Porretta, E., Zhang, P., Nelson, S. (2007) CD4+CD25+ transforming growth factor-beta producing T cells are present in the lung in murine tuberculosis and may regulate the host inflammatory response. *Clinical and Experimental Immunology*. **148** (3): 537-45

Masopust, D., Vezys, V., Marzo, A. L., Lefrancois, L. (2001) Preferential localisation of effector memory cells in nonlymphoid tissue. *Science*. **291** (5512): 2413-7

Matsumoto, S., Matsuo, T., O'hara, N., Hotokezaka, H., Naito, M., Minami, J., Yamada, T. (1995) Cloning and sequencing of a unique antigen MPT70 from *Mycobacterium tuberculosis* H37Rv and expression in BCG using *E. Coli*-mycobacteria shuttle vector. *Scandinavian Journal of Immunology*. **41**: 281-287

Matsuo, T., Matsumoto, S., O'hara, N., Kitaura, H., Mizuno, A., Yamada, T. (1995) Differential transcription of the MPB70 genes in two major groups of *Mycobacterium bovis* BCG substrains. *Microbiology*. **141**: 1601-1607

Maue, A. C., Waters, W. R., Davis, W. C., Palmer, M. V., Minion, F. C., Estes, D. M. (2005) Anaylsis of immune responses directed toward a recombinant early secretory antigenic target six-kilodalton protein-culture filtrate protein 10 fusion protein in *Mycobacterium bovis*-infected cattle. *Infection and Immunity*. **73** (10): 6659-67

Maue, A. C., Waters, W. R., Palmer, M. V., Nonnecke, B. J., Minion, F. C., Brown, W. C., Norimine, J., Foote, M. R., Scherer, C. F., Estes, D. M. (2007) An ESAT-6:CFP10 DNA vaccine administered in conjunction with *Mycobacterium bovis* BCG confers protection to cattle challenged with virulent *M. bovis*. *Vaccine*. **25** (24): 4735-46

Maxwell, K. W., Marcus, S. (1968) Phagocytosis and intracellular fate of *Mycobacterium tuberculosis*: *in vitro* studies with guinea pig peritoneal and alveolar mononuclear phagocytes. *Journal of Immunology*. **101** (1): 176-82

McCorry, T., Whelan, A. O., Welsh, M. D., McNair, J., Walton, E., Bryson, D. G., Hewinson, R. G., Vordermeier, H. M., Pollock, J. M. (2005) Shedding of *Mycobacterium bovis* in the nasal mucus of cattle infected experimentally with tuberculosis by the intranasal and intratracheal routes. *The Veterinary Record*. **157** (20): 613-8

McDonald, R. A., Delahay, R. J., Carter, S. P., Smith, G. C., Cheeseman, C. L. (2008) Perturbing implications of wildlife ecology for disease control. *Trends in Ecology and Evolution*. **23** (2): 53-6

McNair, J., Corbett, D. M., Girvin, R. M., Mackie, D. P., Pollock, J. M. (2001) Characterisation of the early antibody response in bovine tuberculosis: MPB83 is an early target with diagnostic potential. *Scandinavian Journal of Immunology*. **53** (4): 365-71

McShane, H., Pathan, A. A., Sander, C. R., Goonetilleke, N. P., Fletcher, H. A., Hill, A. V. (2005) Boosting BCG with MVA85A: the first candidate subunit vaccine for tuberculosis in clinical trials. *Tuberculosis (Edinb).* **85** (1-2): 47-52

McSwiggan, D. A., Collins, C. H. (1974) The isolation of *M. kansasii* and *M. xenopi* from water systems. *Tubercle*. **55** (4): 291-7

Means, T. K., Lien, E., Yoshimura, A., Wang, S., Golenbock, D. T., Fenton, M. J. (1999). The CD14 ligands lipoarabinomannan and lipoploysaccharide differ in their requirement for Toll-like receptors. *Journal of Immunology*. **163**: 6748-6755

Medina, E., Ryan, L., LaCourse, R., North, R. J. (2006) Superior virulence of *Mycobacterium bovis* over *Mycobacterium tuberculosis* (Mtb) for Mtb-resistent and Mtb-susceptible mice is manifest as an ability to cause extrapulmonary disease. *Tuberculosis (Edinb).* **86** (1): 20-7

Medzhitov, R., Janeway, C. Jr. (2000) The toll receptor family and microbial recognition. *Trends in Microbiology*. **8** (10): 452-6

Meher, A. K., Bal, N. C., Chary, K. V., Arora, A. (2006) *Mycobacterium tuberculosis* H37Rv ESAT-6-CFP-10 complex formation confers thermodynamic and biochemical stability. *The FEBS Journal*. **273** (7): 1445-62

Meher, A. K., Lella, R. K., Sharma, C., Arora, A. (2007) Analysis of complex formations and immune response of CFP-10 and ESAT-6 mutants. *Vaccine*. **25** (32): 6098-106

Melby, P. C., Andrade-Narvaez, F. J., Darnell, B. J., Valencia-Pacheco, G., Tryon, V. V., Palomo-Cetina, A. (1994) Increased expression of proinflammatory cytokines in chronic lesions of human cutaneous leishmaniasis. *Infection and Immunity*. **62** (3): 837-42

Mellman, I., Steinman, R. M. (2001) Dendritic cells: specialised and regulated antigen processing machines. *Cell*. **106** (3): 255-8

Mendez-Samperio, P., Ayala, H., Trejo, A., Ramirez, F. A. (2004) Differential induction of TNF-alpha and NOS2 by mitogen-activated protein kinase signalling pathways during *Mycobacterium bovis* infection. *The Journal of Infection*. **48** (1): 66-73

Menzies, F. D., Neill, S. D. (2000) Cattle-to-cattle transmission of bovine tuberculosis. *The Veterinary Journal*. **160** (2): 92-106

Metchnikoff, E. (1905) Immunity in the infectious diseases. Macmillan Press, New York.

Mikaelian, I., Nanney, L. B., Parman, K. S., Kusewitt, D. F., Ward, J. M., Naf, D., Krupke, D. M., Eppig, J. T., Bult, C. J., Seymour, R., Ichiki, T., Sundberg, J. P. (2004) Antibodies that label paraffin-embedded mouse tissues: a collaborative endeavour. *Toxicologic Pathology*. **32** (2): 181-91

Minnikin, D. E., Goodfellow, M. (1980) Lipid composition in the classification and identification of acid-fast bacteria. *Society for Applied Bacteriology Symposium Series*. **8**: 189-256

Mischenka, V. V., Kapina, M. A., Eruslanov, E. B., Kondratieva, E. V., Lyadova, I. V., Young, D. B., Apt, A. S. (2002) Mycobacterial dissemination and cellular responses after 1-lobe restricted tuberculosis infection of genetically susceptible and resistant mice. *The Journal of Infectious Diseases.* **190**: 2137-45

Mittrucker, H. W., Steinhoff, U., Kohler, A., Krause, M., Lazar, D., Mex, P., Miekley, D., Kaufmann, S. H. (2007) Poor correlation between BCG vaccination-induced T cell responses and protection against tuberculosis. *Proceedings of the National Acadamy of Sciences of the USA*. **104** (30): 12434-9

Monaghan, M. L., Doherty, M. L., Collins, J. D., Kazda, J. F., Quinn, P. J. (1994) The tuberculin test. *Veterinary Microbiology*. **40** (1-2): 111-24

Moore, K. W., de Waal Malefyt, R., Coffman, R. L., O'Garra, A. (2001) Interleukin-10 and the interleukin-10 receptor. *Annual Review of Immunology*. **19**: 683-765

Morrison, W. I., Bourne, F. J., Cox, D. R., Donnelly, C. A., Gettinby, G., McInerney, J. P., Woodroffe, R. (2000) Pathogenesis and diagnosis of infections with *Mycobacterium bovis* in cattle. Independent Scientific Group on cattle TB. *The Veterinary Record*. **146** (9): 236-42

Mosmann, T.R., Cherminski, H., Bond, M.W., Giedlin, M.A., Coffman, R.L. (1986) Two types of murine helper T cell clone. 1. Definition according to profiles of lymphokine activities and secreted proteins. *Journal of Immunology*. **136** (7): 2348-57

Mostowy, S., Tsolaki, A. G., Small, P. M., Behr, M. A. (2003) The *in vitro* evolution of BCG vaccines. *Vaccine*. **21**: 4270-4274

Muirhead, R.H., Gallagher, J., Burn, K.J. (1974) Tuberculosis in wild badgers in Gloucestershire: Epidemiology. *The Veterinary Record*. **95**: 552-555

Muller, M. C., Merx, K., Weisser, A., Kreil, S., Lahaye, T., Hehlmann, R., Hochhaus, A. (2002) Improvement of molecular monitoring of residual disease in leukemias by bedside RNA stabilisation. *Leukemia.* **16** (12): 2395-9

Munder, M., Eichmann, K., Modolell, M. (1998) Alternative metabolic states in murine macrophages reflected by the nitric oxide synthase/arginase balance: competitive regulation by CD4+ T cells correlates with Th1/Th2 phenotype. *Journal of Immunology*. **160** (11): 5347-54

Munro, J. M., Pober, J. S., Cotran, R. S. (1989) Tumour necrosis factor and interferon-gamma induce distinct patterns of endothelial activation and associated leukocyte accumulation in skin of *Papio anubis*. *American Journal of Pathology*. **135** (1): 121-33

Mustafa, T., Wiker, H. G., Mørkve, O., Sviland, L. (2008) Differential expression of mycobacterial antigen MPT64, apoptosis and inflammatory markers in multinucleated giant cells and epithelioid cells in granulomas caused by *Mycobacterium tuberculosis*. *Virchows Arch; An International Journal of Pathology*. **452** (4): 449-56

National Farmers Union (accessed January 2008): http://www.nfuonline.com/

Nemeth, Z. H., Lutz, C. S., Csoka, B., Deitch, E.A., Leibovich, S. J., Gause, W. C., Tone, M., Pacher, P., Vizi, E. S., Hasko, G. (2005) Adenosine augments IL-10 production by macrophages through an A_{2B} receptor-mediated posttranscriptional mechanism. *The Journal of Immunology*. **175**: 8260-8270

Ng, K. H., Watson, J. D., Prestidge, R., Buddle, B. M. (1995) Cytokine mRNA expressed in tuberculin skin test biopsies from BCG vaccinated and *Mycobacterium bovis* inoculated cattle. *Immunology and Cell Biology*. **73**: 362-368

Nicolle, D., Fremond, C., Pichon, X., Bouchot, A., Maillet, B., Ryffel, B., Quesniaux, V.J. (2004) Long term control of *Mycobacterium bovis* BCG infection in the absence of toll-like receptors (TLRs): investigation of TLR2-, TLR6-, or TLR2-TLR4- deficient mice. *Infection and Immunity*. **72**: 6994-7004

O'Brien, D. J., Schmitt, S. M., Fitzgerald, S. D., Berry, D. E., Hickling, G. J. (2006) Managing the wildlife reservoir of *Mycobacterium bovis*: the Michigan, USA, experience. *Veterinary Microbiology*. **112**: 313-26

Olert, J., Wiedorn, K., Goldmann, T., Kuhl, H., Mehraein, Y., Scherthan, H., Niketeghad, F., Vollmer, E., Muller, A. M., Muller-Navia, J. (2001) HOPE fixation: a novel fixing method and paraffin embedding technique for human soft tissues. *Pathology: Research and Practice*. **197**: 823-826

Olleros, M. L., Guler, R., Vesin, D., Parapanov, R., Marchal, G., Martinez-Soria, E., Corazza, N., Pache, J. C., Mueller, C., Garcia, I. (2005) Contribution of transmembrane tumour necrosis factor to host defense against *Mycobacterium bovis* bacillus Calmette-Guerin and *Mycobacterium tuberculosis* infections. *American Journal of Pathology*. **166** (4): 1109-20

Olmstead, A., Rhode, P. W. (2004) An impossible undertaking: the eradication of bovine tuberculosis in the United States. *The Journal of Economic History*. **64**: 734-772

Orme, I. (1998) Cellular and genetic mechanisms underlying susceptibility of animal models to tuberculosis infection. *Novartis Foundation Symposium*. **217**: 112-7

Orme, I. M. (2006) Preclinical testing of new vaccines for tuberculosis. A comprehensive review. *Vaccine*. **24**: 2-19

Orme, I. M., McMurray, D. N., Belisle, J. T. (2001) Tuberculosis vaccine development: recent progress. *Trends in Microbiology*. **9** (3): 115-8

Orme, I. M., Roberts, A. D., Griffin, J. P., Abrams, J. S. (1993) Cytokine secretion by CD4+ T lymphocytes acquired in response to *Mycobacterium tuberculosis* infection. *Journal of Immunol.ogy.* **151** (1): 518-25

Pace, L., Pioli, C., Doria, G. (2005) IL-4 modulation of CD4+CD25+ T regulatory cell-mediated suppression. *Journal of Immunology*. **174** (12): 7645-53

Palmer, M. V., Waters, W. R., Thacker, T. C. (2007) Lesion development and immunohistochemical changes in granulomas from cattle experimentally infected with *Mycobacterium bovis*. *Veterinary pathology*. **44** (6): 863-74

Palmer, M. V., Whipple, D. L., Olsen, S. C., Jacobson, R. H. (2000) Cell mediated and humoral immune responses of white-tailed deer experimentally infected with *Mycobacterium bovis*. *Research in Veterinary Science*. **68** (1): 95-8

Palmer, M.V., Waters, W.R., Whipple, D.L. (2002) Aerosol delivery of virulent *Mycobacterium bovis* to cattle. *Tuberculosis (Edin*b). **82** (6): 275-82

Palomino, J. C., Martin, A., Portaels, F. (2007) Rapid drug resistence detection in *Mycobacterium tuberculosis*: a review of colourimetric methods. *Clinical Microbiology and Infection*. **13** (8): 754-62

Peters, W., Ernst, J. D. (2003) Mechanisms of cell recruitment in the immune response to *Mycobacterium tuberculosis*. *Microbes and Infection*. **5** (2): 151-158

Petit, J. F., Wietzerbin, J., Das, B. C., Lederer, E. (1975) Chemical structure of the cell wall of *Mycobacterium tuberculosis* var. *bovis*, strain BCG. *Zeitschrift fur Immunitatsforschung, Experimentelle und Klinische Immunologie*. **149** (2-4): 118-25

Pitulle, C., Dorsch, M., Kazda, J., Wolters, J., Stackebrandt, E. (1992) Phylogeny of rapidly growing members of the genus Mycobacterium. *International Journal of Systematic Bacteriology*. **42** (3): 337-43

Podlaski, F. J., Nanduri, V. B., Hulmes, J. D., Pan, Y. C., Levin, W., Danho, W., Chizzonite, R., Gately, M. K., Stern, A. S. (1992) Molecular characterisation of interleukin 12. *Archives of Biochemistry and Biophysics*. **294** (1): 230-7

Pollock, J. M., Andersen, P. (1997) Predominant recognition of the ESAT-6 protein in the first phase of interferon with *Mycobacterium bovis* in cattle. *Infection and Immunity*. **65** (7): 2587-92

Pollock, J. M., McNair, J., Bassett, H., Cassidy, J. P., Costello, E., Aggerbeck, H., Rosenkrands, I., Anderson, P. (2003) Specific delayed type hypersensitivity responses to ESAT-6 identify tuberculosis infected cattle. *Journal of Clincial Microbiology*. **41**: 1856-60

Pollock, J. M., McNair, J., Welsh, M. D., Girvin, R. M., Kennedy, H. E., Mackie, D. P., Neill, S. D. (2001) Immune responses in bovine tuberculosis. *Tuberculosis (Edinb).* **81** (1-2): 103-7

Pollock, J. M., Neill, S. D. (2002) *Mycobacterium bovis* infection and tuberculosis in cattle. *Veterinary Journal*. **163** (2): 115-27

Pollock, J. M., Pollock, D. A., Campbell, D. G., Girvin, R. M., Crockard, A. D., Neill, S. D., Mackie, D. P. (1996) Dynamic changes in circulating and antigen-responsive T-cell subpopulations post *Mycobacterium bovis* infection in cattle. *Immunology*. **87** (2): 236-41

Pope, L. C., Butlin, R. K., Wison, G. J., Woodroffe, R., Erven, K., Conyers, C. M., Franklin, T., Delahay, R. J., Cheeseman, C. L., Burke, T. (2007) Genetic evidence that culling increases badger movement: implications for the spread of bovine tuberculosis. *Molecular Ecology*. **16** (23): 4919-29

Porphyre, T., Stevenson, M. A., McKenzie, J. (2008) Risk factors for bovine tuberculosis in New Zealand cattle farms and their relationship with possum control strategies. *Preventative Veterinary Medicine*. **86** (1-2): 93-106

Powell, M. J., Thompson, S. A., Tone, Y., Waldmann, H., Tone, M. (2000) Posttranscriptional regulation of IL10 gene expression through sequences in the 3'-untranslated region. *Journal of Immunology*. **165** (1): 292-6

Pratt, R. J., Grange, J. M., Williams, V. G. (2005) Tuberculosis, a foundation for nursing and healthcare practice. Hodder Education, London, Chapter 2.

Pym, A. S., Brodin, P., Brosch, R., Huerre, M., Cole, S. T. (2002) Loss of RD1 contributed to the attenuation of the live tuberculosis vaccines *Mycobacterium bovis* BCG and *Mycobacterium microti*. *Molecular Microbiology*. **46** (3): 709-17

Qie, Y. Q., Wang, J. L., Zhu, B. D., Xu, Y., Wang, Q. Z., Chen, J. Z., Wang, H. H. (2008) Evaluation of a new recombinant BCG which contains mycobacterial antigen ag85B-mpt64 (190-198)-mtb8.4 in C57/BL6 mice. *Scandinavian Journal of Immunology*. **67** (2): 133-9

Radosevic, K., Wieland, C. W., Rodriguez, A., Weverling, G. J., Mintardjo, R., Gillissen, G., Vogels, R., Skeiky, Y. A. Hone, D. M., Sadoff, J. C., van der Poll, T., Havenga, M., Goudsmit, J. (2007) Protective immune responses to a recombinant adenovirus type 35 tuberculosis vaccine in two mouse strains: CD4 and CD8 T cell epitope mapping and role of interferon gamma. *Infection and Immunity*. **75** (8): 4105-15

Radunz, B. (2006) Surveillance and risk management during the latter stages of eradication: experiences from Australia. *Veterinary Microbiology*. **112** (2-4): 283-90

Rao, V., Dhar, N., Shakila, H., Singh, R., Khera, A., Jain, R., Naseema, M., Paramasivan, C. N., Narayanan, P. R., Ramanathan, V. D., Tyagi, A. K. (2005) Increased expression of *Mycobacterium tuberculosis* 19 kDa lipoprotein obliterates the protective efficacy of BCG by polarizing host immune responses to the Th2 subtype. *Scandinavian Journal of Immunology*. **61** (5): 410-7

Rescigno, M. (2002) Dendritic cells and the complexity of microbial infection. *Trends in Microbiology*. **10** (9): 425-61

Reynolds, D (2006) A review of tuberculosis science and policy in Great Britain. *Veterinary Microbiology*. **112**: 119-126

Rhodes, S. G., Buddle, B. M., Hewinson, R. G., Vordermeier, H. M. (2000) Bovine tuberculosis: immune responses in the peripheral blood and at the site of active disease. *Immunology*. **99**: 195-202

Rhodes, S. G., Hewinson, R. G., Vordermeier, H. M. (2001) Antigen recognition and immunomodulation by gamma delta T cells in bovine tuberculosis. *Journal of Immunology*. **166** (9): 5604-10

Rhodes, S. G., Sawyer, J., Whelan, A. O., Dean, G. S., Coad, M., Ewer, K. J., Waldvogel, A. S., Zakher, A., Clifford, D. J., Hewinson, R. G. (2007) Is interleukin-4delta3 splice variant expression in bovine tuberculosis a marker of protective immunity? *Infection and Immunity*. **75** (6): 3006-13

Ritacco, V., Lopez, B., De Kantor, I. N., Barrera, L., Errico, F., Nader, A. (1991) Reciprocal cellular and humoral immune responses in bovine tuberculosis. *Research in Veterinary Science*. **50** (3): 365-7

Roach, D. R., Bean, A. G., Demangel, C., France, M. P., Briscoa, H., Britton, W. J. (2002) TNF regulates chemokine induction essential for cell recruitment, granuloma formation and clearance of mycobacterial infection. *Journal of Immunology*. **168** (9): 4620-7

Robert, C., Fuhlbrigge, R. C., Kieffer, J. D., Ayehunie, S., Hynes, R. O., Cheng, G., Grabbe, S., von Andrian, U. H., Kupper, T. S. (1999) Interaction of dendritic cells with skin endothelium: A new perspective on immunosurveillance. *Journal of Experimental Medicine*. **189** (4): 627-36

Romani, N., Koide, S., Crowley, M., Witmer-Pack, M., Livingstone, A. M., Fathman, C. G., Inaba, K., Steinman, R. M. (1989) Presentation of exogenous protein antigens by dendritic cells to T cell clones. Intact protein is presented best by immature, epidermal Langerhans cells. *Journal of Experimental Medicine*. **169** (3): 1169-78

Rook, G. A., Adams, V., Hunt, J., Palmer, R., Martinelli, R., Brunet, L. R. (2004) Mycobacteria and other environmental organisms as immunomodulators for immunoregulatory disorders. *Springer Seminars in Immunopathology*. **25** (3-4): 237-55

Rook, G. A., Hernandez-Pando, R., Dheda, K., Teng Seah, G. (2004) IL-4 in tuberculosis: implications for vaccines design. *Trends in Immunology*. **25** (9): 483-8

Roque, S., Nobrega, C., Appelberg, R., Correia-Neves, M. (2007) IL-10 underlies distinct susceptibility of BALB/c and C57BL/6 mice to *Mycobacterium avium* infection and influences efficacy of antibiotic therapy. *Journal of Immunology*. **178** (12): 8028-35

Rothel, J. S., Jones, S. L., Corner, L. A., Cox, J. C., Wood, P. R. (1990) A sandwich enzyme immunoassay for bovine interferon-gamma and it's use for the detection of tuberculosis in cattle. *Australian Veterinary Journal*. **67** (4): 134-7

Rousset, F., Garcia, E., Defrance, T., Peronne, C., Vezzio, N., Hsu, D. H., Kastelein, R., Moore, K. W., Banchereau, J. (1992) Interleukin 10 is a potent growth and differentiation factor for activated human B lymphocytes. *Proceedings of the National Academy of Sciences of the USA*. **89** (5): 1890-3

Rutz, S., Janke, M., Kassner, N., Hohnstein, T., Krueger, M., Scheffold, A. (2008) Notch regulates IL-10 production by T helper 1 cells. *Proceedings of the National Academy of Sciences of the USA*. doi: 10.1073/pnas.0712102105

Ryan, A. A., Wozniak, T. M., Shklovskaya, E., O'Donnell, M. A., Fazekas de St Groth, B., Britton, W. J., Triccas, J. A. (2007) Improved protection against disseminated tuberculosis by *Mycobacterium bovis* bacillus Calmette-Guerin secreting murine GM-CSF is associated with expansion and activation of APCs. *Journal of Immunology*. **179** (12): 8418-24

Said-Salim, B., Mostowy, S., Kristof, A. S., Behr, M. A. (2006) Mutations in *Mycobacterium tuberculosis* Rv0444c, the gene encoding anti-SigK, explain high level expression of MPB70 and MPB83 in *Mycobacterium bovis*. *Molecular Microbiology*. **62** (5): 1251-63

Sakula, A. (1982) Robert Koch: Centenary of the discovery of the tubercle bacilli, 1882. *Thorax.* **37** (4): 246-51

Sallusto, F., Lenig, D., Förster, R., Lipp, M., Lanzavecchia, A. (1999) Two subsets of memory T lymphocytes with distinct homing potentials and effector functions. *Nature*. **401** (6754): 798-12

Sanders, B., Skansen-Saphir, U., Damm, O., Hakansson, L., Andersson, J., Andersson, U. (1995) Sequential production of Th1 and Th2 cytokines in response to live bacillus Calmette-Guerin. *Immunology*. **86** (4): 512-518

Saunders, B. M., Cooper, A. M. (2000) Restraining mycobacteria: role of granulomas in mycobacterial infections. *Immunology and Cell Biology*. **78** (4): 334-41

Scantlebury, M., Hutchings, M. R., Allcroft, D. J., Harris, S. (2004) Risk of disease from wildlife reservoirs: badgers, cattle, and bovine tuberculosis. *Journal of Dairy Science*. **87** (2): 330-9

Schafer, M.P., Fernback, J.E., Ernst, M.K. (1999) Detection and characterisation of airborne *Mycobacterium tuberculosis* H37Ra particles, a surrogate for airborne pathogenic *Mycobacterium tuberculosis*. *Aerosol Science and Technology*. **30**: 161-173

Schandene, L., Alonson-Vega, C., Willems, F., Gerard, C., Delvaux, A., Velu, T., Devos, R., de Boer, M., Goldman, M. (1994) B7/CD28-dependent IL5 production by human resting T cells is inhibited by IL10. *Journal of Immunology*. **152** (9): 4368-74

Schlesinger, L.S., Bellinger-Kawahara, C.G., Payne, N.R., Horwitz, M.A. (1990) Phagocytosis of *Mycobacterium tuberculosis* is mediated by human monocyte complement receptors and complement component C3. *Journal of Immunology*. **144** (7): 2771-80

Schlesinger, L. S., Hull, S. R., Kaufman, T. M. (1994) Binding of the terminal mannosyl units of lipoarabinomannan from a virulent strain of *Mycobacterium tuberculosis* to human macrophages. *Journal of Immunology*. **152** (8): 4070-9

Schluger, N. W., Rom, W. N. (1998) The host immune response to tuberculosis. *American Journal of Respiratory and Critical Care Medicine*. **157**(3): 679-91

Schmitt, S. M., Fitzgerald, S. D., Cooley, T. M., Bruning-Fann, C. S., Sullivan, L., Berry, D., Carlson, T., Minnis, R. B., Payeur, J. B., Sikarskie, J. (1997) Bovine tuberculosis in free-ranging white-tailed deer from Michigan. *Journal of Wildlife Disease.* **33**: 749–758.

Schnappinger, D., Ehrt, S., Voskuil, M. I., Liu, Y., Mangan, J. A., Monahan, I. M., Dolganov, G., Efron, B., Butcher, P. D., Nathan, C., Schoolnik, G. K. (2003) Transcriptional adaptation of *Mycobacterium tuberculosis* within macrophages: insights into the phagosomal environment. *The Journal of Experimental Medicine*. **198** (5): 693-704

Schultz, R. M., Kleinschmidt, W. J. (1983) Functional identity between murine gamma interferon and macrophage activating factor. *Nature*. **305** (5931): 239-40

Scott, P., Natovitz, P., Coffman, R. L., Pearce, E., Sher, A. (1988) Immunoregulation of cutaneous leishmaniasis. T cell lines that transfer protective immunity or exacerbation belong to different T helper subsets and respond to distinct parasite antigens. *Journal of Experimental Medicine*. **168** (5): 1675-84

Seah, G. T., Rook, G. A. (2001) IL-4 influences apoptosis of mycobacterium- reactive lymphocytes in the presence of TNF-alpha. *Journal of Immunology*. **167** (3): 1230-7

Seder, R. A., Ahmed, R. (2003) Similarities and differences in CD4+ and CD8+ effector and memory T cell generation. *Nature Immunology*. **4** (9): 835-42

Seder, R. A., Germain, R. N., Linsley, P. S., Paul, W. E. (1994) CD28-mediated costimulation of interleukin 2 (IL2) production plays a critical role in T cell priming for IL4 and interferon gamma production. *Journal of Experimental Medicine*. **179** (1): 299-304

Sendide, K., Deghmane, A. E., Pechkovsky, D., Av-Gay, Y., Talal, A., Hmama, Z. (2005) *Mycobacterium bovis* BCG attenuates surface expression of mature class II molecules through IL-10 dependent inhibition of cathepsin S. *Journal of Immunology*. **175** (8): 5324-32

Shi, C., Wang, X., Zhang, H., Xu, Z., Li, Y., Yuan, L. (2007) Immune responses and protective efficacy induced by 85B antigen and early secreted antigenic target-6 kDa antigen fusion protein secreted by recombinant bacille Calmette-Guérin. *Acta Biochimica et Biophysica Sinica (Shanghai)*. **39** (4): 290-6

Shirma, G. M., Kazwala, R. R., Kambarage, D. M. (2003) Prevalence of bovine tuberculosis in cattle in different farming systems in the eastern zone of Tanzania. *Preventive Veterinary Medicine*. **57** (3): 167-72

Skinner, M. A., Buddle, B. M., Wedlock, D. N., Keen, D., de Lisle, G. W., Tascon, R. E., Ferraz, J. C., Lowrie, D. B., Cockle, P. J., Vordermeier, H. M., Hewinson, R. G. (2003a) A DNA prime-*Mycobacterium bovis* BCG boost vaccination strategy for cattle induces protection against bovine tuberculosis. *Infection and Immunity*. **71** (9): 4901-7

Skinner, M. A., Parlane, N., McCarthy, A., Buddle, B. M. (2003b) Cytotoxic T cell responses to *Mycobacterium bovis* during experimental infection of cattle with bovine tuberculosis. *Immunology*. **110** (2): 234-41

Skinner, S. J., Deleault, K. M., Fecteau, R., Brokks, S. A. (2008) Extracellular signal-regulated kinase regulation of tumour necrosis factor-alpha mRNA nucleocytoplasmic transport requires TAP-Nxt1 binding and the AU-rich element. *Journal of Biology and Chemistry*. **283** (6): 3191-9

Smith, D. W., Wiegeshaus, E., Navalkar, R., Grover, A. A. (1966) Host-parasite relationships in experimental airborne tuberculosis. I. Preliminary studies in BCG-vaccinated and nonvaccinated animals. *Journal of Bacteriology*. **91** (2): 718-24

Sozzani, S., Sallusto, F., Luini, W., Zhou, D., Piemonti, L., Allavena, P., Van Damme, J., Valitutti, S., Lanzavecchia, A., Mantovani, A. (1995) Migration of dendritic cells in response to formly peptides, C5a and a distinct set of chemokines. *Journal of Immunology*. **155** (7): 3292-5

Sprent, J., Surh, C. D. (2001) T cell memory. *Annual Review of Immunology*. **20**: 551-79

Srinivasan, M., Sedmak, D., Jewell, S. (2002) Effect of fixatives and tissue processing on the content and integrity of nucleic acids. *American Journal of Pathology*. **161**: 1961

Steinman, R. M., Pack, M., Inaba, K. (1997) Dendritic cells in the T cell areas of lymphoid organs. *Immunological Reviews*. **156**: 25-37

Stenger, S., Mazzaccaro, R.J., Uyemura, K., Cho, S., Barnes, P. F., Rosat, J. P., Sette, A., Brenner, M. B., Porcelli, S. A., Bloom, B. R., Modlin, R. L. (1997) Differential effects of cytolytic T cell subsets on intracellular infection. *Science*. **276** (5319): 1684-7

Stenger, S., Modlin, R. L. (2002) Control of *Mycobacterium tuberculosis* through mammalian toll-like receptors. *Current Opinion on Immunology*. **14** (4): 452-7

Stober, C. B., Lammas, D. A., Li, C. M., Kumararatne, D. S., Lightman, S. L., McArdle, C .A. (2001) ATP-mediated killing of *Mycobacterium bovis* bacilli Calmette-Guerin within human macrophages is calcium dependent and associated with the acidification of mycobacteria-containing phagosomes. *Journal of Immunology*. **166** (10): 6276-86

Streilein, J. W., Grammer, S. F. (1989) *In vitro* evidence that Langerhans cells can adopt two functionally distinct forms capable of antigen presentation to T lymphocytes. *Journal of Immunology*. **143** (12): 3925-33

Sturgill-Koszycki, S., Schlesinger, P. H., Chakraborty, P., Haddix, P. L., Collins, H. L., Fok, A. K., Allen, R. D., Gluck, S. L., Heuser, J., Russell, D. G. (1994) Lack of acidification in Mycobacterium phagosomes produced by exclusion of the vesicular proton-ATPase. *Science*. **263** (5147): 678-81

Sung, K. L., Saldivar, E., Phillips, L. (1994) Interleukin-1 beta induces differential adhesiveness on human endothelial cell surfaces. *Biochemical and Biophysical Research Communications*. **202** (2): 866-72

Sweeney, F.P., Courtenay, O., Hibberd, V., Hewinson, R.G., Reilly, L.A., Gaze, W.H., Wellington, E.M. (2007) Environmental monitoring of *Mycobacterium bovis* in badger feces and badger sett soil by real time PCR, as confirmed by immunofluorescence, immunocapture and cultivation. *Applied and Environmental Microbiology*. **73** (22): 7471-3

Szabo, S. J., Dighe, A. S., Gubler, U., Murphy, K. M. (1997) Regulation of the interleukin (IL)-12R beta 2 subunit expression in developing T helper 1 (Th1) and Th2 cells. *Journal of Experimental Medicine*. **185** (5): 817-24

Takayama, K., Wang, C., Besra, G.S. (2005) Pathway to synthesis and processing of mycolic acids in *Mycobacterium tuberculosis*. *Clinical Microbiology Reviews*. **18** (1): 81-101

Tanaka, S., Sato, M., Onitsuka, T., Kamata, H., Yokomizo, Y. (2005) Inflammation cytokine gene expression in different types of granulomatous lesions during asymptomatic stages of bovine paratuberculosis. *Veterinary Pathology*. **42**: 579-88

Thacker, T. C., Palmer, M. V., Waters, W. R. (2006) Correlation of cytokine gene expression with pathology in white-tailed deer (*Odocoileus virginianus*) infected with *Mycobacterium bovis*. *Clinical and Vaccine Immunology*. **13** (6): 640-7

Thacker, T. C., Palmer, M. V., Waters, W. R. (2007) Associations between cytokine gene expression and pathology in *Mycobacterium bovis* infected cattle. *Veterinary Immunology and Immunopathology*. **119** (3-4): 204-13

Tone, M., Powell, M. J., Tone, M., Thompson, S. A., Waldmann, H. (2000) IL-10 gene expression is controlled by the transcription factors Sp1 and Sp3. *Journal of Immunology*. **165** (1): 286-91

Turner, J., Gonzalez-Juarrero, M., Ellis, D. L., Basaraba, R. J., Kipnis, A., Orme, I. M., Cooper, A. M. (2002) *In vivo* IL10 production reactivates chronic pulmonary tuberculosis in C57BL/6 mice. *Journal of Immunology*. **169** (11): 6343-51

Ulrichs, T., Kosmiadi, G. A., Trusov, V., Jorg, S., Pradl, L., Titukhina, M., Mishenko, V., Gushina, N., Kaufmann, S. H. (2004) Human tuberculous granuloma induce peripheral lymphoid follicle-like structures to orchestrate local host defence in the lung. *Journal of Pathology*. **204** (2): 217-28

Umland, S. P., Razac, S., Shah, H., Nahrebne, D. K., Egan, R. W., Billah, M. M. (1998) Interleukin 5 mRNA stability in human T cells is regulated differently than interleukin 2, interleukin 3, interleukin 4, granulocyte/macrophage colony-stimulating factor and interferon gamma. *American Journal of Respiratory Cell and Molecular Biology*. **18** (5): 631-42

Underhill, D. M., Ozinsky, A. (2002) Toll-like receptors: key mediators of microbe detection. *Current Opinion in Immunology*. **14**: 103-110

Van Embden, J. D., Van Gorkom, T., Kremer, K., Jansen, R., Van Der Zeijst, B. A., Schouls, L. M. (2000) Genetic variation and evolutionary origin of the direct repeat locus of *Mycobacterium tuberculosis* complex bacteria. *Journal of Bacteriology*. **182** (9): 2393-401

Van Pinxteren, L. A., Ravn, P., Agger, E. M., Pollock, J., Andersen, P. (2000) Diagnosis of tuberculosis based on the two specific antigens ESAT-6 and CFP10. *Clinical and Diagnostic Laboratory Immunology*. **7** (2): 155-60

Vieira, P. L., Christensen, J. R., Minaee, S., O'Neill, E. J., Barrat, F. J., Boonstra, A., Barthlott, T., Stockinger, B., Wraith, D. C., O'Garra, A. (2004) IL10 secreting regulatory T cells do not express Foxp3 but have comparable regulatory function to naturally occurring CD4+CD25+ regulatory cells. *Journal of Immunology*. **172** (10): 5986-93

Villarreal-Ramos, B., McAulay, M., Chance, V., Martin, M., Morgan, J., Howard, C. J. (2003) Investigation of the role of CD8+ T cells in bovine tuberculosis *in vivo*. *Infection and Immunity*. **71** (8): 297-303

VLA (2006): http://www.defra.gov.uk/vla/Default.htm

VLA, IAH and QUB (2005) *Mycobacterium bovis* pathogenesis: http://www.2.defra.gov.uk/research/project_data

Vordermeier , H. M., Cockle, P. J., Whelan, A. O., Rhodes, S. Chambers, M. A., Clifford, D., Huygen, T., Tascon, R., Lowrie, D., Colston, M. J., Hewinson, R. G. (2000) Effective vaccination of cattle with the mycobacterial antigens MPB83 and MPB70 does not compromise the specificity of the comparative intradermal tuberculin skin test. *Vaccine.* **19**: 1246-55

Vordermeier , H. M., Rhodes, S. G., Dean, G., Goonetilleke, N., Huygen, K., Hill, A. V. S., Hewinson, R. G., Gilbert, S. C. (2004) Cellular immune responses induced in cattle by heterologous prime-boost vaccination using recombinant viruses and bacilli Calmette-Guérin. *Immunology*. **112**: 461-470

Vordermeier , H. M., Whelan, A., Cockle, P. J., Farrant, L., Palmer, N., Hewinson, R. G. (2001) Use of synthetic peptides derived from the antigens ESAT-6 and CFP-10 for differential diagnosis of bovine tuberculosis in cattle. *Clinical and Diagnostic Laboratory Immunology*. **8** (3): 571-8

Vordermeier, H. M., Chambers, M. A., Cockle, P. J., Whelan, A. O., Simmons, J., Hewinson, R. G. (2002) Correlation of ESAT-6 specific gamma interferon production with pathology in cattle following *Mycobacterium bovis* BCG vaccination against experimental bovine tuberculosis. *Infection and Immunity*. **70** (6): 3026-32

Vordermeier, H. M., Cockle, P. C., Whelan, A., Rhodes, S., Palmer, N., Bakker, D., Hewinson, R. G. (1999) Development of diagnostic reagents to differentiate between *Mycobacterium bovis* BCG vaccination and *M. bovis* infection in cattle. *Clinical and Diagnostic Laboratory Immunology*. **6** (5): 675-82

Vordermeier, H. M., Hewinson, R. G. (2006) Development of cattle TB vaccines in the UK. *Veterinary Immunology and Immunopathology*. **112**: 38-48

Wacker, M. J., Godard, M. P. (2005) Analysis of one-step and two-step real-time RT-PCR using SuperScript III. *Journal of Biomolecular Techniques*. **16** (3): 266-71

Wade, H. W. (1952) Demonstration of acid-fast bacilli in tissue sections. *American Journal of Pathology.* **28** (1): 157-70

Waldvogel, A. S., Lepage, M. F., Zakher, A., Reichel, M. P., Eicher, R., Heussler, V. T. (2004) Expression of interleukin 4, interleukin 4 splice variants and interferon gamma mRNA in calves experimentally infected with *Fasciola hepatica*. *Veterinary Immunology and Immunopathology*. **97** (1-2): 53-63

Wangoo, A., Johnson, L., Gough, J., Ackbar, R., Inglut, S., Hicks, D., Spencer, Y., Hewinson, G., Vordermeier, M. (2005) Advanced granulomatous lesions in *Mycobacterium bovis*-infected cattle are associated with increased expression of type I procollagen, gammadelta (WC1+) T cells and CD 68+ cells. *Journal of Comparative Pathology*. **133** (4): 223-34

Watanabe, Y., Watari, E., Matsunaga, I., Hiromatsu, K., Dascher, C. C., Kawashima, T., Norose, Y., Shimizu, K., Takahashi, H., Yano, L., Sugita, M. (2006) BCG vaccine elicits both T-cell mediated and humoral immune responses directed against mycobacterial lipid components. *Vaccine*. **24** (29-30): 5700-7

Waters, W. R., Palmer, M. V., Nonnecke, B. J., Thacker, T. C., Scherer, C. F., Estes, D. M., Jacobs, W. R. Jr., Glatman-Freedman, A., Larsen, M. H. (2007) Failure of a *Mycobacterium tuberculosis* DeltaRD1 DeltapanCD double deletion mutant in a neonatal calf aerosol *M. bovis* challenge model: comparisons to responses elicited by *M. bovis* bacille Calmette Guerin. *Vaccine*. **25** (45): 7832-40

Wayne, L. G., Diaz, G. A. (1967) Autolysis and secondary growth of *Mycobacterium tuberculosis* in submerged culture. *Journal of Bacteriology*. **93** (4): 1374-81

Wayne, L. G., Sohaskey, C. D. (2001) Nonreplicating persistence of mycobacterium tuberculosis. *Annual Review of Microbiology*. **55**: 139-63

Wedlock , D. N., Keen, D. L., McCarthy, A. R., Andersen, P., Buddle, B. M. (2002) Effect of different adjuvants on the immune responses of cattle vaccinated with *Mycobacterium tuberculosis* culture filtrate proteins. *Veterinary Immunology and Immunopathology*. **86**: 79-88

Wedlock, D. N., Denis, M., Painter, G. F., Ainge, G. D., Vordermeier, H. M., Hewinson, R. G., Buddle, B. M. (2008) Enhanced protection against bovine tuberculosis after coadministration of *Mycobacterium bovis* BCG with a Mycobacterial protein vaccine-adjuvant combination but not after coadministration of adjuvant alone. *Clinical and Vaccine Immunology*. **15** (5): 765-72

Wedlock, D. N., Denis, M., Skinner, M. A., Koach, J., le Lisle, G. W., Vordermeier, H. M., Hewinson, R. G., van Drunen Littel-van den Hurk, S., Babiuk, L. A., Hecker, R., Buddle, B. M. (2005) Vaccination of cattle with a CpG oligodeoxynucleotide-formulated mycobacterial protein vaccine and *Mycobacterium bovis* BCG induces levels of protection against bovine tuberculosis superior to those induced by vaccination with BCG alone. *Infection and Immunity*. **73** (6): 3540-6

Wedlock, D. N., Denis, M., Vordermeier, H. M., Hewinson, R. G., Buddle, B. M. (2007) Vaccination of cattle with Danish and Pasteur strains of *Mycobacterium bovis* BCG induce different levels of IFN gamma post vaccination, but induce similar levels of protection against bovine tuberculosis. *Veterinary Immunology and Immunopathology*. **118** (1-2): 50-8

Wedlock, D. N., Skinner, M. A., Parlane, N. A., Vordermeier, H. M., Hewinson, R. G., de Lisle, G. W., Buddle, B. M. (2003) Vaccination with DNA vaccines encoding MPB70 or MPB83 or a MPB70 DNA prime-protein boost does not protect cattle against bovine tuberculosis. *Tuberculosis (Edinb)*. **83** (6): 339-49

Wedlock, D. N., Vesosky, B., Skinner, M. A., de Lisle, G. W., Orme, I. M., Buddle, B. M. (2000) Vaccination of cattle with *Mycobacterium bovis* culture filtrate proteins and interleukin-2 for protection against bovine tuberculosis. *Infection and Immunity*. **68** (10): 5809-15

Wellcome Trust Sanger Institute (accessed January 2008): http://www.sanger.ac.uk/Projects/Microbes/

Wells, W. F., Ratcliffe, H. L., Crumb, C. (1948) On mechanics of droplet nuclei infection: quantitative experimental air-borne tuberculosis in rabbits. *American Journal of Hygiene*. **47**: 11-28

Welsh, M. D., Cunningham, R. T., Corbett, D. M., Girvin, R. M., McNair, J., Skuce, R. A., Bryson, D. G., Pollock, J. M. (2005) Influence of pathological progression on the balance between cellular and humoral immune responses in bovine tuberculosis. *Immunology*. **114** (1): 101-111

Whelan, A. O., Wright, D. C., Chambers, M. A., Singh, M., Hewinson, R. G., Vordermeier, H. M. (2008) Evidence for enhanced central memory priming by live *Mycobacterium bovis* BCG vaccine in comparison with killed BCG formulations. *Vaccine*. **26** (2): 166-73

Whipple, D. L., Bolin, C. A., Miller, J. M. (1996) Distribution of lesions in cattle infected with *Mycobacterium bovis*. *Journal of Veterinary Diagnostic Investigation*. **8** (3): 351-4

White, P.C., Benhin, J.K. (2004) Factors influencing the incidence and scale of bovine tuberculosis in cattle in southwest England. *Preventive Veterinary Medicine*. **63** (1-2): 1-7

Widdison, S., Schreuder, L. J., Villarreal-Ramos, B., Howard, C. J., Watson, M., Coffey, T. J. (2006) Cytokine expression profiles of bovine lymph nodes: effects of *Mycobacterium bovis* infection and bacilli Calmette-Guérin vaccination. *Clinical and Experimental Immunology*. **144**: 281-289

Widdison, S., Watson, M., Piercy, J., Howard, C., Coffey, T.J. (2008) Granulocyte chemotactic properties of *M. tuberculosis* versus *M. bovis*-infected bovine alveolar macrophages. *Molecular Immunology*. **45** (3): 740-9

Wiedorn, K. H., Olert, J., Stacey, R. A., Goldmann, T., Kuhl, H., Matthus, J., Vollmer, E., Bosse, A. (2002) HOPE-a new fixing technique enables preservation and extraction of high molecular weight DNA and RNA of > 20 kb from paraffin-embedded tissues. Hepes-glutamic acid buffer mediated organic solvent protection effect. *Pathology: Research and Practice*. **198**: 735

Wiker, H. G., Nagai, S., Hewinson, R. G., Russell, W. P., Harboe, M. (1996) Heterogeneous expression of the related MPB70 and MPB83 proteins distinguish various substrains of *Mycobacterium bovis* and *Mycobacterium tuberculosis* H37Rv. *Scandinavian Journal of Immunology*. **43**: 374-380

Witchell, J., Varshney, D., Gajjar, T., Wangoo, A., Goyal, M. (2008) RNA isolation and quantitative PCR from HOPE and formalin fixed bovine lymph node tissues. *Pathology: Research and Practice*. **204** (2): 105-11

Wood, P. R., Corner, L. A., Rothel, J. S., Baldock, C., Jones, S. L., Cousins, D. B., McCormick, B. S., Francis, B. R., Creeper, J., Tweddle, N. E. (1991) Field comparisons of the interferon-gamma assay and the intradermal tuberculin test for the diagnosis of bovine tuberculosis. *Australian Veterinary Journal*. **68** (9): 286-90

Xu, L. L., Warren, M. K., Rose, W. L., Gong, W., Wang, J. M. (1996) Human recombinant monocyte chemotactic protein and other C-C chemokines bind and induce directional migration of dendritic cells *in vitro*. *Journal of Leukocyte Biology*. **60** (3): 365-71

Xue, T., Stavropoulos, E., Yang, M., Ragno, S., Vordermeier, M., Chambers, M., Hewinson, G., Lowrie, D. B., Colston, M. J., Tascon, R. E. (2004) RNA encoding the MPT83 antigen induces protective immune responses against *Mycobacterium tuberculosis* infection. *Infection and Immunity*. **72**: 6324-6329

Yamamoto, T., Lasco, T. M., Uchida, K., Goto, Y., Jeevan, A., McFarland, C., Ly, L., Yamamoto, S., McMurray, D. N. (2007) *Mycobacterium bovis* BCG vaccination modulates TNF-alpha production after pulmonary challenge with virulent *Mycobacterium tuberculosis* in guinea pigs. *Tuberculosis (Edinb).* **87** (2): 155-65

Yang, S. B., Song, C. H., Yang, C. S., Kim, S. Y., Lee, K. S., Shin, A. R., Lee, J. S., Nam, H. S., Kim, H. J., Park, J. K., Paik, T. H., Jo, E. K. (2005) Role of the phosphatidylinositol 3-kinase and mitogen-activated protein kinase pathways in the secretion of tumour necrosis factor-alpha and interleukin-10 by the PPD antigen of *Mycobacterium tuberculosis*. *Journal of Clinical Immunology*. **25** (5): 482-90

Young, J. S., Gormley, E., Wellington, E. M. (2005) Molecular detection of *Mycobacterium bovis* and *Mycobacterium bovis* BCG (Pasteur) in soil. *Applied and Environmental Microbiology*. **71** (4): 1946-52

Zahrt, T.C. (2003) Molecular mechanisms regulating persistent *Mycobacterium tuberculosis* infection. *Microbes and Infection*. **5** (2); 159-67

Zhu, G., Xiao, H., Mohan, V. P., Tanaka, K., Tyagi, S., Tsen, F., Salgame, P., Chan, J. (2003) Gene expression in the tuberculous granuloma: analysis by laser capture microdissection and real-time PCR. *Cellular Microbiology*. **5** (7): 445-453

Zinkernagel, R. M. (2000) On immunological memory. *Philosophical Transactions of the Royal Society of London. Series B, Biological Sciences*. **355** (1395): 369-71

Appendix

Appendix 1

Oligonucleotide sequences and molecular properties

Genetic sequences of the designed GAPDH, IFN-γ, TNF-α, IL10 and IL4 primer and probe oligonucleotides specific to the bovine mRNA sequence (BLAST):

Blue: Forward and Reverse primers

Red: Dual labelled probe

GAPDH – PCR product 87 base pairs long

BLAST accession number: AJ000039 (Bos Taurus mRNA)

CGCATCGGGCGCCTGGTCACCAGGGCTGCTTTTAATTCTGGCAAAGTGGACATCGTCGCCATCAATGACCCCTTCATTGA
CCTTCACTACATGGTCTACATGTTCCAGTATGATTCCACCCACGGCAAGTTCAACGGCACAGTCAAGGCAGAGAACGGGA
AGCTCGTCATCAATGGAAAGGCCATCACCATCTTCCAGGAGCGAGATCCTGCCAACATCAAGTGGGGTGATGCTGGTGCT
GAGTATGTGGTGGAGTCCACTGGGGTCTTCACTACCATGGAGAAGGCTGGGGCTCACTTGAAGGGTGGCGCCAAGAGGG
TCATCATCTCTGCACCTTCTGCCGATGCCCCCATGTTTGTGATGGGCGTGAACCACGAGAAGTATAACAACACCCTCAAGA
TTGTCAGCAATGCCTCCTGCACCACCAACTGCTTGGCCCCCCTGGCCAAGGTCATCCATGACCACTTTGGCATCGTGGAG
GGACTTATGACCACTGTCCACGCCATCACTGCCACCCAGAAGACTGTGGATGGCCCCTCCGGGAAGCTGTGGCGTGACG
GCCGAGGGGCTGCCCAGAATATCATCCCTGCTTCTACTGGCGCTGCCAAGGCCGTGGGCAAGGTCATCCCTGAGCTCAA
CGGGAAGCTCACTGGCATGGCCTTCCGCGTCCCCACTCCCAACGTGTCTGTTGTGGATCTGACCTGCCGCCTGGAGAAA
CCTGCCAAGTATGATGAGATCAAGAAGGTGGTGAAGCAGGCGTCAGAGGGCCCTCTCAAGGGCATTCTAGGCTACACTGA
GGACCAGTT

IFN-γ – PCR product 70 base pairs long

BLAST accession number: NM_174086 (Bos Taurus mRNA)

ATTAGAAAAGAAAGATCAGCTACCTCCTTGGGACCTGATCATAACACAGGAGCTACCGATTTCAACTACTCCGGCCTAACT
CTCTCCTAAACAATGAAATATACAAGCTATTTCTTAGCTTTACTGCTCTGTGGGCTTTTGGGTTTTTCTGGTTCTTATGGCCA
GGGCCAATTTTTTAGAGAAATAGAAAACTTAAAGGAGTATTTTAATGCAAGTAGCCCAGATGTAGCTAAGGGTGGGCCTCT
CTTCTCAGAAATTTTGAAGAATTGGAAAGATGAAAGTGACAAAAAAAATTATTCAGAGCCAAATTGTCTCCTTCTACTTCAAAC
TCTTTGAAAACCTCAAAGATAACCAGGTCATTCAAAGGAGCATGGATATCATCAAGCAAGACATGTTTCAGAAGTTCTTGAA
TGGCAGCTCTGAGAAACTGGAGGACTTCAAAAAGCTGATTCAAATTCCGGTGGATGATCTGCAGATCCAGCGCAAAGCCA
TAAATGAACTCATCAAAGTGATGAATGACCTGTCACCAAAATCTAACCTCAGAAAGCGGAAGAGAAGTCAGAATCTCTTTCG
AGGCCGGAGAGCATCAACGTAATGGTCCTCCTGCCTGCAATATTTGAATTTTTAAATCTAAATCTATTTATTAATATTTAATA
TTTTACATTATTTATATGGGGGATATATATTTAGACATCAAAGTATTTATAATAGTAACTTTTATGTCATGAAAATGAGTATCT
ATTAATATATGTGTTATTTATAATTCCTGTATCCTGTGACTATTTCACTTGACCCTTTTTTTTCTGAGTAACTAGGCAAGTCTA
TGGGATTTCAAGGTTTTATCTCAGGGGCCAACTAGGCAGCTAACCTAAGCAAGAATCTGTGGGTTGTGCACTTATTTCACT
TGATGATGTAATGAATGCTGATAAATGAAATGATGCCATCTAGTCACTACTTATCTGAGACTAGATCTGGATTCTGAGCCAC
TACTTTGATGGCATGTCAGACAGCACTTGAATGTGTCAGGCTATATGAC

TNF-α RNA – PCR product 64 base pairs long

BLAST accession number: AF348421 (Bos Taurus mRNA)

ATGAGCACCAAAAGCATGATCCGGGATGTGGAGCTGGCGGAGGAGGTGCTCTCCGAGAAAGCAGGGGGCCCCCAGGGC
TCCAGAAGTTGCTTGTGCCTCAGCCTCTTCTCCTTCCTCCTGGTTGCAGGAGCCACCACGCTCTTCTGCCTGCTGCACTTC
GGGGTAATCGGCCCCCAGAGGGAAGAGCAGTCCCCAGGTGGCCCCTCCATCAACAGCCCTCTGGTTCAAACACTCAGGT
CCTCTTCTCAAGCCTCAAGTAACAAGCCGGTAGCCCACGTTGTAGCCGACATCAACTCTCCGGGGCAGCTCCGGTGGTGG
GACTCGTATGCCAATGCCCTCGTGGCCAACGGTGTGAAGCTGGAAGACAACCAGCTGGTGGTGCCTGCTGACGGGCTTT
ACCTCATCTACTCACAGGTCCTCTTCAGGGGCCAAGGCTGCCCTTCCACCCCCTTGTTCCTCACCCACACCATCAGCCGC
ATTGCAGTCTCCTACCAGACCAGGGTCAACATCCTGTCTGCCATCAAGAGCCCTTGCCACAGGGAGACCCCAGAGTGGGC
TGAGGCCAAGCCCTGGTACGAACCCATCTACCAGGGAGGAGTCTTCCAGCTGGAGAAGGGAGATCGCCTCAGTGCTGAG
ATCAACCTGCCGGACTACCTGGACTATGCCGAGTCTGGGCAGGTCTACTTTGGGATCATCGCCCTGTGA

IL10 – PCR product 69 base pairs long

BLAST accession number: NM_174088 (Bos Taurus mRNA)

ATGCATAGCTCAGCACTACTCTGTTGCCTGGTCTTCCTGGCTGGGGTGGCAGCCAGCCGAGATGCGAGCACCCTGTCTGA
CAGCAGCTGTATCCACTTGCCAACCAGCCTGCCCCACATGCTGCGGGAGCTCCGAGCTGCCTTCGGCGAGGCGAAGACT
TTCTTTCAAATGAAGGACCAACTGCACAGCTTACTGTTGACCCAGTCTCTGCTGGATGACTTTAAGGGTTACCTGGGTTGC
CAAGCCTTGTCGGAAATGATCCAGTTTTACCTGGAAGAGGTGATGCCACAGGCTGAGAACCACGGGCCTGACATCAAGGA
GCACGTGAACTCACTGGGGGAGAAGCTGAAGACCCTGCGGCTGCGGCTGCGGCGCTGTCATCGCTTTCTGCCCTGCGAA
AACAAGAGCAAGGCGGTGGAGAAGGTGAAGAGAGTCTTCAGTGAGCTCCAAGAGAGGGGTGTCTACAAAGCCATGAGTG
AGTTTGACATCTTCATCAACTACATAGAAACCTACATGACAACGAAGATGCAAAAGTGAAGCATTCTAGGGAAGAAGACCT
CCAGGATGGTGACTCTACTAGACTCCATGACGTAAACGGAAGACCTCTGAAATCCAATCCAGGGTTCTGGGAGAGCAGAG
CCAGCTCCCTGGAGACCTGTACTGTGCCTCTCCCCTAGAGTATTTATTACCTCTGATACCTCAGCTCCCACATATATTTATT
TACTGAGCTTCTCTGTGAACTATT

IL4 – PCR product 66 base pairs long

BLAST accession number: NM_173921 (Bos Taurus mRNA)

TGCATTGTTAGCGTCTCCTGGTAAACTAATTGTCTCACATTGTCAGTGCAAATAGAGATACTATTAATGGGTCTCACCTACC
AGCTGATCCCAGTGCTGGTCTGCTTACTGGTATGTACCAGTCACTTCGTCCATGGACACAAGTGTGATATTACCTTAGCAG
AGATCATCAAAACGCTGAACATCCTCACAACGAGAAAGAATTCATGCATGGAGCTGCCTGTAGCAGACGTCTTTGCTGCCC
CAAAGAACACAACTGAGAAGGAAACCTTCTGCAGGGTTGGAATTGAGCTTAGGCGTATCTACAGGAGCCACACGTGCTTG
AACAAATTCCTGGGCGGACTTGACAGGAATCTCAACAGCTTGGCAAGCAAGACCTGTTCTGTGAATGAAGCCAAGACGAG
CACAAGTACGCTGAAAGACCTCTTGGAAAGGCTAAAGACGATTATGAAGGAGAAATACTCCAAGTGTTGAAGCTGAATATT
TTAATTTATGAGTTTTTTATAGCCTTATTTTAAACATATTTATATATCTATAACTCATCATAAAATAAAATATATGTAGAGTCTG
AAAAAA

Table A1: Oligonucleotide (forward primer, reverse primer and dual labelled probes) properties for each gene; GAPDH, IFN-γ, TNF-α, IL10 and IL4 including the potential for the nucleotide to self-anneal (complimentary base sequences).

Oligonucleotide	Base length	Melting temperature (T_m) Salt adjusted method (°C)	GC content (%)	Potential for self annealing
GAPDH				
Forward	19	60	58	None
Reverse	20	60	55	None
Probe	26	70	54	Potential hairpin
IFN-γ				
Forward	23	63	48	None
Reverse	20	63	60	None
Probe	25	69	56	2 hairpins
TNF-α				
Forward	19	62	63	None
Reverse	21	61	52	None
Probe	21	67	67	None
IL10				
Forward	19	62	63	None
Reverse	21	63	57	None
Probe	23	68	61	None
IL4				
Forward	20	58	50	None
Reverse	20	58	50	None
Probe	19	62	63	None

Calculations performed on OligoCalc: an online oligonucleotide properties calculator, www.basic.northwestern.edu+oligocalc.html

Appendix 2

Quantitative RT-PCR: method development

Aim: To optimise cytokine mRNA detection by qRT-PCR using firstly SYBR green methodology to ascertain product specificity followed by dual labelled probe methodology to explore reagent concentrations.

Objectives:

1. Total RNA was extracted from fresh *M. bovis* infected bovine lymph node tissue as per the trizol/chloroform method described in chapter 2. The total RNA was then applied to real time PCR using primer sequences for GAPDH, IFN-γ, TNF-α, IL10, IL4 and a SYBR green method. Following amplification of the target sequence, the PCR product was subjected to increasing temperatures and a dissociation curve plotted to reveal product specificity. Different annealing temperatures were applied to the PCR reactions to ascertain the correct temperature.
2. The total RNA was then applied to dual labelled RT-PCR using specifically designed fluorescent probes to explore the appropriate concentrations of template, primers and probes.

SYBR Green qPCR

Annealing temperature optimisation:

Each of the gene primer sets were designed with an annealing temperature close to 60^{o}C (using the salt adjusted method, Appendix 1; Table A1). To confirm this, the primer sets were applied to real time PCR using SYBR green technology. SYBR green is an intercalating dye that binds to double stranded targets and fluoresces. Therefore, as the number of copies of the amplified target gene increased during PCR, the fluorescence of SYBR green also increased. Following amplification, the PCR product was subjected to a graduated rise in temperature and the level of SYBR green fluorescence recorded at each point. Each target sequence had a particular melting temperature (T_m), and so as this temperature was reached, the PCR product dissociated and produced a specific drop in SYBR green fluorescence. The product should produce only one peak to represent the efficiency of the primer set and also the optimised PCR conditions. To confirm the annealing temperature of each primer set, the PCR machine was

set to apply a graduating annealing temperature across the PCR plate (+/- 10°C of 60°C). In analysis, the PCR reaction that produced a single, clear dissociation curve revealed the optimised annealing temperature for that primer set.

Method

Real time qRT-PCR using SYBR® Green I dye was carried out according to the manufacturers guidelines for the ABsolute™ QRT-PCR Mix (ABgene, UK). A standard reaction mixture (Table A3) was produced and aliquoted (25 µl) into a 96 well clear plate (ABgene, UK) followed by the total RNA template (extracted from fresh *M. bovis* infected lymph node tissue). All reactions were set up on ice.

Table A2: Reagents and suppliers for Dual labelled and SYBR Green qRT-PCR

Reagent	Supplier
ABsolute QRT-PCR SYBR Green mix	ABgene (Epsom, Surrey, UK)
Quantitect™ Probe RT-PCR kit	Qiagen (Crawley, Sussex, UK)
Clear Seal Diamond	ABgene (Epsom, Surrey, UK)
THERMO-FAST ® 96 PCR Plate	Abgene (Epsom, Surrey, UK)
Primer and Probe oligonucleotides	Biomers.net (Ulm, Germany)

Table A3: Standard reaction mixture components used for SYBR® Green qRT-PCR.

Reaction mixture components	Final Concentration
ABsolute™ QRT-PCR SYBR® Green Mix	1x
RNA template	100 ng
Forward Primer	300 nmoles
Reverse Primer	300 nmoles
ABsolute™ QRTase Blend	2 U/µl
RNase-free water	Up to 25 µl

Control reactions were performed with the standard reaction mixture excluding the ABsolute™ QRTase Blend for the no RT negative and substituting the RNA sample for RNase-free water in the no template negative control. Each reaction was completed in duplicate or triplicate. The reaction was carried out within a Quantica Real Time Nucleic Acid Detection System (Techne, UK) to a specific program (Table A4).

Table A4: Amplification program for SYBR® Green qRT-PCR.

First Strand Synthesis 1 cycle	47°C: 30 minutes
QRTase inactivation and polymerase activation 1 cycle	95°C: 15 minutes
Denaturation, Anneal/ Extension 35 cycles	95°C: 15 seconds 60°C: 1 minute
Denaturation 1 cycle	95°C: 30 seconds
Annealing 1 cycle	+/- 10°C of 60°C: 30 seconds
Dissociation Curve 80 cycles	55°C: 10 second hold Increase set point temp. by 0.5°C per cycle

The fluorescent SYBR® Green reading was taken at the annealing/extension stage and dissociation curve (80 cycles at 0.5°C increments) stage (Table A4). The fluorescent readings at the annealing/extension stage were used in quantitative analysis of the specific target gene by calculating a crossing point value. The software (Techne, UK) automatically calculated the crossing point value using the point at which the fluorescence of a reaction reaches a set threshold level relative to the corresponding PCR cycle number. The fluorescent readings taken at the dissociation curve stage were used to produce a dissociation curve (plotting fluorescence versus temperature). It was then possible to determine the specificity of the amplified product and calculate its melting temperature (T_m) and annealing temperature.

Results

Following PCR amplification and the dissociation of the PCR product, each primer set produced a single, clear peak on the dissociation curve at an annealing temperature of 60°C. The dissociation peak of GAPDH PCR product (using 60°C annealing temperature) is displayed in Figure A1 and is representational of the dissociation peaks observed for IFN-γ, TNF-α, IL10 and IL4. It was therefore decided to continue to use 60°C as the annealing temperature of each primer set in subsequent PCR reactions.

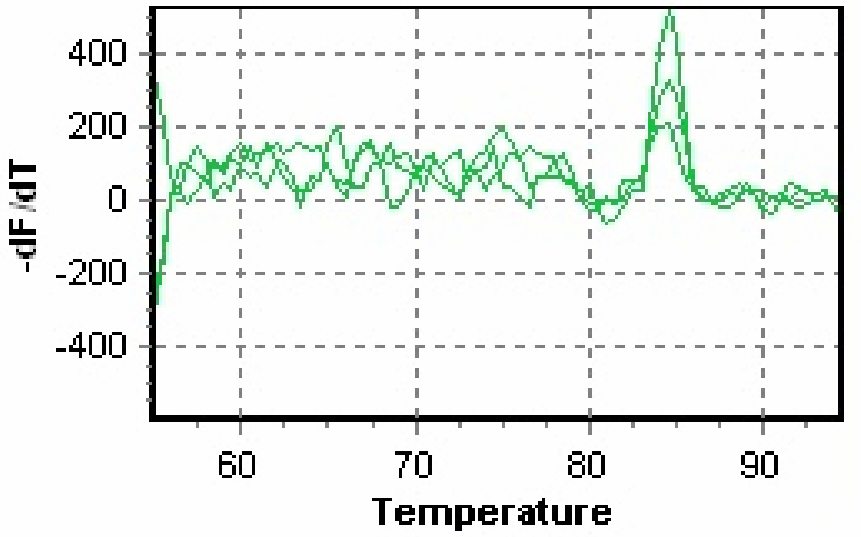

Figure A1: Dissociation peak of GAPDH PCR product (T_m approximately 84°C) following SYBR green RT-PCR. Total RNA extracted from freshly dissected *M. bovis* infected lymph node tissue was used as the template (100 ng) accompanied by GAPDH primers (300 nmoles). The PCR reaction involved an annealing step at 60°C and was performed in triplicate. The graph shows the change in PCR product over varying temperatures (reflected by the negative derivative of the SYBR green fluorescence (dF) relative to the temperature (dT)). As the gradually increasing temperature reaches the specific melting temperature of the PCR product (T_m), the product dissociates and causes a sharp reduction in SYBR green fluorescence. By plotting the data as fluorescence relative to temperature (-dF/dT), the point of dissociation produces a peak on the graph. The presence of one single peak reflects the purity of the PCR product and subsequently the specificity of both primers and PCR conditions (including annealing temperature).

Dual Labelled Probe qRT-PCR

Template concentration:

Due to the importance of conserving the total RNA template extracted from the bovine lymph node tissues, experiments were performed to optimise the concentration of total RNA applied to each reaction. Total RNA concentrations of between 10 and 300 ng were applied to dual labelled probe qRT-PCR using the GAPDH primer set.

Primer and dual labelled probe concentration optimisation:

The efficiency of the reaction and therefore the accuracy of the cytokine analysis were dependent upon the optimisation of the primer and probe concentrations. The primer concentration range as recommended by Qiagen (Crawley, Sussex, UK) was between 400 and 1,000 nmoles. A matrix was used to perform reactions using different primer concentrations (400, 700 and 1,000 nmoles) in nine different combinations of forward and reverse primer (Table A5). The probe concentration range as recommended by Qiagen (Crawley, Sussex, UK) was between 100 and 200 nmoles. QRT-PCR reactions were performed using the optimised primer concentrations and probe concentrations of 100, 150 and 200 nmoles. The primer combination and probe concentration with the lowest crossing point value whilst still maintaining the fluorescence were the optimised values for future experiments.

Table A5: Combinations of reverse and forward primer concentrations (nmoles) used to optimise dual labelled probe qRT-PCR

Forward / Reverse	400 nmoles	700 nmoles	1,000 nmoles
400 nmoles	400/400	400/700	400/1,000
700 nmoles	700/400	700/700	700/1,000
1,000 nmoles	1,000/400	1,000/700	1,000/1,000

Method

Real time qRT-PCR using dual labelled probes was carried out according to the manufacturers' guidelines for Quantitect™ Probe RT-PCR (Qiagen, Crawley, Sussex, UK). A standard reaction mixture (Table A6) was produced and then aliquoted (25 µl) into a 96 well plate followed by the total RNA template extracted from *M. bovis* infected bovine lymph node tissue. All reactions were set up on ice.

Table A6: Standard Reaction mixture components for Dual labelled probe qRT-PCR

Reaction mixture components	Final Concentration
2x QuantiTect Probe RT-PCR Master Mix	1x
RNA template	10-300 ng
Forward Primer	400-1,000 nmoles
Reverse Primer	400-1,000 nmoles
Probe	100-200 nmoles
QuantiTect RT Mix	0.5 µl/reaction
RNase-free water	Up to 25 µl

Control reactions were performed with the standard reaction mixture excluding the QuantiTect RT Mix for the no RT negative and the RNA sample for the no template negative control. Each reaction was completed in duplicate. The reaction was carried out within a Quantica Real Time Nucleic Acid Detection System (Techne, UK) to a specific program (Table A7).

Table A7: Amplification program for dual labelled probe qRT-PCR

Reverse Transcription 1 cycle	 50°C: 30 minutes
Initial Activation step 1 cycle	 95°C: 15 minutes
Denaturation, annealing/extension 40 cycles	 94°C: 15 seconds 60°C: 1 minute

The fluorescent dye reading was taken at the annealing/extension stage (Table A7). The crossing point value was calculated for each reaction and used to determine the relative amount of product formed.

Results

Template concentration:

Table A8: Dual labelled qRT-PCR crossing point (Cp) values of GAPDH mRNA expression (primer and probe concentration 400 and 200 nmoles respectively) in varying quantities of total RNA (10-300 ng) extracted from *M. bovis* infected fresh lymph node tissue

Total RNA template concentration (ng)	Replicate 1 Cp value	Replicate 2 Cp value	Mean Cp value	Standard error of the mean
300	24.67	21.61	23.14	1.53
200	24.69	22.89	23.79	0.90
100	22.25	22.64	22.44	0.19
50	24.68	22.75	23.72	0.96
10	26.94	25.99	26.46	0.47
No RT negative	Negative	Negative		
No template negative	Negative	Negative		

Real time PCR was performed using different concentrations of total RNA extracted from *M. bovis* infected bovine lymph nodes (10-300 ng, Table A8). The reactions using 100 ng of template produced the lowest crossing point values (mean 22.44) in addition to the replicates displaying consistent results (showing the smallest standard error of the mean 0.19, Table A8). The data displayed for GAPDH (Table A8) was representational of that obtained for the other four target genes and it was therefore decided to use 100 ng of total RNA in all future PCR experiments.

Primer concentration:

Real time PCR using different combinations of forward and reverse primer concentrations had an affect on the fluorescence and subsequently the resulting crossing point value of each reaction (Figure A2). The GAPDH primer combination with the lowest crossing point value was 700/700 nmoles (22.2) and this result was also reproduced for the four other gene target primer sets.

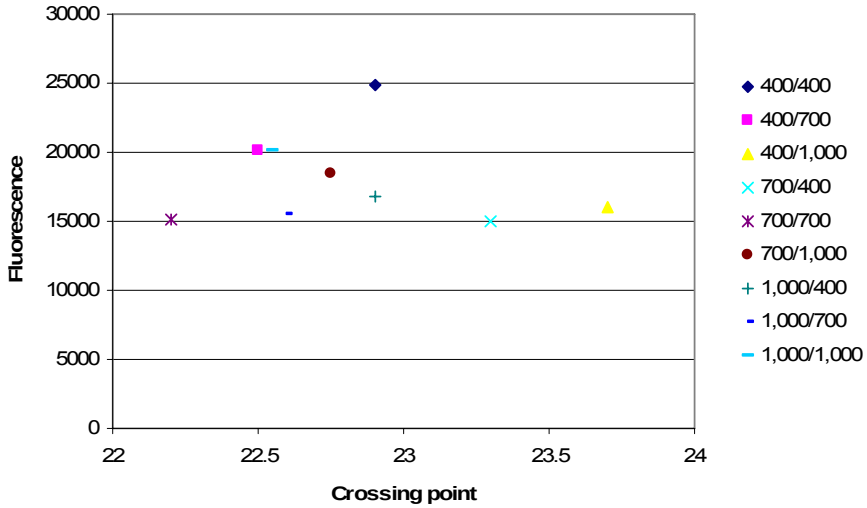

Figure A2: The effect of different GAPDH primer concentrations on the fluorescence and crossing point values for individual PCR reactions. Total RNA extracted from freshly dissected *M. bovis* infected lymph nodes was used as a template (100ng) accompanied by GAPDH primers (nine combinations of forward and reverse concentrations between 400 and 1,000 nmoles) and probes (200 nmoles). The data are displayed as the mean of triplicate reactions, each set involving a different combination of forward and reverse prime concentration.

Probe optimisation:

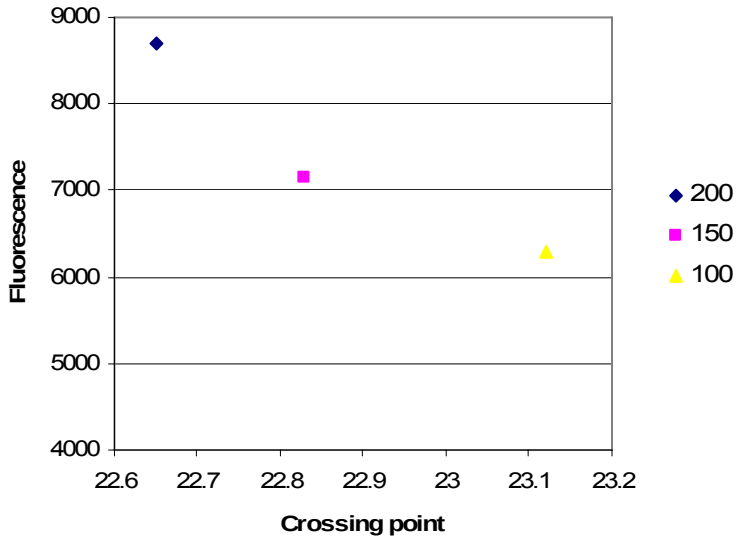

Figure A3: The effect of different GAPDH probe concentrations on the fluorescence and crossing point values for individual PCR reactions. Total RNA extracted from freshly dissected *M. bovis* infected lymph nodes was used as a template (100ng) accompanied by GAPDH primers (700n nmoles) and varying probe concentrations (100, 150 and 200 nmoles). The data are displayed as the mean of triplicate reactions, each set involving a different probe concentration.

Figure A3 displays the results from varying the probe concentration during GAPDH real time PCR. The probe concentration 200 nmoles produced the lowest crossing point value (22.65) and the highest level of fluorescence (8700). As the probe concentration decreased to 150 and 100 nmoles, the crossing point value as decreased (22.83 and 23.12, respectively, Figure A3).

Summary:

The oligonucleotide primer sets designed for GAPDH, IFN-γ, TNF-α, IL10 and IL4 produced single dissociation peaks following real time PCR using SYBR green methodology (represented by Figure A1). This signified the specificity of the primer sets. The larger and clearer dissociation peaks were obtained after applying an annealing temperature of 60^{o}C and so it was decided to use 60^{o}C in future PCR experiments.

As the main QPCR experiments were to be performed using dual labelled probe methodology, it was necessary to perform optimisation experiments using the probes. Due to the importance of conserving the bovine total RNA sample, template optimisation was performed (Table A8). It was revealed that 100 ng was sufficient to produce reliable and relatively low crossing point values. Following template optimisation, different combinations of forward and reverse primer concentrations were applied to the PCR reactions. The primer combination 700/700 nmoles produced the lowest crossing point values whilst maintaining the level of fluorescence (represented by Figure A2). Lastly, the probe concentration was optimised by applying 100, 150 or 200 nmoles of the dual labelled probe to each reaction. The results revealed that 200 nmoles of probe produced the lowest crossing point values and also the highest fluorescence (Figure A3).

The results reveal the effects of differing template, primer and probe concentrations on the sensitivity of the PCR reaction and therefore highlight the importance of being consistent with PCR conditions throughout mRNA expression studies. To aid reproducibility of the results, the concentrations of template, primer and probe (100ng, 700 nmoles and 200 nmoles, respectively) were maintained throughout the gene expression studies.

Available online at www.sciencedirect.com
ScienceDirect
Pathology – Research and Practice 204 (2008) 105–111
PATHOLOGY RESEARCH AND PRACTICE
www.elsevier.de/prp

ORIGINAL ARTICLE

RNA isolation and quantitative PCR from HOPE- and formalin-fixed bovine lymph node tissues

Jaydene Witchell[a], Dhaval Varshney[a], Trusha Gajjar[a], Arun Wangoo[b,1], Madhu Goyal[a,*]

[a]*School of Life Sciences, University of Hertfordshire, Hatfield, Herts AL10 9AB, UK*
[b]*Department of Pathology, Veterinary Laboratories Agency, Weybridge, Addlestone, Surrey KT15 3NB, UK*

Received 2 February 2007; accepted 13 September 2007

Abstract

The use of ribonucleic acid (RNA) extracted from Hepes glutamic acid buffer-mediated organic solvent protection effect (HOPE)-fixed tissues in quantitative reverse transcriptase polymerase chain reaction (qRT-PCR) is fairly novel. We compared qRT-PCR analysis of formalin- and HOPE-fixed, paraffin-embedded lymph node tissues from *Mycobacterium bovis*-infected cattle by extracting total RNA using a commercial kit (Ambion) and a Trizol method. RNA extracted from HOPE-fixed tissues showed comparable quantities between the commercial kit (82.7–107.9 μg/ml total RNA) and the Trizol method (87–161.1 μg/ml total RNA), displaying a high degree of integrity when analyzed by electrophoresis. RNA extracted from formalin-fixed tissues using the commercial kit produced similar concentrations (80.6–145.7 μg/ml total RNA) in comparison to the HOPE tissue; however, the integrity was compromised. Extraction of RNA from the formalin-fixed tissues using Trizol was unsuccessful.

Following qRT-PCR for glyceraldehyde-3-phosphate dehydrogenase (GAPDH), total RNA from HOPE-fixed tissues showed higher levels of target messenger ribonucleic acid (mRNA) (4.05×10^{-2} pg/100 ng total RNA using the commercial kit and 6.45×10^{-2} pg/100 ng total RNA using Trizol) in comparison to formalin-fixed tissues (5.69×10^{-4} pg/100 ng total RNA). This could be attributed to RNA degradation by exposure to formalin fixation. In conclusion, the HOPE fixative proved to be a better source for RNA extraction from cattle lymph nodes and subsequent qRT-PCR.

Keywords: Quantitative polymerase chain reaction; RNA extraction; HOPE fixative; Formalin fixative; *Mycobacterium bovis*

Introduction

Molecular techniques such as quantitative reverse transcriptase polymerase chain reaction (qRT-PCR) are rapidly becoming the preferred methods of disease prevention and diagnosis [8,14,17]. The study of nucleic acids, in particular ribonucleic acid (RNA), has provided vital information on the initial infection and advancement [18] of disease within challenged hosts.

Abbreviations: RNA, ribonucleic acid; mRNA, messenger ribonucleic acid; RT-PCR, reverse transcriptase polymerase chain reaction; qRT-PCR, quantitative RT-PCR; HOPE, Hepes glutamic acid buffer-mediated organic solvent protection effect; GAPDH, glyceraldehyde-3-phosphate dehydrogenase; bp, base pairs; CP value, crossing point value; FFPE, formalin-fixed paraffin-embedded

*Corresponding author. Tel.: +44 1707284624; fax: +44 1707285046.
E-mail address: m.goyal@herts.ac.uk (M. Goyal).
[1]Present address: Veterinary Medicines Directorate, Addlestone, Surrey KT15 3LS, UK.

0344-0338/$ - see front matter © 2007 Elsevier GmbH. All rights reserved.
doi:10.1016/j.prp.2007.09.002

The need for extracting RNA of a high quality is integral in this process [3,4], and considerable effort has been focused on developing methods that enable tissue fixation and archival storage without the associated nucleic acid degradation [2,7]. Archival storage of tissue samples has proved extremely useful in disease pathology and molecular biology due to providing a vast array of material morphologically conserved and with documented clinical backgrounds [6,7]. An example of this is rabies-infected brain tissue samples that were fixed in formalin in the late 1980s, and, 16 years postfixation, RT-PCR analysis of the disease was successfully performed [16].

One of the most widely used fixatives is neutral buffered formalin [2,13], however, much debate has surrounded its practical use for RNA extraction [4]. Variable results have been produced on the efficacy of formalin fixation due to its ability to form methylene bridges between amino acids within the RNA molecule, thus proving extraction methods less reliable [7,13]. As an alternative to formalin, the Hepes glutamic acid buffer-mediated organic solvent protection effect (HOPE) fixative has been shown to conserve RNA integrity [10,19] by avoiding amino acid cross linking. HOPE-fixed, paraffin-embedded human tissues have been used as a source for RNA extraction, producing transcript lengths of up to 2462 nucleotides and allowing the amplification of RT-PCR products of 183 bp in length [19]. More recently, RNA has been extracted from laser microdissected human lung tissue and applied in real-time RT-PCR [5]. However, as far as the authors are aware, HOPE fixation of animal tissues such as bovine material and its use in quantitative real-time PCR (providing actual data on bovine messenger ribonucleic acid (mRNA) concentration) is largely unknown.

In addition to a high-quality starting material, the extraction method itself is important in successfully procuring RNA [7]. Studies on RNA extraction from HOPE-fixed human tissues using the RNeasy kit (Qiagen, Germany), RNAzol B (Campro Scientific, Netherlands) and the GenoPrep mRNA kit on the GenoM- 48 Workstation (GenoVision, Norway) have provided RNA transcripts of variable quality [5,19]. The same methods were applied to formalin-fixed tissues; however, no quantifiable RNA was produced [19]. In this study, we have compared two RNA extraction methods, a commercial kit Optimum^{TM} FFPE kit (Ambion, UK) that is designed for extraction from formalin-fixed tissues [9] and a Trizol (Invitrogen, UK) method that has had much success in non-fixed material [1]. Both of these methods are new in application to HOPE-fixed cattle lymph node tissues. These methods were also performed on formalin-fixed cattle lymph node tissues. The extracted transcript was then analyzed by agarose gel electrophoresis and qRT-PCR to determine the quantity of housekeeping gene glyceraldehyde-3-phosphate dehydrogenase (GAPDH) mRNA. The results will provide information on the reproducibility of the fixative and extraction of RNA using different commercial sources.

Materials and methods

Sample preparation

Tissue samples of cervical and thoracic lymph nodes were taken at post mortem from *Mycobacterium bovis*-infected cattle at the Veterinary Laboratory Agency (VLA, Surrey). Cattle lymph node tissue samples were either fixed in 10% neutral-buffered formalin for 7 days or were incubated in aqueous protection solution HOPE for 14–36 h (0–4 °C) followed by incubation in a premixed ice-cold acetone solution (100 ml acetone and 100 μl HOPE II solution at 0–4 °C) for 2 h and then dehydration with freshly prepared acetone (0–4 °C) for 3×2 h (as per manufacturers instructions, DCS Innovative, Germany). Both fixation methods were followed by embedding of the sections in paraffin wax. The samples were cut into 10 μm sections and placed into microcentrifuge tubes (Eppendorf, $3 \times 10\,\mu m^2$ sections per tube) for subsequent RNA extraction. All tissue fixation and paraffin-embedding were performed at the VLA (Surrey). This study details a representative number of samples performed for total RNA extraction using both methods (three samples of each fixative for each method), however, the isolation procedure was repeated for each fixative more than 10 times to ensure reproducibility of the results.

RNA extraction

Optimum^{TM} formalin-fixed, paraffin-embedded (FFPE) kit (Ambion) method

Total RNA was extracted from both formalin- and HOPE-fixed, paraffin-embedded sections following the manufacturer's instruction manual. Briefly, samples were deparaffinized using xylene at room temperature and dissolved in Proteinase K (60 units/μl) solution (Ambion) at 37 °C for 6 h. RNA extraction buffer (Ambion, UK) was added to the supernatant and vortexed vigorously for 10 s. The sample was passed through a micro filter cartridge by centrifugation, followed by two washes and transferred to a micro elution tube into which 2×10 μl volumes of pre-heated (70 °C) RNA elution solution (Ambion, UK) were added. This was then left at room temperature for 1 min before centrifuging (16,500*g*) for 1 min to elute the RNA.

Trizol extraction method

Following deparaffinization using xylene at 57 °C, both formalin- and HOPE-fixed samples were pulverized in liquid nitrogen and submerged in Trizol (800 µl). The samples were left in a sonicating bath for intervals of 1 min (3 xs) before adding glycogen (1 mg/ml) to aid in pellet visualization. The sample was then passed through a syringe and needle (24G) before the addition of chloroform and the tube contents mixed by vortexing for 30 s. After centrifuging for 10 min at 4 °C, the supernatant was transferred into a new microcentrifuge tube with ice-cold isopropanol (500 µl) and incubated at −20 °C for 4 h. The microcentrifuge tube was then centrifuged for 15 min at 4 °C and the supernatant discarded. The resultant pellet was washed in 70% ethanol and resuspended in RNase-free water.

Spectrophotometry was performed to analyze the extracted total RNA for concentration and purity. Each sample was also run on agarose gel (1%) electrophoresis (using Tris Acetate EDTA (TAE) buffer) to determine the integrity of the RNA by visual analysis of the 28S and 18S rRNA bands.

Quantitative RT-PCR

Quantitative RT-PCR was performed using a dual labeled probe and primer set (amplicon of 87 bp) for the housekeeping gene GAPDH and the Quantitect™ Probe RT-PCR (Qiagen, UK) kit according to the manufacturers' guidelines. Briefly, QuantiTect RT-PCR mastermix (1x), forward primer (0.4 µm), reverse primer (0.4 µm), probe (0.2 µm), and QuantiTect RT mix were added to 100 ng of total RNA to a final volume of 25 µl. The RT-PCR reaction was carried out on a Quantica thermal cycler (Techne, UK) applying the following conditions: 50 °C for 30 min; 95 °C for 15 min; 50 cycles at 94 °C for 15 s, 60 °C for 1 min followed by a 4 °C hold. The probe was dual labeled with a FAM fluorophore at the 5′ end and a Black Hole Quencher (BHQ-1) at the 3′ end (Biomers, Germany). Each reaction was carried out in duplicate and included two negative controls (one excluding reverse transcriptase and another excluding the template). To produce a standard curve specific to GAPDH, an oligonucleotide (107 bp) was designed and manufactured (Biomers) identical to the amplicon produced during PCR of the GAPDH transcript. Known quantities of the designed oligonucleotide were then run alongside the unknown samples to produce a standard curve of crossing point (CP) number (the point at which the amplification curve crosses the threshold line) against concentration (picograms). The results were expressed as picograms of GAPDH mRNA in 100 ng of total RNA (pg/100 ng).

Results

Total RNA extracted from formalin- and HOPE-fixed, paraffin-embedded tissues using the Optimum™ FFPE kit (Ambion)

Total RNA extracted from both formalin- and HOPE-fixed tissues using the Optimum™ FFPE kit (Ambion) produced spectrophotometer results of comparative quantification (the three representative formalin-fixed tissue samples produced 80.6, 145.7 and 97.9 µg/ml total RNA, and the HOPE-fixed tissue samples produced 107.9, 82.7 and 97.3 µg/ml total RNA, Table 1A). The purity of each of these samples was also within range, between 1.7 and 1.9 (260/280 nm ratio, Table 1A). Agarose gel electrophoresis of the RNA extracted from formalin-fixed tissues showed a visible 28S rRNA band (Fig. 1A), and RNA extracted from HOPE-fixed tissues using the same method displayed both 28S and 18S rRNA bands (Fig. 1B). Extracted transcripts for both formalin- and HOPE-fixed tissues displayed successful mRNA expression of the housekeeping gene GAPDH after qRT-PCR (Fig. 2) producing CP values of 34.71 and 28.19, respectively (Table 2). This was converted to quantitative values using the standard curve (Fig. 3), and it was found that the total RNA extracted from HOPE-fixed tissues had a higher level of GAPDH mRNA at 4.05×10^{-2} pg/100 ng of total RNA in comparison to total RNA extracted from formalin-fixed tissues at 5.69×10^{-4} pg/100 ng of total RNA (Table 2).

Total RNA extracted from formalin- and HOPE-fixed, paraffin-embedded tissues using the Trizol method

Total RNA extracted from formalin-fixed tissues using the Trizol method proved unsuccessful as it could

Table 1A. Quantification and purity (as determined by 260/280 nm ratio) of total RNA determined by spectrophotometery isolated from three formalin-fixed (FORM) and three HOPE-fixed, paraffin-embedded cattle lymph node tissue sections using the Optimum™ FFPE kit (Ambion)

Fixation method and sample number	Total RNA quantification (µg/ml)	260/280 nm ratio (purity)
HOPE 1	107.9	1.8
HOPE 2	82.7	1.9
HOPE 3	97.3	1.9
FORM 1	80.6	1.7
FORM 2	145.7	1.8
FORM 3	97.9	1.9

The three tissue sections from each fixative are a representative group of the isolation procedure that was repeated more then 10 times.

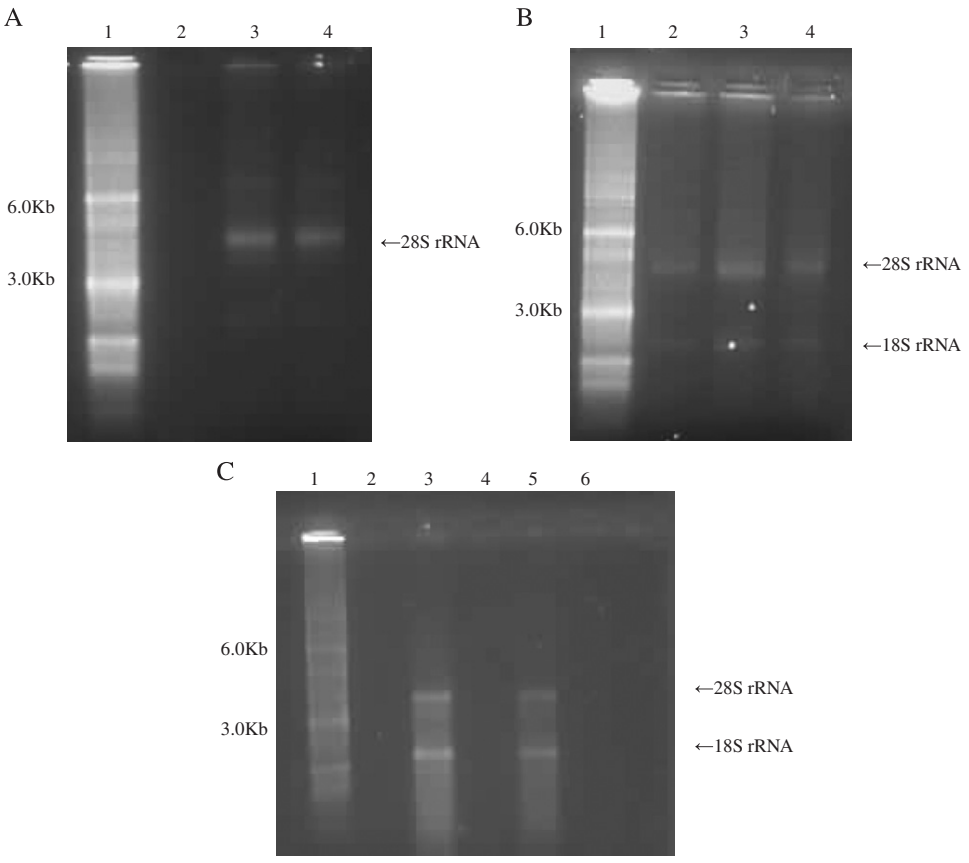

Fig. 1. Agarose gel electrophoresis (ethidium bromide staining) of total RNA samples (1 μg) isolated using the Optimum™ FFPE kit (Ambion, UK) from (A) formalin-fixed (lanes 3 and 4, lane 2 not used) and (B) HOPE-fixed (lanes 2-4) paraffin-embedded cattle lymph node tissues. Agarose gel electrophoresis (ethidium bromide staining) of total RNA samples (1 μg) isolated using the Trizol method (C) from formalin-fixed (lanes 2 and 4) and HOPE-fixed (lanes 3 and 5, lane 6 not used) paraffin-embedded cattle lymph node tissues. Lane 1 was a 0.5-10 kb RNA ladder. Experiments were repeated three times.

not be quantified using spectrophotometry (Table 1B) and the results were confirmed as we did not get any rRNA bands on the agarose gel (Fig. 1C). It subsequently did not produce an amplifiable product above the set threshold in qRT-PCR (Table 2). The concentration of RNA extracted from HOPE-fixed tissues using spectrophotometry for the three representative samples was 87, 146.7, and 161.1 μg/ml total RNA (Table 1B), and the purity was 1.8 and 1.9, respectively (260/280 nm ratio, Table 1B). The total RNA from HOPE-fixed tissues also exhibited strong 28S and 18S rRNA bands when analyzed by gel electrophoresis (Fig. 1C). The extracted transcript displayed successful mRNA expression of the housekeeping gene GAPDH after qRT-PCR (Fig. 2), producing a CP value of 27.39 (Table 2). This was converted to quantitative values using the standard curve (Fig. 3) and found to contain a GAPDH mRNA concentration of 6.45×10^{-2} pg/100 ng of total RNA (Table 2).

All controls used in qRT-PCR were negative, and the standard curve produced an adequate line coefficient of 0.98 and amplification efficiency of 1.9 (Fig. 3).

Discussion

Studies on disease infection and progression are fast becoming reliant on modern molecular techniques such as PCR [17]. The need for intact RNA extraction methods is an extremely important prelude to PCR [3,4] and has seen vast improvements over the last decade [13]. This includes the use of different tissue fixation methods to secure the integrity of RNA during archival storage. In this study, we have compared two fixatives (HOPE and formalin) for their ability to maintain RNA integrity. We have also compared two different RNA extraction methods (a commercial kit (Ambion) and a Trizol method) to determine which method produced the highest quantity of total RNA from tissues fixed in both HOPE and formalin. Using the commercial Optimum™ FFPE kit (Ambion), total RNA extracted from HOPE-fixed tissues showed comparatively similar quantities and was of a similar purity to total RNA extracted from formalin-fixed tissues (statistically, there was no significant difference between the concentration of total RNA extracted from the two fixation methods,

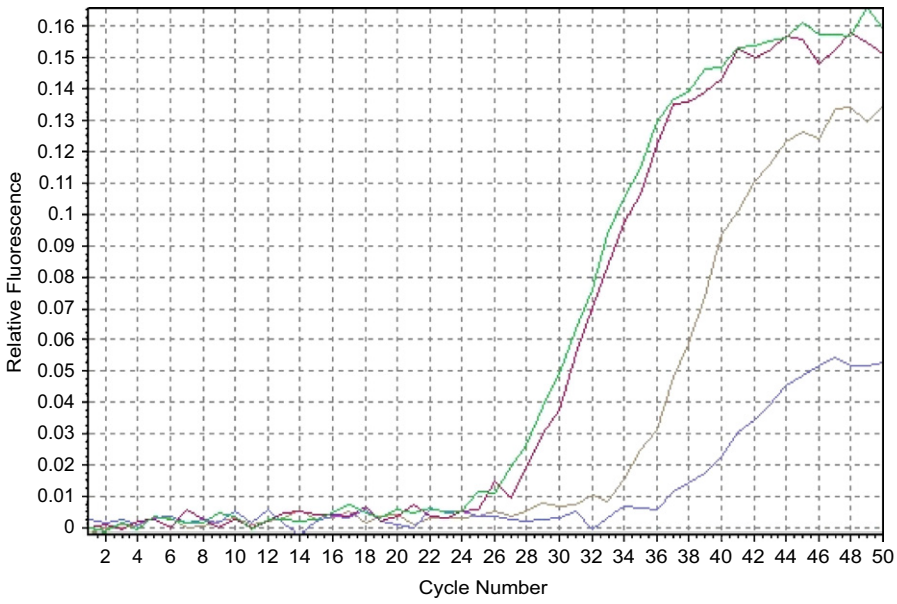

Fig. 2. Real-time RT-PCR of total RNA extracted from both the formalin-fixed and HOPE-fixed, paraffin-embedded tissues using the Optimum™ FFPE kit (brown and red lines, respectively) and the Trizol method (blue and green lines, respectively). The target sequence was an 87 bp fragment of the RNA of bovine glyceraldehyde-3-phosphate dehydrogenase, and each reaction was performed in duplicate.

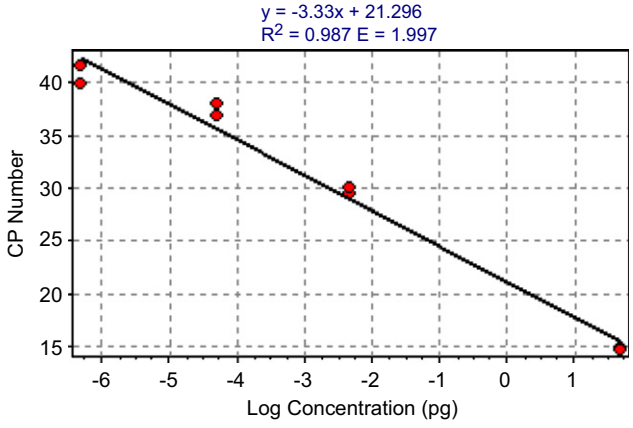

Fig. 3. Real-time RT-PCR of the manufactured standard template (Biomers.net), designed to be identical in sequence to the amplicon produced during the PCR of the GAPDH transcript. Known concentrations of the standard template (50, 5, 5×10^{-3} and 5×10^{-7} pg) were run on qRT-PCR alongside the unknown samples to produce a standard curve of crossing point (CP) value against log concentration (pg). The equation of the plotted line (above the graph) was then used to quantify the GAPDH mRNA concentration within the unknown samples (Table 2).

Mann–Whitney test $p > 0.05$). However, when using qRT-PCR to analyze the content of GAPDH mRNA, the mRNA concentration was higher in HOPE-fixed tissues (4.05×10^{-2} pg/100 ng total RNA) compared to formalin-fixed tissues (5.69×10^{-4} pg/100 ng total RNA), suggesting that HOPE fixation maintained the integrity of the RNA to a much higher degree [19]. This

Table 1B. Quantification and purity (as determined by 260/280 nm ratio) of total RNA determined by spectrophotometery isolated from three formalin-fixed (FORM) and three HOPE-fixed, paraffin-embedded cattle lymph node tissues using the Trizol method

Fixation method and sample number	Total RNA quantification (μg/ml)	260/280 nm ratio (purity)
HOPE 1	146.7	1.8
HOPE 2	87.0	1.8
HOPE 3	161.1	1.9
FORM 1	Negative	Negative
FORM 2	Negative	Negative
FORM 3	Negative	Negative

The three tissue sections from each fixative are a representative group of the isolation procedure that was repeated more then 10 times.

was supported by the agarose gel electrophoresis, as the total RNA extracted from HOPE-fixed tissues displayed both rRNA bands (18S and 28S) in comparison to the one band (28S) shown in total RNA from formalin-fixed tissues. This work agrees with previously published data where it has been shown that total RNA extracted from HOPE-fixed tissues displayed a stronger integrity and therefore a much higher level of detectable mRNA in RT-PCR (5,15,19). This ability of HOPE fixation could be due to the increased rate of acetone tissue dehydration, enabled by the diffusion of a protective solution of amino acids into the sample, thus conserving both its morphological and nucleic acid composition [13].

Table 2. qRT-PCR crossing point (CP) values for the expression of GAPDH mRNA in total RNA (100 ng) extracted from formalin-fixed and HOPE-fixed, paraffin-embedded samples using two methods, the Optimum^{TM} kit (Ambion) and a Trizol method

Total RNA extraction method	Sample fixation method	Average CP value	GAPDH mRNA concentration (pg/100 ng total RNA)
Optimum^{TM} kit (Ambion)	Formalin	34.71	5.69×10^{-4}
	HOPE	28.19	4.05×10^{-2}
Trizol	Formalin	Negative	Negative
	HOPE	27.39	6.45×10^{-2}

Each reaction was performed in duplicate and the average displayed in the table. The average CP values were then converted into quantitative values using the standard curve (Fig. 3) and expressed in picograms (pg) of GAPDH mRNA in 100 ng total RNA.

Using the Trizol method, the HOPE-fixed tissues produced total RNA of a very similar quantity and purity to the total RNA extracted from HOPE-fixed tissues using the commercial kit (statistically, there was no significant difference between the concentration of total RNA using the two extraction methods, Mann–Whitney test $p > 0.05$). The resultant GAPDH mRNA quantity calculated by qRT-PCR was also extremely similar, 4.05×10^{-2} pg/100 ng total RNA extracted using the commercial kit and 6.45×10^{-2} pg/100 ng total RNA extracted using the Trizol method. As previously mentioned, the Ambion kit was successful in extracting total RNA from formalin-fixed tissues, however, we were unable to isolate quantifiable RNA from formalin-fixed tissues using the Trizol method. In the Ambion Optimum^{TM} kit, this is most likely attributed to the proteinase K step in the protocol, which is much more efficient at separating the RNA from its cross-linked matrix [7]. However, the period of sample incubation in proteinase K is extremely long (in our experience, it took 6 h to solubilize only a fraction of the tissue present) and has been reported to take up to 48 h [11], leading to further RNA degradation. The cross-linked matrix is believed to form due to the reaction of RNA with formaldehyde, producing methylene bridges between the amino groups [13]. Due to the absence of formaldehyde in the HOPE fixative method, tissues fixed in HOPE do not possess cross linkage and therefore perform equally well in RNA isolation methods with or without proteinase K solution. Similar results have been reported by Weidorn et al. [19].

In conclusion, this study supports a strong consensus that HOPE fixative is a more appropriate fixative to use for subsequent RNA extraction and molecular techniques. This study is the first to demonstrate the potential of HOPE fixation of *M. bovis*-infected cattle lymph nodes with the subsequent quantifying of gene-specific mRNA within a known amount of total RNA using qRT-PCR. This complements the work already shown on the benefits of HOPE fixative in human tissue types such as lung [5], cancer cells [15], spleen, and heart [19]. Due to the vastly improved nucleic acid conservation, HOPE fixative is being applied to tissues samples used in subsequent disease diagnosis, such as the possible detection and even differentiation of the *Mycobacterium tuberculosis* complex within archived infected mice tissues [12]. In addition to this, this study has highlighted the need to apply, not just the more efficient fixative technique but also the appropriate extraction method specific to the fixative used, adding new methods to those previously reported [5,19]. By considering these factors and exploring the most effective combination of fixative and extraction methods, the quality of molecular techniques such as PCR and their practical use in exploring genetic expression of both host and pathogen can provide a basis for future research into intervention and treatment.

Acknowledgments

We would like to thank Linda Johnson (VLA), Julie Gough (VLA) and the Histopathology department at the VLA (Surrey) for kindly supplying us with the formalin- and HOPE-fixed *M. bovis*-infected, cattle lymph node tissues.

References

[1] D. Barbaric, L. Dalla-Pozza, J.A. Byrne, A reliable method for total RNA extraction from frozen human bone marrow samples taken at diagnosis of acute leukaemia, J. Clin. Pathol. 55 (2002) 865.
[2] B. Bhudevi, D. Weinstock, Detection of bovine viral diarrhoea virus in formalin fixed paraffin embedded tissue sections by real time RT-PCR (Taqman), J. Virol. Meth. 109 (2003) 25.
[3] S.A. Bustin, Quantification of mRNA using real time reverse-transcription polymerase chain reaction, J. Biomol. Tech. 15 (2002) 155.
[4] S.A. Bustin, R. Mueller, Real-time reverse transcription PCR and the detection of occult disease in colorectal cancer, Mol. Aspects Med. 27 (2006) 192.
[5] T. Goldmann, R. Burgemeister, U. Sauer, S. Loeschke, D.S. Lang, D. Branscheid, P. Zabel, E. Vollmer, Enhanced molecular analyses by combination of the

HOPE- technique and laser microdissection, Diagn. Pathol. 1 (2006) 2.
[6] U. Lehmann, H. Kreipe, Real-time PCR analysis of DNA and RNA extracted from formalin-fixed and paraffin-embedded biopsies, Methods 25 (2006) 409.
[7] F. Lewis, N.J. Maughan, V. Smith, K. Hillan, P. Quirke, Unlocking the archive – gene expression in paraffin-embedded tissue, J. Pathol. 195 (2001) 66.
[8] L. Louie, A.E. Simor, S. Chong, K. Luinstra, A. Petrich, J. Mahony, M. Smieja, G. Johnson, F. Gharabaghi, R. Tellier, B.M. Willey, S. Poutanen, T. Mazzulli, G. Broukhanski, F. Jamieson, M. Louie, S. Richardson, Detection of severe acute respiratory syndrome coronavirus in stool specimens by commercially available real-time reverse transcriptase PCR assays, J. Clin. Microbiol. 44 (2006) 4193–4196.
[9] M. Macluskey, R. Baillie, H. Morrow, S.L. Schor, A.M. Schor, Extraction of RNA from archival tissues and measurement of thrombospondin-1 mRNA in normal, dysplastic and malignant oral tissues, Br. J. Oral. Maxillofac.Surg. 44 (2006) 116.
[10] J. Olert, K. Weidorn, T. Goldmann, H. Kühl, Y. Mehraein, H. Scherthan, F. Niketeghad, E. Vollmer, A.M. Müller, J. Müller-Navia, HOPE fixation: a novel fixing method and paraffin-embedding technique for human soft tissues, Pathol. Res. Prac. 197 (2001) 823.
[11] A. Pollet, Y.C. Bedard, S.Q. Li, T. Rohan, R. Kandel, Correlation of p53 mutations in ThinPrep-processed fine needle aspirates with surgically resected breast cancers, Mod. pathol. 13 (2001) 1173.
[12] R. Sen Gupta, D. Hillemann, T. Kubica, G. Zissel, J. Muller-Quernheim, J. Galle, E. Vollmer, T. Goldmann, HOPE fixation enables improved PCR-based detection and differentiation of *Mycobacterium tuberculosis* complex in paraffin-embedded tissues, Pathol. Res. Pract. 199 (2003) 619.
[13] M. Srinivasan, D. Sedmak, S. Jewell, Effect of fixatives and tissue processing on the content and integrity of nucleic acids, Am. J. Pathol. 161 (2002) 1961.
[14] S.E. Stroup, S. Roy, J. McHele, V. Maro, S. Ntabaquzi, A. Siddique, G. Kang, R.L. Guerrant, B.D. Kirkpatrick, R. Fayer, J. Herbein, H. Ward, R. Haque, E.R. Houpt, Real-time PCR detection and speciation of cryptosporidium infection using Scorpion probes, J. Med. Microbiol. 55 (2006) 1217.
[15] E. Vollmer, J. Galle, D.S. Lang, S. Loeschke, H. Schultz, T. Goldmann, The HOPE technique opens up a multitude of new possibilities in pathology, Rom. J. Morphol. Embryol. 47 (2006) 15.
[16] S. Wacharapluesadee, P. Ruangvejvorachai, T. Hemachudha, A simple method for detection of rabies viral sequences in 16-year old archival brain specimens with one-week fixation in formalin, J. Virol. Meth. 134 (2006) 267.
[17] P.R. Wakeley, N. Johnson, L.M. McElhinney, D. Marston, J. Sawyer, A.R. Fooks, Development of a real-time, TaqMan reverse transcription-PCR assay for detection and differentiation of lyssavirus genotypes 1, 5, and 6, J. Clin. Microbiol. 43 (2005) 2786.
[18] S. Widdison, L.J. Schreuder, B. Villarreal-Ramos, C.J. Howard, M. Watson, T.J. Coffey, Cytokine expression profiles of bovine lymph nodes: effects of *Mycobacterium bovis* infection and bacilli Calmette-Guérin vaccination, Clin. Exp. Immunol. 144 (2006) 281.
[19] K.H. Wiedorn, J. Olert, R.A. Stacey, T. Goldmann, H. Kühl, J. Matthus, E. Vollmer, A. Bosse, HOPE-a new fixing technique enables preservation and extraction of high molecular weight DNA and RNA of >20 kb from paraffin-embedded tissues. Hepes–glutamic acid buffer mediated organic solvent protection effect, Pathol. Res. Pract. 198 (2002) 735.

Tuberculosis (2008) **88**, 610—615

available at www.sciencedirect.com

ScienceDirect

journal homepage: http://intl.elsevierhealth.com/journals/tube

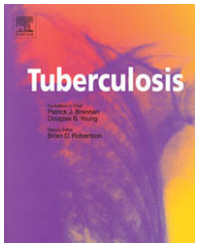

Cytokine mRNA expression in cattle infected with different dosages of *Mycobacterium bovis*

Hima Chandana Boddu-Jasmine [a], Jaydene Witchell [a], Martin Vordermeier [b], Arun Wangoo [c,d], Madhu Goyal [a,*]

[a] *School of Life Sciences, University of Hertfordshire, College Lane, Hatfield, Herts AL10 9AB, UK*
[b] *TB Research group, Veterinary Laboratories Agency, Weybridge, Addlestone, Surrey KT15 3NB, UK*
[c] *Department of Pathology, Veterinary Laboratories Agency, Weybridge, Addlestone, Surrey KT15 3NB, UK*

Received 20 March 2008; received in revised form 6 June 2008; accepted 7 June 2008

KEYWORDS
Colony-forming units;
HOPE fixed tissues;
RNA extraction;
Quantitative reverse transcriptase polymerase chain reaction;
Mycobacterium bovis

Summary
Cytokine mRNA expression of pro-inflammatory cytokines, i.e., interferon-gamma (IFN-γ), tumor necrosis factor-alpha (TNF-α) and anti-inflammatory cytokines, i.e., interleukin-4 (IL-4), interleukin-10 (IL-10) was quantified using quantitative reverse transcriptase polymerase chain reaction (qRT-PCR) in cattle infected with different doses (1—1000 colony-forming units (cfu)) of *Mycobacterium bovis*. RNA was extracted from the Hepes glutamic acid buffer mediated organic solvent protection effect (HOPE) fixed lymph node tissues using Trizol method.

The expression levels of all the four cytokines gradually increased in cattle infected with 1 cfu—1000 cfu. Statistical significance ($P < 0.05$) was observed for the cytokines IFN-γ, IL-4 and IL-10 between the cattle infected with 1 cfu and 1000 cfu. Though there was an increase in the expression levels of TNF-α from cattle infected with 1 cfu—1000 cfu, this difference in expression was not statistically significant ($P > 0.05$). The increase in the levels of IFN-γ indicates that the host may be responding to control the infection and the increased level of IL-4 and IL-10 which are anti-inflammatory cytokines, suggests that these cytokines are trying to protect the host by reducing the inflammation and also by controlling the levels of TNF-α (the cytokine that may cause tissue damage).

Abbreviations: mRNA, messenger ribonucleic acid; cfu, colony-forming units; qRT-PCR, quantitative reverse transcriptase polymerase chain reaction; HOPE, Hepes glutamic acid buffer mediated organic solvent protection effect; IFN-γ, interferon-gamma; TNF-α, tumor necrosis factor-alpha; IL-4, interleukin-4; IL-10, interleukin-10.

* Corresponding author. Tel.: +44 17 07 284 624; fax: +44 17 07 285 046.
E-mail address: m.goyal@herts.ac.uk (M. Goyal).
[d] Present address: Veterinary Medicine Directorate, Addlestone, Surrey KT15 3LS, UK.

1472-9792/$ - see front matter © 2008 Elsevier Ltd. All rights reserved.
doi:10.1016/j.tube.2008.06.003

Introduction

Bovine tuberculosis (TB), caused by *Mycobacterium bovis* (*M. bovis*), is a zoonotic infection in a wide range of domestic and wild mammalian hosts. The infected cattle can transmit infection to other cattle and humans.[1] It is one of the major economic problems for the agricultural trade and industry in several countries. The prevalence of *M. bovis* infection in cattle is increasing rapidly in some countries, including the UK and Ireland.[2] The organism infects a wide range of mammalian hosts and eradication of the disease is difficult if there is an extensive reservoir in a wild life population. Existing evidence suggests that the European badger is the main wild life reservoir in the UK and Ireland.[3]

The innate immune response is extremely effective in removing the tubercle bacilli, but following the failure of the innate immune system, the cell-mediated immune system (CMI) is initiated as the bacteria remains intra-cellular.[1] This leads to the induction of a large number of cytokines, some of which are essential for the control of infection.[4] The magnitude of infection is not only related to the virulence of the infected bacilli but also to the immunity of the host, infecting dose of bacilli and environmental factors. From previous studies, it has been concluded that the inhalation of a small number of mycobacteria can initiate the lesions, which are equivalent in number to the quantity of organisms delivered[5] and when large infective doses of *M. bovis* are delivered intranasally, it results in extensive infection and progression of the disease in challenged animals. As the size of the challenge dose was reduced, severity of the disease decreased. In the same way, when the immune response was observed in cattle infected with different magnitudes of *M. bovis*, animals challenged with a higher dose lead to CMI response, and the production of anti-*M.bovis* antibodies. Low doses of *M. bovis* lead to gradual development of CMI and little or no antibody response.[6] During natural infection, a small number of bacilli (2 or more cells) have been shown to be enough to initiate tuberculosis in a potential host.[7] Recent studies by Dean et al. reported that 1 cfu is sufficient to induce a disease in cattle,[8] and the degree of lesion advancement and granuloma distribution was similar between the lowest dose group (1 cfu) and the highest dose of the four groups (1000 cfu).[9] Therefore, in the present study we have extended the previous work to determine the mRNA cytokine expression in the HOPE fixed lymph node tissues of cattle infected with 1, 10, 100 and 1000 cfu using qRT-PCR. Cytokine expression was assessed at 26 weeks post-infection.

HOPE fixative has been shown to conserve RNA integrity by avoiding amino acid cross-linking.[10,11] RNA extracted from HOPE fixed human tissues has been successfully used in RT-PCR for PCR products ranging from 220 to 663 base pairs.[12] Hence this study also demonstrates the potential of HOPE fixation of *M. bovis* infected cattle lymph node tissues with the subsequent quantification of gene specific mRNA using qRT-PCR.

Materials and methods

Experimental infection of cattle with *M. bovis*, post-mortem of the infected cattle and HOPE fixation of infected samples were carried out at Veterinary Laboratories Agency (VLA), Weybridge, Surrey, UK.

Experimental animals

Twenty Friesian Holstein heifers, that were six months old, with no history of tuberculosis, were intratracheally infected with 1, 10, 100, and 1000 cfu doses of *M. bovis* (Field strain GB − AF 2122/97), as reported by Dean et al. Briefly, an endotracheal tube (80 cm) holding a fine cannula was used to inject 1.5 ml of prepared inoculum into an anesthetized animal. The animals were euthanized at 26 weeks post-infection by intravenous injection of sodium pentobarbitone and lymph nodes were collected aseptically. From each dosage group, four cattle were included in this study. Three lymph nodes (caudal mediastinal, left-bronchial and cranial mediastinal)[8] from each calf and in total 12 lymph node samples were obtained for each group.

Preparation of tissue samples

The infected lymph node tissues were incubated in the aqueous HOPE solution for 14—36 h (0—4 °C) and then incubated in acetone (0—4 °C) for 2 h, followed by dehydration with freshly prepared acetone (0—4 °C) for 3 × 2 h (as per manufacturer's instructions, DCS Innovative, Germany). This was followed by embedding of the sections in paraffin wax.[11]

Subsequent RNA extraction and study of cytokine gene expression were carried out for these HOPE fixed samples at the University of Hertfordshire, Hatfield, UK.

Isolation of total RNA

The HOPE fixed tissue blocks were kept at −20 °C for 10 min before sectioning. These tissue blocks were cut into 10 μm sections using a microtome.

The sections were deparafinized using xylene (1 ml) at 57 °C for 10 min in an eppendorf. The samples were centrifuged and the pellet formed was washed with ethanol. The pellet was pulverized in liquid nitrogen and Trizol (800 μl) reagent was added. This was followed by sonication for 2—3 min. Glycogen (1 mg/ml) was added; the samples were then passed through a syringe and needle (24 G) before the addition of chloroform (160 μl) and the tube contents mixed by vortexing for 30 s. After centrifuging for 10 min at 4 °C, the supernatant was transferred into a new micro centrifuge tube with ice cold isopropanol (500 μl) and incubated at −20 °C for 4 h. This was followed by centrifugation and the resultant pellet was washed in 70% ethanol and resuspended in 50 μl of RNase free water and stored at −70 °C. Concentration and purity of the extracted RNA were analyzed using a spectrophotometer and the quality was checked using Agarose gel electrophoresis. DNase treatment was performed for the total RNA before qRT-PCR using Turbo DNA free kit (Ambion, Warrington, UK) to reduce the genomic DNA contamination.

Quantitative RT-PCR

One step qRT-PCR was carried out within a Quantica thermal cycler (Techne, Staffordshire, UK) using

Quantitect™ probe RT-PCR master mix (Qiagen, West Sussex, UK) that allows both reverse transcription and PCR to take place in a single tube.

Primers and probes oligonucleotide sequence

Oligonucleotide primer and dual labelled probe sequenced for qRT-PCR (sequences were designed at VLA, Weybridge, Surrey, UK). Primers and probes sequences are as follows.

IFN-γ:
Forward primer — 5′-C AGAAAGCGGAAGAGAAGTCAGA-3′
Reverse primer — 5′-CAGGCAGGAGGACCATTACG-3′
Probe — FAM: 5′-TCTCTTTCGAGGCCGGAGAGCATCA-3′: BHQ-1
TNF-α:
Forward primer — 5′-CGGTGGTGGGACTCGTATG-3′
Reverse primer — 5′-GCTGGTTGTCTTCCAGCTTCA-3′
Probe — FAM: 5′-CAATGCCCTCGTGGCCAACGG-3′: BHQ-1
IL-10:
Forward primer — 5′-GGTGATGCCACAGGCTGAG-3′
Reverse primer — 5′-AGCTTCTCCCCCAGTGAGTTC-3′
Probe — FAM: 5′-CACGGGCCTGACATCAAGGAGCA-3′: BHQ-1
IL-4:
Forward primer — 5′-GCCACACGTGCTTGAACAAA-3′
Reverse primer — 5′-TCTTGCTTGCCAAGCTGTTG-3′
Probe — FAM: 5′-TCCTGGGCGGACTTGACAGG-3′: BHQ-1

Probes for Taqman analysis were labeled at the 5′ end with the reporter dye FAM (6-carboxyfluorescein) and at the 3′ end with the quencher dye BHQ-1 (Black Hole Quencher).

qRT-PCR for quantification of cytokine mRNA

qRT-PCR was carried out according to the manufacturer's guidelines for Quantitect™ probe RT-PCR kit (Qiagen, UK), with 200 ng of RNA template, Quantitect™ probe RT-PCR master mix with the final concentration of 1×, Quantitect™ RT mix of 0.5 μl/reaction, forward and reverse primers with final concentration of 700 nmoles and probe with 200 nmoles. Each reaction was performed in duplicate with one positive and two negative controls (one excluding the template and the other excluding the reverse transcriptase enzyme).

The reactions were carried out within a Quantica thermal cycler, applying the programme: reverse transcription (1 cycle) at 50 °C for 30 min, initial activation step (1 cycle) at 95 °C for 15 min followed by denaturation, annealing/extension step (50 cycles) at 94 °C for 15 s and 60 °C for 1 min.

Statistical analysis

All the statistical analyses were carried out using Microsoft Excel 2002 (Microsoft Co., Redmond, WA, USA) and non-parametric statistical tests. The Kruskal—Wallis test and Mann—Whitney *U* test were used to analyze the significance of IFN-γ, TNF-α, IL-10 and IL-4 expression levels between the cattle infected with 1, 10, 100 and 1000 cfu doses. Effects with a *P* value of <0.05 were considered significant.

Results

Pro- and anti-inflammatory cytokine gene expression was compared in cattle infected with 1, 10, 100 and 1000 cfu of *M .bovis*. The expression for IFN-γ, TNF-α, IL-10 and IL-4 expression was observed in all the tissue samples. The cytokine gene expression was observed to increase with the increase in dosage of *M. bovis*.

The average copy number of different cytokines in the lymph node tissues of cattle infected with different doses is shown in Table 1. There was a gradual increase in the expression of IFN-γ from 1 cfu to 1000 cfu (4.23-fold increase) (Figure. 1a). A statistical significance ($P<0.05$) was observed between the cattle infected with 1 cfu and 1000 cfu and also between the cattle infected with 10 cfu and 1000 cfu (3.88-fold change). A slight increase in the level of IFN-γ expression was observed in animals infected with 10 cfu and 100 cfu as compared to animals infected with 1 cfu (1.99 and 1.09-fold increase, respectively), however, this difference was not statistically significant ($P>0.05$).

TNF-α mRNA levels were determined as shown in the Table 1. Though there was an increase in the expression from cattle infected with 1 cfu—1000 cfu (2.83-fold changes), but this difference was not statistically significant ($P>0.05$). There was a slight increase in the level of TNF-α expression in the animals infected with 10 cfu and 100 cfu as compared to animals infected with 1 cfu (2.23 and 1.03-fold increase, respectively) (Figure. 1b). This difference was also not statistically significant ($P>0.05$).

Similarly when IL-4 expression was quantified (Table 1), there was an increase in the level of expression from 1 cfu to 1000 cfu (3.15-fold change) (Figure. 1c). Mann—Whitney *U* test showed the statistical significance ($P<0.05$) between the cattle infected with 1 cfu and 1000 cfu and between the cattle infected with 10 cfu and 1000 cfu

Table 1 The average copy number of cytokines (IFN-γ, TNF-α, IL-4 and IL-10) expression in the cattle infected with 1, 10, 100 and 1000 cfu of *M. bovis*.

Cytokines	Experimental dose			
	1 cfu (molecules/μl)	10 cfu (molecules/μl)	100 cfu (molecules/μl)	1000 cfu (molecules/μl)
IFN-γ	213,500	234,665	425,825	904,750
TNF-α	252,450	260,675	565,000	715,125
IL-4	200,875	221,125	449,250	633,000
IL-10	93,850	288,975	450,000	510,750

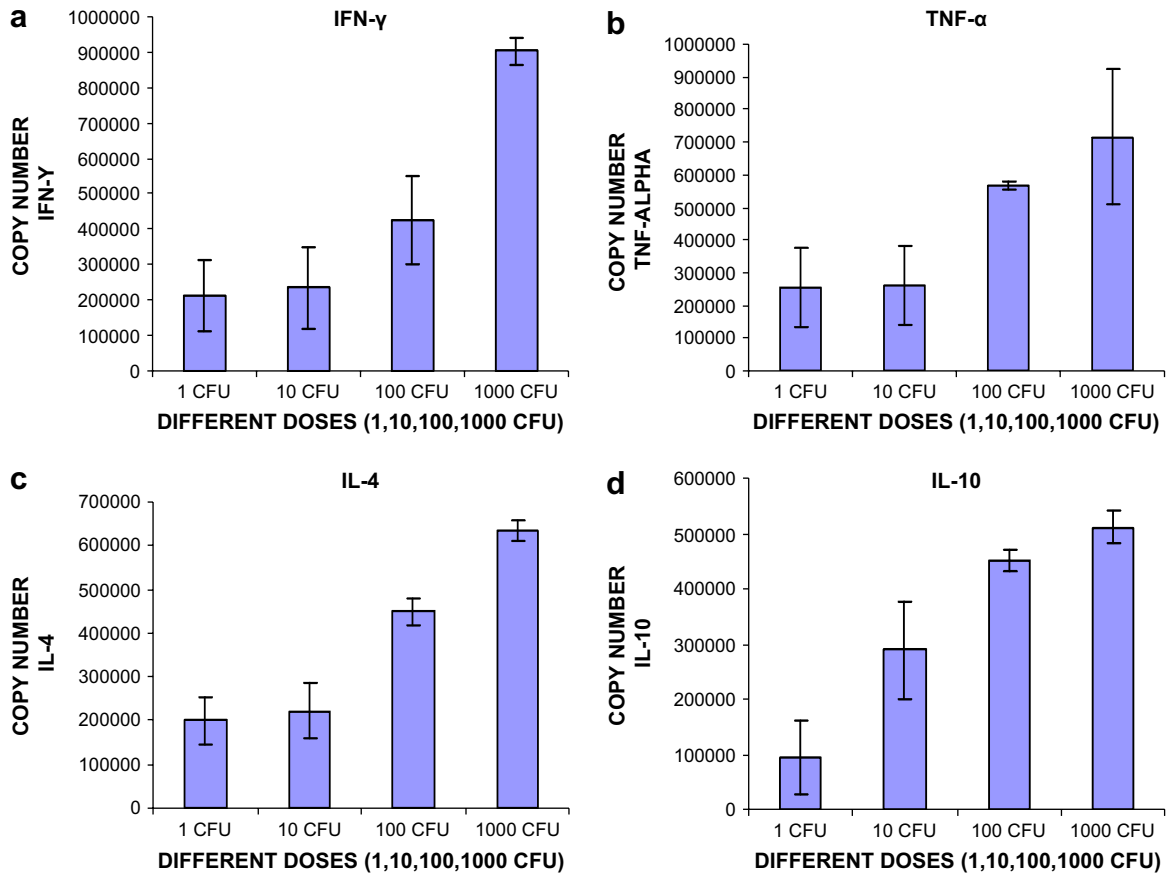

Figure. 1 The level of expression of cytokines — (a) IFN-γ, (b) TNF-α, (c) IL-4 and (d) IL-10 in the cattle experimentally infected with 1, 10, 100, 1000 cfu of *M. bovis*. The level of cytokine expression was determined by qRT-PCR. The copy number of cytokines in each group represents the average of the three lymph node (cranial mediastinal, left bronchial and caudal mediastinal) taken from each dose.

(2.86-fold change). The increase in the level of expression in cattle infected with 10 cfu and 100 cfu (1.10 and 2.23-fold change, respectively) was not statistically significant ($P > 0.05$).

The IL-10 expression levels gradually increased in the cattle infected with 1 cfu—1000 cfu (5.44-fold change) as shown in Figure. 1d. Mann—Whitney *U* test showed the statistical significance between the cattle infected with 1 cfu and 100 cfu (3.07-fold change) and between the cattle infected with 1 cfu and 1000 cfu of *M. bovis* ($P < 0.05$).

Discussion

In this study we analyzed the cytokine gene expression in the lymph nodes from cattle infected with 1, 10, 100 and 1000 cfu of *M. bovis*. The key objective of this study was to compare the expression levels of pro-inflammatory and anti-inflammatory cytokines in the bovine lymph nodes of cattle infected intratracheally with logarithmic increasing doses of *M. bovis* using qRT-PCR. This would help to understand the immune response in cattle naturally infected with *M. bovis* (4—6 bacilli) versus those infected experimentally (more than 1000 cfu). Previous study carried out by our group on the cattle infected with *M. bovis* showed that 1 cfu of *M. bovis* induced pathology equivalent to that was seen in animals infected with 1000 cfu of *M. bovis*.[8] In this study we have carried out further work on the same set of cattle (used only four cattle out of five for 1 cfu and 10 cfu dose) and analyzed the expression of four cytokine genes (IFN-γ, TNF-α, IL-10 and IL-4) that are known to be essential for the host defence against tuberculosis and play a major role in regulating the formation of granulomatous lesions.[13] The expression of the four cytokines was also measured in the fresh lymph nodes obtained from non-infected cattle using real time PCR (unpublished data). These non-infected cattle showed expression of all the cytokines and the expression of IFN-γ, TNF-α and IL-4 was significantly lower ($P < 0.05$, Mann—Whitney *U* Test) than in the cattle infected with 1, 10, 100 and 1000 cfu of *M.bovis*. The expression of IL-10 was also lower in the non-infected cattle but the difference was not significant ($P > 0.05$, Mann—Whitney *U* Test) when compared with cattle infected with 1 cfu or 10 cfus. However, the expression was significantly lower ($P < 0.05$) when compared with cattle infected with 100 cfu and 1000 cfu of *M. bovis*.

Our results show that IFN-γ expression levels gradually increased as the dose of infection was increased from 1 cfu

to 1000 cfu. The increase in the IFN-γ level was statistically significant when the results of 1 cfu infected lymph nodes were compared with 1000 cfu and 10 cfu with 1000 cfu. This cytokine is known to play a major role in protection and pathology during infection.[14] Previous studies on immunohistochemistry assay for cytokine IFN-γ, showed that the expression was more apparent in the lymph nodes from animals infected with higher doses of *M. bovis*.[9] The increased levels of IFN-γ mRNA with the potential of a developing humoral response is a characteristic of a Th-0 type response and associated with increased pathogenesis.[15] Previous work carried out by Dean et al. on minimum infective dose of *M. bovis* did not find a correlation between dose of *M. bovis* and pathology score or the time to detect the IFN-γ positivity. This may be because the systemic responses measured by Dean et al. are not totally reflective of responses at the site of disease and may also include antigens that are not part of tuberculin.

The level of TNF-α mRNA was not significantly different in different dosage groups though there was increase in the cytokine expression from 1 cfu to 1000 cfu. The possible reason is that this cytokine is primarily involved in the initial stages of innate immunity.[16] Generally TNF is a multi-potent cytokine which plays a part in apoptosis, cell activation and differentiation.[18] The role of TNF during TB is both antibacterial and production of inflammatory response. A study performed by Widdison et al.[17] on non-infected and *M. bovis* experimentally infected (1.3×10^4 cfu) cattle, showed significant decrease in the expression level of TNF-α in the infected animals at 16 weeks post-infection. The two possible reasons for the discrepancies in the expression of TNF-α level between the two studies could be due to the time point at which samples were taken (26 within this study and 16 weeks post-infection in Widdison et al.) and also the dose of *M. bovis* used for infection, which was lower in our study. One of the other possible reasons for this might be that the levels are controlled by other anti-inflammatory cytokines (IL-4 and IL-10).

The expression of anti-inflammatory cytokines IL-4 and IL-10 was also measured in this study as these cytokines potentially have a major role in the pathogenesis of mycobacterial infection.[19] The IL-4 gene expression was observed in animals infected with 1 cfu and 10 cfu and there was an increase in the expression levels in the lymph node of animals infected with 100 cfu and 1000 cfu. This increase was statistically significant, when the results of animals infected with 1 cfu were compared with 1000 cfu and 10 cfu with 1000 cfu. IL-4 mRNA levels in *Mycobacterium tuberculosis* infected humans have been reported to increase significantly with established pulmonary TB.[20] In bovine TB the expression of IL-4 m-RNA was reported to be relatively low until 6–8 weeks of post-inoculation thereafter it peaked and remained at high levels for 2 weeks, followed by a sharp decrease.[21]

IL-10 cytokine expression levels gradually increased when the animals were infected with 1 cfu–1000 cfu and there was a statistically significant difference between the animals infected with 1 cfu–100 cfu and between the animals infected with 1 cfu–1000 cfu. Previous studies of bovine infection (10^6 cfu) in cattle have shown that IL-10 mRNA levels were low at 5 weeks of infection with an increase at 26 weeks post-infection.[15] The low expression of Th-2 cytokines (IL-4 and IL-10) during early stages of infection shown by previous studies[15,21] may be because during the early stages of infection Th-1 response to TB infection is activated and IFN-γ is the predominant cytokine. In the later stages of infection the response shifts to a combined IFN-γ and IL-4 mediated response and subsequently an IL-4 dominant Th-2 response as the infection progresses.[22,23] The increased expression of these anti-inflammatory cytokines in the later stages may be to control the expression of pro-inflammatory cytokines and regulate the Th-1 and Th-2 balance during TB.

In conclusion, the trends in cytokine mRNA expression seen in this study were encouragingly similar to those previously reported,[9,15,20] and centered primarily on a Th-1 type response that evolved into a Th-2 type later in the disease process.

By scrutinizing the expression of these cytokines and pathology of the cattle infected with a logarithmically increasing dose of *M. bovis*, whilst the pathology remains the same in cattle infected with both low and high doses of *M. bovis*[9] the expression of cytokines varies. Irrespective of the pathology the expression of pro-inflammatory and anti-inflammatory cytokines increased as the dose of infection increased. All the cytokines were detected after 26 weeks post-infection, even in the cattle infected with the lower doses. As the amount of cytokines produced were elevated, in the cattle infected with high doses of *M. bovis* it may be possible that less amount of cytokine expression is required to prevent the disease at low dose of infection and high amount of cytokine is required when the cattle are infected with higher doses of *M. bovis* as shown in our study.

Thus, as the general response to cytokine expression was dependent on the dose of infection it is possible that the infection with 1 cfu of *M. bovis* activates the immune response to a lesser degree, compared to the cattle infected with higher doses. This is because less antigenic stimulation is seen when cattle are inoculated with lower doses of *M. bovis*.

This study also supports a strong consensus that HOPE fixative can be an appropriate fixative to use for subsequent RNA extraction and molecular techniques. This study demonstrates the potential of HOPE fixation of *M. bovis* infected cattle lymph node with the subsequent quantifying of gene specific mRNA using qRT-PCR. This complements the work already shown on the benefits of HOPE fixative in human tissue types such as lungs,[24] cancer cells,[25] spleen and heart.[12] Due to the vastly improved nucleic acid conservation, HOPE fixative being applied to tissue samples used in subsequent disease diagnosis and even differentiation of the MTB complex within archived infected mice tissues.[26]

Consideration of these factors and exploration of the most effective combination of fixative and PCR methods and their use in exploring the cytokine expression can provide an aid for the outgoing research to develop an effective vaccine against the organism responsible for TB.

Acknowledgements

We would like to thank Shelly Rhodes of the TB Research group (VLA) for kindly providing sequences for cytokine primers and probes. Also we would like to thank Julie Gough of the Histopathology department (VLA) for preparation and supplying HOPE-fixed *M. bovis* infected cattle lymph node tissues.

Funding: This study was partially funded by the Department for Environment, Food and Rural Affairs, London, United Kingdom.

Competing interests: None declared.

Ethical approval: Not required.

References

1. Pollock JM, Welsh J, McNair J. Immune responses in bovine tuberculosis: towards new strategies for the diagnosis and control of disease. *Vet Immunol Immunopathol* 2005;**108**(1–2): 37–43.
2. Phillips CJ, Foster CR, Morris PA, Teverson R. The transmission of *Mycobacterium bovis* infection to cattle. *Res Vet Sci* 2003;**74**(1):1–15.
3. Morris RS, Pfeiffer DU, Jackson R. The epidemiology of *Mycobacterium bovis* infections. *Vet Microbiol* 1994;**40**(1–2): 153–77.
4. Henderson RA, Watkins SC, Flynn JL. Activation of human dendritic cells following infection with Mycobacterium tuberculosis. *J Immunol* 1997;**159**(2):635–43.
5. Costella E, Doherty ML, Quigley FC, O'Reilly PF. A study of cattle to cattle transmission in *Mycobacterium bovis* infection. *Vet J* 1998;**155**(3):245–50.
6. Pollock JM, Neill SD. *Mycobacterium bovis* infection and tuberculosis in cattle. *Vet J* 2002;**163**(2):115–27.
7. Schafer MP, Fernback JE, Ernst MK. Detection and characterization of airborne *Mycobacterium tuberculosis* H37Ra particles, a surrogate for airborne pathogenic *Mycobacterium tuberculosis*. *Aerosol Sci Technol* 1999;**30**(2):161–73.
8. Dean GS, Rhodes SG, Coad M, Whelan AO, Cockle PJ, Clifford DJ, et al. Minimum infective dose of *Mycobacterium bovis* in cattle. *Infect Immun* 2005;**73**(10):6467–71.
9. Johnson L, Dean GS, Rhodes SG, Hewinson RG, Vordermeier HM, Wangoo A. Low-dose *Mycobacterium bovis* infection in cattle results in pathology indistinguishable from that of high-dose infection. *Tuberculosis* 2007;**87**(1):71–6.
10. Olert J, Wiedorn KH, Goldmann T, Kuhl H, Mehraein Y, Scherthan H, et al. HOPE fixation: a novel fixing method and paraffin-embedding technique for human soft tissues. *Pathol Res Pract* 2001;**197**(12):823–6.
11. Witchell J, Varshney D, Gajjar T, Wangoo A, Goyal M. RNA isolation and quantitative PCR from HOPE and formalin-fixed bovine lymph node tissues. *Pathol Res Pract* 2008;**204**(2):105–11.
12. Wiedorn KH, Olert J, Stacy RP, Goldmann T, Kuhl H, Matthus J, et al. HOPE – a new fixing technique enables preservation and extraction of high molecular weight DNA and RNA of >20 kb from paraffin-embedded tissues. *Pathol Res Pract* 2002; **198**(11):735–40.
13. Roach DR, Bean AG, Demangel C, France MP, Bricoe H, Britton WJ. TNF regulates chemokine induction essential for cell recruitment, granuloma formation, and clearance of mycobacterial infection. *J Immunol* 2002;**168**(9):4620–7.
14. Cooper AM, Dalton DK, Stewart TA, Griffin JP, Russel DG, Orme IM. Disseminated tuberculosis in interferon gamma gene-disrupted mice. *J Exp Med* 1993;**178**(6):2243–7.
15. Welsh MD, Cunningham RT, Corbett DM, Girvin RM, McNair J, Skuce RA, et al. Influence of pathological progression on the balance between cellular and humoral immune responses in bovine tuberculosis. *Immunology* 2005;**114**(1):101–11.
16. Pratt RJ, Grange JM, Williams VG. *Tuberculosis: a foundation for nursing and health practice*. London: Hodder Education; 2005 [chapter 2].
17. Widdison S, Schreuder LJ, Villarreal-Ramos B, Howard CJ, Watson M, Coffey TJ. Cytokine expression profiles of bovine lymph nodes: effects of *Mycobacterium bovis* infection and bacille Calmette–Guérin vaccination. *Clin Exp Immunol* 2006;**144**(2):281–9.
18. Ehlers S. Role of tumour necrosis factor (TNF) in host defence against tuberculosis: implications for immunotherapies targeting TNF. *Ann Rheum Dis* 2003;**62**:ii37.
19. Rojas M, Oliver M, Gros P, Barrera LF, Garcia LF. TNF-alpha and IL-10 modulate the induction of apoptosis by virulent *Mycobacterium tuberculosis* in murine macrophages. *J Immunol* 1999; **162**(10):6122–31.
20. Seah GT, Scott GM, Rook GA. Type 2 cytokine gene activation and its relationship to extent of disease in patients with tuberculosis. *J Infect Dis* 2000;**181**(1):385–9.
21. Rhodes SG, Palmer N, Graham SP, Bianco AE, Hewinson RG, Vordermeier HM. Distinct response kinetics of gamma interferon and interleukin-4 in bovine tuberculosis. *Infect Immun* 2000;**68**(9):5393–400.
22. Orme IM, Roberts AD, Griffin JP, Abrams JS. Cytokine secretion by CD4 T lymphocytes acquired in response to *Mycobacterium tuberculosis* infection. *J Immunol* 1993;**151**(1): 518–25.
23. Jiao X, Lo-Man R, Winter N, Derlaud E, Gicquel B, Leclerc C. The shift of Th1 to Th2 immunodominance associated with the chronicity of *Mycobacterium bovis* bacille Calmette–Guerin infection does not affect the memory response. *J Immunol* 2003;**170**(3):1392–8.
24. Goldmamm T, Burgemeister R, Sauer U, Loeschke S, Lang DS, Zabel P, et al. Enhanced molecular analyses by combination of the hope-technique and laser microdissection. *Diagn Pathol* 2006;(1):2.
25. Vollmer E, Galle J, Lang DS, Loeschike S, Schultz H, Goldmann T. The HOPE technique opens up a multitude of new possibilities in pathology. *Rom J Morphol Embryol* 2006; **47**(1):15–9.
26. Sen Gupta R, Hillemann D, Kubica T, Zissel G, Galle J, Vollmer E, et al. Hope fixation enables improved PCR-based detection and differentiation of *Mycobacterium tuberculosis* complex in paraffin-embedded tissues. *Pathol Res Pract* 2003;**199**(9):619–23.